Towards Continuous Biomanufacturing
A Computational Approach for the Intensification of Monoclonal Antibody Production

A thesis submitted to Imperial College London for the degree of Doctor of Philosophy

by

Maria M. Papathanasiou

Centre for Process Systems Engineering, Department of Chemical Engineering, Imperial College London,

United Kingdom.

June 2017

To the loving memory of my uncle Nikos,

Declaration of Originality

I hereby certify that this is my own work and any material that is not mine in this work has been appropriately acknowledged.

Maria M. Papathanasiou

Copyright Declaration

Acknowledgements

This is the second, but final time, I am writing this text to express my gratitude to those ones (new & old) who never left my side during these 4.5 painful, but memorable years. As I am writing this, I am waiting for the final decision on my thesis. Feelings are mixed and stress is off the roof. For sure not the greatest moment for decisions, but certainly the best one to feel grateful for the support I have received throughout this process. This experience made me realize that apart from those people who stood by me, I am also thankful to those ones who didn't. To those ones who tried to kill my dreams and successfully failed. To all those people, the good and bad Samaritans of my PhD journey, I'd like to dedicate the following lines.

Far and foremost, my deepest gratitude goes to **Prof. Stratos Pistikopoulos**, the person who celebrated my success stories and supported my failures. I could never believe that I would be so lucky to be blessed with such an inspirational supervisor. I would like to thank you Professor for teaching me how to become a fighter, stand for what I deserve, always with dignity and kindness. Being my academic father for those 4.5 years, you have showed me my strengths and helped me improve my weaknesses. Thank you for trusting me, even during the most difficult times, for having my back like a second father and for pushing me out of my comfort zone showing me what I can really achieve (even though sometimes I couldn't see it myself). I will be forever grateful for all the knowledge (technical and non) I gained next to you and I promise you I will always be smiling no matter the circumstances. It is a great honor to be your academic daughter. Secondly I would like to thank **Prof. Sakis Mantalaris**. As I was writing the first version of my "Acknowledgements", I wanted to thank you for the mentoring and collaboration during these years. After what followed, however, I'd like to thank you for far more beyond that. Next to you I have experienced moments of insecurity, moments where I questioned myself and my skills, moments where in the name of good manners I had to hide my feelings and moments where strategic thinking was key. For all those moments that made me stronger, I'd like to thank you. Hadn't it been for personalities like yours, I wouldn't have become the warrior I am today.

To my examiners: **Dr. Cleo Kontoravdi, Prof. Eva Sorensen**, thank you for showing me that nothing can stand between me and my dreams. Thank you for revealing my inner strength to turn anger into productivity and prove to myself first that everything you really want is possible. Thank you for making me of steel so no one can ever question me again!

Prof. Nilay Shah this paragraph is rightfully dedicated to you. It is the least I can do to express how grateful I am for your support. Thank you for recognizing who I am and for

rewarding me for that. May you always motivate people as you motivated me. The (academic) world needs more people of your kind.

During this journey, I had the chance to meet and collaborate with exceptional people that I'd like to thank. **Prof. Massimo Morbidelli & Dr. Thomas Mueller-Spaeth**, thank you for all your help and mentoring during this project. **Dr. Ana Quiroga**, thank you for the collaboration in the upstream project & moral support ☺. **Muxin, Ioana, Styliana, Romain** thank you for the collaboration! The financial support received from the OPTICO European Project (GA No 280813) and Texas A&M University is also gratefully acknowledged.

My parametric brothers: **Niko & Richard**, thank you for being there, always supportive! I will never forget the years we spent together, the good and the bad times, the laughter and the tears, the Texan experience we shared…Gang, for all those moments I'd like to thank you and for never losing trust in me. **Fabi**, you are naturally the next one to thank! Thank you for being an amazing collaborator and becoming an invaluable friend. I'm truly thankful for your patience with all my stupid chromatography questions and the pink Luxemburgerli boxes!!! Don't forget, next stop: US of A, it's a date. **Eleni**, this "thank-you letter" would never be complete without your name in it. You are the person who encouraged me to embark on this journey, the person who always has an objective advice and a warm heart ready to embrace me when I need it the most. You're not just a friend, you are the bigger sister I never had. Next one in line is you **Andrianos**. Words are not enough to describe how grateful I am to have met you and honored to be able to call you "friend". Thank you for being there with a hug and ready to fight for and with me. I love you for life. **Niko** (Chrys.) this is a shout out to you. To all the dark, secret, deep (sometimes not so deep :P) conversations we had and our full-fat parties when our hearts desired it the most (ode to Lidl pizza!). I found a friend in you and I promise to be there for you as you were for me during those dark-ish months. **Gizem** canim!! Thank you for never leaving my side, for standing stronger than the distance and for being a patient listener. Your words were giving me strength in the worst of moments. Cok seviyorum and I'm really excited for what is coming!!! ☺ ☺ **Keeran**, I'll be forever grateful for having met you my Caribbean celebrity! Being so extra for once again, I must admit that your positivity and trust in me have been a huge drive that helped me pull through. Miss you loads. **Katerina,** this "thank you" goes to you for listening patiently to all my thoughts & insecurities and helping me win them. For sharing to my dreams and living them with me. Thank you for being a friend for all those years that were the beginning of a lifetime. Pack your bags girl, it's happening! **Monty**, thank you for the collaboration but above all thank you for being a friend. I will never forget those amazing months we spent being flat-mates, the super Pokemon moments (not the most proud ones of our lives hehe), the tortilla adventures and that Hollister afternoon. To you, new but true friend, **Filippo**: No matter how strange this

"international" friendship might seem, for me this is one of the treasures of this life. You have been one of the very few people who selflessly cared of how I was doing and kept distracting me from my worries with the most entertaining conversations & trip planning. To this new-born friendship that has already created memories (testata!), un abbraccio forte!!! When I was putting together the people I wanted to thank, you couldn't be missing, **Roberto**. Believe it or not, those months would have never been the same without you. Even though you will casually say "Come oooon….I did nothing!" (admit it , you already thought about it), for me you have done a lot…even though the years we know each other are still countable :P I will never forget how you believed in me when I didn't and how you motivated me to fight for what is mine. Hopefully, I'll find the words to explain to you (and to myself) someday, somehow, the strange things that life does and surprises us and suddenly time seems just so relative ;) (maybe it is the same miracle as that one of alcohol that is sugar in disguise!?!)…for now, just buy an umbrella cause I'm on my way! Un bacio x

Turan, my Spanish sister, thank you for everything!!! I am grateful to God for having you in my life. Thank you & Fran for being always there with a warm hug and delicious food (that cannot be forgotten, reference to quinoa tabouleh) to help me stand up again. I'm excited to see what life has saved for us. Here's to endless tea-conversations and whatsapp screenshots. Te echo de menos y ti amo mucho! **Sofia** all the words and pages in the world wouldn't be enough to describe what you mean to me. It's you that life sent me as living proof that friends can be family. Thank you flat-mate, sister, friend, gym-buddy, psychotherapist, alter ego... Those years were only the beginning and no distance or circumstance is strong enough to break our bond.

Last, but certainly not least, I'd like to express my deepest gratitude to **my family**. I have been blessed with the most loving and caring parents and brother anyone could ask for. Thank you for making me a fighter, for teaching me that values & morals are higher than degrees and for always showing me the truth no matter how painful it might be sometimes. I will be forever grateful to belong in this family and I promise to always make you proud. I love you with all my heart!

Before closing this letter (finally!!!), I'd like to share the most important lesson I have learned from this journey: ***"Vincit qui se vincit"***… in free translation: the one who conquers himself can conquer everything. And so I did… And so I will!!!

Abstract

Current industrial trends encourage the development of sustainable, environmentally friendly processes with reduced energy and raw material consumption. Meanwhile, the increasing market demand as well as the tight regulations in product quality, necessitate efficient operating procedures that guarantee products of high purity. In this direction, process intensification via continuous operation paves the way for the development of novel, eco-friendly processes, characterized by higher productivity compared to batch (Nicoud, 2014). The shift towards continuous operation could advance the market of high value biologics, such as monoclonal antibodies (mAbs), as it would lead to shorter production times, decreased costs, as well as significantly less energy consumption (Konstantinov and Cooney, 2015, Xenopoulos, 2015). In particular, mAb production comprises two main steps: the culturing of the cells (upstream) and the purification of the targeted product (downstream). Both processes are highly complex and their performance depends on various parameters. In particular, the efficiency of the upstream depends highly on cell growth and the longevity of the culture, while product quality can be jeopardized in case the culture is not terminated timely. Similarly, downstream processing, whose main step is the chromatographic separation, relies highly on the setup configuration, as well as on the composition of the upstream mixture. Therefore, it is necessary to understand and optimize both processes prior to their integration. In this direction, the design of intelligent computational tools becomes eminent. Such tools can form a solid basis for the: (i) execution of cost-free comparisons of various operating strategies, (ii) design of optimal operation profiles and (iii) development of advanced, intelligent control systems that can maintain the process under optimal operation, rejecting disturbances. In this context, this work focuses on the development of advanced computational tools for the improvement of the performance of: (a) chromatographic separation processes and (b) cell culture systems, following the systematic PAROC framework and software platform (Pistikopoulos et al., 2015). In particular we develop model-based controllers for single- and multi-column chromatographic setups based on the operating principles of an industrially relevant separation process. The presented strategies are immunized against variations in the feed stream and can successfully compensate for time delays caused due to the column residence time. Issues regarding the points of integration in multi-column systems are also discussed. Moreover, we design and test in silico model-based control strategies for a cell culture system, aiming to increase the culture productivity and drive the system towards continuous operation. Challenges and potential solutions for the seamless integration of the examined bioprocess are also investigated at the end of this thesis.

Table of Contents

List of Figures

List of Tables

List of Equations

Nomenclature

Abbreviations	
BHK	Baby Hamster Kidney cells
CHO	Chinese Hamster Ovary cells
CHP	Combined Heat and Power
CIP	Clean-in-Place
CoGs	Cost of Goods
CSS	Cyclic Steady State
CTC	Continuous Countercurrent Tangential Chromatography
CQA	Critical Quality Attributes
DAE	Differential and Algebraic Equations
DF	Diafiltration
Dmax	Disturbances upper bound
Dmin	Disturbances lower bound
DSP	Downstream Processing
EMA	European Medicines Agency
FDA	US Food and Drug Administration
GSA	Global Sensitivity Analysis
HCP	Host Cell Proteins
HEK	Human Embryonic Kidney epithelial cells
IEX	Ion-exchange
MAbs	Monoclonal Antibodies

MCSGP	Multicolumn Countercurrent Solvent Gradient Purification
MHE	Moving Horizon Estimation
mp-MPC	Multi-parametric Model Predictive Control
mp-LP	Multi-parametric Linear Programming
mp-MILP	Multi-parametric Mixed Integer Linear Programming
mp-MIQP	Multi-parametric Mixed Integer Quadratic Programming
mp-P	Multi-parametric Programming
mp-QP	Multi-parametric Quadratic Programming
MPC	Model Predictive Control
MPT	Multi Parametric Toolbox
NC	Control Horizon
NLP	Nonlinear Programming
ODAE	Ordinary Differential and Algebraic Equations
ODE	Ordinary Differential Equations
OH	Output Horizon
OSD	Oral Solid Dosage
P	Terminal weights for the states
PAROC	Parametric Optimization and Control
PAT	Process Analytical Technologies
PCC	Periodic Countercurrent Chromatography
PDAE	Partial Differential and Algebraic Equations
PE	Parameter Estimation
PPP	Pentose Phosphate Pathway

PSA	Pressure Swing Adsorption
PTM	Post-translational Modifications
Q	Weights on the states
QbD	Quality by Design
QR	Weights on the outputs
R	Weights on the inputs
SIMO	Single-Input Multiple-Output
SISO	Single-Input Single-Output
SMB	Simulating Moving Bed
TCA	Tricarboxylic Acid
Umax	Input upper bound
Umin	Input lower bound
UF	Ultrafiltration
USP	Upstream Processing
Xmax	States upper bound
Xmin	States lower bound
Ymax	Output upper bound
Ymin	Output lower bound

Physical and Mathematical Quantities

$\mathbf{A_{col}}$	Column cross section	cm^2
$\boldsymbol{C_{asp}}$	Constant used in the calculation of the specific growth rates	-
$\boldsymbol{C_{asn}}$	Constant used in the calculation of the specific growth rates	-

C_{arg}	Constant used in the calculation of the specific growth rates	-
$c(z,t)_{i,h}$	Liquid phase concentration of species i in column h	mg/mL
$c_{av_{i,s}}$	Average concentration of species i in stream s	mg/mL
$c^{0}_{i,h}$	Initial concentration of species i in column h	mg/mL
c^{feed}_{i}	Feed concentration of species i	mg/mL
$c^{in}_{i,h}$	Inlet concentration of species i in column h	mg/mL
$c^{out}_{i,h}$	Outlet concentration of species i in column h	mg/mL
$H_{i,h}$	Overall Henry constant of species i in column h	mg/mL
$H^{I}_{i,h}$	Henry constant for the adsorption site 1of species i in column h	mg/mL
$H^{II}_{i,h}$	Henry constant for the adsorption site 2of species i in column h	mg/mL
H_{mod}	Henry constant of the modifier	mg/mL
k_i	Lumped mass transfer coefficient of species i	min^{-1}
L_{col}	Column length	cm
K_{MET}	Glutamate priority term	mM
K_{glc}	Saturation constant for growth on glucose	mM
K_{glu}	Saturation constant for growth on glutamate	mM
K_{asp}	Saturation constant for growth on aspartate	mM
K_{arg}	Saturation constant for growth on arginine	mM
K_{asn}	Saturation constant for growth on asparagine	mM
$K_{glc,lim}$	Saturation constant for growth on glucose	mM
$K_{glu,lim}$	Saturation constant for growth on glutamate	mM
$K_{asp,lim}$	Saturation constant for growth on aspartate	mM

$K_{arg,lim}$	Saturation constant for growth on arginine	mM
$K_{asn,lim}$	Saturation constant for growth on asparagine	mM
$M_{glyc,glc}$	Requirement of glucose to produce alanine (Energy)	mmol/Cell·h
$M_{tca,glc}$	Requirement of glucose to produce energy (TCA cycle) per cell	mmol/Cell·h
$M_{tca,glu}$	Requirement of glutamate to produce ATP (TCA cycle) per cell	mmol/Cell·h
$m_{mab,x}$	Maintenance	mmol/Cell·h
$\mathbf{n_{col}}$	Number of columns	-
$\mathbf{n_{comp}}$	Number of components	-
$\mathbf{n_{outlet}}$	Number of outlet streams	
$\mathbf{q(z,t)_{i,h}}$	Solid phase concentration of species i in column h	mg/mL
$\mathbf{Pur_{av_j}}$	Average purity at cycle j	-
$\mathbf{Q_h}$	Flow rate of column h	mL/min
Q_{MET}	Effect of glutamate concentration on glucose uptake	-
$Q_{x,glc}$	Glucose consumed per cell for growth	mmol/Cell·h
$Q_{glyc,glc}$	Specific glucose consumption rate to produce lactate and alanine	mmol/Cell·h
$Q_{tca,glc}$	Specific consumption of glucose to produce energy through the TCA cycle	mmol/Cell·h
$Q_{glu,arg}$	Glutamate produced from arginine	mmol/Cell·h
$Q_{x,glu}$	Glutamate consumed per cell for growth	mmol/Cell·h
$Q_{tca,glu}$	Saturation constant for growth on glucose	mmol/Cell·h
$Q_{tca,asp}$	Saturation constant for growth on aspartate	mmol/Cell·h
$\mathbf{q^I_{i,h}}$	Saturation constants	mg/mL

$q^{II}_{i,h}$	Saturation constant	mg/mL
Y_j	Yield at cycle j	-
$Y_{x,glc}$	Yield of glucose on biomass	Cell/mmol
$Y_{glyc,glc}$	Requirement of glucose to produce lactate (Energy) per cell	Cell/mmol
$Y_{tca,glc}$	Requirement of glucose to produce energy (TCA cycle) per cell	Cell/mmol
$Y_{x,glu}$	Yield of glutamate on biomass	Cell/mmol
$Y_{tca,glu}$	Requirement of glutamate to produce ATP (TCA cycle) per cell	Cell/mmol
$\alpha_{i,1}, \ldots, \alpha_{i,8}$	Coefficients used in the isotherms for the MCSGP process	-
ε_i	Column porosity for component i	-
μ	Growth rate	h^{-1}
μ_d	Death rate	h^{-1}
μ_{max}	Maximum theoretical growth rate	h^{-1}
$\mu_{d,max}$	Maximum theoretical death rate	h^{-1}

Subscripts

h	Column index
i	Species index
j	Cycle index
s	Stream index
t	Time
$t_{cycletime}$	Cycle duration
z	Space coordinate

Chapter 1.

Introduction

Monoclonal antibodies (mAbs) play a vital role in the treatment of infectious diseases, cancer and autoimmune diseases (Torphy, 2002). Despite their beneficial properties, mAbs are now facing competition stemming from: (i) the emergence of biosimilars and other therapeutic agents of similar properties, (ii) lower production costs and (iii) shorter time-to-market. Moreover, current industrial trends indicate a shift towards eco-efficient processes of reduced environmental footprint that consequently leads to re-evaluation of standard practice (Xenopoulos, 2015, Klutz et al., 2016). Klutz et al. (2016) recently presented a study where they compared: (i) a fed-batch (single fed-batch fermentation unit, followed by six downstream unit operations, run sequentially), (ii) a continuously operated process (perfusion bioreactor and six downstream unit operations, run simultaneously) and (iii) a hybrid model (fed-batch upstream with continuous downstream). Especially in the case of the downstream, the study reports that continuous operation is approximately 8 € per gram of mAb more favorable than the batch. The latter is mainly attributed to better utilization of the chromatography resin as well as the viral retention filtration material. Overall, the hybrid model results in 15% reduction in the cost of goods and is proposed as the most successful solution. A similar study by Walther et al. (2015) demonstrates that integrated continuous biomanufacturing could reduce the total cost (operating and capital) up to 55% compared to batch. Continuously operated processes could also reduce the environmental footprint. As reported by Plumb (2005) by shifting from batch to a continuous operation utility and energy requirements could be cut up to 95%. Moreover, due to its higher efficiency and lower utility consumption, continuously operated equipment is reported to be significantly smaller in size, leading therefore to further cost savings (Plumb, 2005, Nichols, 2008, Hillier, 2013). Indicatively, Langer and Rader (2014) report that commercial manufacture involves bioreactors over 1,000‑2,000L that require large-scale industrial operations and equipment. A shift to continuous operation would involve smaller equipment and other operations (e.g. mixing, heating, cooling, etc) at smaller scale making the process more eco-efficient.

Recently there has been increasing interest in the investigation of the improvement possibilities of the processes currently used for the production of mAbs (Girard et al., 2015, Walther et al., 2015, Klutz et al., 2016). Most of the related studies suggest the transition from batch to continuous operation, as the solution towards steady-state operation, where product purity would remain constant throughout the process (Steinebach et al., 2016a, Zydney, 2016). Furthermore, a shift from batch to continuous operation promises significant decrease in the holdup steps, thus decreasing both the production time and the risk of product degradation (Gillespie et al., 2012, Gospodarek et al., 2014, Steinebach et al., 2016a, Zydney, 2016).

MAb production consists of the upstream and the downstream processing. Upstream considers the culturing of the cells that are used as the expression system for the production of the targeted product, while downstream processing involves a series of separation/purification steps of the upstream mixture. Currently, cell culture systems are operated to a great extent in fed-batch mode, while separation processes are characterized by periodic, batch profiles. Therefore, a shift from batch to a fully integrated, continuous operation is not a trivial task and is associated with a plethora of challenges. The latter can arise from the optimal equipment design, quality assurance as well as monitoring and control of the new production line. More specifically, in the case of the upstream it is necessary to ensure that the continuous system will be characterized by similar or higher productivity, improved product quality, while the equipment size will be decreased (Chon and Zarbis-Papastoitsis, 2011). As reported by Konstantinov and Cooney (2015), stable cell lines need to be developed that will ensure high productivity for longer periods (e.g. 3 months). In the same fashion, there is eminent need for the design of media formulations that can support high cell densities and optimization of the cell culture conditions in order to ensure high cell density and productivity. Similarly, in downstream processing and in particular in the case of chromatographic separation processes, it is essential to optimize and/or re-design current equipment in order to allow handling of larger load volumes, while minimizing equipment and material cost. In addition, under high titers, downstream processing can become significantly expensive, mostly due to equipment and consumables costs (Dünnebier et al., 2001, Chon and Zarbis-Papastoitsis, 2011, Strube et al., 2012, Gronemeyer et al., 2014), thus setting its optimization a priority. Although, the concept of continuous upstream is being discussed since 1986 (Arathoon and Birch, 1986), in the case of downstream knowledge is still limited. Nowadays there are several manufacturers that offer small-scale continuous chromatography systems (e.g. BioSC® & Varicol® by Novasep, Periodic Countercurrent Chromatography (PCC) & Straight-through Processing (STP) by GE Healthcare, Contichrom® by Chromacon). However, significant experience in continuous chromatography needs to be gained in process scale-up in order to ensure successful operation at large scale. Moreover, apart from advances in the chromatography steps, developments in other downstream unit operations are required (e.g. continuous ultrafiltration/diafiltration) (Konstantinov and Cooney, 2015).

From a process standpoint, it is necessary to ensure that the integrated bioprocess is efficiently monitored and controlled in order to achieve maximum and stable product quality and yield. Control and monitoring of such complex processes is a challenging task that is now coupled with continuous operation, rendering online measurements even more challenging to

obtain. At the moment in batch operation, each process unit is controlled independently without need of communication between the different monitoring/control equipment. However, in continuous operation the feedback across process units is required, pointing towards the development of global control schemes, where the entire process flow is supervised. The development of advanced computational tools can facilitate changes in the current state-of-the-art of biomanufacturing, providing a basis for cost-free simulations. In addition, it can pave the way towards the design of advanced optimization strategies and control policies that will ensure feasible, optimal and stable operation. Furthermore, in-silico experimentation allows the comparison of various operating scenarios that can significantly reduce labor time and cost and identify process limitations and bottlenecks.

1.1 Aims & Objectives

Aiming to facilitate the shift from batch to continuous operation, this work presents the development of advanced computational tools that will enable the intensification of monoclonal antibody production through continuous operation. MAb production consists of two main parts: (1) the upstream processing, where the cells are cultured and the therapeutic agent is produced and (2) the downstream processing that involves the isolation/purification of the targeted product. Acknowledging that currently downstream processing is the most costly and limiting part of the bioprocess, we devote the main focus of this work to the development of advanced control strategies for a series of industrially relevant, chromatographic separation systems. The key objective of this study is the design of "smart control strategies" that obey the governing laws of the system at hand, while ensuring continuous monitoring and stable operation. However, in a fully integrated bioprocess, the need of global control policies becomes eminent. Therefore, in this work we also investigate the design of control strategies for a cell culture system in a bioreactor. The development of a global approach for the control of the continuous bioprocess is also discussed. The control policies presented in this work are of model-based nature and are developed within the generic PAROC framework/software platform for the design and in-silico testing of advanced controllers (Pistikopoulos et al., 2015). The rest of the manuscript is organized as follows:

- **Chapter 2.** Monoclonal Antibody Biomanufacturing**:**

  This chapter presents the current state-of-the-art in monoclonal antibody manufacturing. Here we discuss the standard practice both in upstream and downstream processing and we investigate the potential and bottlenecks of the shift

form batch to continuous operation. Moreover, the role of computational tools in this transition is discussed.

- **Chapter 3.** Chromatographic Separation Processes**:**

  The main focus of this work is the development of advanced control strategies for chromatographic separation systems. This chapter is dedicated to the operating principles of chromatography. Works on optimization and control of such systems are also discussed here.

- **Chapter 4.** Model-based Control of Single-Column Chromatographic Systems**:**

  Here we present the development of advanced control strategies of a single-column chromatographic separation system, based on the operating principles of an industrial process. We design and test in-silico 3 different control schemes: (a) 3 Single-Input Single-Output controllers under continuous feed, (b) a Single-Input Multiple-Output controller under continuous feed and (c) a Single-Input Multiple-Output controller under periodic feeding strategy. Aiming to overcome issues with unavailable measurements and to design a continuous monitoring approach, we suggest a novel concept, where we track the integral of the outlet concentrations of the mixture components. The behavior of the controllers under various flow rates and disturbances is also assessed.

- **Chapter 5.** Model-based Control of Multi-Column Chromatographic Systems *following the PAROC framework***:**

  This chapter focuses on the development of advanced control schemes for multi-column chromatographic systems. We consider a twin-column system; based on the principles of an industrially relevant separation process and we present the design and testing of a novel control scheme, where the two columns are monitored in a centralized/decentralized fashion. Moreover, we present a novel approach, where the recycling streams are treated as disturbance aiming to minimize the feedback information required during online monitoring.

- **Chapter 6.** Model-based Control of Cell Culture Systems**:**

  In this chapter we investigate the development of an advanced, model-based control strategy for a cell culture system aiming to improve the process productivity. Firstly we present a dynamic optimization study that is used as a basis for the development

of the model-based controllers. Furthermore, we design and test 3 advanced controllers of different sampling strategies. The controllers' performance is assessed and compared.

- **Chapter 7.** Conclusions & Future Directions**:**

  In this chapter a summary of this work is presented and current/future directions for the continuation of this work are discussed.

- **Appendix A:** Computational Tools

  Appendix A presents all theoretical aspects related to this work. Namely we illustrate the theory behind: (i) Global Sensitivity Analysis and (b) Multi-parametric Model Predictive Control.

- **Appendix B:** Downstream Process

  Appendix B demonstrates additional studies/collaborations related to the downstream systems examined in this work. In particular, we illustrate: (a) the process model of the MCSGP process, developed by the Morbidelli Group (ETH, Zürich), (b) a sensitivity analysis study on the control parameters, executed on the single-column system, (c) a collaborative work on the development and comparison of PID controllers for the single-column case and (d) a preliminary investigation of the periodicity in the control laws during the "closed-loop" validation of the controllers designed for the single-column case.

- **Appendix C:** Upstream Process

  Appendix C presents complementary work performed on the upstream system. More specifically here we illustrate: (a) a collaborative project for the development and experimental validation of the dynamic model used to describe the cell culture system and (b) an additional control study, where no outlet is considered.

The work presented on the development of control strategies for the downstream purification process was conducted in the framework of the European OPTICO Project for "Model-based Optimization and Control for Process Intensification in Chemical and Biopharmaceutical Systems" (G.A. No 280813). This collaborative initiative consisted of a 13-partner industrial/academic consortium. The current work was conducted in collaboration with ChromaCon AG and ETH Zürich (the Morbidelli Group) on the industrial process unit Multi-column Counter-current Solvent Gradient Purification process. The mathematical model for

this unit have been previously developed and validated by ETH Zürich (the Morbidelli Group), while the current thesis focused on the development of advanced control techniques. The work conducted on the development of control strategies for the bioreactor system, is based on a previously developed and validated model by Dr. Ana Quiroga. This thesis focused on the investigation of different control strategies on the respective system.

Chapter 2.

Monoclonal Antibody Biomanufacturing

2.1 Current status and needs

2.1.1 Fundamentals

MAbs are "Y" shaped molecules, consisting of two light and two heavy chains connected by disulfide bonds. Each light chain (approximately 25 kDa) is composed of two successive domains (the constant and the variable), while the heavy one (approximately 50 kDa) considers one constant and one variable region. The variable regions are responsible for antigen binding, while the constant regions are responsible for the biological functions. In general, based on their heavy chains, we distinguish 5 classes of antibodies: IgG, IgA, IgM, IgE and IgD (Sommerfeld and Strube, 2005). Their targeted selectivity makes them a very powerful and attractive method for the treatment of cancer, various autoimmune diseases or organ transplantations (Bai, 2011).

MAbs act as the leading product in the rapidly increasing market of high value biologics and their sales are considered to increase twice as fast as other biotechnological drugs. According to market projections, the value of mAb market is expected to increase up to 75 billion USD by 2025 (Mabion, 2013). Their demand depends highly on the patient population, however, their high cost (approximately $35000 p/a per patient for mAbs treating cancer conditions) (Farid, 2007) has given rise to alternative, more affordable solutions. Indicatively, biosimilars form a new class of lower-cost therapeutics and designed to be similar to existing biological medicines (Blackstone and Fuhr, 2012, E.M.A, 2016b). Biosimilars are considered to be biopharmaceutical drugs that are manufactured to have active properties similar to those of previously licensed therapeutics. They demonstrate no clinically meaningful differences to the original product and are usually produced using alternative expression systems (Love et al., 2013). Since the approval of the first biosimilar product in the European Union (2006) their market has been rapidly increasing, looking at the moment at 21 approved products by the European Medicines Agency (EMA) solely (E.M.A, 2016b). Moreover, in March 2015 biosimilars penetrated the US market with their first product being approved by the U.S. Food and Drug Administration (F.D.A, 2015a). However, biosimilars are not generic equivalents of the originator product and their properties are highly associated to the processes used for their manufacturing (Mellstedt et al., 2008). As patents of biotechnological companies on mAbs gradually expire (Konstantinov and Cooney, 2015), there is an eminent need for the mAb market to answer to competition by moving towards novel processes that will secure patents on mAb manufacturing and subsequently decelerate the emergence of similarly manufactured drugs. Shifting to more cost-effective solutions and smart manufacturing shows great

potential and can result into higher process yield, cheaper end-products and shorter production times (Blackstone and Fuhr, 2012, Xenopoulos, 2015).

2.1.2 Current status in mAb biomanufacturing

The production of mAbs consists of two main parts: (a) the upstream processing (USP) and the downstream processing (DSP). The former refers to the culturing of the cells in bioreactors and the production of the targeted product, while the latter involves a sequence of separation/purification steps responsible for the isolation of the antibody from the upstream harvest. Currently, the biomanufacturing of mAbs considers fed-batch cell culture systems and batch separation processes (Xenopoulos, 2015).

2.1.2.1 Upstream Processing (USP)

The design of an optimal process of high yield is a challenging task, accompanied by a variety of factors that need to be considered and examined. Figure 2.1 illustrates some of those problem parameters that are discussed below.

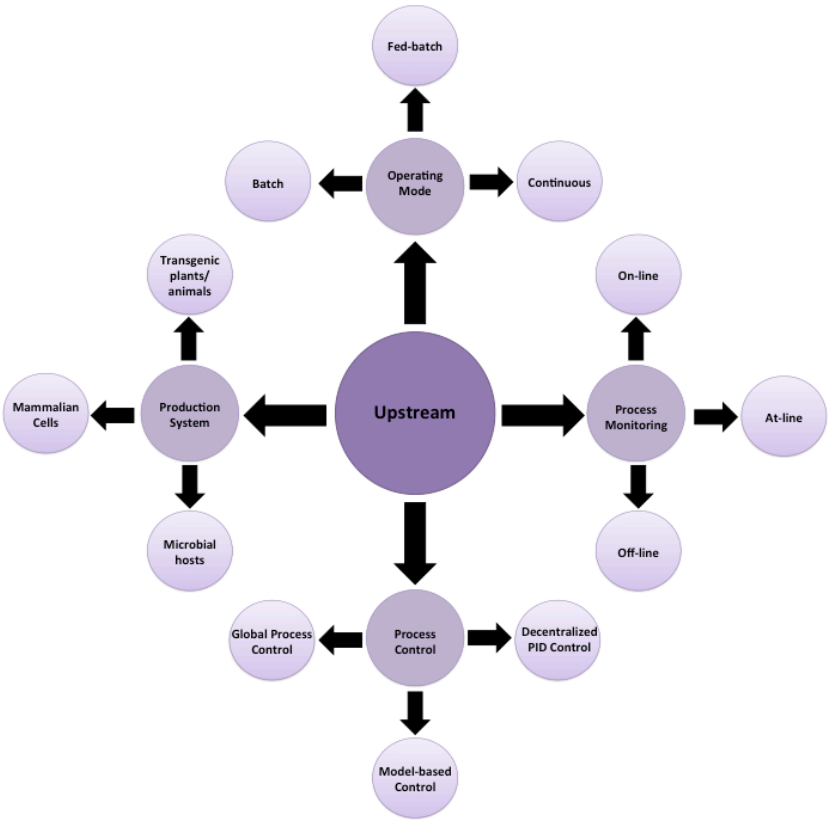

Figure 2.1 Factors that need to be considered during the design of an upstream process in monoclonal antibody production.

(i) **Production systems**: Current state-of-the-art in upstream processing of monoclonal antibodies and other biopharmaceutical products dictates mammalian cell culture systems as the preferred expression system (Zhu, 2012). Mammalian cells have the distinct advantage to produce active molecules with humanlike post-translational modifications (PTM) identical to native endogenous proteins, including glycosylation, formation of disulphide bonds and proteolytic processing; which are known to be essential for the biological function and pharmacokinetics of the final product (Berlec and Strukelj, 2013). Most marketed biologic drugs are produced in Chinese Hamster Ovary (CHO) cells, murine myeloma lymphoblastoid-like cells (NS0 and Sp2/0-Ag14), Human Embryonic Kidney epithelial cells (HEK 293), and Baby Hamster Kidney (BHK-21) cells. Despite their successful entry in the manufacturing industry, mammalian cells cultures face significant challenges such as low yield, high medium costs and slow growth (Zhang, 2010) when compared to bacteria and/or yeast (approximately 3fold lower) (Báez et al., 2005, Birch et al., 2008, Zhang, 2010). To enhance the expression of the recombinant proteins, different approaches have been implemented such as cell engineering, vector design, screening tools, culture medium composition and operating conditions optimization, and control strategies (Zhu, 2012).

(ii) **Operating mode:** Here various types of configurations are considered. Batch cultures are closed systems, which contain a limited amount of nutrients. In this case, cell death is caused by nutrient starvation or toxic metabolites accumulation. On the other hand, in fed-batch cultures, a concentrated feeding medium is supplied to cover the nutritional requirements of the cells; consequently, the integral viable cell density and volumetric productivity are increased. Fed-batch cultures are widely used in the biopharmaceutical industry because of their reduced direct costs, high harvest concentration and robust, reproducible, manufacturing outcomes (Zhang, 2010). In perfusion and continuous manufacturing configurations, fresh medium is added continuously with the difference laying on the content of outflow. In perfusion the cells are retained inside the bioreactor, and the removed broth is cell-free, containing the product in relatively low titer. Continuous processes do not have internal or external cell-retention devices. The advantages of these systems are the steady state operation, reduced equipment size, streamlined process flow, low-cycle times, and reduced capital cost (Konstantinov and Cooney, 2015). Nevertheless, issues such as phenotypic instability of the cell line over long culture periods in use need to be addressed prior to the selection of the appropriate expression system (Barnes et al., 2004, Bailey et al., 2012).

(iii) **Process control & monitoring**: In order to ensure optimal operation that will lead to stable product quality, advanced control and monitoring tools are required. Currently available electrochemical and optical sensors enable the monitoring of the physical and physicochemical culture conditions (pH, temperature and dissolved oxygen online measurements). However, for the control of the product titer and quality it is necessary to measure additional parameters, such as: cell density, nutrient concentration and level of toxic metabolites (Konstantinov and Cooney, 2015). Despite the advances in online sampling for at-line analysis (e.g. BioProfile analyzers) and online probes (e.g. near-infrared spectroscopy technology) there is still a wide gap between monitoring technologies and control techniques. Therefore there is eminent need to fill this technological gap and drastically improve the sustainability of biopharmaceutical processes.

2.1.2.2 Downstream Processing (DSP)

Similarly to USP, Figure 2.2 illustrates they key issues that need to be addressed during the design of a downstream process.

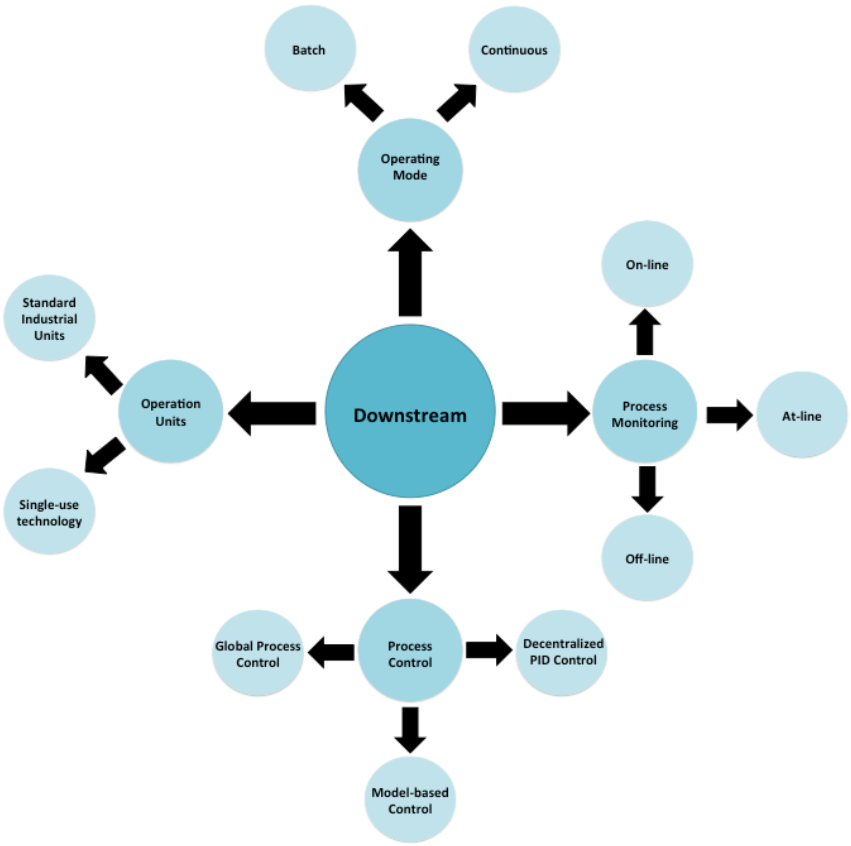

Figure 2.2 Factors that need to be considered during the design of a downstream process in monoclonal antibody production.

Unlike USP, DSP is a sequential procedure, involving a series of separation/purification steps until the required product purity is achieved. Firstly, the cell culture mixture containing the targeted product is centrifuged and filtered. Following that, a step performed with Protein A chromatography, serves as a product capture step and results in high purity and concentration of the drug (Figure 2.3). This is followed by two polishing steps, where usually ion-exchange chromatography is used. Finally, a virus filtration step is required, followed by ultrafiltration/diafiltration (UF/DF) for the formulation and concentration of the final product (Kelley, 2009a, Kelley et al., 2009). Here we discuss some of the key aspects that need to be considered during the design of the optimal downstream process train.

(i) **Operation units:** For the first clarification step, centrifugation is the current preferred method. However it is not able to significantly reduce the amount of solids present in the medium and return a centrate suitable for capture chromatography. Therefore, depth filtration is required for the removal of host cell proteins (HCP) (Kelley et al., 2009). At this stage, alternatives such as flocculation can also be considered, offering higher clarity than centrifugation (Shpritzer et al., 2006). The primary capture step is usually performed with Protein A chromatography, however ion-exchange chromatography can be considered as well. The preferred method for the polishing step is normally defined by the nature of the product and the impurities. Here, Protein A and ion-exchange chromatography can both be used. For increased efficiency and minimization of the polishing steps, alternatives such as mixed-mode resins (Carta and Jungbauer, 2010) and/or the use of membrane adsorbers can also be considered (Zhou and Tressel, 2006). Traditionally, column chromatography utilizes stainless steel equipment. However, recent trends that necessitate the minimization of production costs, have given rise to novel technologies, such as single-use equipment. The emergence of disposable technologies (e.g. chromatographic units, filters, centrifuges) offers great opportunities towards the design of more cost-efficient processes of similar or improved productivity (Lim et al., 2007, Shukla and Gottschalk, 2013).

(ii) **Operating mode:** Currently, industrial downstream manufacturing utilizes multiple batch unit operations, designed to handle feeds of 2-5 g/L (Gronemeyer et al., 2014). Industrially standardized procedures followed in DSP, ensure products of high purity, limiting, however, the amount recovered in the end of the process cycle as they can only handle certain volume of loads. Aiming to increase process efficiency, significant advances have been made towards the development of semi- or fully continuous chromatographic processes. The latter gave rise to novel semi-continuous

separation configurations, such as the Periodic Counter-Current Chromatography (PCC), the Multicolumn Countercurrent Solvent Gradient Purification Process (MCSGP) the Continuous Countercurrent Tangential Chromatography (CTC) and the Sequential Multicolumn Chromatography (SMCC) (Ströhlein et al., 2006a, Aumann et al., 2007, Godawat et al., 2012, Ng et al., 2014, Dutta et al., 2015, Zydney, 2016). Apart from increased productivity, continuous DSP guarantees a significant decrease in the respective Cost of Goods (COGs) as raw materials, such as eluents, are recycled. Moreover, product quality can be significantly improved, as in continuous processing hold-up steps (e.g. harvest vessels, intermediate storages) can be eliminated (Klutz et al., 2016).

(iii) **Process control & monitoring:** Currently, measurements regarding product quality rely mostly on ultraviolet (UV) detectors and automated HPLC systems. The accuracy of the former is highly sensitive and linked to experimental factors, while the latter provide infrequent measurements on the average concentrations of the mixture components (Grossmann et al., 2008). In addition, in order to obtain the suitable controller feedback, lengthy experimental procedures are required (Konstantinov and Cooney, 2015), leading to significant delays in the process operation. Traditionally, the outlet of chromatography columns is continuously monitored by ultraviolet/visible (UV/VIS) detectors; while in lab-scale, light scattering and mass spectroscopy equipment are also used (Carta and Jungbauer, 2010). UV detectors are considered to be effective as proteins usually exhibit a strong absorbance signal at 280 nm (applicable also in the case of monoclonal antibodies). Despite the existence of some online measurements on protein concentration, the detection of impurities in the mixture is still performed through offline procedures, such as size exclusion chromatography for the detection of fragments and/or aggregates and immunoasays for the detection of host cell proteins and DNA (Moorhouse et al., 1997, Wakankar et al., 2011, Healthcare, 2015). In the case of aggregates, other methods may also be used based on their size (Cordoba-Rodriguez, 2008, Paul and Hesse, 2013). Regulatory bodies also suggest few analytical procedures that can assist the identification of impurities (ICH Q6B) and they are discussed below (section 2.1.3). Moreover, there are attempts to allow for on-line available measurements, such as the one by EMD Milipore & Momenta Pharmaceuticals (Doneanu et al., 2012), where they present a procedure for the online identification of host cell proteins using two-dimensional liquid chromatography coupled with high resolutions mass spectroscopy, followed by high throughput HCP quantification. Currently, regulatory bodies encourage the development of advanced

Process Analytical Technologies (PAT) that will provide the necessary information timely, minimizing human error (F.D.A et al., 2004, Low et al., 2007).

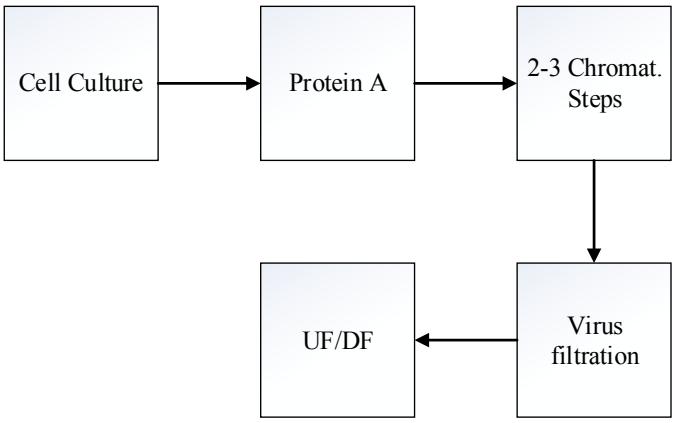

Figure 2.3 Sequence of processes involved in DSP.

2.1.3 Industrialization of monoclonal antibodies

2.1.3.1 Typical production process

Figure 2.4 illustrates a standard process sequence followed in the production of mAbs. Usually, mammalian cells are chosen as the expression system and are grown in suspension culture in large bioreactors (5-25 thousand liter) (Kelley, 2009b). Most of mAbs products are derived from CHO, NS0 or Sp2/0 cell lines (Wurm, 2004). A typical production process is run for 7-14 days in fed-batch mode, where discrete feeds with nutrients are added to the bioreactor. Before inoculation of the production bioreactor, an expansion of a cell bank vial and subsequent growth of the cells in seeding bioreactors is performed (Zhang, 2010).Currently, mAb titers vary between 1-10 g/L while the bioreactor production volumes range from 5,000 L to 25,000 L (Butler, 2005, Sharfstein, 2008).

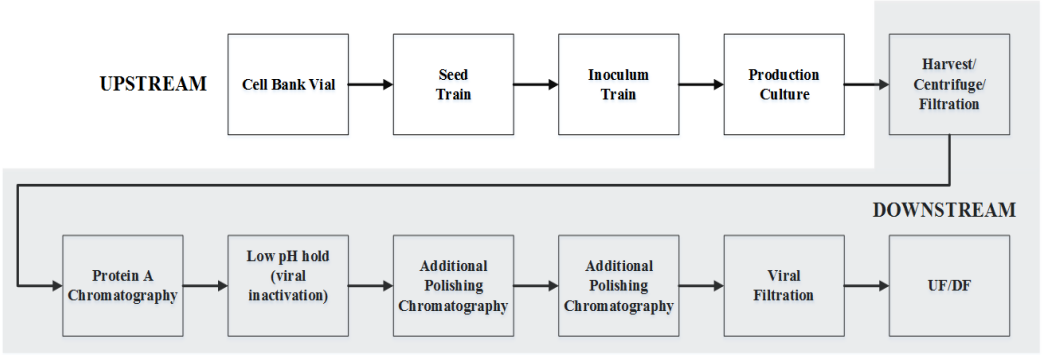

Figure 2.4 Indicative production process of mAbs. Upstream processing steps are depicted in the white area, while the grey area illustrates the downstream purification steps (adapted from Kelley 2009 & Liu 2010).

The downstream processing cascade involves various separation processes, including different chromatographic purification steps. Starting with the initial centrifugation and filtration (often referred as *primary recovery*), the mixture is clarified from suspended solids, such as cells or cell debris. Following the primary recovery, a standard downstream process sequence includes successive capture, purification and polishing steps, each with one or more operations (Carta and Jungbauer, 2010). In most of the cases in mAb production, the capture step is realized through Protein A affinity chromatography. The selectivity of Protein A affinity chromatography can result in high purities up to >95% in a single step (Shukla et al., 2007, Perez-Almodovar and Carta, 2009, Shukla and Thömmes, 2010). This step is usually employed after harvest operations (where the supernatant is clarified from cells and cell debris) and significantly reduces the volume of the product stream, as a higher concentration in the post-Protein A capture pool is achieved. Nevertheless, Protein A adds another impurity in the stream, that of the leached Protein A ligand that has to be removed by the following purification steps.

From a process perspective, Protein A is often the limiting step as large volumes from the culture supernatant are loaded on relatively smaller and expensive columns (Shukla et al., 2007). Moreover, as Protein A carries out the elution at low pH values, there is the risk for the formation of soluble high molecular weight aggregates, thus reducing the product yield and burdening the polishing steps with further clearance from the aggregate species that can be antigenic (Shukla and Thömmes, 2010, Zydney, 2016, Johnson et al., 2017). Besides the removal of impurities, also viral inactivation steps are required (Q5A, Shukla and Thömmes, 2010, Johnson et al., 2017). Therefore, low pH treatment is employed as it has been proven to efficiently inactivate retroviruses from various biological products (Shukla et al., 2007). The following two polishing steps are responsible for the removal of host cell proteins, DNA, aggregates, fragments and leached Protein A from the capture step (Voitl et al., 2010, Zhang et al., 2014b, Khalaf et al., 2016). Typically in mAb downstream processing, two subsequent chromatographic steps are employed based on ion-exchange (IEX) chromatography. The latter is performed for the removal of both process and product related impurities. While IEX chromatography can also be applied in capture steps it is mainly used for polishing applications. With the pH being in between the pI of the antibody and the pI of most host cell proteins, significant removal of HCPs can be achieved. Additionally, aggregates can also be removed. Due to the pI of most mAbs, which is often in the range of 7.5-9.5, cation-exchange polishing is often performed in bind-elute mode, aiming at the removal of HCP, DNA as well as aggregates, while anion-exchange polishing is performed in flow-through mode, with impurities such as DNA and HCP adsorbing on the resin, while the target protein is collected

in the flow-through (Carta and Jungbauer, 2010, Voitl et al., 2010). Viral filtration follows to complement the viral inactivation step that is performed after the primary recovery. Lastly, an ultrafiltration/ diafiltration step is applied for the concentration of the final product as well as buffer exchange. As discussed earlier (section 2.1.2.2), there is a variety of measurements obtained during the downstream processing to determine Critical Quality Attributes, as well as product purity and process yield.

2.1.3.2 Critical Quality Attributes (CQAs) and regulatory approval

Monoclonal antibodies are associated with stringent regulations that define their purity and composition. According to the ICH Q6B note on "Specifications: Test Procedures and Acceptance Criteria for Biological/Biotechnological Products", for a drug to be considered acceptable for its intended use it needs to comply with pre-defined specifications. The latter correspond to "a list of tests, references to analytical procedures, and appropriate acceptance criteria which are numerical limits, ranges, or other criteria for the tests described".

Table 2.1 CQAs commonly observed in biopharmaceutical proteins (adapted from Eon-Duval et al. (2012), ICH Q6B & EMA "Guideline: Development, production, characterization and specifications for monoclonal antibodies and related products" (2016)).

Product-related impurities & substances	Process-related impurities	Contaminants
Aggregation	Residual DNA	Adventitious agents (e.g. bacteria, mycoplasma, viruses)
Fragmentation	Residual Host Cell Proteins (HCPs)	Endotoxins
C- and N- terminal modifications	Raw material-derived impurities (e.g. leached Protein A)	
Oxidation		
Deamidation/isomerization		
Glycosylation		
Glycation		
Conformation		
Disulfide bond modifications/free thiols		

The characterization of a biological product includes the determination of physicochemical properties, biological activity, immunochemical properties, purity and impurities "(ICH

Q6B). Based on regulatory announcements (ICH Q6B) as well as information provided in the open literature (Shukla et al., 2007, Carta and Jungbauer, 2010, Eon-Duval et al., 2012) impurities are classified into two main categories: (a) product-related and (b) process-related impurities. The first one relates to impurities that result from the product, such as aggregates, while process-related impurities evolve from the process itself, such as HCPs. Besides the removal of these impurities, one needs to consider that mAbs undergo different modifications. Therefore, announcements published by the International Conference on Harmonization (ICH) and other regulatory bodies (EMA, FDA) identify the necessary Critical Quality Attributes (CQA) alongside with their allowed ranges. CQA refers to "a physical, chemical, biological or microbiological property or characteristic that should be within an appropriate limit, range or distribution to ensure the desired product quality". CQAs are considered to highly affect product safety and efficacy, hence it is suggested that they are closely monitored. For the purposes of this work, we focus particularly on the aspects of purity and hence the removal of impurities is considered, while for the rest of the specifications, such as glycosylation, the reader is referred to ICH Q6B.

The determination of absolute and/or relative "purity" is usually highly method-dependent and is determined using a combination of methods (ICH Q6B). Due to their complex molecular characteristics and production process, the end-drug substances can include multiple molecular entities and variants (e.g. glycoforms or charge variants). It is advised that the properties of the latter are assessed and compared to the desired product in order to ensure that the presented heterogeneity has no effect on the activity, efficacy and safety of the drug. In the event that the tested variants demonstrate properties similar to the desired product they can be characterized as "product-related substances" and not impurities. In case they are found to affect the activity, efficacy and/or safety of the drug they are classified as "product-related impurities" and they need to be within certain limits (ICH Q6B). On the other hand, "process-related" impurities are variants occurring during the production process and do not have properties similar to the desired product thus jeopardizing the drug activity, efficacy and/or safety. These can result from cell substrates (e.g. HCP, DNA), cell culture (e.g. antibiotics) or downstream processing (e.g. leached Protein A). Last but not least, contaminants (e.g. bacteria) adventitiously introduced in the production process "should be strictly avoided and/or suitably controlled with appropriate in-process acceptance criteria or action limits for drug substance or drug product specifications" (ICH Q6B). Table 2.1 presents an indicative summary of product- and process- related impurities, as well as types of contaminants that are often encountered in the production of mAbs.

Table 2.2 demonstrates the appropriate requirements that need to be met in order to ensure the safety of a protein pharmaceutical. Limits on other types of impurities may depend on their type and/or effect on the drug activity, efficacy and/or safety and are therefore decided upon characterization and collection of preclinical/clinical data (Eon-Duval et al., 2012). ICH Q6B suggests an indicative list of analytical techniques that can be used for the detection and/or quantification of impurities in biological and biotechnological products. In the case of process-related impurities; for host cell proteins, a sensitive assay (such as immuoassay) can assist the detection of a wide range of proteins, while DNA levels from host cells can be identified via direct analysis (e.g. hybridization techniques). Chromatographic and/or electrophoretic methods can be applied for the detection of product truncation, dissociation and polymerization (EMA "Guideline: Development, production, characterization and specifications for monoclonal antibodies and related products" (2016)).

Table 2.2 General guidlines for purity of protein pharmaceuticals (adapted from Carta and Jungbauer (2010)).

Criteria	Requirement
Specific protein content	>99.9%
Dimer/oligomer content	<1.0%
Ligand leakage	Usually < 1 ppm
Virus content	Absence with a probability of $<10^{-9}$
DNA content	<10 pg/dose
Endotoxin content	5 EU kg^{-1} h^{-1}
Prion content	Absence with a probability of $<10^{-9}$

2.2 From batch to continuous operation: *A paradigm shift*

Recent trends in biomapharmaceutical processing are investigating the possibility of operating the process steps in a continuous fashion, envisioning the development of a fully integrated, continuous bioprocess. Continuous biomanufacturing is currently a promising solution towards

(i) Improved productivity
(ii) Decreased COGs

(iii) Reproducible product quality and

(iv) Decreased process times.

The shift to continuous operation will offer the opportunity to reduce the capital cost through significant decrease in the equipment size and footprint (e.g. small bioreactors and chromatography columns, elimination of hold tanks) (Konstantinov and Cooney, 2015). Continuous bioreactors and purification columns are characterized by high volumetric productivity, cell density and utilization rate respectively that allow for multifold decrease in the equipment size that will result in similar or higher product volumes. Indicatively, Langer (2011) reports that a single 50 L perfusion bioreactor can produce the same amount of product as a 1,000 L bioreactor operating in fed-batch mode. Moreover, reduction in buffer volumes offered by continuous chromatography as well as the decreased start-up/shut-down procedures will allow the development of processes of lower environmental classification. Continuous processing offers also decreased molecule residence time in the reactor as well as elimination of the holdup steps that can risk product quality (Konstantinov and Cooney, 2015).

Process intensification through continuous operation has already, successfully been applied to various industries (Anderson, 2001, Laird, 2007), aiming to decrease the environmental footprint, while increasing process productivity and product quality. The initiatives of Novartis-MIT for continuous crystallization (Quon et al., 2012) and the GSK-Pfizer partnership for the development of continuous processing technology for oral solid dosage (OSD) drugs (Taylor, 2015) demonstrate the industrial importance of this trend in the biopharmaceutical sector. In the market of recombinant proteins, Genzyme and Bayer are leading adapters of perfusion and other continuous manufacturing processes (Langer, 2011), while Novasep, GE Healthcare, Knauer and ChromaCon are some of the equipment manufacturers offering small- and pilot-scale continuous chromatography systems. Warikoo et al. (2012) demonstrate one of the first fully continuous pilot-scale bioprocesses for the production of a mAb and a recombinant human enzyme. They design and use a system composed by a 12 L perfusion bioreactor connected to 4-column Periodic Countercurrent Chromatography and they successfully demonstrate the production and purification of the desired products.

Regulatory directives for Quality by Design (*QbD*) and the rising competition from less-expensive solutions (e.g. biosimilars) are now urging mAb manufacturing towards significant changes in the current state-of-the-art (del Val et al., 2010, Konstantinov and Cooney, 2015). Moreover, recent presentations and reports by the US FDA show that regulatory authorities

have started to embrace the shift from batch to continuous operation in mAb manufacturing, pointing out its potential and needs (Chatterjee, 2012). There are no regulatory announcements inhibiting continuous processing. On the contrary, regulatory bodies such as the FDA and EMA embrace technological advances that can lead to more efficient processes of lower cost. The latter is supported by recent announcements from the FDA (2004, 2015b) where they urge manufacturers to make a step towards innovative pharmaceutical manufacturing. Moreover, the benefits of novel PAT technologies (such as reduction of production cycles and increased automation to minimize human error) are acknowledged and their development is encouraged (FDA 2015). Currently, challenges such as process control, scale-up and contamination avoidance are discussed (Langer and Rader, 2014).

It is true that such a ground-breaking change in the status quo requires thorough consideration and investigation of several factors that affect both process counterparts (USP & DSP). The vision of a fully integrated bioprocess can also be facilitated through gradual development of each process independently, leading to hybrid intermediates (e.g. continuous upstream and batch downstream) (Godawat et al., 2015, Konstantinov and Cooney, 2015). Technological advances are therefore required in both USP & DSP in order to ensure that the "new" bioprocess will bring substantial improvements.

Perfusion systems are already being used to a certain extent for the production of recombinant proteins (Hernandez, 2015) by leading manufacturers such as Genzyme, Eli Lilly, Bayer, Novartis, Merck-Serono and Lonza. However there are still open challenges to be addressed such as the design of media formulations to support high cell densities as well as the stability of the cell line in use (Konstantinov and Cooney, 2015). Stability in the protein (mAb) quality attributes is a crucial parameter that needs to be assessed in order to ensure that the selected cell line will be able to support long term culturing. Barnes et al. (2004) report that in long-term cultures of GS-NS0 cells there is a threshold above which mAb production is limited by saturation of the translational/secretory machinery of the cell. Similarly, Bailey et al. (2012) demonstrate decrease in the productivity of long-term cultured GS-CHO cells, relating the phenomenon to the potentially altered cell metabolism of late generation cells and their different response to environmental conditions. However a more recent publication (Konstantinov and Cooney, 2015) shows constant product quality of a mAb for 30 days cultivation of CHO cells.

USP systems have been extensively studied (Arathoon and Birch, 1986) and their technological evolution is expected to be fast (Konstantinov and Cooney, 2015), however downstream processing is still facing significant challenges. Recent studies identify the latter

as the most costly and limiting factor of the bioprocess. DSP is associated with approximately 80% of the manufacturing costs in bioprocessing (Hunt et al., 2001, Girard et al., 2015) and currently handles limited amount of volumes, thus limiting further improvements in the upstream process (Dünnebier et al., 2001, Chon and Zarbis-Papastoitsis, 2011, Strube et al., 2012, Gronemeyer et al., 2014). As mentioned earlier, there are a few manufactures offering small-scale continuous chromatographic separation processes. However, such kinds of equipment are rather new. Therefore, significant understanding and experience on their dynamics needs to be accumulated prior to their implementation. Issues regarding process performance and capacity utilization need to be addressed as they significantly affect product purity, production costs and yield. Besides this, process robustness is one of the main challenges, as batches out of specifications due to variations need to be avoided (Jungbauer, 1993, Degerman et al., 2009, Ng et al., 2012, Angarita et al., 2013). Moreover, the need of technological advances in continuous viral inactivation and UF/DF as well as PAT is also reported (Konstantinov and Cooney, 2015, De Palma, 2016).

There is therefore eminent need to design of a systematic approach that will minimize investment costs and potential risks. A robust, integrated experimental/computational approach can serve as the tool to obtain the information required for the design of an efficient, continuous bioprocess. However, currently, there are no standardized methods indicating the nature and the amount of the experiments that will provide the essential information needed for the optimization of the system. As a result, the information coming from experiments is often overwhelming and requires costly and time-consuming procedures to be retrieved. To compliment and facilitate experimentation, comes the design of advanced computational tools that provides a solid basis for cost-free simulations, comparisons of different operating scenarios, as well as design of tailor-made experiments, thus minimizing labor cost and time (Royle et al., 2013).

2.3 The Role of Computational Tools

Although regulatory authorities are supportive of this paradigm shift towards continuous manufacturing, the adaptation of novel processing methodologies by the key industrial players is relatively slow. Concerns arising from the uncertain efficiency of new equipment as well as the overwhelming investment costs make the shift from batch to continuous operation a challenging process (Konstantinov and Cooney, 2015). As pointed out by the FDA (Chatterjee, 2012), questions regarding the optimal sample frequency and on-line/in-line data management need to be answered prior to the development and adaptation of novel,

continuous production lines. Moreover, issues regarding the integration of analytical tools, as well as the uniformity in the control approach need to be addressed Ierapetritou et al. (2016).

Table 2.3 Selected list of publications on computational tools used in the assistance of bio- and pharmaceutical process development.

Research Area	Reference
Pharmaceutical process development	Barton and Lee (2002), Farid (2007), Gernaey and Gani (2010), Reklaitis et al. (2010), Boukouvala et al. (2012), Pollock et al. (2012), Lakerveld et al. (2013), Liu et al. (2014a), Zhang et al. (2014a), Lakerveld et al. (2015), Rogers and Ierapetritou (2015), Sahlodin and Barton (2015), Xenopoulos (2015), Ierapetritou et al. (2016), Sebastian Escotet-Espinoza et al. (2016), Singh et al. (2016a), Singh et al. (2016b), Haas et al. (2017), Wang et al. (2017), Wang and Georgakis (2017)
Cell culture systems	Schubert et al. (1994), Ozturk et al. (1997), Farid et al. (2000), Frahm et al. (2003), Sidoli et al. (2004), Kontoravdi et al. (2005b), Teixeira et al. (2005), Jenzsch et al. (2006), Teixeira et al. (2006), Kontoravdi et al. (2007), Teixeira et al. (2007), Gnoth et al. (2008), Lam et al. (2008), Karra et al. (2010), Kontoravdi et al. (2010), Kiparissides et al. (2011c), Sercinoglu et al. (2011), Aehle et al. (2012), Jedrzejewski et al. (2014), Green (2015), Kiparissides et al. (2015), Quiroga et al. (2016)
Chromatographic processes	Dünnebier et al. (2000), Dünnebier and Klatt (2000), Klatt et al. (2000), Dünnebier et al. (2001), Teoh et al. (2001a), Teoh et al. (2001b), Engell and Toumi (2005), Nagrath et al. (2005), Degerman et al. (2006), Kawajiri and Biegler (2006a), Degerman et al. (2007), Farid (2007), Chan et al. (2008a), Grossmann et al. (2010), Krattli et al. (2011), Müller-Späth et al. (2011), Getaz et al. (2012), Westerberg et al. (2012), Bentley and Kawajiri (2013), Bentley et al. (2013), Close et al. (2013), Krättli et al. (2013b), Behrens et al. (2014), Close et al. (2014b), Li et al. (2014), Liu et al. (2014b), Ng et al. (2014), Suvarov et al. (2014), Papathanasiou et al. (2016b), Papathanasiou et al. (2017)

In order to be able to tackle the aforementioned challenges, a thorough investigation and understanding of the system is required. The latter necessitates the execution and comparison of various operating scenarios that will elucidate the process dynamics, as well as the optimal design and/or operating conditions. In this direction, advanced computational tools can prove to be of high importance as they provide low-cost test platforms, where the results can be obtained rapidly (Klatt and Marquardt, 2009, Gernaey et al., 2012, Rogers and Ierapetritou, 2015). The development of tractable mathematical models provides a solid basis to quantitatively study the characteristics of complex and multilevel interactions. Multi-scale mathematical models combined with experimentally-derived characterization will allow an early determination of the process bottlenecks at minimum experimental cost. These models can also be used for testing purposes of different operating scenarios and initial conditions, as well as for the design of advanced optimization strategies and control policies that will lead to optimal and stable operation. Table 2.3 summarizes few of the recent contributions where Process Systems Engineering has played a central role in the simulation/prediction and investigation of various biopharmaceutical systems.

2.3.1 The PAROC Framework & Software Platform

The development and testing of the computational tools discussed above, requires the application of robust procedures that can guarantee the efficiency of the designed optimization and control policies. Moreover, from a computational perspective, the mathematical models describing such processes are usually highly complex and require significant computational force in order to be simulated. In addition, nonlinearities present in the model equations might render the optimization and control studies impossible to perform. Therefore, prior to the execution of the in-silico experimentation, the design of a detailed computational protocol is required that will guarantee seamless development and testing of the respective tools.

In this work we follow the PAROC (PARametric Optimization and Control) framework and software platform (Figure 2.5) for the design and testing of advanced controllers (Pistikopoulos et al., 2015). PAROC is a comprehensive framework that allows the execution and design of advanced optimization and control studies based on high-fidelity, dynamic mathematical models. The framework comprises four distinct steps: (i) high fidelity modeling and analysis, (ii) model approximation, (iii) model based control and ‘closed-loop’ control system validation and (iv), moving horizon estimation techniques that are discussed in detail below. The presented framework has been successfully applied in various case studies for: (a) the control and estimation of the anesthesia process (Nascu et al., 2014), (b) the simultaneous

design and control of a Combined Heat and Power (CHP) system (Diangelakis et al., 2014), (c) the control and estimation of a distillation column (Nascu et al., 2014, Pistikopoulos et al., 2015) and (c) the development of advanced control strategies of chromatographic systems (Papathanasiou et al., 2016a).

2.3.1.1 High-fidelity Modeling and Analysis

As mentioned above, mathematical models play a vital role in the in-silico experimentation. Following the procedure suggested by Kiparissides et al. (2011a), the first step of the framework is dedicated to the formulation and validation of a rigorous, dynamic model, based on first principles. Once the model structure has been finalized, the impact of the parameter uncertainty on the model output is assessed (Global Sensitivity Analysis, GSA) (Appendix A) and the significant parameters are estimated using experimental data (Parameter Estimation, PE). The model predictability is also evaluated and the model is used for both open loop simulations of the examined system, as well as optimization studies. Within PAROC, the actions described here are executed using gPROMS® ModelBuilder (P.S.E, 1997-2016) for the model simulation and the optimization, while the GSA and PE are performed using gPROMS® ModelBuilder in conjunction with MATLAB®, via the gO:MATLAB interface.

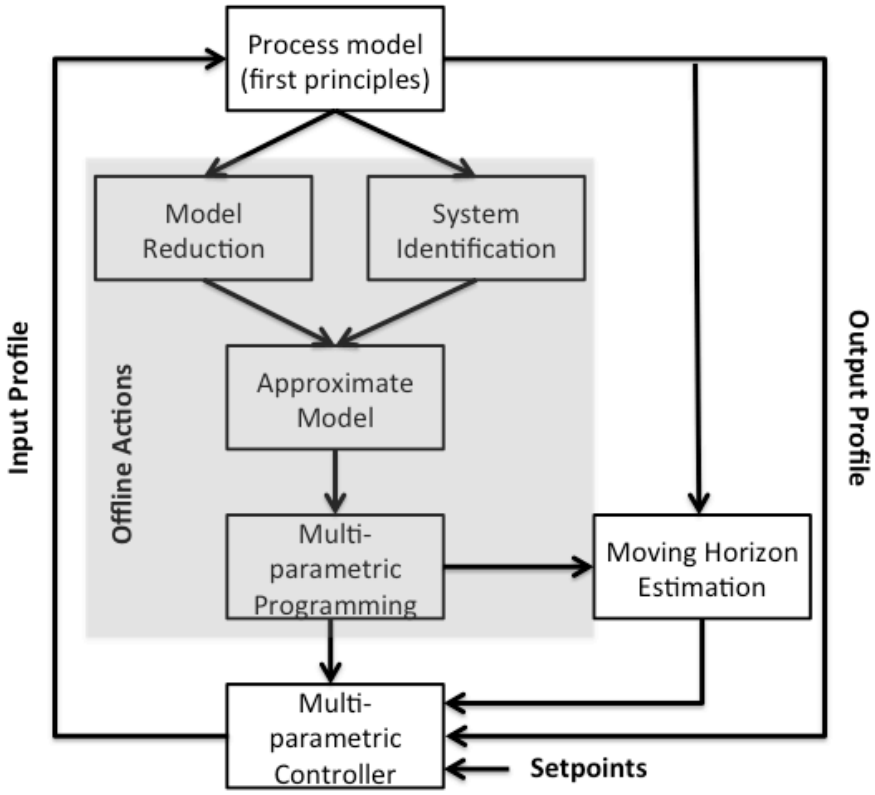

Figure 2.5 The PAROC framework and software platform (adapted from Pistikopoulos et al. (2015)).

2.3.1.2 Model approximation

Usually, the models designed in the previous step contain large sets of Partial and/or Ordinary Differential and Algebraic Equations (PDAE and/or ODE) that involve highly nonlinear terms, thus leading to computationally expensive simulations. Therefore, it is often necessary to simplify the model formulation and replace it with a linear system representation that will allow control studies to be successfully performed (Rivotti et al., 2012, Lambert et al., 2013). PAROC suggests the model approximation to be realized either via (i) system identification or (ii) model reduction techniques. The principal difference of the two methods is that the latter is based on formal techniques that reduce the model complexity, while maintaining the physical interpretation of its entities, while system identification is based on statistical methods that may lead to linear representations without physical meaning. However, both methods aim to design a linear, model (state space) that is suitable for the formulation and solution of the control problem later on. In this work, we perform the model approximation via system identification, using the System Identification Toolbox (*ident*) from MATLAB®.

2.3.1.3 Model-based control and Closed-loop validation

The state space model designed in the previous step is used here for the formulation of the control problem, employing receding horizon policies. PAROC suggests the development of advanced controllers based on multi-parametric programming techniques (Appendix A). Based on the latter, the optimization problem is solved offline thus improving the performance of the controller during the online operation (Pistikopoulos, 2000). The control formulations are solved within MATLAB® using the Parametric OPtimization (POP) toolbox (Oberdieck et al., 2016) designed for the solution of explicit/multi-parametric programming problems. As documented by , the POP toolbox consists of three elements: a problem solver, Oberdieck et al. (2016) problem generator and a problem library. In the problem solver, a variety of algorithms for the solution of multi-parametric programming problems are implemented. For the case of multi-parametric-Linear Programing (mp-LP) and multi-parametric-Quadratic Programing (mp-QP) problems, a geometrical, a combinatorial and a connected-graph algorithm is available, as well as a link to the Multi-Parametric Toolbox (MPT) (Kvasnica et al., 2004). For the case of multi-parametric-Mixed Integer Linear Programing (mp-MILP) and multi-parametric-Mixed Integer Quadratic Programing (mp-MIQP) problems, a decomposition-based algorithm as well as an exhaustive enumeration algorithm is implemented, combined with four different comparison procedures. The problem generator enables the random generation of test problems for the four problem classes, which can be solved. It is important to note that not only the numerical values of the problems are

randomly generated, but also the sparsity of the matrices generated. This aims at avoiding the generation of structurally similar problems. Lastly, the problem library consists of 4 test sets, which have been used to benchmark the solution algorithms within POP. For more information on the POP toolbox and multi-parametric Model Predictive Control (mp-MPC) framework the reader is referred to Oberdieck et al. (2016), Pistikopoulos et al. (2015) and Appendix A. Following the solution of the control problem, the designed controllers are tested in-silico against the process model. This is a 'closed-loop' procedure, where the dynamic model is simulated in tandem with the controller and the performance of the latter is assessed. For the closed-loop validation we use gPROMS® ModelBuilder for the model simulation in tandem with MATLAB®, utilizing the gO:MATLAB interface.

2.3.1.4 Moving Horizon Estimation (MHE)

The framework allows also moving horizon estimation techniques to be applied, where processes are noisy or there is limited amount of feedback information available. In those cases, Kalman filter is commonly applied (Welch and Bishop, 2001), however, the use of constrained estimation techniques such as the moving horizon estimation (MHE) can lead to significant improvements of the estimation result by adding system knowledge (Rao, 2000, Darby and Nikolaou, 2007). MHE is an estimation method that obtains the estimates by solving a constrained optimization problem given a number, or horizon, of past measurements. It has the ability to obtain both the state information and the noise sequence over the horizon (Rawlings and Mayne, 2009). It should be noted that for the purposes of this work MHE techniques are not employed.

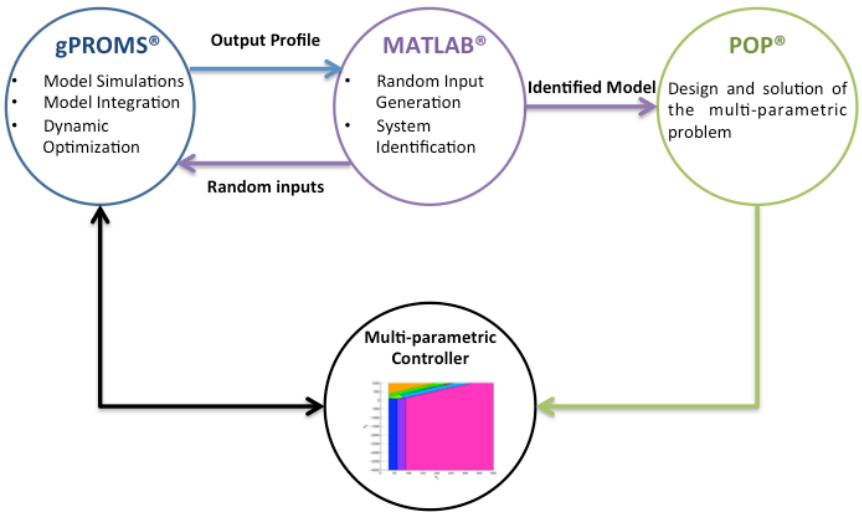

Figure 2.6 Software integration utilized by the PAROC framework and software platform.

Chapter 3.

Chromatographic Separation Processes

1. **The mathematical model of the MCSGP process presented in this chapter has been developed and validated by the Morbidelli Group (ETH Zürich). The model is also presented in Appendix A of Papathanasiou et al. (2016). Advanced control strategies for the multicolumn countercurrent solvent gradient purification process. AIChE J., 62: 2341–2357. doi:10.1002/aic.15203s*

3.1 Introduction

Downstream processing plays a vital role in the production of mAbs. Industrial production of mAbs involves a series of filtration/purification steps aiming to achieve the required purity levels (Chon and Zarbis-Papastoitsis, 2011). In particular, the bioreactor harvest is initially clarified with filtration/centrifugation and is further processed by a sequence of chromatographic steps until the desired quality is reached. Firstly, a capture step is applied where the harvest volume is reduced and the majority of the impurities are removed. Usually, another three chromatographic steps follow that are responsible for viral inactivation/filtration and the formulation of the product in the final concentration (Kelley, 2009a, Chon and Zarbis-Papastoitsis, 2011). The chromatographic steps are usually based on protein A or ion exchange technologies and there are cases, where multiple purification cycles per harvest are required, thus leading to a combination of these methods. The downstream process is finalized with a polishing step, where human pathogenic agents are removed (Gottschalk, 2005, Chon and Zarbis-Papastoitsis, 2011).

Industrial downstream manufacturing utilizes multiple batch unit operations, designed to handle feeds of 2-5 g/L (Gronemeyer et al., 2014). Industrially standardized procedures ensure products of high purity, limiting, however, the amount recovered in the end of the process cycle. Current separation techniques can process average amount of harvests, constraining optimization efforts to increase product volumes in the upstream. However, recent advances in the upstream lead to increased titers (over 5 g/L), challenging the purification process even more. As a result, the production cost has shifted from the upstream to the purification process as novel equipment and processes are required in order to be able to handle the increased product volumes resulting from the upstream (Lim et al., 2007, Schaber et al., 2011). Recent figures indicate that downstream processing is associated with 80% of the total cost of the bioprocess (Hunt et al., 2001, Girard et al., 2015) and currently acts as a limiting factor for the optimization of the upstream.

Improvements in cell culture titers, along with new regulatory directives (such as QbD and PAT) and the emergence of novel therapeutics of lower production costs (e.g. biosimilars) (Cramer and Holstein, 2011) urge the current state-of-the-art in downstream processing towards ground-breaking changes. In this direction several advances have been made both in the materials used, as well as in the operating strategies of purification processes. Several works have demonstrated chromatographic separation processes of increased capacity, achieved by either changes in the purification procedure or the use of novel technologies (e.g.

single use technologies) (Shukla and Gottschalk, 2013). Although the recovery yield is one of the dominant factors that characterize the efficiency of downstream processing, it is not the only criterion. Particularly in the case of mAbs, process efficiency is also evaluated by the purity of the end-product that is coupled with strict regulations (Kurz, 2007). The combined objective of high purity and yield that follow a reverse analogy, gave rise to novel chromatographic separation processes of semi-continuous nature, such as Periodic Counter-Current Chromatography, the Multicolumn Countercurrent Solvent Gradient Purification Process and the Continuous Countercurrent Tangential Chromatography (Zydney, 2016). The shift from batch to semi-continuous and eventually to continuous processing in chromatographic processes offers the opportunity for standardized procedures, common for all biopharmaceutical products and therefore stable product quality. In addition, the continuous nature promises significant reduction in equipment size and consequently in the capital costs (Konstantinov and Cooney, 2015). Last but not least, batch processing is characterized by several hold up steps that risk product quality, while in continuous operation those are minimized and therefore product quality is significantly improved.

Evidently, a shift from batch to continuous operation necessitates the current state-of-the-art to be redesigned both in terms of equipment, as well as operating strategies. Additionally, novel control and monitoring technologies are required in order to ensure that the process will run uninterrupted at optimal levels.

This chapter is organized as follows: Section 3.2 illustrates the basic principles of chromatographic separation processes. Types of mathematical models, as well as the operating modes used are discussed here. Section 3.3 is particularly focused on the description of the Multicolumn Countercurrent Solvent Gradient Purification process, while section 3.4 discusses main challenges and relevant works on the optimization and control of chromatographic systems.

3.2 Chromatography

3.2.1 Basic principles

Downstream processing can be defined as the integration of product isolation and purification in a single process that consists of logical sequenced steps (Jagschies, 2000). The aim is to extract the desired product (usually a protein or a peptide) from a mixture of biological products that resulted from the upstream process. Therefore, process planning is essential in order for the product to meet the quality criteria. A rigorous design of the downstream strategy, optimization of the process parameters and process scale-up from the laboratory to industrial scale is required (Jagschies, 2000). Since the early 1970s chromatography has been widely used for the purification of several therapeutic agents, such serum proteins (Curling, 1980). Chromatographic purification usually constitutes the final step of the downstream purification process and therefore it is highly affected by the earlier steps such as the selection of raw materials and the product isolation. The selection of the appropriate chromatographic process depends mainly on the composition of the mixture subjected to separation.

Chromatography has proved to be a powerful tool when it comes to the isolation of the desired product from a mixture that contains a broad range of compounds (Guiochon, 2012). The separation process utilizes the differences in the equilibrium constants of the components in a diphasic system and elutes each component in separate, distinct time frames (elution bands). In principle, a chromatographic system consists of a mobile and a stationary phase that need to be in relative motion and excellent contact, for the concentrations in the stationary phase to be close to their equilibrium values (Guiochon, 2012). The mixture components equilibrate between the mobile and the stationary phase and as the former percolates through the second, rapid mass transfer takes place, driving the components to the column exit. Table 3.1 summarizes the main chromatographic techniques used and their selection method.

Table 3.1 Chromatographic methods and their separation criteria.

Method	Separation Criterion
Gel filtration	Particle size
Ion exchange	Particle charge
Hydrophobic interaction & reversed phase chromatography	Hydrophobicity
Affinity chromatography	Biospecific interaction

In this work we focus on the development of control strategies of a chromatographic separation process based on ion-exchange (IEX) technologies. In bioprocessing, IEX chromatography is performed for the removal of both process and product related impurities. While IEX chromatography can also be applied in capture steps (Miesegaes et al., 2012) it is mainly used for polishing applications (Carta and Jungbauer, 2010). With the pH being in between the pI of the antibody and the pI of most HCPs, a good removal of HCPs can be achieved. Additionally, aggregates can also be removed. In particular:

- Cation-exchange polishing is often performed in bind-elute mode, aiming at the removal of HCP, DNA as well as aggregates and fragments (Carta and Jungbauer, 2010, Zhang et al., 2014b, Khalaf et al., 2016).
- Anion-exchange polishing is performed in flow-through mode, with impurities such as DNA and HCP adsorbing on the resin, while the target protein is collected in the flow-through (Carta and Jungbauer, 2010, Voitl et al., 2010).

In IEX, the columns are packed with ion-exchanger particles that contain charged ion-exchange groups that are attached to a solid matrix with covalent bonds. The exchangers can be either cation or anion exchangers (Jandera and Lembke, 2000). The isolation and concentration of the desired component is realized through the selective adsorption of the sample on the chromatographic medium (Jagschies, 2000). As a general rule, the efficiency of chromatographic separation processes is assessed by the final product recovery and purity. However, yield and purity follow a reverse analogy and therefore there is an inherent trade-off during the optimization of the process. Thus, the optimal point should be identified, where

the process is characterized by maximum product recovery, while meeting the purity constraints.

$$Product\ Recovery = \frac{Amount\ of\ product\ in\ the\ outlet\ product\ stream}{Amount\ of\ product\ in\ the\ feed\ stream}$$

$$Product\ Purity = \frac{Amount\ of\ product\ in\ the\ outlet\ product\ stream}{Total\ amount\ of\ the\ productstream}$$

3.2.2 Types of chromatography & Mathematical modeling

In the attempt to understand the dynamics of chromatography Guiochon (2012) distinguishes chromatographic processes based on the following criteria:

(i) The equilibrium isotherm: The process can be characterized either as *linear* on *nonlinear* based on the profile of the isotherm. Usually, in analytical applications the volume of the samples is small or they are highly diluted and therefore any curvature on the isotherm can be ignored, thus classifying the process as linear. However, in the case of concentrated solutions (or preparative chromatography) the effect of the aforementioned curvature can no longer be neglected (nonlinear chromatography).

(ii) Influence of axial dispersion & resistance mass transfer on band profiles: Neglecting these phenomena, leads to an *ideal* chromatography model, where infinite column efficiency is assumed. Alternatively, considering the dispersion in the direction of the concentration gradient as well as the fact that equilibration between the mobile and the stationary phases is not instantaneous, results into *nonideal* chromatographic models.

The classification described above results into four distinct theories that are illustrated in Table 3.2. With respect to mathematical modeling, all the combinations provide relatively simple solutions with the exception of nonideal, nonlinear chromatography, where only numerical solutions are possible (Guiochon, 2012).

Table 3.2 Chromatographic theories and their main assumptions.

	Linear	**Nonlinear**
Ideal	Component pulses move independently from one another, without changes in their profiles.	Influence of nonlinear phase equilibrium thermodynamics is considered. Individual elution profiles cannot be obtained independently. Final outcome depends on the amount of components present in the mixture.
Nonideal	Influence of kinetic phenomena on band profiles is considered. Pulses move independently at constant velocity.	Column efficiency and nonlinear behavior both taken into consideration.

Aiming to describe and understand the phenomena taking place during chromatographic separations, several types of models have been developed. The models are classified into two main theory categories: (i) The Theory of Linear Chromatography and (ii) The Theory of Nonlinear Chromatography. Based on the above, models that fall in the first category, neglect any curvature in the isotherm, while the others consider phase equilibrium thermodynamics. Table 3.3 summarizes the main model types for the two categories.

Apart from plate and statistical models that are found in linear chromatography, the majority of chromatographic models is based on the general mass balances for the different components along the column (Guiochon et al., 1994, Guiochon, 2012, Nicoud, 2015), combined with mass-transfer expressions (Gritti and Guiochon, 2012a) and an appropriate adsorption isotherm (Guiochon et al., 1994). Regarding the mass transport from the liquid bulk to the adsorption site, various expressions, which are based on different assumptions, can be found in the literature. These concepts are, in order of increasing complexity, instantaneous equilibrium (Varma and Morbidelli, 1997), lumped mass-transfer coefficient (Carta and Jungbauer, 2010), external film diffusion (Gritti and Guiochon, 2012b) and discretization along the pore length (Guiochon et al., 1994), which can also be combined with discretized pore models (de Neuville et al., 2013). Therefore the choice of the right model equation set and its associated assumptions depends highly on the examined system, its dynamics as well as the purpose that the process model is called to meet.

Table 3.3 Mathematical models in chromatography and their key assumptions (adapted from Guiochon (2012)).

Model		Key Assumptions
Plate Models	Craig Model	Batch operation
(Empirical)	Martin-Synge Model	Continuous operation
Statistical Models		Various individual contributions in the mechanism of band broadening and column efficiency are related. Gaussian band profiles
Equilibrium-Dispersive Model		Infinite fast mass transfer across the column with finite extent of axial dispersion
Lumped Kinetic Model		Relates the variation of the local concentration of solute in the stationary phase and the extent of the local deviation from equilibrium through a kinetic equation
The General Rate Model		Accounts for all possible contributions in the system with respect to mass transfer kinetics
Ideal Model of Chromatography		Considers infinite column efficiency
Moderate Column Overload		Band profiles depend on the initial curvature of the isotherm

3.2.3 Continuous chromatography

Chromatography is an expensive separation technique and thus it is preferred when other methods are not adequate for the separation of high-value molecules. Particularly the market of high-value biologics (e.g. peptides, proteins and antibodies) uses solvent gradient batch chromatography for the separation and purification of the targeted product (Aumann and Morbidelli, 2007). The advantages of continuous processes, such as higher purity, less solvent

consumption and increased productivity, make continuous, countercurrent separation processes more attractive compared to batch. One of the most popular continuous chromatographic processes is the Simulating Moving Bed (SMB).

Since its emergence in 1960's SMB has gained attention and has been applied in numerous industries (e.g. sugars, petrochemicals, pharmaceuticals). SMB is a multi-column process, where the columns are connected to each other creating a circulation loop (Kawajiri and Biegler, 2006b). This technique is suitable for the separation of two-fraction mixtures and it is highly attractive as it reaches high purity only with partial separation of the two fractions. However, in cases where the mixture needs to be separated in three fractions with the desired component to be the intermediate (weak impurities, targeted product and strong impurities), the SMB process, which separates the mixture in only two fractions, is no longer sufficient. A feasible solution would be the consecutive use of two SMBs, however this would increase the cost of the process significantly. In this direction Aumann and Morbidelli (2005) designed and patented the MCSGP process, for the continuous separation of multicomponent mixtures with three (or more) components. The basic principles and the operation of MCSGP are described in Section 3.3.

3.3 The Multicolumn Countercurrent Solvent Gradient Purification Process (MCSGP)

MCSGP is a continuous, multicolumn separation process used for the purification of various biomolecules. The process is based on the principles of SMB, utilizing at the same time the benefits of gradient chromatography. The initial design was for a three-fraction separation process with linear solvent gradients. The gradients can also be step, piecewise linear or nonlinear (Aumann and Morbidelli, 2007). The principle of MCSGP was first presented by Ströhlein et al. (2006a), while in 2007, Aumann & Morbidelli described the operation of the six-column process and presented the determination procedure of its parameters patented in 2006 (EP 05405327.7). The process was then reduced to a three-column, semi-continuous system (Aumann and Morbidelli, 2008). The latter was expanded to a setup consisting of four columns, where the fourth column can be used either for loading (Müller-Späth et al., 2010a) or for different types of cleaning in place (CIP) (Müller-Späth et al., 2009). The latest development is the twin-column setup (Krättli et al., 2013b, Müller-Späth et al., 2013). The MCSGP process has been successfully applied for the separation of several mixtures.

Table 3.4 Main applications of the MCSGP process.

Application	Reference
6-column system for the purification of industrial stream containing 46% Calcitonin	Aumann and Morbidelli (2007)
Peptide Purification using the Multicolumn Countercurrent Solvent Gradient Purification (MCSGP) Process (ChromaCon, ETH, Novartis)	Aumann et al. (2009)
3-column system for the separation of three mAb charge variants	Müller-Späth et al. (2008)
MCSGP as capture step for mAb purification from clarified cell culture supernatant	Müller-Späth et al. (2010a)
3-column system used for the purification of three commercially available mAbs (Bevacizumab, Trastuzumab, and Cetuximab)	Müller-Späth et al. (2010b)
Purification of a synthetic peptide using multi-column chromatography (Contichrom® & MCSGP) (ChromaCon, Bristol-Myers Squibb, KAI Pharmaceuticals)	Ströhlein et al. (2012)
Purifying Common Light-Chain Bispecific Antibodies: A Twin-Column, Countercurrent Chromatography Platform Process (ChromaCon & Merus)	Müller-Späth et al. (2013)
Multifraction separation MCSGP (from three to four fractions)	Krättli et al. (2013a)

Currently, purification equipment based on MCSGP is commercially available by ChromaCon AG and LEWA Bioprocess Technology Group and has been used by several manufacturers (e.g. Bristol-Myers Squibb, Clariant, Merck Serono, Novartis) in case studies presented in Table 3.4. The work presented in this thesis is based on a case study separation performed using the ContiChrom HPLC unit used for the separation of a monoclonal antibody from product-related impurities (ChromaCon, 2017).

3.3.1 The twin-column MCSGP process for ternary mixture separations

Let us consider here a general case where a ternary mixture is fed in a batch mode to the setup and the separation is achieved by the application of a modifier gradient. From thereafter, the terminology suggested by Ströhlein et al. (2006a) is adapted, according to which impurities characterized by weak adsorptivity are lumped into one fraction called weak impurities (W), the product (P) that corresponds to the targeted compound and the strongly adsorbing impurities are lumped under the term strong impurities (S). Elution of the different components is performed by a linear modifier gradient, which decreases the adsorptivity of

the different components. Figure 3.1 illustrates a simplified chromatogram for such a separation, where five stages can be identified:

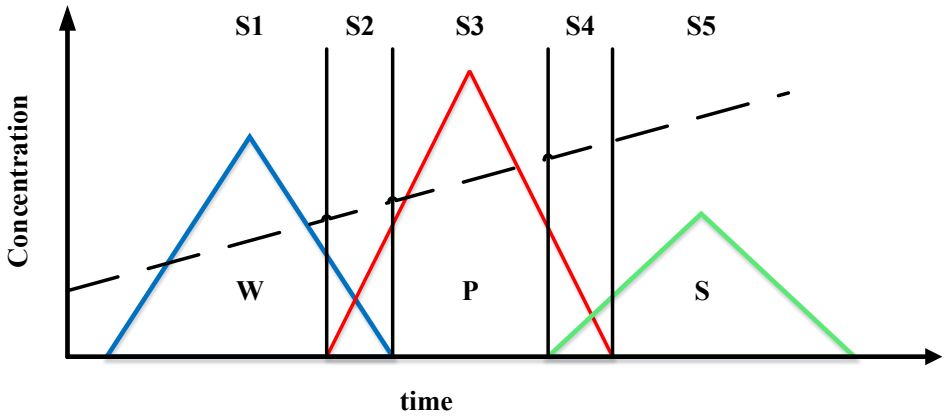

Figure 3.1 Elution profile in gradient chromatography.

(i) S1: The column elutes weak impurities (W).
(ii) S2: A mixture of weak impurities and product (P) is eluted.
(iii) S3: The targeted product exits the column.
(iv) S4: A mixture of strong impurities (S) and product (P) is eluted.
(v) S5: Strong impurities are removed from the column.

The dotted line illustrated in Figure 3.1, represents the gradient applied to the modifier throughout one process cycle. The efficiency of the process is evaluated based on the final purity and recovery yield of the targeted product. However, the latter is eluted at S3 and can be found in mixtures with W and S, during S3 and S4 respectively. Therefore, it is necessary to find the optimal operating procedure that will prolong the elution window of the targeted product (S3), maintaining high product purity (minimizing the amount of impure fractions). On that end, the internal recycle of the impure mixture fractions in the MCSGP process, increases the increases the recovery yield and guarantees high product purity.

The twin-column MCSGP setup comprises two identical chromatographic columns based on IEX principles (Krättli et al., 2013b). During the process cycle, the columns alternate between batch and interconnected mode, with the latter facilitating the internal recycle of the impure stream fractions. In particular, during the first interconnected (continuous) phase (I1), column 2 starts empty and equilibrated (Figure 3.2). Simultaneously, the outlet flow of column 1 enters column 2 mixed with an additional fraction of adsorbing eluent (E). After the completion of I1, the two columns start operating in batch mode (B1 phase), where the feed (F) is introduced to column 2 and the product is eluted from column 1. In I2 phase the recycling stream containing the impure fraction of product and strong impurities exits column

1 and enters column 2. By the end of I2 phase, column 2 starts eluting pure W (B2 phase). B2 phase finishes when the overlapping region of W and P reach the end of column 2. At this point the first switch (Switch 1) has been completed and the two columns swap positions. Therefore, column 1 will go through the recycling and feeding tasks as described above, while column 2 will continue with the gradient elution (Krättli et al., 2013b).

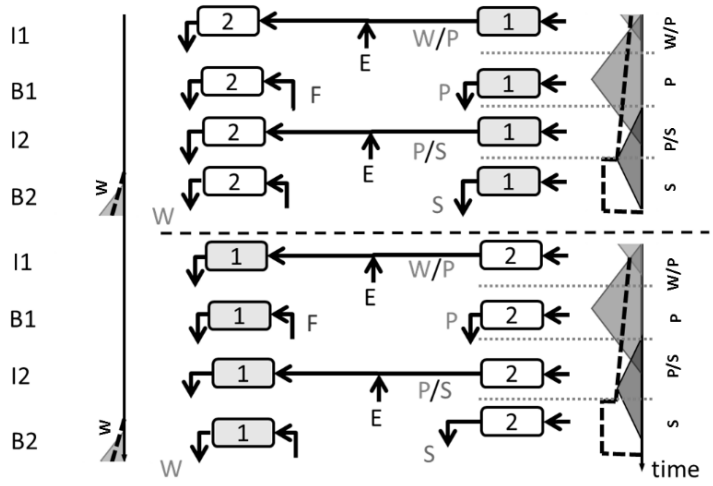

Figure 3.2 The twin-column MCSGP setup (Krättli et al., 2013b, Papathanasiou et al., 2016a).

3.3.2 Mathematical modeling of the MCSGP process

Here we focus on the twin column system, used for the separation and purification of an antibody from a cell culture mixture. Based on IEX technology, the MCSGP process is described by a PDAE model that was firstly presented by Müller-Späth et al. (2008). The model is based on lumped kinetics and considers:

(i) Weak adsorbing mAb variant: antibody fragments. The latter can be of various types (AbsoluteAntibody, 2017), however for the purposes of this work they are lumped thereafter under the term *weak impurities (W).*

(ii) Product variant: mAb (P)

(iii) Strong adsorbing impurities: antibody aggregates. Aggregates can be dimers or of higher order. In general, dimers have, due to their structure, a similar adsorption behavior to the target protein, and represent therefore the most challenging strong adsorbing impurity (Cordoba-Rodriguez, 2008, Paul and Hesse, 2013). For the purposes of this work aggregates are lumped and considered as a single impurity under the term *strong impurities* (S). For the controller development a correlation between input and output variables is required, however without absolute values as explained in Section 3.3.2.1.

Appendix B presents the process model that describes the events taking place during separation. The model uses the differential mass balances for the calculation of the component concentrations as suggested by (Guiochon et al., 1994, Guiochon, 2002) and uses equations commonly encountered in liquid chromatography (Appendix B). Usually, the mass balance equation of chromatography is characterized by a series of assumptions that accompany the majority of such models and as reported by Guiochon et al. (1994) they do not limit significantly the range of validity of the derived mass balance equation set.

(i) The column is assumed to be radially homogeneous. There are studies discussing the influence of column heterogeneity on the elution profiles (Miyabe and Guiochon, 1999), however radial homogeneity is encountered in most of the developed models and is a good approximation for well-packed columns, as they are used in industry.

(ii) In preparative chromatography, the compressibility of the mobile phase is almost always neglected. That characterizes the majority of mathematical models in preparative chromatography, for aqueous solutions at pressures between 1-5 bar, this is a good approximation.

(iii) As shown by Martin et al. (1973), the diffusion coefficients in liquids do not depend highly on pressure, thus the axial dispersion coefficient is considered to remain constant.

(iv) In liquid chromatography, the differences between the partial molar volumes in the two phases do not exceed a few percentage (Riedo, 1982, Kováts, 1985), therefore they are considered to be the same.

(v) In liquid chromatography it usually assumed that the solvent or the weak solvent (in the case of a mixed mobile phase) is not adsorbed (Kováts, 1985) one could exclude its mass balance from the equation set.

(vi) Thermal effects are neglected. In order for all the physico-chemical parameters to remain constant, the column is assumed to operate under constant conditions (i.e. temperature, pressure, mobile phase flow rate). While for reversed-phase systems, the performance depends highly on the temperature; this is not the case for IEX chromatography.

The mathematical model used to describe the events taking place during the purification of the mAb using the MCSGP process has been previously developed and validated by the Morbidelli Group (ETH Zürich) (Ströhlein et al., 2006a, Ströhlein et al., 2006b, Melter et al., 2007, Melter et al., 2008). The model equations are described in detail in Appendix B, while here an overview of the process model structure is given. The model comprises two main parts: (a) the equation set describing the mass balances for the mixture components & the

isotherms and (b) the mass balances around the columns. The latter is variable, depending on the system configuration (Figure 3.2) and is explained below (sections 3.3.2.3 and 3.3.2.4).

3.3.2.1 Chromatography mass balance and isotherms

The model used in this work, is the linear driving force model with a lumped mass-transfer coefficient, which can also be expressed as a function of the adsorbed amount (Ng et al., 2014, Steinebach et al., 2016a). The model uses a competitive bi-Langmuir isotherm to describe the adsorption behavior of proteins (Guiochon, 2002, Ströhlein et al., 2006a). Generally, in ion-exchange chromatography (Kopaciewicz et al., 1983), the most commonly used concepts are: (a) the multi-component Langmuir isotherm (Carta and Jungbauer, 2010), (b) the steric mass-action law (Brooks and Cramer, 1992) and (c) colloidal models (Guélat et al., 2013). A third consideration in biomolecule separation is the idea of lumping several components into one pseudo-component (Forrer et al., 2008, Pfister et al., 2016), which allows faster simulations while still capturing the main trends. In the model used in this work, a relatively simple structure is adopted, which however contains all relevant mass-transport and adsorption effects and their impact on the process performance.

There is a variety of models that can be found in the open literature based on the separation type and operating mode. Those may consider a series of different assumptions (e.g. axial dispersion, mass transfer limitation), initial/boundary conditions and/or level of detail (e.g. modeling at the pore level). In that context and based on the separation dynamics, the model developer can consider: (a) different expressions for the isotherms (Gerontas et al., 2013, Close et al., 2014a, Ng et al., 2014, Kumar et al., 2015), (b) monitoring the concentration at the pore level (Küpper et al., 2009, Steinebach et al., 2016b), (c) modeling the distribution of analytes based on the ion charge (in ion exchange chromatography) (Drgan et al., 2009) or (d) follow a more macro-scale approach such as the one presented by Wang et al. (2002), in cases where the model does not require a great level of detail. There are also other approaches such as the one presented by Guzlek et al. (2010), where the chromatographic system is resembled to and modeled as a series of continuous-stirred reactors. The aforementioned cases, along with many more contributions in the open literature, present the development of mathematical models that adequately describe the systems of interest. Their principal differences usually lay on the level of detail they monitor, as well as the assumptions upon which the equation sets are built. Both those elements however are product of the purpose of use of the developed model. In principal, chromatographic models should be designed based on the system dynamics, considering however the purpose of their end-use. Models that are characterized by high level of mathematical complexity and detail can prove to be valuable when it comes to

studies on the interactions taking place within the chromatographic system. Nevertheless, such rigorous models tend to involve a large number of parameters that require significant amount of experiments in order to be determined. In addition, such models may be used for further computational studies (such as optimization and control) can potentially require high computational effort. As a result the trade-off between model rigor and computational demand needs to be assessed based on the purpose for which the mathematical model is developed (Dünnebier et al., 1998).

Particularly in cases where the purpose of the study is the development of control schemes and estimation techniques (Dünnebier et al., 2001, Engell and Toumi, 2005, Degerman et al., 2007, Küpper et al., 2009, Behrens et al., 2014, Holmqvist and Magnusson, 2016) the mathematical model is expected to provide accurate information on the input-output interaction. Usually, models of moderate complexity are preferred as they are able to describe the process dynamics without excessive computational requirements (Dünnebier et al., 1998). Furthermore, in the case of model-based control studies, the process models are often simplified in order to meet the specifications required for the control problem formulation as discussed in Chapter 2. Such procedures can be realized through linear state space modeling techniques and/or complete discretization followed by linearization, leading subsequently to simplified systems that look into the input/output interactions. In this direction, the model presented in Appendix B, which has been previously presented and validated in several works (Ströhlein et al., 2006a, Aumann and Morbidelli, 2007, Aumann et al., 2007, Stroehlein et al., 2007, Aumann and Morbidelli, 2008, Müller-Späth et al., 2008, Aumann et al., 2009, Grossmann et al., 2010, Müller-Späth et al., 2010a, Aumann et al., 2011, Muller-Spath et al., 2011), is considered to adequately describe the effects taking place in the chromatographic system that are of interest for the development of the control schemes presented here (Chapter 4 and Chapter 5).

3.3.2.2 Mass balances around the columns

The model discussed above and presented in Appendix B describes the separation dynamics within the columns and does not depend on the system configuration that is the connection of different columns in a multi-column process (interconnected/batch, Figure 3.2). However, based on the system configuration, the mass balances around the columns may differ within the process cycle. Subsequently, the design equations of the system for the two operating modes are as follows:

3.3.2.3 Batch mode

During batch operation (Figure 3.3a) the stream entering the column is not mixed with any other stream. Therefore we simply assume that anything that enters the column, exits at constant flow rate (Equation 3.1) for both columns.

$$c_{i,in} \cdot Q_{i,in} = c_{i,out} \cdot Q_{i,out}$$

Equation 3.1 Column mass balance during batch operation

Where $c_{i,in}$ *(mg/mL)* and $c_{i,out}$ *(mg/mL)* represent the inlet and outlet concentrations of component i, while $Q_{i,in}$ *(mL/min)* and $Q_{i,out}$ *(mL/min)* represent the inlet and outlet flow rate respectively.

3.3.2.4 Interconnected (continuous) mode

In the continuous mode the two columns operate under a different strategy. The column on the right side (Figure 3.1) is not affected by the operation of the column on the left and therefore its mass balance remains the same as in batch (Equation 3.1). On the other hand, the elution volumes from the column in the right position are mixed with additional fractions of modifier (Figure 3.3b) and enter the column on the left. Therefore the mass balance for the latter is described by Equation 3.2 and Equation 3.3.

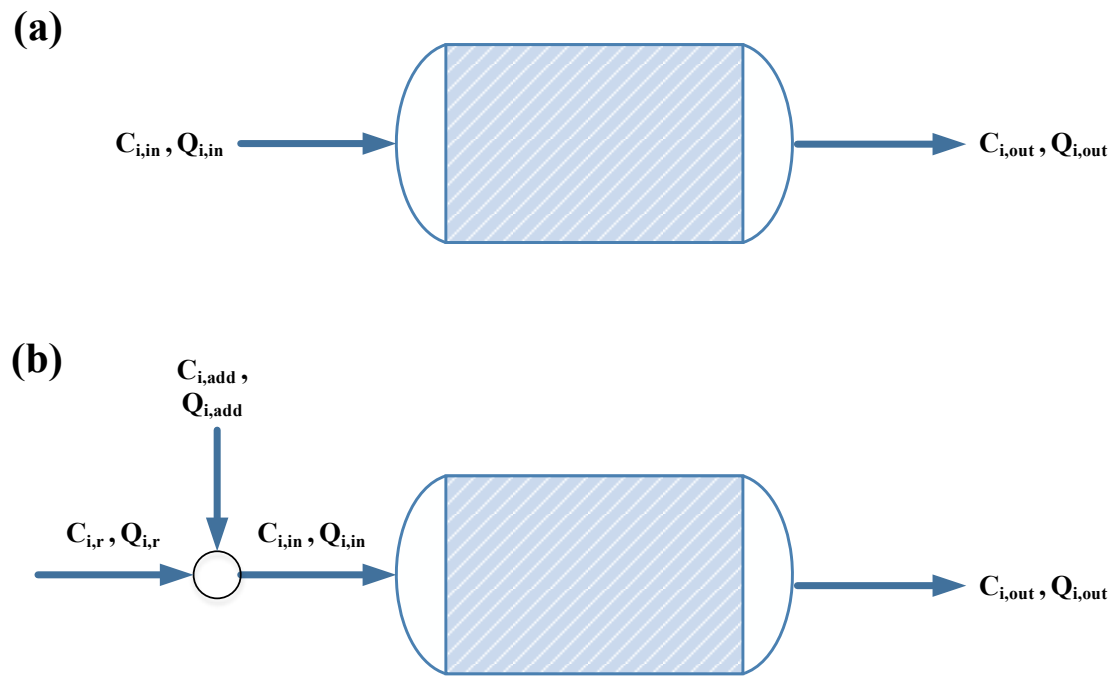

Figure 3.3 Column configuration under: (a) batch and (b) interconnected operation.

$$c_{i,in} = \frac{c_{i,add} \cdot Q_{i,add} + c_{i,r} \cdot Q_{i,r}}{Q_{i,in}}$$

Equation 3.2 Mass balance around the column receiving the internal recycle stream during interconnected operation.

$$Q_{i,in} = Q_{i,out} = Q_{i,add} + Q_{i,r}$$

Equation 3.3 Inlet flow rate of the column receiving the internal recycle stream during interconnected operation.

Where $c_{i,add}$ *(mg/mL)* and $c_{i,r}$ *(mg/mL)* represent the additional and the internally recycled concentrations of component i, while $Q_{i,add}$ *(mL/min)* and $Q_{i,r}$ *(mL/min)* represent the flow rates of the additional and the internally recycled stream respectively. $Q_{i,in}$ *(mL/min)* and $Q_{i,out}$ *(mL/min)* represent the inlet and outlet flow rate respectively

3.4 Optimization and Control of Chromatographic Systems

3.4.1 Optimization under Cyclic Steady State (CSS)

Similarly to Pressure Swing Adsorption (PSA) systems, chromatographic systems belong to the family of periodic systems that constitutes a challenging type of models to optimize and control. Their periodic nature and the PDAE model that describes them challenge the development of advanced optimization and control studies on such systems. Due to their periodic nature, cyclic processes require significant computational effort in order to be simulated and optimized. For this reason there have been many studies reported in the literature aiming to accelerate the acquisition of cyclic steady state (CSS). This issue has been mostly studied for PSA systems, the dynamics of which resemble continuous, multi-column chromatographic processes. Two main approaches are presented below:

3.4.1.1 Direct dynamic simulation

Unger et al. (1997) proposed a direct dynamic simulation approach. According to this method, the numerical procedures aim to obtain the CSS directly, without solving the entire PDAE model. This is realized by posing a point boundary condition (Equation 3.4) that requires the initial and the final state of the system within a cycle to be the same.

$$\left\| \boldsymbol{x(t_{cycletime})_k} - \boldsymbol{x(t_0)_k} \right\| \leq \boldsymbol{ess_k}$$

Equation 3.4 Boundary condition posed to enforce CSS in periodic systems.

Here, k is the iteration counter, $x(t_0)_k$ represents the initial state of the system, $x(t_{cycletime})_k$ is the state of the system after a cycle and ess_k shows the development of $\left\| x(t_{cycletime})_k - x(t_0)_k \right\|$ of cycles computed. Consequently, if a very small ess_k is chosen

then a very large number of cycles has to be computed in order for Equation 3.4 to be satisfied (Unger et al., 1997). Direct dynamic simulation is a robust and relatively simple approach, since there is only need for the solution of a system of differential equations (Unger et al., 1997, Dünnebier et al., 2000). On the other hand, only stable cycles can be found and the convergence is determined by the properties of the system at hand.

3.4.1.2 Global discretization

Another approach to calculate CSS has been presented by Nilchan and Pantelides (1998). This global discretization method, suggests the discretization of model equations both in space and time. The resulting system will be a large nonlinear algebraic system and can be solved by an Nonlinear Programming (NLP) solver. Equation 3.4 is included in the general model formulation aiming to enforce CSS. The challenge of this method, apart from the spatial initial guess, is that it requires an initial guess for the temporal profiles of the variables that needs to be obtained from the results of dynamic simulations, close to the CSS.

Table 3.5 Direct dynamic simulation and full discretization approach used in literature for the achievement of CSS.

Approach	Reference
Maximization of feed velocity in SMB (s.t purity and recovery constraints). Comparison of simultaneous, single-discretization approach (Jiang et al., 2003) and the global discretization method (Nilchan and Pantelides, 1998). Full discretization does not increase the optimal throughput	Kawajiri and Biegler (2006b)
Nonlinear adsorption profile of SMB renders the application of full-discretization approaches difficult. Very fine grid required thus making the problem stiff.	Dünnebier et al. (2000)
Maximizing product recovery under purity constraint in SMB, using **Equation 3.4** for the CSS.	Klatt et al. (2000)
Traditional dynamic optimization approach for product recovery optimization in a two-bed PSA system, using **Equation 3.4** for the CSS.	Khajuria and Pistikopoulos (2013)
Modeling & optimization of reversed-phase purification system using indirect optimization method, aiming to maximize productivity under purity constraints.	Degerman et al. (2007)

Another important issue is the specification of the grid in the time domain, which for stiff differential equations results in extremely large systems, due to very fine discretization. Depending on the dynamics and special characteristics of the system, the appropriate optimization method needs to be chosen in order to obtain the optimal operation profile without requiring extensive computational force. Table 3.5 illustrates some of the contributions using the above-described methods for the optimization of cyclic processes.

3.4.2 Control of chromatographic systems

The definition of the objective function and the operating constraints is of key importance for optimization and/or control studies of any system. Chromatographic systems fall in the class of multi-objective optimization, where we are interested in maximizing both product purity and yield. Other objectives might be the minimization of production cost and/or production time (Table 3.6). A detailed review of the relevant literature can be found in Engell and Toumi (2005). Besides the objective function, another key aspect in the control studies of chromatographic processes is the selection of the control variables. The quality and quantity of the final product can be affected by various parameters, however the following aspects paly the most vital role in gradient chromatography:

(i) The initial and final concentrations of the eluent that facilitates the separation of the mixture components (modifier): The modifier gradient is responsible for the quantity of the eluting fractions.
(ii) The feed flow rate: The choice of the feed flow rate and therefore the flow rate within the column determines the speed that the components travel in the column and therefore the speed of the elution.
(iii) Switching times: In multi-column processes, the time that the mixture spends in each configuration can significantly affect the quality of the targeted product.

In addition to the above, the operational system constraints need to be satisfied at all times. Usually they consider: the maximum flow rate that can be applied to the system and minimum thresholds for the purity and recovery of the final product. Constraints for temperature and pressure could also be included but their effects are neglected in liquid chromatography (Guiochon et al., 1994). Their periodic nature and the complex mathematical models that describe those systems render the control of chromatographic processes a challenging task.

Table 3.7 summarizes some of the contributions focusing on the control of chromatographic separation processes, using different techniques in order to ensure the design of robust control strategies. Significant developments are required in order to facilitate full automation of current chromatographic processes. To the extent of the author's knowledge, currently there are no standardized procedures for the control of chromatographic columns and their operation significantly resides on statistical tools and experimentally validated processes.

Manufacturers offer various solutions that allow frequent sampling and feedback measurements. For example, UV/VIS detectors are commonly used in chromatography and offer on-line measurements (within seconds) on the elution profiles of the mixture components based on UV-adsorption. However, such systems measure at a single wavelength, which does not allow direct correlation to product purity. Therefore, complementary information is required that will more accurately determine the composition of the monitored stream. The latter is achieved by at-line HPLC units that can be coupled with automated sampling devices, to provide the required information. Such measurements can be achieved within reasonable time limits and within the process cycle time (Grossmann, 2009). Moreover, a variety of offline tests (such as chromatography and immunoassays) are available and ensure that the final product specifications are met (for more information the reader is referred to Chapter 2). Significant advancements have been made towards the automation and simplification of the operation that have lead to the availability of various software tools, such as UNICORN (GE Healthcare), BioSC® (Novasep), PurityChrom Bio (Knauer) and ChromIQ (ChromaCon AG) that allow process monitoring and results analysis.

Table 3.6 Optimization objectives often used for chromatographic processes (an indicative list of contributions).

Objective function	Reference
Maximization of the production rate.	Natarajan et al. (2000), Gallant (1996), Felinger and Guiochon (1992), Golshan and Guiochon (1990)
Increase of yield (within a particular range).	Jandera et al. (1998)
Maximization of the production rate times yield.	Felinger and Guiochon (1996)
Minimization of the production cost.	Gallant et al. (1996)
Maximization of process efficiency.	Golshan-Shirazi and Guiochon (1991)
Maximization of the specific production rate.	Felinger and Guiochon (1993)
Dynamic optimization for the maximization of the amount of purified product, subject to purity and yield constraints.	Teoh et al. (2001b)
Comparison of different objective functions (cost minimization, recovery yield maximization and annual net profit maximization).	Chan et al. (2008b)
Investigation of trade-off of throughput maximization and desorbent minimization.	Kawajiri and Biegler (2008) & Dünnebier et al. (2000)
Comparison of 3 different objective functions (purity, yield, purity & yield.)	Degerman et al. (2006)

Table 3.7 Control of chromatographic processes (an indicative list).

Control Application	Reference
Open-loop control for the simultaneous maximization of recovery yield and production rate in batch chromatography.	Holmqvist and Magnusson (2016)
Model predictive control for the maintenance of product purity in the presence of disturbances.	Toumi and Engell (2004)
Iterative setpoint optimizing control on the MCSGP process for ternary separation.	Behrens et al. (2014)
Process control concept for batch-chromatography.	Dünnebier et al. (2001)
Cycle-to-cycle' control of SMB processes.	Grossmann et al. (2008)
Model Predictive Control of the MCSGP process.	Grossmann et al. (2010)
Online control of the twin-column MCSGP process.	Krättli et al. (2013b)
Closed-loop control of the MCSGP process.	Krättli et al. (2011)

Given the strict purity constraints and the complexity coupled with such systems, it is essential to ensure that the control strategies designed will be able to handle the system variations/disturbances, ensuring optimal operation and CSS. To that end, model-based control offers the advantage of transferring the knowledge from the process model to the controller, thus ensuring optimal operation. Additionally, particularly in the case of Model Predictive Control (MPC) the future state of the system can be predicted and therefore the appropriate control actions can be calculated. The aim of MPC is to provide a sequence of control actions over a future horizon that will optimize the controller performance based on predictions of the system states (Pistikopoulos, 2009). In particular, explicit/multi-parametric MPC combines the advantages of MPC with the ability to solve the optimization problem offline. In this fashion, the control inputs are derived as a set of explicit functions of the system states (Bemporad et al., 2002). An important advantage of multi-parametric Model Predictive Control (mp-MPC) is that the computed control laws can be easily tested and implemented on embedded devices (Dua et al., 2008). The optimal control laws are retrievable immediately through simple function evaluations, enabling fast response without the computational requirements of a computer in the background. In addition, it provides a deeper understanding of the process behavior based on the critical regions, how many and

which constraints are active. Moreover, for small, industrial scale systems, such as the MCSGP process, there is need for micro-devices that will be embedded on the setup ('MPC on a chip') (Pistikopoulos, 2012). More details for the theory behind mp-MPC can be found in Appendix A.

In this work we focus on the development of advanced, intelligent controllers for: (i) chromatographic separation processes based on the principles of MCSGP and (ii) a cell culture system, using the mp-MPC technology. The following two chapters are dedicated to the work that has been performed for a single-chromatographic column (Chapter 4) and a multi-column system (Chapter 5). Finally, the development of advanced optimization and control strategies for a cell culture system is presented (Chapter 6).

Chapter 4.

Model-based Control of Single-Column Chromatographic Systems

*Parts of this work have been performed in the framework of the OPTICO European Project (G.A. No.280813).

**The results presented in this chapter have been included in the following publications:

2. *Papathanasiou et al. (2016). Advanced control strategies for the multicolumn countercurrent solvent gradient purification process. AIChE J., 62: 2341–2357. doi:10.1002/aic.15203*
3. *Papathanasiou et al. (2016). "Development of advanced control strategies for periodic systems: An application to chromatographic separation processes", 2016, In American Control Conference (ACC). IEEE. pp. 4175-4180.*
4. *Papathanasiou et al. (2016). "A control strategy for periodic systems – application to the twin-column MCSGP", 2015, In Computer Aided Chemical Engineering, Elsevier, Volume 37, pp. 1505-1510.*

4.1 Introduction

As discussed in Chapter 3, chromatography is one of the most important steps in mAb manufacturing, as it determines the quality of the antibody and is applied both for initial separation and late-stage purification of the upstream mixtures. In addition, due to its volume limitations it restricts biomanufacturing from moving to higher titers. To add to that, the material and equipment costs associated with chromatographic processes (Dünnebier et al., 2001, Chon and Zarbis-Papastoitsis, 2011, Strube et al., 2012, Gronemeyer et al., 2014) necessitate the development of advanced tools that will ensure optimal operation of reduced cost and maximum productivity, under purity constraints.

There have been several works in the open literature that examine the control of such processes with the objective to increase the recovery yield, maintaining high product purity. Suvarov et al. (2014) presents an adaptive 'cycle-to-cycle' control strategy, based on a discrete time model for the maximization of the productivity of an SMB unit. Grossmann et al. (2010) suggests a 'cycle-to-cycle' MPC approach for the control of MCSGP (6-column configuration), while Krättli et al. (2011) and Krättli et al. (2013b) employed PID techniques for the control of the four- and the twin-column MCSGP respectively. Few of the main challenges discussed in the open literature are: (i) the achievement of CSS that will ensure process stability, (ii) the online feedback during the operation of the controller, as measurements are challenging to obtain, particularly in continuous processes, (iii) efficient rejection of disturbances and (iv) simplification of the optimization and/or control problem that often requires excessive computational force to be solved.

Aiming to tackle the above-mentioned challenges, in this chapter, we present a methodology for the control of a single-column system, based on the operating principles of the MCSGP process, employing mp-MPC strategies. The chapter is organized as follows: Section 4.2 describes the single-column system and focuses on the analysis of the input/output dynamics. Sections 4.3, 4.4 and 4.5 demonstrate the development of advance multi-parametric controllers for the following systems: (i) three single-input single-output systems under constant feeding, (ii) a single-input multiple-output system under constant feeding and (iii) single-input multiple-output system under variable feeding treated as disturbance. The controllers are developed and tested in-silico against the process model. Following that, a novel strategy is presented in Section 4.6, used to treat the inherent time delay of such systems. Finally, in Section 4.7 we assess the behavior of the SIMO controller (considering disturbances) under various flow rate values. This chapter focuses on the design of a control scheme that is able to track the system, capturing its main features (such as the periodicity and

system non-linearity), as well as dealing with challenges such as variations in the feed composition and time delays. Although in chromatographic separation ultimately the process performance in terms of purity and yield needs to be considered, the described controller has a more fundamental purpose of tracking the behavior of the system under various conditions. Hence such a controller can keep the system operating at a defined set-point in a cyclic manner. It is assumed that the conditions that result in optimal purity and yield can be experimentally and/or computationally pre-defined.

4.2 Single-column System

4.2.1 The system

The single-column system shown in Figure 4.1 is a chromatographic column based on IEX technology, following the principles of MCSGP (Section 3.3). Here we consider the separation of a ternary mixture resulting from a cell culture system, including:

(i) Weak adsorbing impurities (W)
(ii) Antibody that is the targeted product (P)
(iii) Strong adsorbing impurities (S)

As mentioned in Chapter 3, weak impurities refer to antibody fragments, the product variant refers to the mAb, while strong adsorbing impurities refer to antibody aggregates. Indicatively, Müller-Späth et al. (2013) and Krättli et al. (2013b) describe the type of fragments and aggregates that can be found in antibodies of IgG-class, as the one considered here. Also, we assume that modifier is used for the separation process at a certain flow rate value (within the permitted range for the given equipment). In this case, the column is operated continuously and we distinguish two cases: (i) constant and (ii) periodic feeding. The system (Figure 4.1a) is described by the model equations presented in Appendix B, while the mass balance around the column is calculated by Equation 3.1.

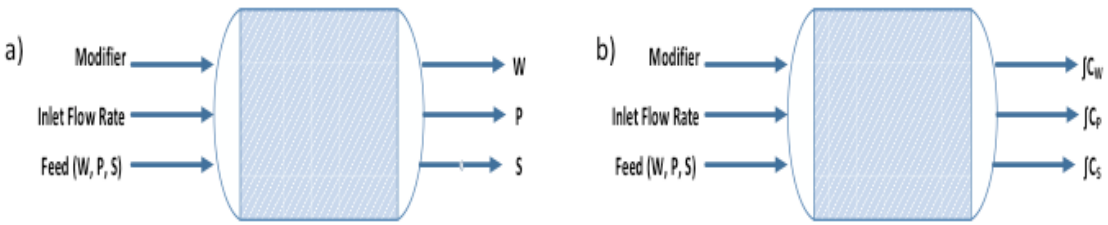

Figure 4.1 a) Single-column system based on the principles of the MCSGP process (5x3 system) and (b) Single-column system based on the principles of MCSGP, tracking the integrals of the outlet concentrations (5x3 system).

4.2.2 Input – Output selection

4.2.2.1 Output selection: The concept of the integral

According to standard practice, the optimization and control studies performed on chromatographic systems consider the maximization of recovery yield under purity constraints (Section 3.2). However, according to Equation B.10 and Equation B.11 (Appendix B), purity and yield are computed based on the average concentrations of the eluted mixture components and therefore we are interested only in their final values by the end of each process cycle. Consequently, that renders them "discrete-type" outputs and leads to 'cycle-to-cycle' control strategies. The selection of continuous variables as outputs, would facilitate the derivation of tailor-made control laws and tighter process monitoring, as the controller would receive feedback in a continuous (or semi-continuous) fashion. Moreover, the outputs chosen for the formulation of the control problem should be ideally measurable or their measurements should not require lengthy experimental procedures.

Towards this direction and aiming to tackle the aforementioned challenges, in this work we suggest tracking of the integral of the outlet concentrations of the mixture components (Figure 4.1b). Currently the quantities of the eluted components can be identified using standard UV detectors that are widely used in such processes. The latter can be translated into the concentration of the eluted quantity using a linear relationship between the total mass injected in the column and the area below the peak of the chromatogram (Equation 4.1). This linear relationship holds within a certain range (approximately up to 1000 AU, representative range for such separation processes). Current setups are equipped with computational systems able to provide within seconds accurate, automated information on the area below the elution peak and therefore the eluted component quantity. This information can be used for the calculation of the integral of the eluted concentration via commercially available software (such as MATLAB®) and returned to the controller as feedback. The use of the proposed output offers continuous monitoring of the outlet stream throughout the process cycle and therefore allows the controller to act timely in case of disturbances and/or deviations of the assigned setpoints. In addition, continuous (or pseudo-continuous at the range of seconds) tracking of the system offers the flexibility to use a series of measurements as controller feedback and minimize the risk of failure. For example the designed controllers can initially receive frequent feedback within seconds from the UV/VIS monitors as described above and later on be updated by more accurate measurements resulting from the HPLC that requires longer analysis time. This two-step verification of the process state allows the controller to re-estimate a better forward action in case the original feedback received from the UV is not accurate enough. Finally, yield and purity can be post-calculated offline as per current standard practice as they are

based on the average concentrations over a process cycle, which are related to the concept of the integral. Similarly to any other online control strategy, it heavily resides on the availability of online (or at-line) measurements. Therefore, risks related to noise and/or unavailable measurements can be encountered here as well. However, due to the model-based nature of the proposed controllers, the presented approach can benefit from the process model when measurements are unavailable. More specifically, in a sudden event where the detectors fail to return a feedback measurement to the controller, the output from the high-fidelity process model can be used. The latter can be simulated in tandem with the online operation and provide measurements in cases of emergency. The latter can be updated later on by actual experimental values when available. Last but not least, the proposed controllers do not intend to completely eliminate the operator, who can interfere at any point and re-adjust the process parameters appropriately.

$$m_i = K_i \cdot A_i$$

Equation 4.1 Linear relationship between the total mass injected in the column and the area below the peak of the chromatogram

Where m_i is the quantity of the eluted component i, K_i is the absolute response factor for component i and A_i is the area below the peak on the chromatogram.

4.2.2.2 Input selection: Sensitivity tests

As discussed in Section 3.4.2 the right choice of the control variables is of vital importance. Given the complexity of the mathematical model, it is essential to reduce the computational force required for the control studies to be executed. Therefore, the control problem formulation needs to be simplified in a meaningful manner, following a rigorous procedure that will ensure that the main system interactions are considered and the controller will return satisfactory results. Consequently, the 5 input – 3 output system (5x3) is subjected to sensitivity tests, where the inputs are varied within the permitted range and their effect on the output behavior is monitored. Figure 4.2 illustrates the strategy applied to the inputs, where we excite within the allowed range: (i) the modifier concentration, (ii) the flow rate and (iii) the feed composition. Each input is varied separately in order to identify the individual effect it has on the monitored outputs (synergetic/antagonistic effects are not considered here). Based on the experimental procedures followed for the operation of the MCSGP the three variables are excited within the ranges shown in Table 4.1 and are representative for applications in mAb purification (Grossmann et al., 2010, Krättli et al., 2013b). The illustrated bounds are in line and have been defined experimentally by the Morbidelli Group (ETH Zürich). Due to confidentiality agreement with the Morbidelli Group (ETH Zürich) the exact values cannot be disclosed and therefore only estimates are provided. Although this

work focuses on the purification of a mAb and the bounds used in the sensitivity test are representative for bioseparations, the reader is referred to Appendix B where a more extended sensitivity test on the modifier is available in order to examine cases where the separation requires modifier concentration greater than 4 mg/mL.

Each input is varied independently and therefore synergetic/antagonistic effects are not considered here. The pulse strategy applied here is in line with the input strategy applied in the industrial operation of MCSGP (Section 3.3.1) and therefore it is preferred to a multisine approach. In order to allow an objective handling of the system, the time points and the duration of the pulses are randomly generated and chosen for each variable. Firstly the modifier concentration is perturbed from its starting value (2.48 mg/mL), following 3 sequential changes (+8%, -19% and +61%) starting at the 60^{th}, 136^{th} and 200^{th} minute respectively with 10 min duration (Figure 4.2). It is important to underline that between changes the system is let free to reach steady state. The latter allows unbiased monitoring of each perturbation independently. In this fashion, during changes in the modifier concentration the system is operated under constant flow rate (0.6 mL/min) and constant feeding with predefined composition (0.07, 0.4 and 0.04 mg/mL for weak impurities, product and strong impurities respectively). As depicted in (Figure 4.3) the modifier concentration affects significantly the eluting component quantities. More specifically, we observe that in the beginning when the modifier concentration is constant the eluted component quantities are constant as well. However, the first increase in the modifier concentration (60^{th} minute) results in an increase in the eluted quantities. In particular we observe a 72%, 67% and 43% increase in the eluted concentrations of weak impurities, product and strong impurities respectively. From a physicochemical perspective it is expected that an increase in the modifier concentration will result into higher eluted quantities, as the modifier is the salt that induces the separation. Moreover, it is observed that the perturbation in the modifier concentration affected the weak impurities the most. The latter is also in line with the physics of the system as such kinds of impurities are characterized by decreased charge and are the ones that are relatively easy to separate and elute. Conversely, the strong impurities require significantly increased modifier concentration in order to be eluted and thus are less affected by small changes. Following that, the modifier concentration is decreased (-19%) and re-stabilized to its original value after 10 min (Figure 4.2a). These two consecutive changes firstly allow the components to be accumulated in the column (during low modifier concentration) and then rapidly washed out resulting in the peaks observed at the 143^{rd} minute (Figure 4.3). Lastly, the modifier concentration is increased to 4 mg/mL in order to cover the whole range of concentrations used in mAb purification (Figure 4.2a) that results into 200^{th} minute (Figure 4.3). This jump in the modifier concentration leads to >100% increase in the

eluted quantities that is, however, a cumulative effect stemming both from the increase in the modifier concentration as well as in the accumulation of the latter within the column. Contrary to the modifier concentration, the inlet flow rate does not seem to affect the quantities of the eluted components. In particular the inlet flow rate follows 3 consecutive perturbations between the 266th and the 470th minute that result in no significant change in the quantity of the eluted concentrations (Figure 4.3). This in accordance both with the mathematical model and the experimental procedure as the modifier concentration is used to calculate the Henry constant in a highly nonlinear equation, while the flow rate participates in a linear fashion in the general mass balance (Appendix B) that results into lower impact on the total amounts of the eluting components. According to the basic chromatographic principles (Guiochon et al., 1994), the modifier concentration affects the liquid-solid equilibrium in a highly nonlinear fashion and consequently the accumulation and/or elution of the components at the end of each process cycle. On the other hand, the flow rate affects the speed of the elution (i.e. the process kinetics) but not the thermodynamics of the chromatographic system.

Table 4.1 Upper and lower bounds used for the sensitivity tests. In the case of the feed composition: the concentrations of weak impurities, the product and strong impurities are varied within ± 10% from the base case values (0.07, 0.4 and 0.04 mg/mL respectively)

Variable	Upper bound	Lower bound	Units
Modifier concentration (**Figure 4.2**a)	4	2	mg/mL
Inlet flow rate (**Figure 4.2**c)	1	0.2	mL/min
Feed composition (**Figure 4.2**b)	+10% from the base case value	-10% from the base case value	mg/mL

In the case of the feed composition, the concentrations of the mixture components are varied simultaneously as they are present in the upstream harvest and therefore cannot be controlled independently. More specifically, the feed composition follows 2 perturbations between the 530th and the 610th minute (Figure 4.2b). The first change corresponds to a +10% increase from the base case value (Table 4.1) and the second to a -10% decrease respectively, while the system is left to stabilize in between. The variation window ±10% has been experimentally predefined by the Morbidelli Group and corresponds to repetitive variations that result from the upstream process used for the production of the mAb studied in this work. The changes applied to the feed composition result in <10% changes in the eluted quantities.

To summarize, it is observed (Figure 4.3) that the most significant deviation in the output profiles occurs from changes in the modifier concentration. This is followed by changes in the feed composition, while the flow rate seems to have no significant effect on the quantity of the eluted components. It should be underlined that both the modifier concentration and the inlet flow rate can be controlled by the operator. Conversely, the feed composition depends on the upstream process and cannot be controlled. Nevertheless, in standardized processes, the variation range of the composition of the feed stream can be experimentally predefined, thus allowing us to treat it as measured disturbance with known bounds. Consequently, based on the sensitivity tests presented here, the system is reduced to a 1 x 3 input – output system with the modifier concentration as the sole input and the integrals of the outlet concentrations of the three mixture components as outputs.

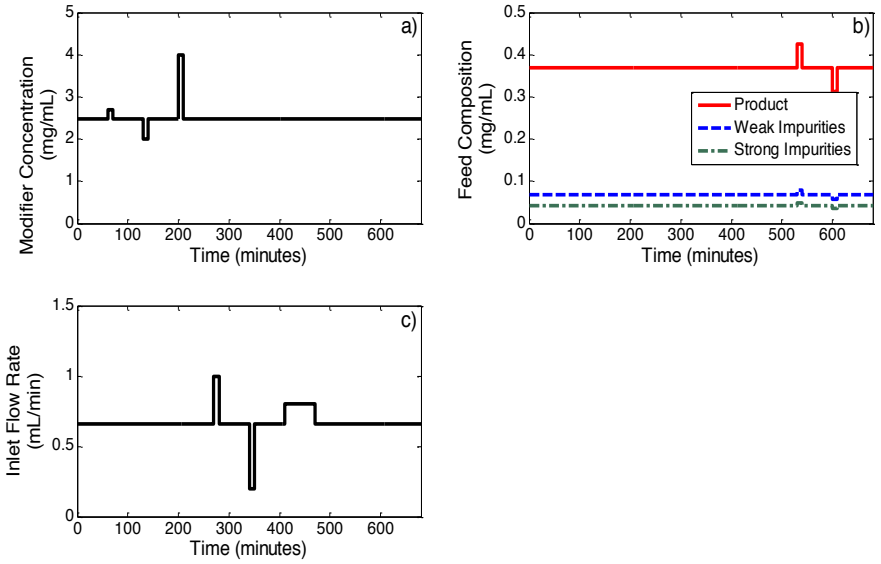

Figure 4.2 Pulse input strategy as applied for the sensitivity tests and the development of the state space models for (a) the modifier concentration (mg/mL), (b) feed composition (mg/mL) and (c) the inlet flow rate (mL/min).

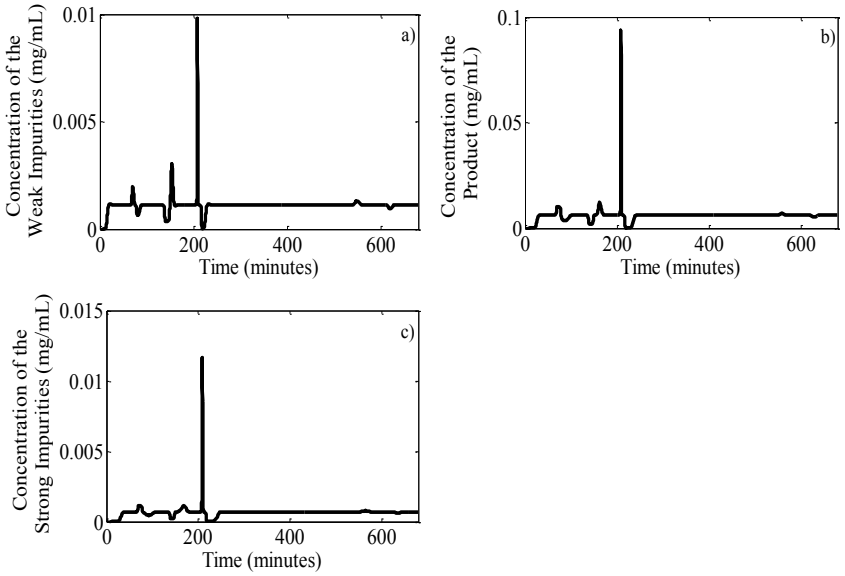

Figure 4.3 Output profiles as resulted from the sensitivity tests for the outlet concentration of (a) the weak impurities, (b) the product and (c) the strong impurities.

It should be underlined that according to standard practice the modifier concentration is changed following a smoother gradient profile. The changes presented in this section are more abrupt and can potentially result in extreme profiles in the system behavior. However, this ensures that the system has been computationally excited based on extreme conditions and any other profile smoother than the one examined here should still be captured by the presented strategy.

4.2.3 Reduced systems under investigation

Following the input/output selection presented above, the input system is considering a single entity (modifier concentration), while the outputs correspond to the integrals of the outlet concentrations of the mixture components. In addition, the feed introduced to the chromatographic column can be considered as measured disturbance (Section 4.2.2.2). In order to fully explore the system dynamics and behavior, we examine the development of advanced controllers for the following systems:

(i) Single Input – Single Output (SISO): We develop 3 independent controllers considering the modifier concentration as input and the integral of the outlet concentration of every mixture component as output, respectively (Section 4.3).

(ii) Single Input – Multiple Output (SIMO), *without* disturbance: We design a controller, monitoring the integrals of the outlet concentrations simultaneously, using the modifier concentration as the control variable (input). In this case, the feed is not considered as disturbance (Section 4.4).

(iii) Single Input – Multiple Output (SIMO), *with* disturbance: The design of this controller is based on the one described above (ii), however here we consider the feed as measured disturbance. (Section 4.5).

For all the cases the flow rate is maintained at a constant value and is not considered in the formulation of the control problem.

4.3 Single Input – Single Output Controllers

The 3 SISO controllers developed in this section are based on the cases presented in Figure 4.4. Namely:

(i) Case 1: SISO controller with modifier used as control variable and the integral of the outlet concentration of the weak impurities ($\int C_W$) considered as output.

(ii) Case 2: SISO controller with modifier used as control variable and the integral of the outlet concentration of the targeted product ($\int C_P$) considered as output.

(iii) Case 3: SISO controller with modifier used as control variable and the integral of the outlet concentration of the strong impurities ($\int C_S$) considered as output.

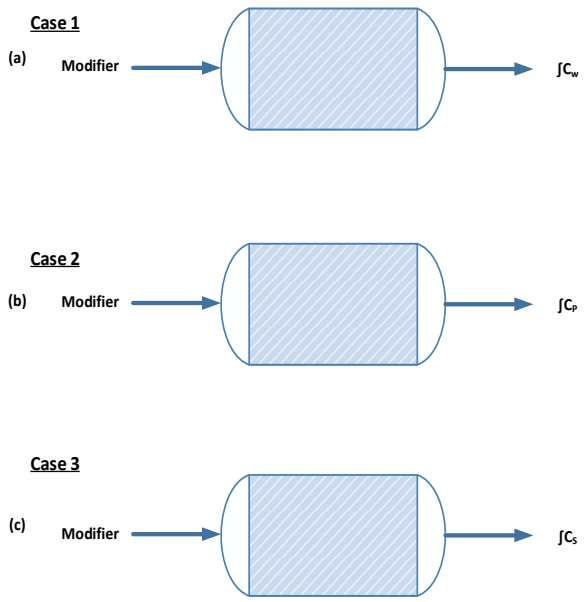

Figure 4.4 The three Single Input - Single Output (SISO) systems, considering the modifier concentration as input and the integral of the outlet concentration of the (a) weak impurities (Cw), (b) product (C_P) and (c) strong impurities (C_S) as output.

4.3.1 Model approximation

The process model (Appendix B) comprises complex, nonlinear equations that challenge the control studies. Therefore, as discussed in Section 0, the equation set needs to be simplified

and transformed into a form suitable for the formulation of the control problem. Therefore a system identification step for the design of discrete, linear state space models that capture the system dynamics is applied. The process model is simulated under a random pulse input strategy in order to ensure that the system is adequately excited (within the range of interest). The input/output data set is stored and processed using the identification toolbox in MATLAB® (*ident*). Figure 4.2 (a & b) illustrates the input strategy as applied to the 3 systems described above (Figure 4.3), while the output behavior is depicted in Figure 4.5.

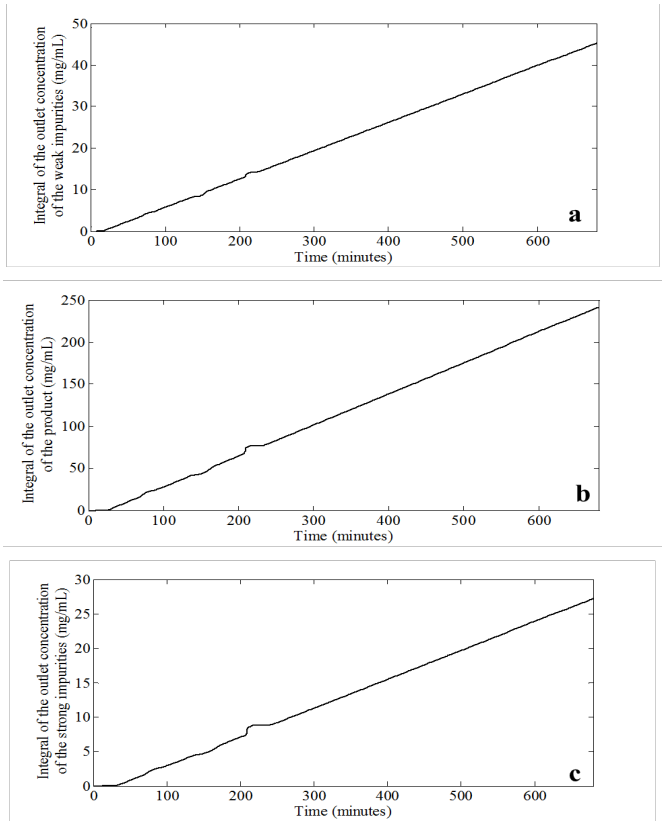

Figure 4.5 Output profiles as resulted from the sensitivity tests for the integral of the outlet concentration of (a) the weak impurities, (b) the product and (c) the strong impurities.

The presented data sets are used for the design of 3 linear, state space models. Equation 4.2 demonstrates the general formulation of a state space without disturbances. The details of the designed models are summarized in Table 4.2. Figure 4.6 illustrates the comparison of the state space model and the process model simulation.

$$x(t + T_s) = Ax(t) + Bu(t)$$

$$y(t) = Cx(t)$$

Equation 4.2 General formulation of a linear state space model (without disturbance).

Where x, u, y correspond to the states, control actions (modifier concentration) and outputs ($\int C_W$, $\int C_P$, $\int C_S$) respectively, t represents the time, T_s is the sampling time and A, B, C

represent the matrices of the state space model. The matrices for the state space models are given below.

(i) ***Case 1:*** *Modifier concentration - Integral of weak impurities*

$$A = \begin{bmatrix} 0.9992 & 0.0003385 \\ 0.0001287 & 0.9996 \end{bmatrix}$$

$$B = \begin{bmatrix} 7.417e-06 \\ 1.358e-05 \end{bmatrix}$$

$$C = [-52.42 \quad 451]$$

(ii) ***Case 2:*** *Modifier concentration - Integral of product*

$$A = \begin{bmatrix} 0.999 & -0.0005434 \\ -4.204e-05 & 0.9984 \end{bmatrix}$$

$$B = \begin{bmatrix} 0.0002333 \\ 0.0001817 \end{bmatrix}$$

$$C = [-1151 \quad 2185]$$

(iii) ***Case 3:*** *Modifier concentration - Integral of strong impurities*

$$A = \begin{bmatrix} 0.9951 & 0.01566 \\ 0.004947 & 0.9797 \end{bmatrix}$$

$$B = \begin{bmatrix} 0.01079 \\ -0.0134 \end{bmatrix}$$

$$C = [-147.1 \quad -125.3]$$

Table 4.2 Characteristics of the three SISO state space models

Input Variable	Output Variable (Integral of the outlet concentration)	Number of States	Sampling Time (s)	%Fit
Modifier Concentration	Weak Impurities	2	6	95.98%
Modifier Concentration	Product	2	6	87.04%
Modifier Concentration	Strong Impurities	2	6	66.58%

Based on the on the operating strategy of the MCSGP process (Section 3.3.1) and in order to ensure that the main events (loading, elution etc) are captured, we choose a sampling time of 6 seconds (0.1 min) for the design of the state space models (Figure 4.6). Additional graphs are illustrated in Figure 4.7, where the state space models presented in Table 4.2 are tested against a different set of inputs (Figure 4.7 a & b).

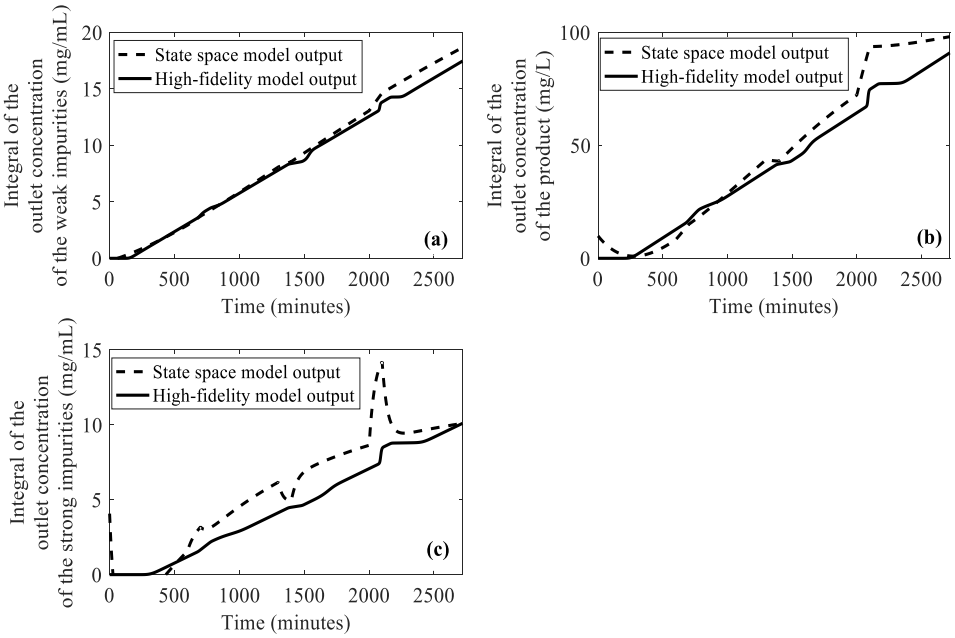

Figure 4.6 Comparison of the three state space models designed above [state space model simulation (---) against the high-fidelity process model (—)] for (a) the weak impurities, (b) the product and (c) the strong impurities, with 95.98%, 87.04% and 66.58% fit respectively.

It should be underlined that the state space model is an intermediate step performed in order to facilitate the formulation and solution of the control problem later on (please refer to Chapter 2) by transforming the problem into a discrete, linear representation suitable for mp-MPC (Rivotti et al., 2012, Lambert et al., 2013). Here, the chosen method relies on the principles of system identification, where an input and an output data set are correlated based on linear combinations (MATLAB®, Mathworks). Therefore, the states of the presented, linear model do not correspond to physical entities of the examined system and any physical interactions/dynamics are eliminated in this step. Thus, the state space model does not classify as a "result" but rather as an "intermediate compensation" to facilitate the controller design.

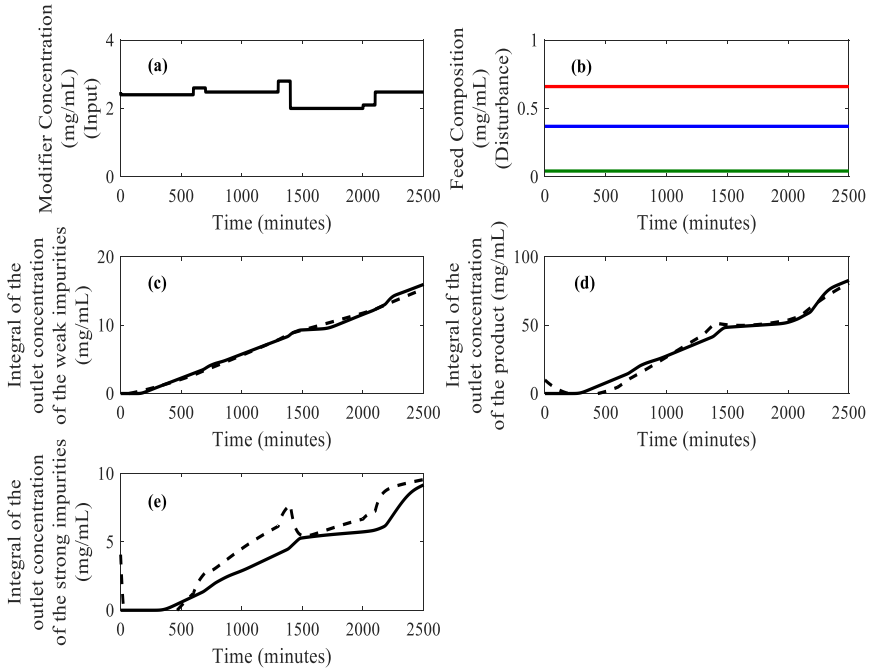

Figure 4.7 Validation of the state space models presented in Table 4.2 against a different of input/disturbance profiles: (a) modifier concentration (mg/mL) used as input for the validation, (b) feed composition used as disturbance [blue: concentration of the weak impurities (mg/mL), red: concentration of the product (mg/mL) and green: concentration of the strong impurities (mg/mL)], (c) comparison of the state space models for weak impurities against the high-fidelity process model, (d) comparison of the state space model for the product against the high-fidelity process model and (e) comparison of the state space model for strong impurities against the high-fidelity process model [where state space model simulation is the dotted line (---) and the high-fidelity process model the continuous line (─)].

Based on the above, sophisticated analysis on the statistical significance of the model parameters and/or the mismatch would increase the computational expense without significant benefit in the system performance. Similar techniques that could bring the problem into a linear, discrete form could also be applied (such as full-discretization, followed by linearization as presented by Grossmann et al. (2010)). The latter however, when applied to such complex systems usually results into an overwhelming number of equations increasing both the risk of human error as well as the computational demand.

The validation of the state space model designed here is assessed in two steps. Firstly, the mismatch between the output of the designed linear model and the output of the high-fidelity model (output set) is compared. At this stage, a "satisfactory" state space model is not the one that would necessarily demonstrate the least mismatch, but a model that is capable of capturing the trends followed by the original output (high-fidelity process model). The second and most important validation of the accuracy of the state space model comes from the controller validation itself (please refer to Chapter 2 & section 4.3.3). Following the formulation and solution of the control problem (based on the linear, state space model), the controller performance is assessed against the high-fidelity process model. Here, the

controller is responsible to minimize the error between the output and the output setpoint. Should it fail to present a satisfactory behaviour, it is advisable that the operator re-assesses the tuning parameters used for the controller design (please refer to section 4.3.2) and/or the design/rationale of the state space model.

Based on the fact that state space model in this work is used for the formulation of mp-MPC schemes that are of receding horizon nature, the fitting of the linear, state space, discrete time model is relevant only within the length of the output and control horizon chosen for the design of the controller. Furthermore, it is in the nature of mp-MPC to account for process model-approximate model mismatch at every iteration. Given that the discretization step used for the design of the state space model is 6 seconds and the maximum control horizon chosen throughout the design of the mp-MPC controllers in this work is 10, the accuracy of the designed models is relevant for a horizon of 1 minute. Following this, a new process model – approximate model mismatch is taken into account into the mp-MPC formulation, thus neutralizing the approximation gap.

Therefore, the state space models presented above are considered suitable for the formulation and solution of the control problem. At this stage they are considered satisfactory as they capture the main trends of the outputs of the high-fidelity model (Figure 4.6 & Figure 4.7). It is observed that the fit of all three models is satisfactory and therefore they can be used for the development of the controller later on.

4.3.2 Design of the mp-MPC controllers

The state space models described above are used for the design of three, independent multi-parametric controllers for the single-column design. Figure 4.8 illustrates the control scheme as designed for the three cases presented above.

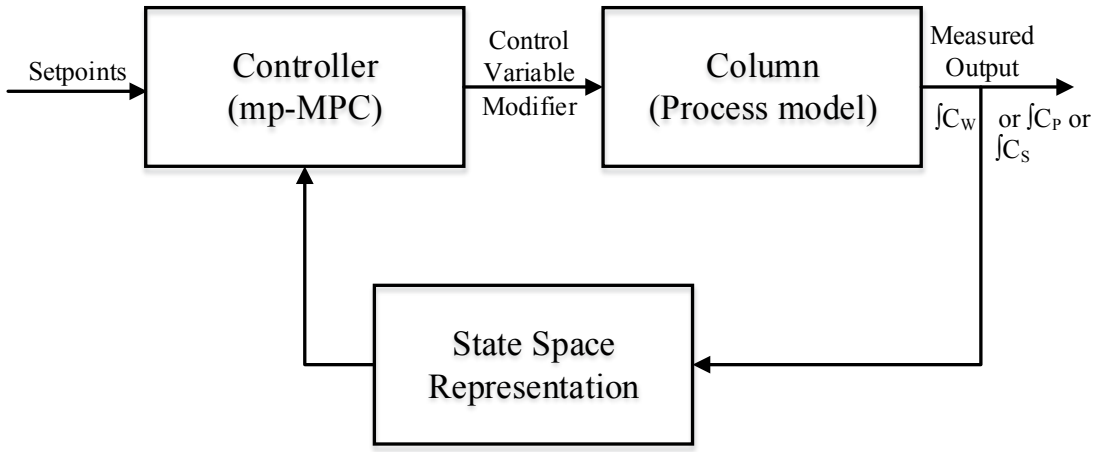

Figure 4.8 mp-MPC control scheme followed for the 3 SISO controllers.

In particular, each controller is designed based on the state space models derived in section 4.3.1. The setpoints for the controller are defined by the operator and concern the integrals of the outlet concentrations of the three mixture components. The controllers use the modifier concentration as manipulating variable and are developed based on mp-Programming strategies (Appendix A). Table 4.3 illustrates the tuning parameters used for the development of the three controllers. The problems are solved using the POP toolbox (Oberdieck et al., 2016) within MATLAB®. Figure 4.9 illustrates the solution maps of the three controllers, as a function of two problem parameters. There are 28, 53 and 80 critical regions depicted for Controller 1, 2 and 3 respectively.

Table 4.3 mp-MPC tuning parameters as used for the design of the three SISO controllers (where *I* is the identity matrix).

Tuning Parameters	Explanation	Controller 1 *(Case 1)*	Controller 2 *(Case 2)*	Controller 3 *(Case 3)*
OH	Output Horizon	10	10	10
NC	Control Horizon	8	8	8
Q	Weights on the states	$100 \cdot I$	$100 \cdot I$	$100 \cdot I$
QR	Weights on the outputs	1000	1000	100
R	Weights for the inputs	1	1	1
Umin	Input upper bound	0	0	0
Umax	Input lower bound	12	12	12
Total number of critical regions		96	118	317

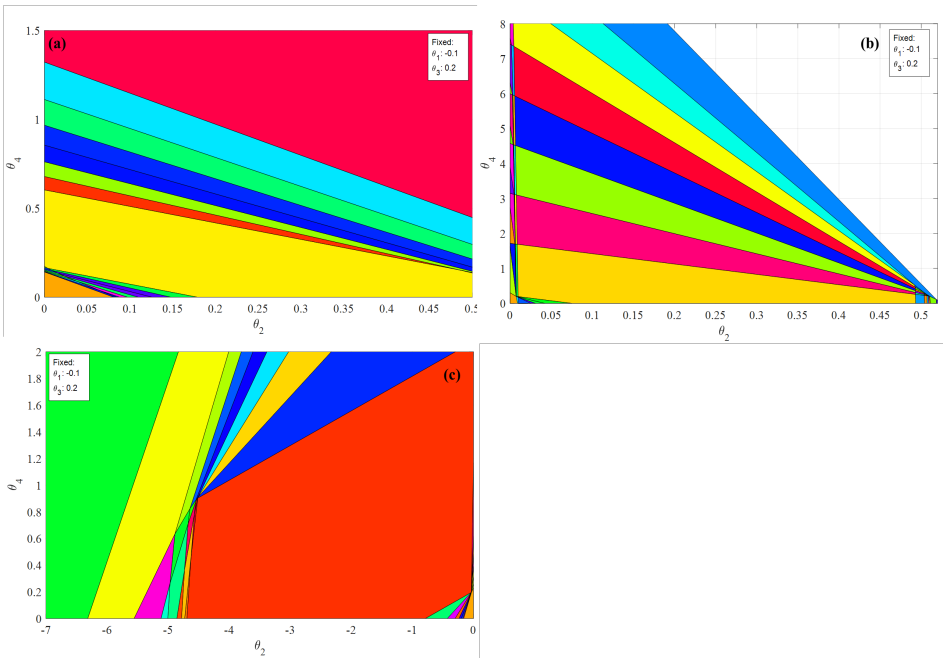

Figure 4.9 Two-dimensional projection of the critical regions polyhedral, for: (a) Controller 1, (b) Controller 2 and (c) Controller 2. All the images are based on the following values: States: x_1= -0.1, x_2=θ_2, Output: $\int C_i = 0.2$ and Output Setpoint: $\int C_i^{set} = \theta_4$, where $i = W, P, S$.

4.3.3 In-silico evaluation of the controller performance

Following the design of the controllers, their performance is evaluated in-silico. The process model is simulated in gPROMS® ModelBuilder v.4.2.0 in tandem with the controller (MATLAB®) through the gO:MATLAB interface The results shown below correspond to three independent model simulations, one for each developed controller. All the simulations are performed under the assumption of continuous feeding of, experimentally predefined composition (Table 4.4) and under constant flow rate (0.6 mL/min).

Table 4.4 Feed composition as considered for the in-silico controller validation[1].

Component	Concentration in the feed (mg/mL)
Weak impurities	0.07
Product	0.4
Strong impurities	0.04

[1]Due to confidentiality agreement with the Morbidelli Group (ETH Zürich) the exact values cannot be disclosed and therefore only estimates are provided.

Figure 4.10a, Figure 4.11a and Figure 4.12a illustrate the comparison between the model output and the desired output setpoint. It can be observed that there is a fairly good agreement between the monitored output and the setpoint, however the system responds with a repetitive time delay. Additionally, it can be observed that all three controllers indicate cyclic input profiles (Figure 4.10b, Figure 4.11b and Figure 4.12b). This implies that both the designed state space models and the developed controllers have incorporated the periodic nature of the examined process and could therefore lead to strategies that will ensure CSS. Moreover, the input profiles are in agreement with the physical and chemical properties of the system. As per the original process, elution can only take place after a respective increase in the modifier concentration. The latter is observed when the input profiles (Figure 4.10b, Figure 4.11b and Figure 4.12b) are correlated to the relevant setpoint changes (Figure 4.10a, Figure 4.11a and Figure 4.12a). More specifically, whenever an increase in the setpoint is encountered, the modifier concentration increases. However, this increase is not random and is directly related to the differences between the setpoints. For example, the difference between the second and third setpoint of the strong adsorbing impurities (Figure 4.12a) is less when compared to the one between the third and the fourth. Therefore, the modifier concentration is expected to increase much more during the 3rd setpoint change. This is also observed in the input profile that is suggested by Controller 3 (Figure 4.12b). It can be observed that the periodic profile

seen in the input strategies is also shown in the choice of critical regions (Figure 4.10c, Figure 4.11c and Figure 4.12c). This could be translated into periodic control laws that force the system to effectively reach CSS. In particular, Controller 2 (Figure 4.11) that corresponds to the tracking of the targeted product shows a consistent, cyclic profile in the choice of critical regions and effectively the assigned control laws.

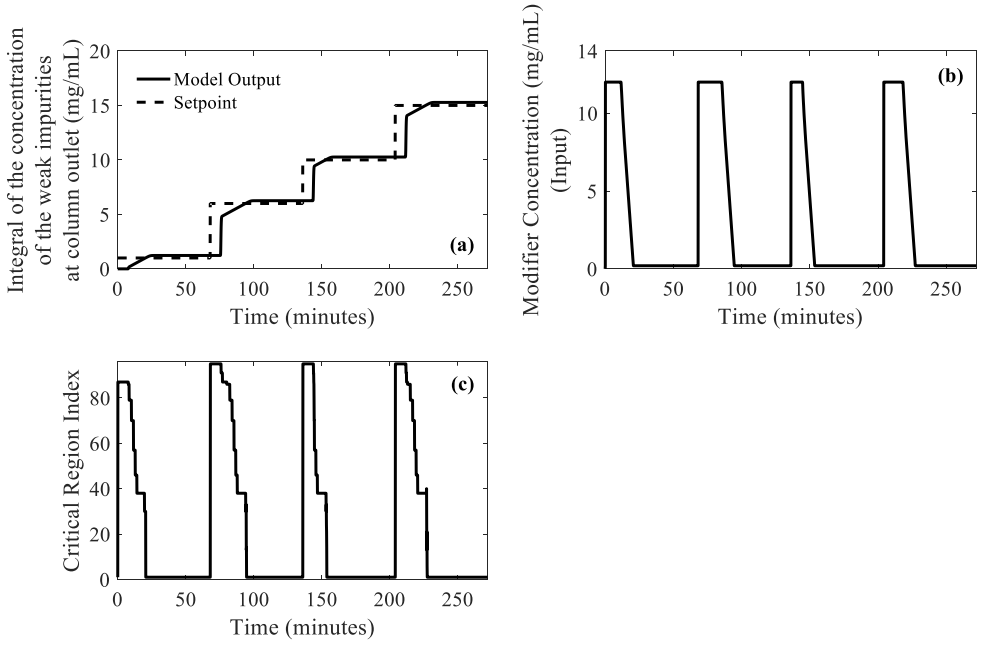

Figure 4.10 Results from the 'closed-loop' validation of Controller 1 (weak impurities): (a) comparison of the model output (—) and the output setpoint (---), (b) input profile as generated by the controller and (c) selection of critical regions.

Particularly in the case of the product (Controller 2) (Figure 4.11a) a repetitive offset is observed, starting from 10% overshoot in the second setpoint and followed by 5% and 3% overshoot in the third and fourth setpoint respectively. The decrease in the offset throughout the simulation could be attributed to the model-based nature of the controller as well as to the receding horizon theory behind it that allows the controller to gain knowledge both from the process model and its past actions.

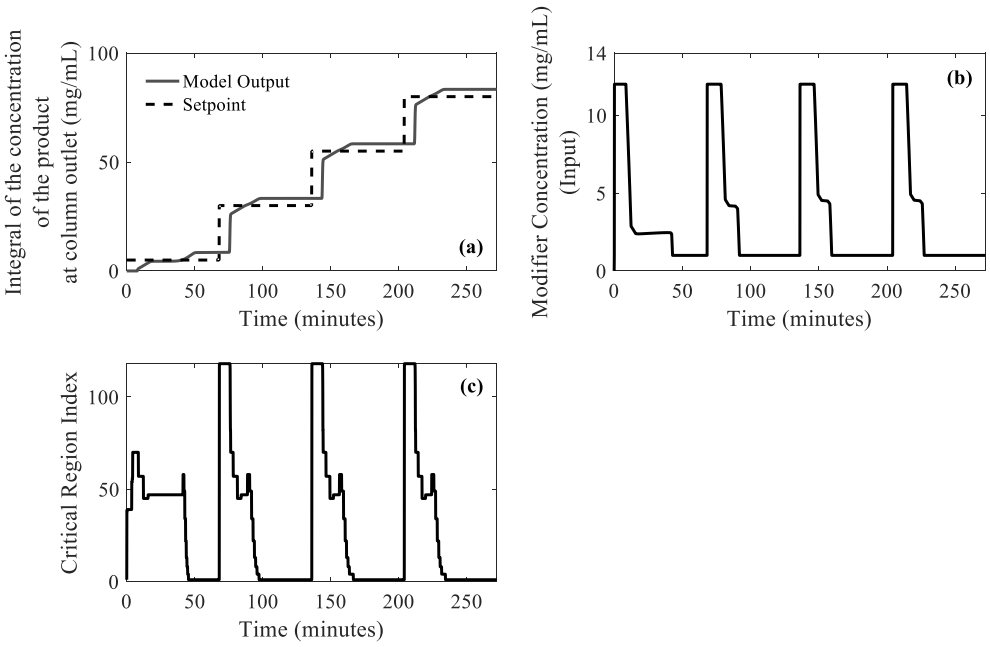

Figure 4.11 Results from the 'closed-loop' validation of Controller 2 (product): (a) comparison of the model output (—) and the output setpoint (---), (b) input profile as generated by the controller and (c) selection of critical regions.

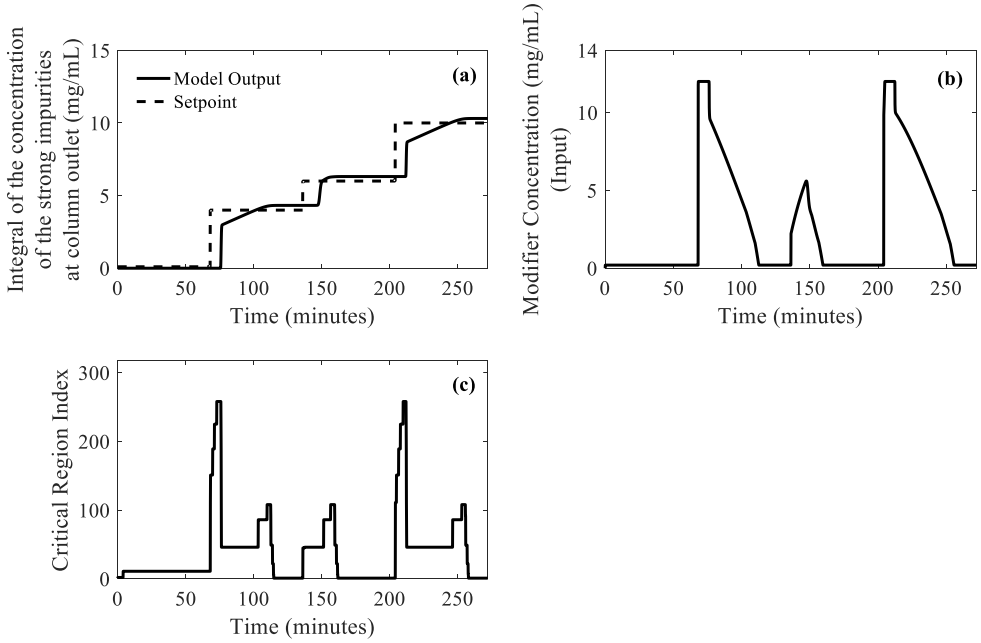

Figure 4.12 Results from the 'closed-loop' validation of Controller 3 (strong impurities): (a) comparison of the model output (—) and the output setpoint (---), (b) input profile as generated by the controller and (c) selection of critical regions.

The deviations observed here could be due to the fact that in this case study the feeding is not considered in the formulation of the control problem; thus the controller is not trained to recognize the amount of components entering the column. Moreover, as discussed in

Appendix B, the tuning parameters (Table 4.3) may affect the controller behavior in various ways with particular interest in the QR/R ratio that defines the effect of the controller input on the output. Consequently, a different choice of weights for the input and/or output may lead to improved performance (Appendix B). When required, such types of offsets can be handled using the "integral state" presented by Sakizlis et al. (2004a) that aims to track and decrease the setpoint/output mismatch, introducing the error as an additional state in the objective function.

4.3.4 Conclusions

In this section we investigate a single chromatographic column system, used for the separation of a ternary mixture containing weak impurities, antibody and strong impurities. In order to fully understand its dynamics, in this case study the system is decomposed to 3 SISO systems, monitoring the integrals of the outlet concentrations of the mixture components. The designed controllers manage to track the predefined setpoints returning periodic input profiles that are in accordance with the governing physicochemical properties of the system. The presented controllers are based on a novel concept introduced in section 4.2.2.1 that suggests tracking of the integral of the outlet concentrations of the mixture components at the column outlet. It is observed that the proposed strategy can lead to continuous process monitoring and periodic control laws, as the outputs can be continuously tracked throughout the process cycle. In the case of the product (Controller 2) repetitive, decreasing offset is observed. As discussed earlier this can be attributed to: (i) the elimination of the feed from the controller problem and (ii) the choice of weights that define the input/output behavior in the control problem.

The results presented in this section, consider that feed is introduced continuously in the system. This however, does not always comply with the process operating conditions, as columns are usually loaded following a periodic (batch) strategy. In addition, it is observed that the setpoints are reached with a repetitive time delay that is common for all three controllers. Additionally, the system at hand is based on the principles of MCSGP that considers a nonlinear-nonideal type of model. Based on the latter, the component elution bands cannot be obtained independently from one another and therefore the three mixture components need to be monitored and controlled simultaneously under a uniform input strategy. Starting from the latter finding, in the following section (Section 4.4) we combine the three outlet concentrations in a single control strategy and we design a SIMO controller under continuous feeding.

4.4 Single Input – Multiple Output Controller *(without disturbance)*

As mentioned previously, the studied system is based on the assumption that the elution bands of the mixture components cannot be obtained independently and therefore they need to be monitored simultaneously. In addition, in order for the system to reach CSS a uniform modifier strategy is required. Therefore, in this section we study a 1x3 SIMO system (Figure 4.13), where we control the modifier concentration and we track the integrals of the three outlet concentrations of the mixture components under the same input strategy (Figure 4.13). For this case study, we consider a continuous feeding of known composition Table 4.4. It should be underlined that this case study aims to design a controller that is able to track the system, capturing its main features such as the periodicity and system non-linearity. Although in chromatographic separation ultimately the process performance in terms of purity and yield needs to be considered, the described controller has a more fundamental purpose and therefore numeric results for these parameters are not further discussed.

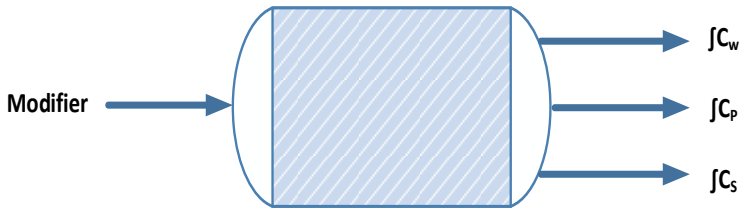

Figure 4.13 The three Single Input - Multiple Output (SIMO) system, considering the modifier concentration as input and the integral of the three outlet concentrations as outputs.

4.4.1 Model approximation

Here we combine the approximate models developed in Section 4.3.1 to design a new, linear state space model of the formulation presented in Equation 4.2, considering however 3 outputs. Table 4.5 illustrates the details of the state space model that was constructed based on the 3 models designed in section above (Section 4.3.1), therefore the fitting of the linear model to the process models is the same as the ones presented for the 3 SISO controllers.

Table 4.5 Characteristics of the SIMO state space model without disturbance.

Input Variable	Output Variable (Integrals of the outlet concentration)	Number of States	Sampling Time (s)
Modifier Concentration	Weak impurities, Product & Strong impurities	6	6

The matrices of the formulation are given below, while the fit is the same as presented in Section 4.3.1, as the state space is built based on the three SISO systems developed previously.

$$A = \begin{bmatrix} 0.9992 & 0.0003385 & 0 & 0 & 0 & 0 \\ 0.0001287 & 0.9996 & 0 & 0 & 0 & 0 \\ 0 & 0 & 0.999 & -0.0005434 & 0 & 0 \\ 0 & 0 & -4.204e-05 & 0.9984 & 0 & 0 \\ 0 & 0 & 0 & 0 & 0.9951 & 0.01566 \\ 0 & 0 & 0 & 0 & 0.004947 & 0.9797 \end{bmatrix}$$

$$B = \begin{bmatrix} 7.417e-06 \\ 1.358e-05 \\ 0.0002333 \\ 0.0001817 \\ 0.01079 \\ -0.0134 \end{bmatrix}$$

$$C = \begin{bmatrix} -52.42 & 451 & 0 & 0 & 0 & 0 \\ 0 & 0 & -1151 & 2185 & 0 & 0 \\ 0 & 0 & 0 & 0 & -147.1 & -125.3 \end{bmatrix}$$

4.4.2 Design of the mp-MPC controllers

Following the procedure presented above (Section 4.3.3), the state space model (Section 4.4.1) is used for the formulation and solution of the mp-MPC problem presented in Figure 4.14. The controller considers the modifier concentration as the manipulating variable and the integrals of the outlet concentrations of the three mixture components as outputs. The problem is formulated using the tuning parameters presented in Table 4.6. In order to explore the system dynamics in an objective manner, we maintain the weights for all measured outputs (*QR*) equal. The problem is solved using the POP® toolbox within MATLAB® (Oberdieck et al., 2016).

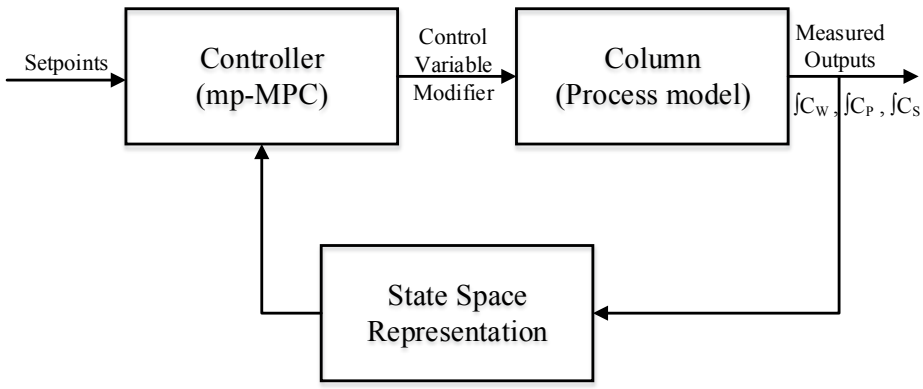

Figure 4.14 mp-MPC control scheme followed for the SIMO controller without disturbance.

Table 4.6 mp-MPC tuning parameters as used for the design of the SIMO controller without disturbances (where *I* is the identity matrix).

Tuning Parameter	Explanation	Value
OH	Output Horizon	4
NC	Control Horizon	2
Q	Weights on the states	1·*I*
QR	Weights on the outputs	[1 1 1]
R	Weights for the inputs	1·*I*
Umin	Input upper bound	0
Umax	Input lower bound	12
Total number of critical regions		6

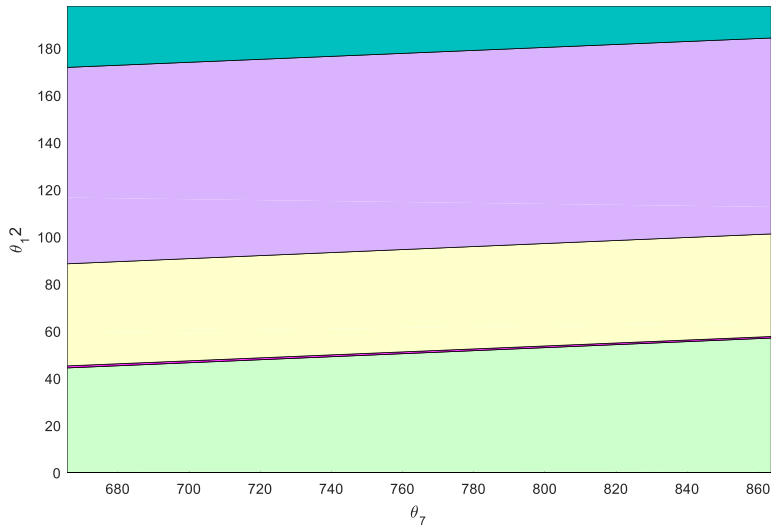

Figure 4.15 Two-dimensional projection of 5 critical regions polyhedral. States: $x_1 = -0.0005$, $x_2 = 0.0044$, $x_3 = -0.0009$, $x_4 = 0.0018$, $x_5 = -0.0039$, $x_6 = -0.0034$, Outputs: $\int C_i = [\theta_7\ 5\ 1]$, Output Setpoints: $\int C_W^{set} = 2$, $\int C_P^{set} = 5$, $\int C_S^{set} = \theta_{12}$, where $i = W, P, S$.

4.4.3 In-silico evaluation of the controller performance

The controller designed in the previous step is tested in a closed-loop fashion against the process model. Both the controller (MATLAB®) and the mathematical model (gPROMS® ModelBuilder v. 4.2.0) are simulated in tandem (via gO:MATLAB) and the controller behavior is assessed. For the simulation we consider constant feeding of fixed composition (Table 4.4) and constant flow rate (0.6 mL/min), while in this case the three outputs are monitored simultaneously. In this example, the setpoints are obtained by validated model simulations and the setpoints are changed instantaneously. It can be observed (Figure 4.16) that the proposed controller tracks the predefined setpoints efficiently, without significant offset (< 3%). Exceptions to the latter are the last setpoints of the weak and strong impurities (Figure 4.16 a & c), where 3% and 11% overshoots are observed. In a real-time application that could potentially entail certain risks associated with increased impurity amount in the final product formulation that would make the latter fall out of the regulatory specifications, depending on the product of interest. However, as discussed in section 4.4.2, also here, the controller is not trained to recognize the amount of components entering the column. Moreover, the tuning parameters (Table 4.6) may affect the controller behavior in various ways with particular interest in the QR/R ratio that defines the effect of the controller input on the output (Appendix B). Consequently, a different choice of weights for the input and/or output may lead to improved performance (Appendix B). When required, such types of offsets can be handled using the "integral state" presented by Sakizlis et al. (2004a) that aims to track and decrease the setpoint/output mismatch, introducing the error as an additional state in the objective function.

In addition to the above, based on the original MCSGP process, we are interested in purifying the targeted product (Figure 4.16b) and therefore monitoring its behavior is of vital importance. With respect to the impurities, we are interested in removing them in controlled time intervals and clean the columns from strong adsorbing components by the end of each cycle. According to standard practice, the setpoints for the controller are obtained via optimization procedures (both experimental and computational) that define parameters such as the optimal feeding strategy and the process switching times between the two modes (batch and interconnected, please see section 3.3.2). Therefore, the application of the presented controller on the experimental setup would look into a set of optimized setpoints that would be more representative of the separation process.

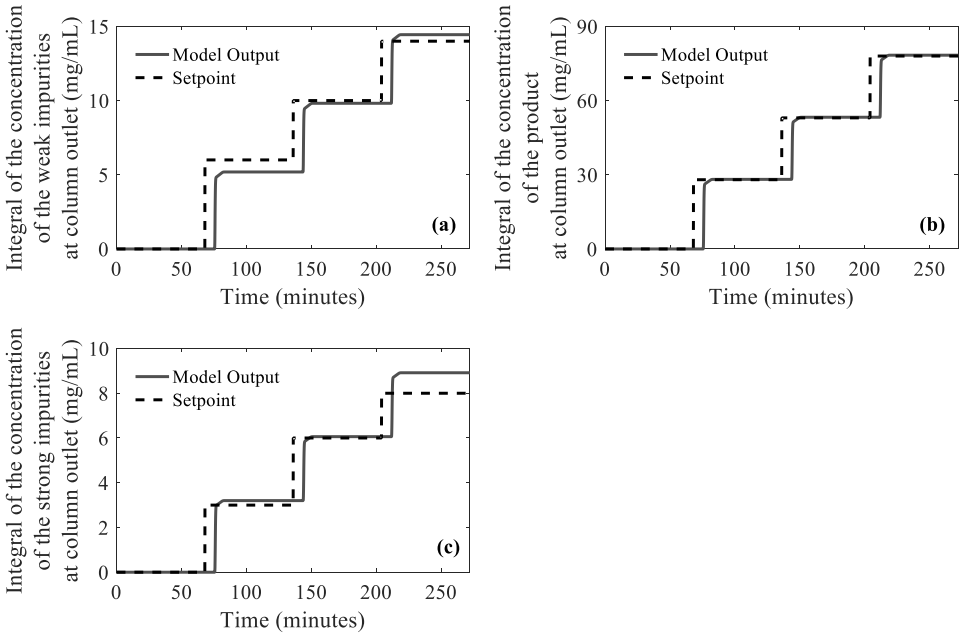

Figure 4.16 Comparison of the predefined setpoint (---) and the output of the process model simulation (—) as resulted from the controller closed-loop validation for (a) weak impurities, (b) product and (c) strong impurities over time [under constant feed (Table 4.4) and flow rate (0.6 mL/min)].

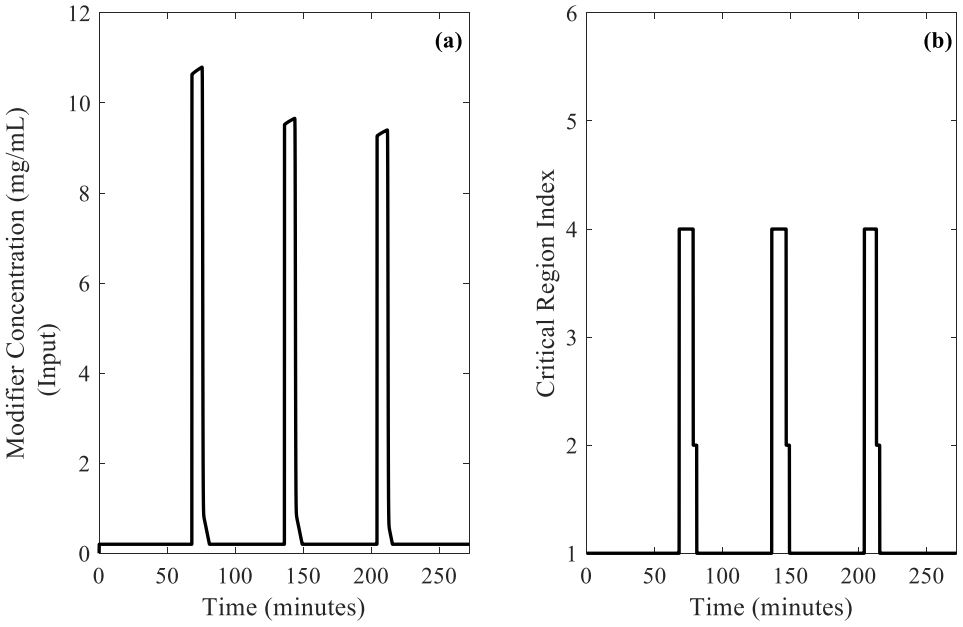

Figure 4.17 (a) Input profiles as generated by the controller and (b) Evolution of the critical regions/control laws during the 'closed-loop' controller validation

The simulation results shown in Figure 4.16 are a result of the controller input, illustrated in Figure 4.17a. It is observed that the controller introduces modifier into the system following a repetitive, periodic profile. The changes observed in the input profile, occur rapidly due to the instantaneous change of the predefined setpoints (Figure 4.16). The input behavior can be

explained based on the physicochemical properties of the system, as the controller increases the modifier concentration (Figure 4.17a) whenever elution is required (Figure 4.16). It is observed that the controller gradually decreases the modifier concentration at every step. That could be attributed to the fact that modifier is accumulated in the column and therefore the process model and effectively the controller realize that only the necessary amount of eluent needs to be provided. The latter is a distinct advantage of the model-based nature of the proposed control strategy, as the knowledge of the process model has been transferred to the controller. Subsequently, this can lead to smart control systems that provide eco-friendly, sustainable solutions that decrease the use of raw materials.

The periodicity observed in the input is also depicted on the choice of critical regions (Figure 4.16b). The controller inherently chooses critical regions in a periodic manner, thus leading to cyclic control laws. This can be considered as an indication that the system periodic nature has been successfully transferred from the process model to the designed controller, the application of which can lead to stable operation under CSS. Lastly, the monitored outputs are characterized by a repetitive time delay of approximately 8 min that is studied in section 4.6.

4.4.4 Gradient setpoint change

As mentioned above (Section 4.4.3) in the 'closed-loop' simulation of the controller the setpoints are changed instantaneously, leading to rapid control actions and therefore a more aggressive input profile. However, in chromatographic separations the elution takes place gradually, following a gradient profile. Particularly in the MCSGP process, the elution peaks are of approximately 1.5 min duration and therefore this needs to be considered in the design and/or evaluation of the presented control scheme. Based on this, we assess the controller capabilities to track gradient elution profiles of 1.5 min duration. Therefore, we repeat the step described in section 4.4.3 under a different setpoint strategy, where each change occurs following a slope of 1.5 min.

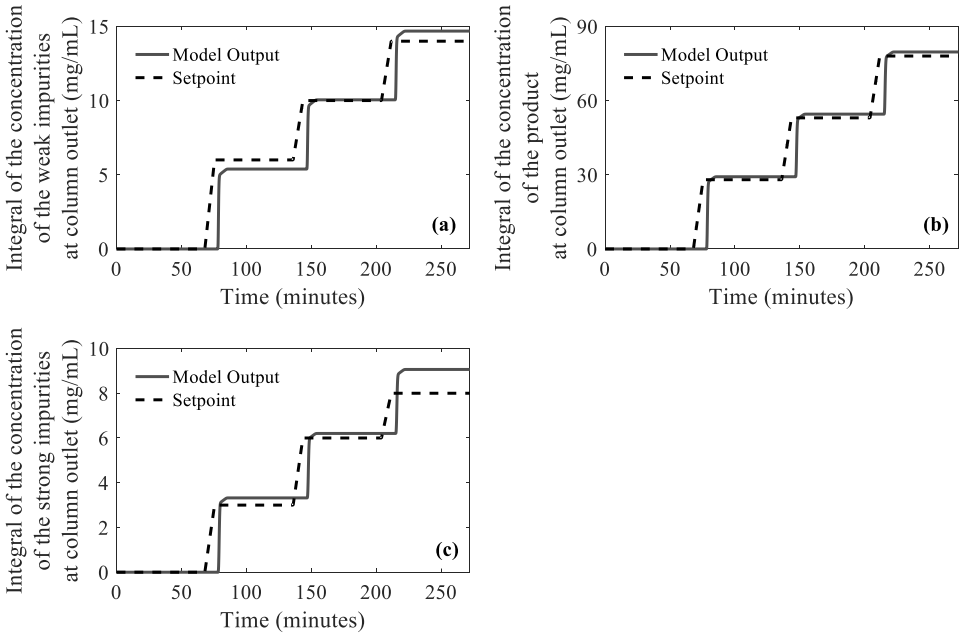

Figure 4.18 Comparison of the predefined setpoint following gradient change of 1.5 min and the output of the process model simulation as resulted from the controller closed-loop validation for (a) weak impurities, (b) product and (c) strong impurities over time [under constant feed (Table 4.4) and flow rate (0.6 mL/min)].

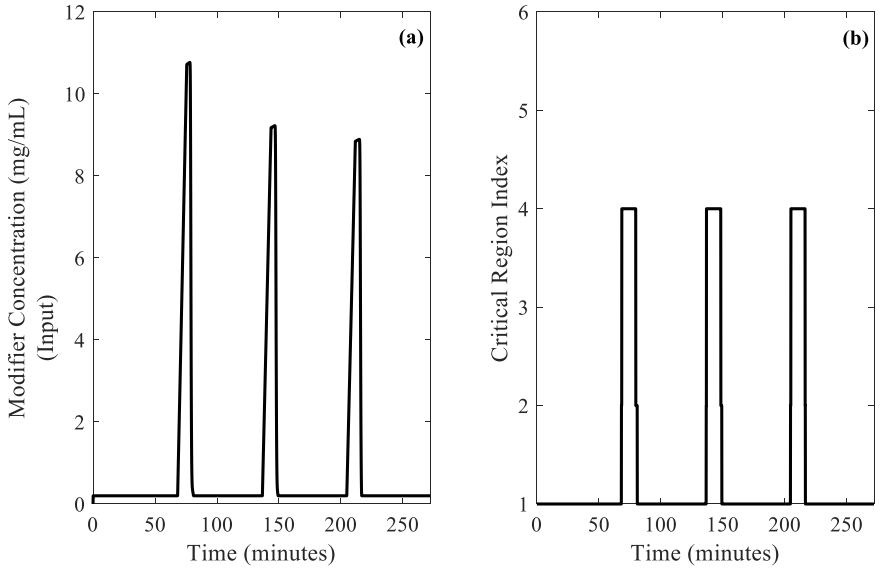

Figure 4.19 (a) Input profiles as generated by the controller and (b) Evolution of the critical regions/control laws during the 'closed-loop' controller validation under gradient setpoint change.

As illustrated in Figure 4.18 the setpoints (dotted line) are changed following a gradient of 1.5 min, however this does not seem to affect significantly the behavior of the outputs, as the results from the process model (continuous line) are the same with the ones presented in the section above (Section 4.4.3) where the setpoints are changed instantaneously. Contrary to the output behavior, a significant change in the input profile is observed (Figure 4.19a). More

specifically, the input actions (modifier concentration) are now characterized by a smoother profile particularly at the time points where the setpoints are changed. Moreover, the input strategy as shown in Figure 4.19a is also very similar to the experimental strategy applied in the MCSGP process, upon whose design the presented controllers are based.

It is observed that the controller manages to track efficiently the predefined setpoints (Figure 4.18) returning a periodic input profile (Figure 4.19a) that corresponds to periodic control laws in the selection of critical regions (Figure 4.19b). Moreover, the main characteristics of the presented strategy discussed in section 4.4.3 are maintained here as well. More specifically, the controller obeys the governing principles of the examined system, feeding only the essential concentration of modifier required for the elution. However, it is observed that although the applied gradient change in setpoints represents the system in a more accurate manner, the time delay observed in section 4.4.3 persists. Lastly, the overshoots discussed previously are observed here as well (Figure 4.18) particularly in the last setpoints of weak and strong impurities (4% and 11,5% respectively). As demonstrated later on (section 4.5) the addition of the feed stream as disturbance in the control problem offers significant improvements in the final controller behavior. Moreover, the main objective of the proposed controllers is to efficiently track the system, maintaining key features such as the periodicity. Therefore, attributes such as purity and/or yield are not assessed here. Nevertheless, since the proposed control strategy can efficiently track the system under various conditions, it can be expected that it will return satisfactory results also in real-time application, where the process is operated under pre-optimized setpoints.

4.4.5 Conclusions

This section demonstrates the development of a single-input multiple-output controller, where the integrals of the three outlet concentrations of the mixture components are monitored simultaneously under a unified modifier concentration profile. The behavior of the designed controller is assessed under continuous feeding of predefined concentration (Table 3.1) and constant flow rate (0.6 mL/min). The proposed controller manages to efficiently track the predefined setpoint under a physicochemically meaningful, periodic input strategy that promises stable operation. Moreover, the periodicity observed both in the modifier profile, as well as in the selection of control laws (critical regions) provides an indication that the cyclic nature of the system and process has been successfully transferred from the process model to the designed controller. In order to mimic the original process and in particular the gradient elution that occurs in such chromatographic separation processes, here we demonstrate a new strategy where the setpoints are changed following a slope of 1.5 min duration. The proposed approach does not improve the controller performance per se in terms of setpoint tracking,

however, it leads to smoother input profiles of gradient nature that resemble current industrial practice.

The controllers discussed in this section consider continuous feeding of predefined composition that is not taken into consideration during the formulation of the control problem. However, according to standard practice feed is introduced into the system in a periodic fashion and its composition can vary, depending on the upstream batch. In order to immunize the control scheme against periodic feeding, as well as against the variations in its composition, in the next section (Section 4.5) we examine the design of a single-input multiple-output controller that considers the feed composition as disturbance and its performance is assessed.

4.5 Single Input – Multiple Output Controller *(with disturbance)*

The previous two sections (Section 4.3 and 4.4) focus on the development of advanced control strategies, considering continuous feeding. However, in industrial application of chromatographic processes, feed is usually introduced in a periodic manner. As mentioned in section 4.2.2, in the cases studied in this work, the feed corresponds to the upstream harvest, thus its composition cannot be manipulated. Therefore, in this section we examine the development of an advanced mp-MPC controller considering the feed as measured disturbance. We elaborate on the work presented in section 4.4, and we consider a system (Figure 4.20) with one input (modifier concentration), three outputs (integrals of the outlet concentrations of the mixture components) and measured disturbances (feed) of experimentally predefined bounds (± 10% from the base case value).

Figure 4.20 The three Single Input - Multiple Output (SIMO) systems, considering the modifier concentration as input and the integral of the outlet concentration of the (a) weak impurities (C_w), (b) product (C_P) and (c) strong impurities (C_S) as output.

4.5.1 Model approximation

The input strategy presented in Figure 4.2 (a & b) is used for the design of a linear state space model of the characteristics presented in Table 4.7.

Table 4.7 Characteristics of the SIMO state space model with the feed as disturbance.

Input Variable	Output Variable (Integrals of the outlet concentration)	Measured Disturbance	Number of States	Sampling Time (s)
Modifier Concentration	Weak impurities, Product & Strong impurities	Feed composition	4	6

Given the fact that here we include measured disturbances, the mathematical formulation considers one additional matrix that represents the impact of the disturbances on the system states (Equation 4.3). The state space model is validated against the mathematical, process model and results into: 94.88%, 94.93% and 93.06% fit for the three outputs respectively. Figure 4.21 illustrates the comparison between the state space model (dotted line) and the process model (continuous line).

$$x(t + T_s) = Ax(t) + Bu(t) + Dd(t)$$

$$y(t) = Cx(t)$$

Equation 4.3 General formulation of a linear state space model (with measured disturbance).

Where *x, u, y* are the states, inputs (modifier concentration) and outputs ($\int C_W$, $\int C_P$, $\int C_S$) respectively, *t* corresponds to the time, T_s is the sample time and *A, B, C, D* represent the matrices of the state space model.

$$A = \begin{bmatrix} 0.9998 & 0.0003667 & 0.0004885 & -9.137e-05 \\ 0.0009448 & 0.9971 & -0.003154 & -0.001599 \\ -0.001027 & 0.0003536 & 0.999 & 0.001881 \\ 0.000969 & 0.001559 & 0.0005033 & 0.9976 \end{bmatrix} B = \begin{bmatrix} -6.252e-06 \\ 4.514e-05 \\ 6.337e-05 \\ -3.396e-05 \end{bmatrix}$$

$$C = \begin{bmatrix} 545.6 & 101.1 & 17.69 & 7.422 \\ 2925 & 660.2 & 102.6 & -67.49 \\ 331.9 & 78.42 & 17.12 & -11.23 \end{bmatrix}$$

$$D = \begin{bmatrix} 1.557e-05 & 8.449e-05 & 9.616e-06 \\ -9.018e-05 & -0.0004893 & -5.57e-05 \\ -3.487e-05 & -0.0001892 & -2.154e-05 \\ 3.698e-05 & 0.0002007 & 2.284e-05 \end{bmatrix}$$

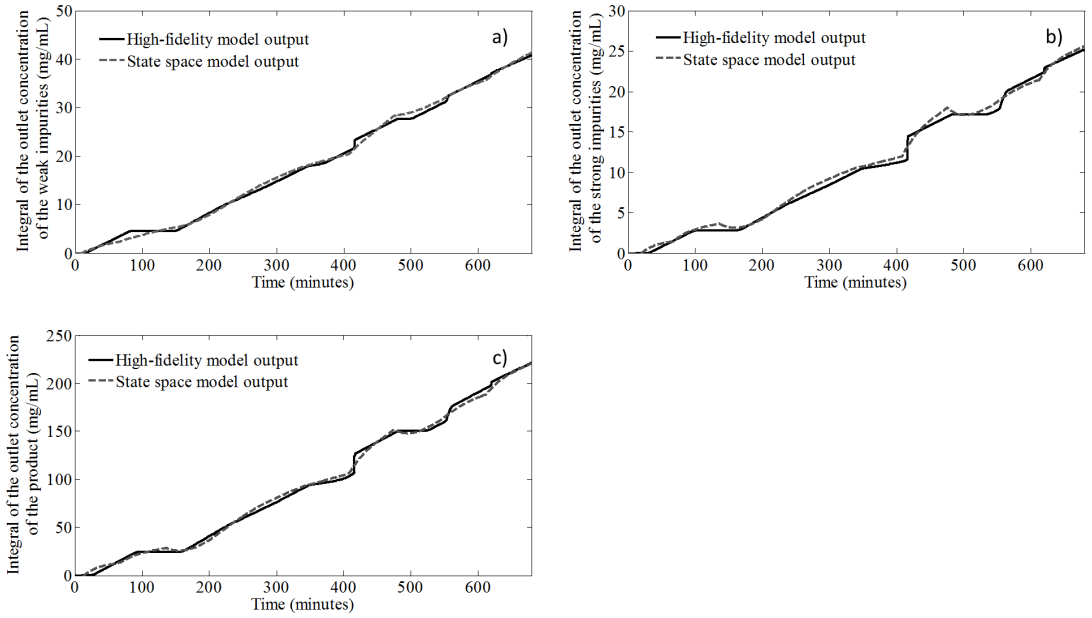

Figure 4.21 Comparison of the state space model simulation (---) against the high-fidelity process model (—) for (a) the weak impurities, (b) the product and (c) the strong impurities, with 94.88%, 94.93% and 93.06% fit respectively.

As mentioned earlier (section 4.3.1) the state space model does not classify as a "result" but rather as an "intermediate compensation" to facilitate the controller design. Therefore, on the same basis, the state space model designed here is considered satisfactory and is used for the design of the controller.

4.5.2 Design of the mp-MPC controllers

The state space model described above is used for the design of an advanced multi-parametric controller for the nominal single-column case. We consider the modifier concentration as the manipulated variable (input), the concentrations of the components in the feed stream (measured disturbances) and the integrals of the outlet concentrations (tracked outputs) (Figure 4.22). The mp-MPC settings are illustrated in Table 4.8. The integral of the product is characterized by a higher coefficient in the QR matrix of the mp-programming problem formulation (Table 4.8) as it is in fact the output of interest. To compensate both for variations in the feed composition as well as for the periodic strategy applied in the feeding, the control formulation considers the feed composition as disturbance. The bounds of the latter can be experimentally pre-defined and therefore it is treated as measured disturbance with known bounds. As mentioned previously, in this work we examine the separation/purification of a monoclonal antibody from an upstream mixture and the case study is based on the MCSGP process. Therefore the bounds for the feed composition have been defined from experiments performed by the Morbidelli Group (ETH Zürich) and are shown in Table 4.8. The lower bound of 0 mg/mL corresponds to the cases where no feeding

is introduced to the system. Usually the feed composition varies ± 10% from the base case value presented in Table 4.4 and therefore the upper bound is defined accordingly. Due to confidentiality agreement with the Morbidelli Group (ETH Zürich) the exact values of the feed composition cannot be disclosed and thus here we provide close estimates.

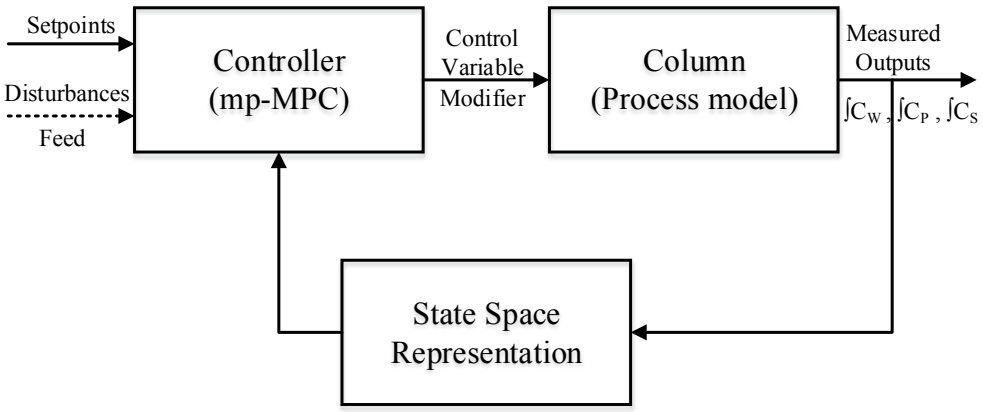

Figure 4.22 mp-MPC scheme designed for the SIMO controller considering the feed as disturbance.

Table 4.8 mp-MPC tuning parameters as used for the design of the SIMO controller under measured disturbances (where *I* is the identity matrix).

Tuning Parameter	Explanation	Value	Tuning Parameter	Explanation	Value
OH	Output Horizon	4	**Umin**	Input upper bound	0
NC	Control Horizon	2	**Umax**	Input lower bound	12
Q	Weights on the states	$1 \cdot I$	**Dmin**	Disturbance upper bound	[0 0 0]
QR	Weights on the outputs	$[10^2\ 10^4\ 10^2]$	**Dmax**	Disturbance lower bound	[0.0748 0.4059 0.0462]
R	Weights for the inputs	$1 \cdot I$	**Total Number of Critical Regions**		9
P	Terminal weight for the states	Riccati equation*			

* The Riccati equation is as follows: $P = A^T PA - (A^T PB)(B^T PB + R)^{-1}(APB) + Q$, where A and B are the matrices of the state space model and P, R, Q the tuning parameters used for the control problem formulation.

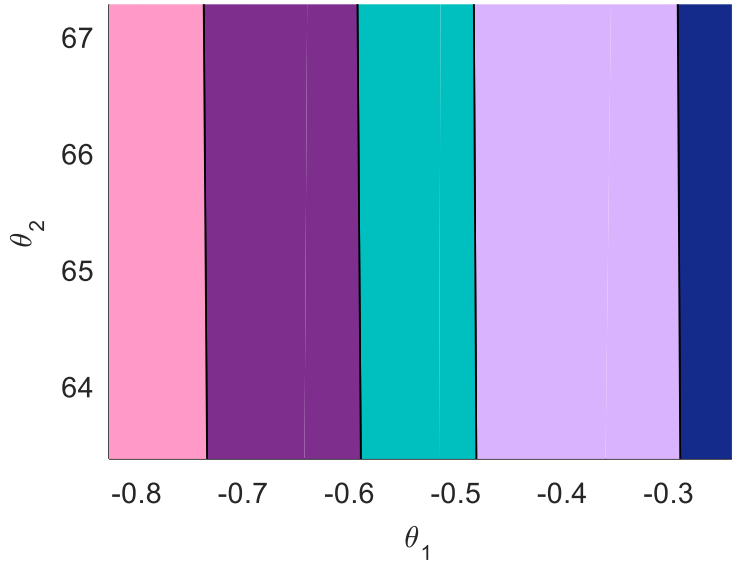

Figure 4.23 Two-dimensional projection of 5 critical regions polyhedral. States: $x_1 = 0.0059$, $x_2 = \theta_2$, $x_3 = 0.1165$, $x_4 = 0.0238$, Disturbances: $C_i^{feed} = [0.01\ 0\ 0.001]$, Outputs: $\int C_i = 1$, Output Setpoints: $\int C_W^{set} = 2$, $\int C_P^{set} = 2$, $\int C_S^{set} = \theta_1$, where $i = W, P, S$.

The problem is solved using the POP® toolbox for robust/explicit mp-MPC, within PAROC (Pistikopoulos et al., 2015, Oberdieck et al., 2016). The solution of the problem resulted in 9 critical regions, 5 of which are depicted in Figure 4.23. The plot is generated based on two of the parameters of the mp-programming problem, while the rest are fixed to a base case value.

4.5.3 In-silico evaluation of the controller performance

The designed controller is validated in-silico against the high-fidelity, nonlinear process model and the output profiles are monitored. The 'closed-loop' validation is performed using the gO:MATLAB interface in gPROMS ModelBuilder® v. 4.2.0. For the controller assessment we consider a constant, base case, average value for the flow rate (0.6 mL/min) and a periodic feeding strategy (Figure 4.24). The feeding strategy applied here is the same as the one adopted in the original MCSGP process (Section 3.3), where feeding is introduced at every column once per cycle for approximately 2 min. Figure 4.24 illustrates the concentrations of the: (a) weak impurities, (b) product and (c) strong impurities present in the feed stream. The feed as presented in Figure 4.24 is defined by the operator and is considered as measured disturbance by the designed controller. It should be underlined that setpoints during the in silico validation are changed following the gradient strategy presented in section 4.4.4 and thus every increase follows a slope of approximately 1.5 min

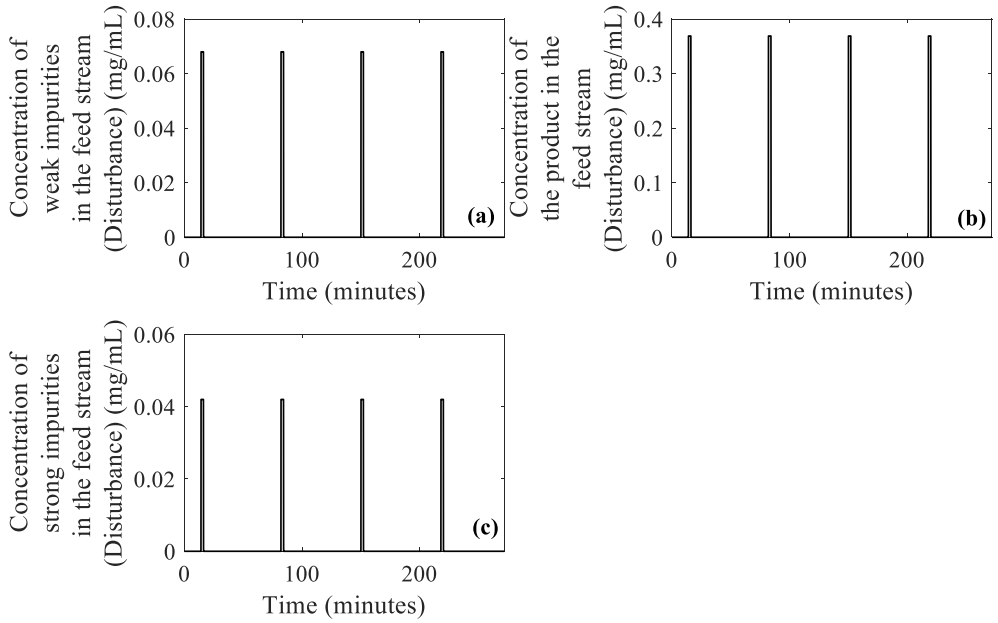

Figure 4.24 Strategy followed for the feed composition (considered as measured disturbance), including: (a) weak impurities, (b) product and (c) strong impurities as indicated by the controller during the 'closed-loop' validation.

Figure 4.25 illustrates the comparison between the output of the process model and the predefined setpoint, where a good agreement is observed. The controller manages to track the setpoints efficiently and with significantly reduced offset compared to the results presented above (Section 4.4). In particular, the weak impurities are characterized by undershoots that are less than 2%, while the product does not demonstrate any deviation from the setpoints (Figure 4.25b). Nevertheless, in the case of strong impurities, deviations from the setpoints are still encountered. Especially the second setpoint is characterized by a 10% undershoot, where the controller does not manage to reach the desired concentration (Figure 4.25c). As discussed earlier, this could be attributed to the control tuning parameters and in particular the QR values determining the weight of the three outputs in the objective function of the control problem (Appendix B). Increasing the weight of the strong impurities could potentially lead to more accurate tracking of the output variable. At this point it should be underlined that the main objective of the proposed controller is to efficiently track the system, maintaining key features such as the periodicity (Figure 4.26). Therefore, attributes such as purity and/or yield are not assessed here. Nevertheless, since the proposed control strategy can efficiently track the system under various conditions, it can be expected that it will return satisfactory results also in real-time application, where the process is operated under pre-optimized setpoints. Here, however, the setpoints are retrieved from simulations of the validated mathematical model and correspond to a case study designed for this work aiming to test the controller behavior under a variety of conditions.

The improved behavior can be attributed to the fact that the control problem examined in this section also considers the feed composition as measured disturbance and therefore the controller is immunized against variations in the feed stream. This observation is also supported by the input profile generated by the controller in the 'closed-loop' validation (Figure 4.26a). The strategy suggested for the modifier is characterized by 4 satellite actions that proceed the main feeding and occur at the same time with the disturbances (Figure 4.26a). It is therefore evident that the addition of the feed stream as disturbance in the control problem improves significantly the behavior of the controller that due to its predictive nature can calculate the optimal actions to account for the upcoming disturbance. Despite the addition of the disturbances in the control problem, the repetitive time delay discussed in the previous sections (Sections 4.3 and 4.4) is observed here as well. This systematic delay is encountered in all outputs (Figure 4.25) and is approximately 8 min.

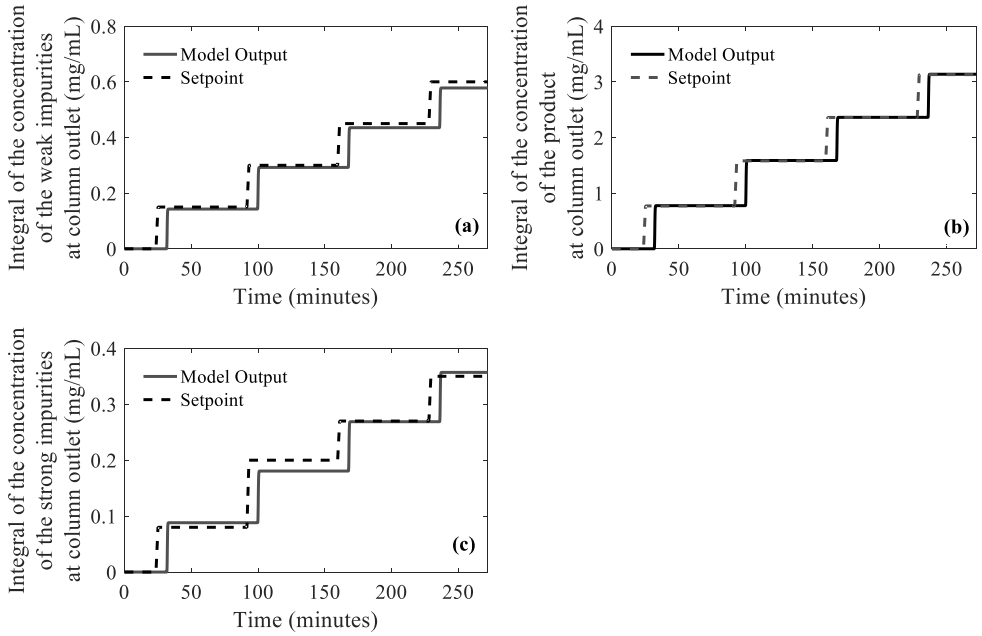

Figure 4.25 Comparison of the predefined setpoint (---) and the output of the process model simulation (—) as resulted from the controller closed-loop validation for (a) weak impurities, (b) product and (c) strong impurities over time [under constant flow rate (0.6 mL/min), considering the feed composition as measured disturbance].

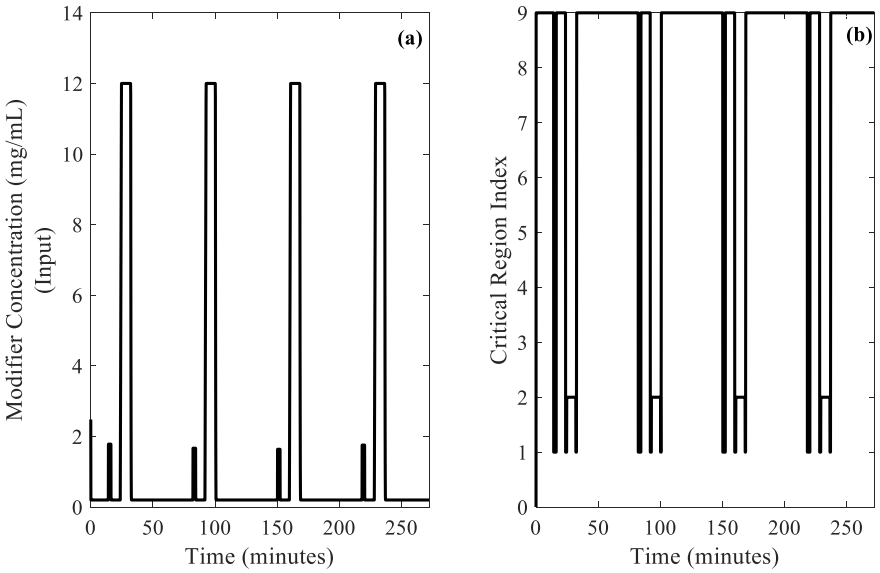

Figure 4.26 (a) Input profiles as generated by the controller and (b) Evolution of the critical regions/control laws during the 'closed-loop' controller validation [under constant flow rate (0.6 mL/min), considering the feed composition as measured disturbance].

Similarly to the previous control schemes, here we observe a periodic profile in the input (Figure 4.26a) that is followed by a cyclic profile in the selection of control laws (Figure 4.26b), inherently suggested by the controller. We can therefore conclude that the periodic nature of the examined process has been successfully transferred from the process model to the linear representation and effectively to the controller, indicating that CSS can be achieved.

4.5.4 Conclusions

This section presents the development of a single-input (modifier concentration) multiple-output (integrals of the outlet concentrations of the three mixture components) controller that considers variations in the feed stream as measured disturbance. The designed controller is tested in silico, under 'closed-loop' validation against the process model and its performance is assessed. The validation is performed under constant flow rate as per the previous proposed schemes (Sections 4.3 and 4.4). The presented controller manages to track the predefined setpoints efficiently, without significant offsets, suggesting a periodic input profile that can lead to stable operation. Moreover, the addition of the feed composition as disturbance in the problem formulation results into satellite, corrective actions in the input as the predictive nature of the controller, allows it to take action for the upcoming disturbance on time.

However, despite the addition of the disturbance, the results continue to demonstrate a repetitive time delay in the output profiles. This delay is encountered at every setpoint change

and is of approximately 8 min. The latter can be associated with the operating flow rate and the residence time of the column at hand. The following section (Section 4.6) is dedicated to thorough the investigation of this delay and suggests a strategy for its elimination.

4.6 Handling the Time Delay: "Setpoint Shift" Strategy

As discussed earlier, the results presented in Sections 4.3, 4.4 and 4.5 are characterized by a repetitive time delay, identical for all problem formulations. Investigating this phenomenon further, we conclude that it is an inherent characteristic of the system and it is directly correlated to the value of the flow rate. More specifically, the time delay shown in the results presented above, corresponds to the residence time and can be calculated using the column volume and the operating flow rate (Equation 4.4) (Guiochon, 2012).

$$t = \frac{V}{Q}$$

Equation 4.4 Residence time as a function of the column volume and operating flow rate.

Where t is the residence time (or time delay), V is the column volume and Q the operating flow rate. The time delay can be calculated a priori at each time point, as both the column volume and the flow rate are known. From an optimization standpoint, the flow rate is one of the most important factors that highly affect the product purity and the elution bands. However, the optimal operating flow rates can be determined beforehand, through dynamic optimization procedures, instead of participating in the control problem as an additional input variable. In that way, the control problem is decreased and therefore the computational force required for its solution is significantly less. Moreover, operating the controller under constant flow rate is also in line with industrial applications as currently pumps installed in chromatographic devices can operate close to a given setpoint (i.e. under constant flow rate).

Here, we pre-calculate the residence time for the given flow rate value and we shift the setpoint accordingly to compensate for the delay ("*setpoint shift* strategy"). In that way we create two sets of setpoints: (a) the ones that are shifted backwards in time and are the ones used by the controller for the input generation and (b) the real setpoints that follow the elution profiles. The proposed strategy is assessed for all the presented control schemes (SISO, SIMO without disturbance and SIMO with disturbance) for the base case of 0.6 mL/min. Table 4.9 summarizes the details of the presented case studies. Due to confidentiality agreement signed with the Morbidelli Group (ETH Zürich), the exact values of the variables cannot be disclosed and therefore the values provided are close estimates of the ones used in the simulations. The simulations are performed under gradient setpoint change (Section 4.4.4).

Table 4.9 Details used for the assessment of the "setpoint shift" strategy applied for the elimination of the time delay in the controller performance.

Column Volume (mL)	Flow Rate (mL/min)	Residence Time (delay) (min)
5	0.6	8

4.6.1 SISO systems

The first controllers to be tested under the "setpoint shift" strategy are the three SISO controllers developed in section 4.3. In addition, the controllers are simulated under the gradient setpoint change, where setpoints are increased following a slope of approximately 1.5 min and continuous feed (Table 4.4). The controllers operate independently from each other, tracking only one output.

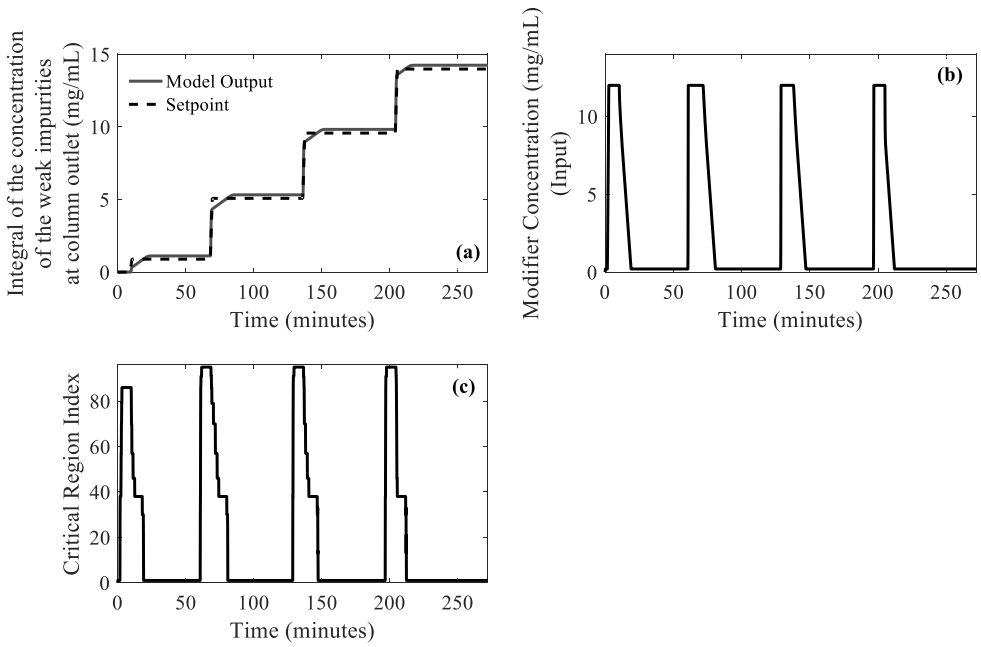

Figure 4.27 Results from the 'closed-loop' validation of Controller 1: (a) comparison of the model output (—) and the output setpoint (---), (b) input profile as generated by the controllers and (c) selection of critical regions, under the 'setpoint shift' strategy.

All the controllers manage to track the setpoints efficiently without significant offsets. However, most importantly, it is observed that the delay has been eliminated from all output profiles (Figure 4.27a, Figure 4.28a and Figure 4.29a). Investigating the input profiles thoroughly (Figure 4.27b, Figure 4.28b and Figure 4.29b), we observe that the input actions

are taken approximately 8 min earlier than before (Section 4.3). The latter is a result of the applied strategy of shifting the setpoints according to the pre-calculated delay.

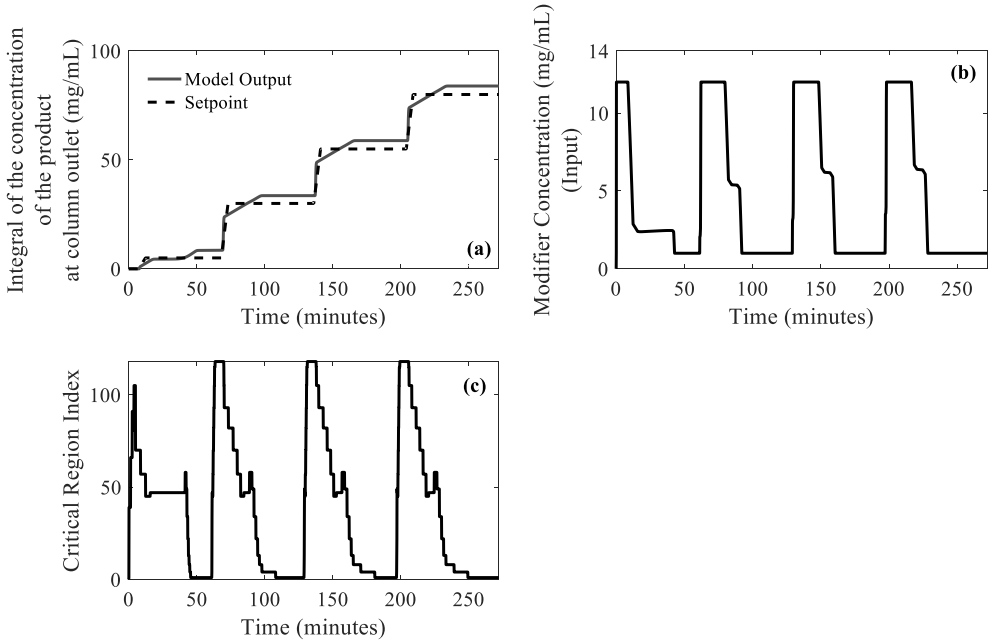

Figure 4.28 Results from the 'closed-loop' validation of Controller 2: (a) comparison of the model output (—) and the output setpoint (---), (b) input profile as generated by the controllers and (c) selection of critical regions, under the 'setpoint shift' strategy.

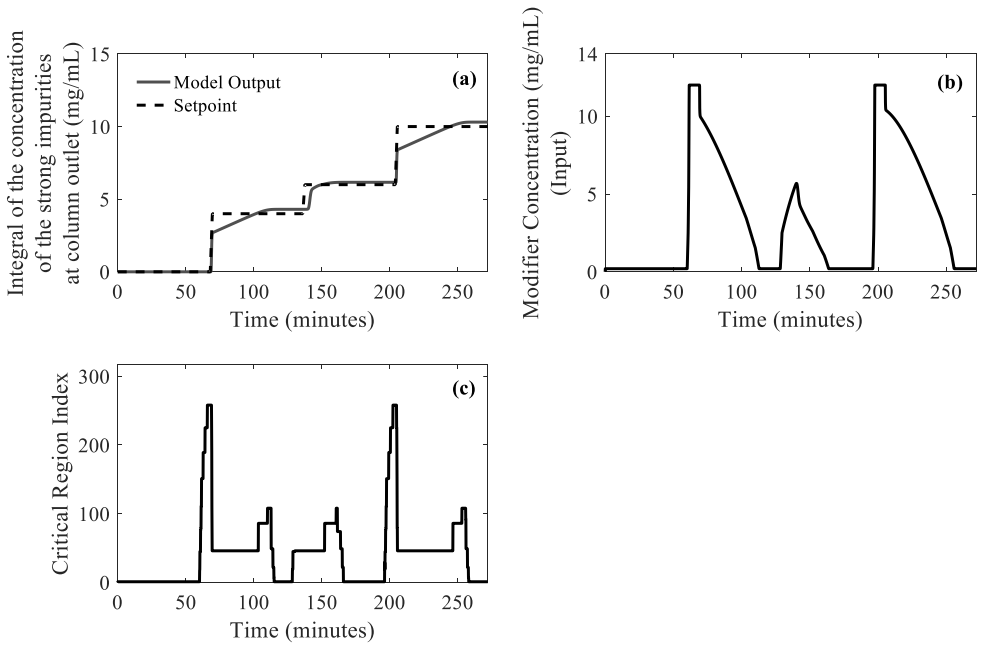

Figure 4.29 Results from the 'closed-loop' validation of Controller 3: (a) comparison of the model output (—) and the output setpoint (---), (b) input profile as generated by the controllers and (c) selection of critical regions, under the 'setpoint shift' strategy.

In addition, we observe that the proposed strategy does not affect the optimal actions in terms of value (Figure 4.27b, Figure 4.28b and Figure 4.29b), however, we observe that the input

profiles are characterized by broader peaks. This can be associated to the combined effect with the gradient elution that is imposed during the closed loop validation that forces the controller to follow a smoother input strategy. To add to that, as illustrated in Figure 4.27c, Figure 4.28c and Figure 4.29c, the choice of control laws continues to be periodic.

4.6.2 SIMO system (without disturbance)

The next control scheme we test under the "setpoint shift" strategy is the single-input multiple-output controller, under continuous feed (Section 4.4). The controller is tested in 'closed-loop' under constant flow rate. It is observed that due to the applied strategy, all the outputs manage to reach the predefined setpoint on time, without time delay (Figure 4.30). Also in this case the input actions are taken 8 min earlier than before (Section 4.4) as the controller can now see the defined setpoint earlier in time.

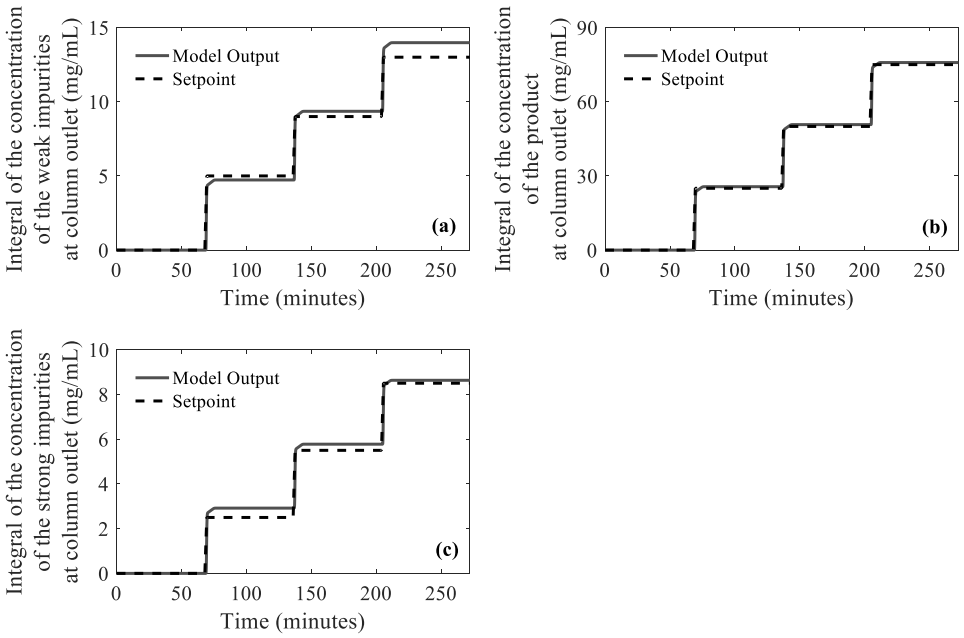

Figure 4.30 Comparison of the predefined setpoint following gradient change of 1.5 min and the output of the process model simulation as resulted from the controller closed-loop validation for (a) weak impurities, (b) product and (c) strong impurities over time [under constant feed (Table 4.4) and flow rate (0.6 mL/min)], under the 'setpoint shift' strategy.

The proposed strategy does not affect either the input values or the periodicity in its profile (Figure 4.31a). However, the control actions presented here are broader compared to the ones demonstrated in section 4.4.4 (Figure 4.18). This could be attributed to the fact that the "setpoint shift" strategy combined with the gradient change in the setpoints, allows the controller to follow the system more closely and therefore provide a more precise input profile based on the system needs. Similarly, the selection of the control laws continues to follow the cyclic profile presented earlier.

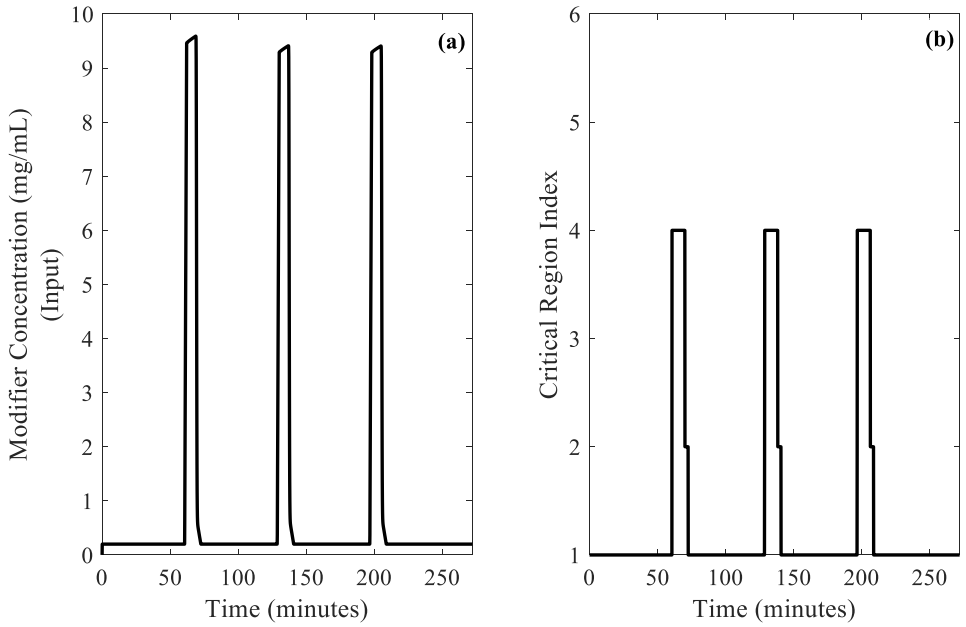

Figure 4.31 (a) Input profiles as generated by the controller and (b) Evolution of the critical regions/control laws during the 'closed-loop' controller validation, under the 'setpoint shift' strategy.

4.6.3 SIMO system (with disturbance)

The last scheme where we apply the "setpoint shift" strategy and we check the controller capabilities is the single-input multiple-output controller that considers variations in the feed stream as measured disturbance (Section 4.5). Also in this case the flow rate is maintained constant throughout the simulation. Figure 4.32 illustrates the comparison between the predefined setpoints and the outputs of the process model, where a good agreement is observed. In particular, the time delay has been completely eliminated for all measured outputs, while the output of interest (Figure 4.32b) demonstrates the most satisfactory behavior. The latter can be attributed to the different weight distribution of the outputs in the objective function (QR matrix) as discussed in section 4.5.2. The input profile (Figure 4.33) is

characterized by the same width in the peaks and a cyclic behavior similar to the results presented above (Figure 4.26a).

However, we observe that here (Figure 4.33) the satellite actions are merged to the main modifier feed. The latter is a result of the setpoint shift and consequently the shift of the input actions backwards in time. As a result, the selection of critical regions presented in Figure 4.33b is different than the one presented above where no shift in the setpoints is applied (Section 4.5). Moreover, also in this case the periodicity in the control laws is maintained, indicating that the proposed scheme can lead to stable operation where CSS can be achieved.

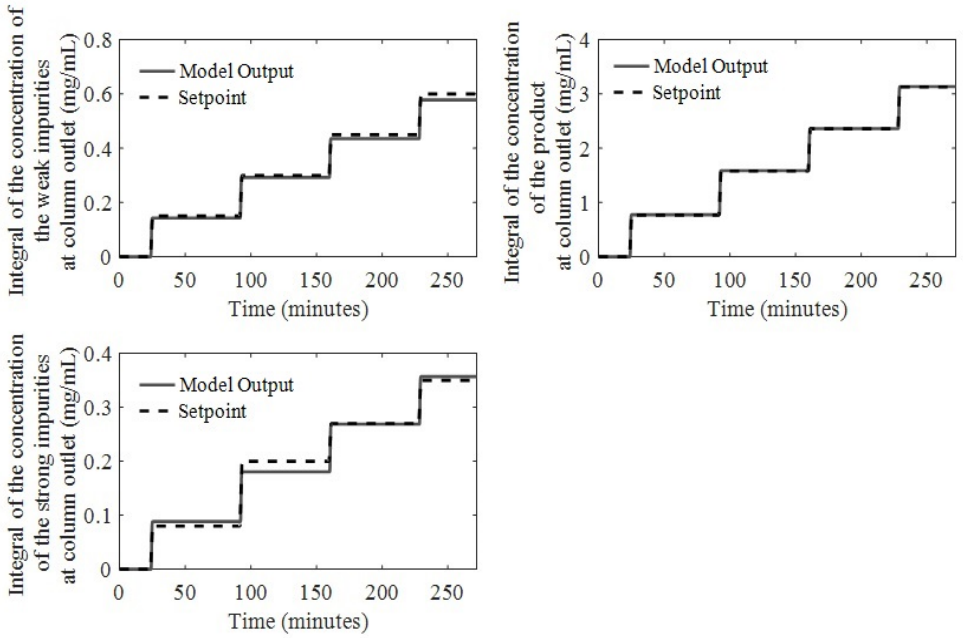

Figure 4.32 Comparison of the predefined setpoint (---) and the output of the process model simulation (—) as resulted from the controller closed-loop validation for (a) weak impurities, (b) product and (c) strong impurities over time [under constant flow rate (0.6 mL/min), considering the feed composition as measured disturbance (Figure 4.24)], under the 'setpoint shift' strategy.

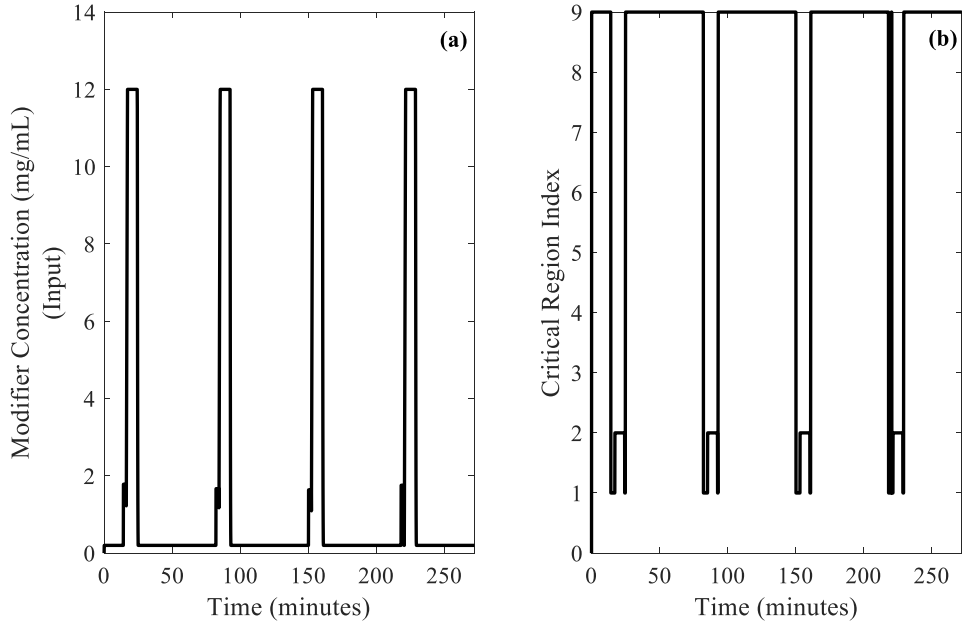

Figure 4.33 (a) Input profiles as generated by the controller and (b) Evolution of the critical regions/control laws during the 'closed-loop' controller validation [under constant flow rate (0.6 mL/min), considering the feed composition as measured disturbance (Figure 4.24)], under the 'setpoint shift' strategy.

4.6.4 Conclusions

In this section we investigate the time delay observed in the assessment of previously developed controllers (Sections 4.3, 4.4 and 4.5). We demonstrate how this delay is associated to the operating flow rate and the column volume. In particular, the repetitive delay corresponds to the residence time that is an inherent characteristic of chromatographic systems and cannot be manipulated by the operator. Aiming to improve the system performance and educate the designed controllers to compensate for this delay, we suggest a novel approach, where the setpoints are shifted in time. More specifically, we exploit the fact that both the column volume and the operating flow rate are known a priori and therefore we use them to pre-calculate the residence time. Following that we create two sets of setpoints. The first one is shifted in time based on the calculated delay and is used to update the controller, while the second corresponds to the desired elution times. This strategy is applied to the three different control schemes presented earlier (Sections 4.3, 4.4 and 4.5) and the controllers are assessed. It is observed that the proposed approach manages to efficiently eliminate the time delay in all examined cases, without affecting the system periodicity and/or optimal control actions. The "setpoint shift" strategy presented here does not seem to significantly affect the controllers performance with respect to setpoint tracking, as the offsets discussed previously are observed here as well. In the following section (Section 4.7) we

consider the most complex case of the SIMO controller with disturbance and we examine its behavior under various flow rate values, following the strategy presented here.

4.7 Controller performance under various Flow Rates

As resulted from the sensitivity tests (Section 4.2.2.2), the flow rate does not affect the quantity of the ingredients extracted by the column. Therefore, the control schemes presented above do not consider the flow rate as part of the problem formulation and the controller performance is assessed under a constant flow rate within the range of interest. However, according to the principles of chromatography (Guiochon, 2012) the flow rate controls the speed of the extraction and effectively the elution profile. As discussed in section 4.6, the operating flow rate in conjunction with the column volume, are responsible for the residence time that results in an inherent time delay affecting the elution.

It is therefore of vital importance to assess the performance of the designed controllers under various flow rate values, covering the whole feasible operating space. Here, we assess the most complex case of the SIMO system with disturbance (Section 4.5) under three different flow rate values (low, average and high ranging from 0 mL/min to 1 mL/min), applying the "setpoint shift" strategy, presented above (Section 4.6). The range chosen for the inlet flow rate is in line with the specifications/feasible operating bounds of the column (pressure over the packed bed) and the resulting linear flow rates are typical for chromatographic processes, described by the mathematical model that is presented in Appendix B. The latter has been validated across this range of conditions and therefore can be trusted for the in-silico validation of the controller (Ströhlein et al., 2006a, Aumann and Morbidelli, 2007, Aumann et al., 2007, Stroehlein et al., 2007, Aumann and Morbidelli, 2008, Müller-Späth et al., 2008, Aumann et al., 2009, Grossmann et al., 2010, Müller-Späth et al., 2010a, Aumann et al., 2011, Muller-Spath et al., 2011). Table 4.10 illustrates the operating details of the three case studies.

Table 4.10 Details used for the assessment of the controller behaviour under various flow rate values.

Column Volume (mL)	Flow Rate (mL/min)	Residence Time (delay) (min)
5	0.2	25
	0.6	8
	1	5

For the comparison studies, the disturbance profile shown in Figure 4.24 is followed. It should be mentioned that in each case, the setpoints are adjusted subjected to the system feasibility. In all three cases (Figure 4.34) the controller successfully meets the setpoint requirements, indicating a cyclic input profile. Depending on the flow rate values, the input profile may, however, vary. More specifically, it is observed that the higher the flow rate, the faster the control action. From a physicochemical point of view, high flow rates indicate higher speed within the column and therefore the input has a more aggressive impact on the output profile. Consequently, the controller has to react faster when operating under maximum flow rate (Figure 4.34a). On the contrary, in the third case, where the controller operates under minimum flow rate, the setpoints are shifted in time (Figure 4.34c.2), as the residence time is prolonged and the control actions are broader (Figure 4.34c.1). It can be observed that the "setpoint shift" strategy presented in Section 4.6 copes well with various flow rate ranges and manages to efficiently eliminate the inherent time delay.

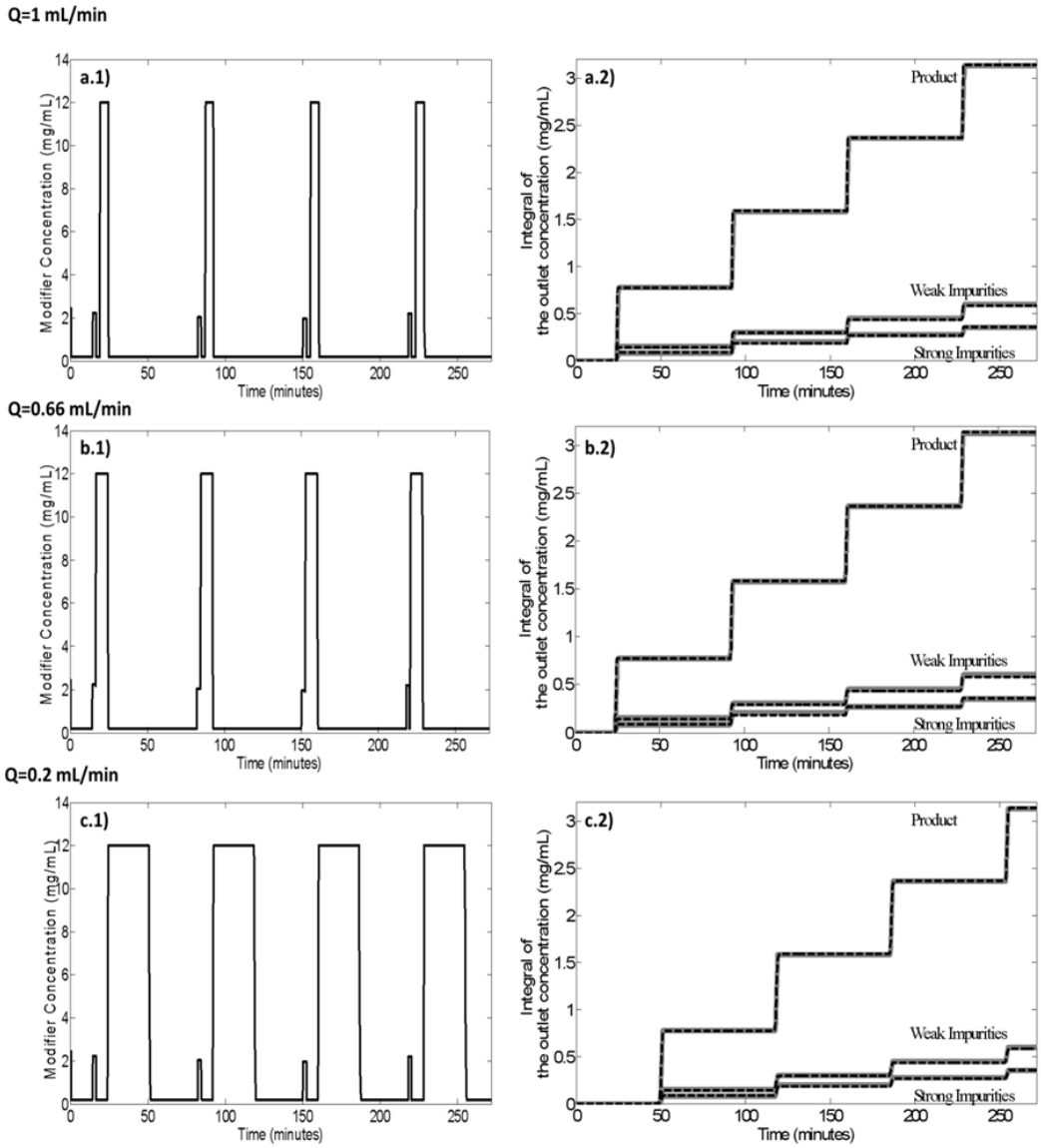

Figure 4.34 Comparison results for three flow rate values (Q= 1, 0.6 and 0.2 mL/min). The column on the left represents the input profile (modifier concentration) indicated by the controller that leads to the output profile (integrals of the components concentrations, right column) [using the setpoint shift strategy].

4.8 Conclusions

In this chapter we present the development of advanced, model-based control strategies for single-column chromatographic systems. We examine a single-column system based on the principles of the MCSGP process, used for the separation of a ternary mixture containing weak impurities, antibody and strong impurities. The main objective of this work is the design and testing of novel control strategies that is able to track the system at hand, while maintaining its key features, such as the periodicity and non-linearity. The case studies presented in this chapter aim to test the developed controllers under a variety of conditions and do not assess their performance based on final purity and/or yield. It is acknowledged that the latter correspond to the main parameters based on which the efficiency of a chromatographic separation is assessed, however the goal of the presented studies is focused on system tracking, that is understanding how the controller can maintain a set-point and reject disturbances and hence using a more fundamental approach. In real-time application the process is pre-optimized (computationally and/or experimentally) and issues such as optimal feeding strategy, optimal flow rate value and switching times are defined prior to the execution and automation of the process. The optimization policies yield thereafter the optimal setpoints under which the controller should operate. Here, we trust the validated mathematical model in order to specify the setpoints for each presented case study.

The first objective of this chapter is to fully explore and understand the system dynamics. For this reason, we execute preliminary sensitivity tests, where the effect of the inputs on the outlet concentrations of the mixture components is assessed (Section 4.2.2). Based on this, we reduce the input set to a single entity (the modifier concentration) that is considered as the most significant for the eluted quantities. Considering the interactions resulting from the sensitivity tests we examine the development of advanced multi-parametric controllers on three case studies: (i) three single-input, single-output systems under continuous feeding (Section 4.3), (ii) a single-input, multiple-output system under continuous feeding (Section 4.4) and (iii) a single-input, multiple-output system under variable feeding, considering the latter as disturbance (Section 4.5). At the same time, we propose a novel strategy (Section 4.2.2), where we track the integral of the outlet concentrations of the mixture components, allowing continuous process control. This can effectively lead to better, ‘tailor-made’ control actions compared to ‘cycle-to-cycle’ control. Practically, the designed controllers can initially receive frequent feedback within seconds from the UV/VIS detectors (Chapter 2 & Chapter 3) and can later also be updated by more accurate measurements resulting from the HPLC that requires longer analysis time. This bi-level feedback offers a two-step verification of the process state and allows the controller to re-estimate a better forward action in case the

original feedback received from the UV is not accurate enough. The integral of the outlet concentrations can be computed using commercially available software packages (e.g. FORTRAN, MATLAB) and linked to a software package used for post-analysis of chromatograms that uses the integral function for the integration of the elution peaks (e.g. UNICORN Control Software by GE Healthcare).

The presented controllers manage to efficiently monitor the system and track the predefined setpoints to a satisfactory extent. As discussed earlier there are cases where the controllers demonstrate increased deviations (under- and over-shoots) from the predefined setpoints, particularly in the case of strong impurities. In an experimental/industrial application this could entail risks related to increased impurity content in the final product formulation that falls out of regulatory specifications. However, it should be underlined that the case studies presented here aim to test the controllers against extreme and fast-changing conditions and ensure that they can track the system adequately and do not necessarily focus on optimizing purity and yield. The latter is usually achieved via optimization studies prior to the industrial application of the setup. Nevertheless, the presence of the offsets is briefly discussed in this chapter and various solutions are proposed in case the issue persists even at events where the process is optimized. Such offsets can be tackled in several ways: (i) through direct tuning of the controller (e.g. increasing the weight of the perturbed output variable), (ii) introduction of an integral state to minimize the offset as part of the objective function in the control problem Sakizlis et al. (2004a) and (iii) state estimation techniques (e.g. Kalman filter) that will allow estimation of the system states and will provide more accurate control actions (Voelker et al., 2010).

All presented control schemes are characterized by periodicity in the input profiles that is inherently suggested by the designed controllers. The latter is of vital importance as it shows that the proposed schemes can lead to cyclic operation, where cyclic steady state can be achieved. The presented systems are characterized by a repetitive time delay that is equal to the column residence time. The latter is directly correlated to column volume and the operating flow rate that has been excluded from the control problem formulation. Nevertheless, under known volume and flow rate, this delay can be pre-computed and therefore it can be handled by a shift of the setpoints in time. On that end, we suggest and test the "setpoint shift" strategy (Section 4.6), where we pre-calculate the residence time and we shift the setpoints in time. The efficiency of the strategy is successfully tested for: (i) all presented cases under average flow rate and (ii) the most complex case (SIMO system with disturbance) under a wide range of operating flow rates (Section 4.7). Chapter 5 is focused on the development of advanced control strategies for multi-column systems, considering a two-

column chromatographic separation setup based on the principles of the MCSGP process. Key challenges such as unavailable measurements at the connection point are also discussed.

Chapter 5.

Model-based Control of Multi-Column Chromatographic Systems *following the PAROC framework*

*Parts of this work have been performed in the framework of the OPTICO European Project (G.A. No.280813).

**The results presented in this chapter have been included in the following publications:

1. *Papathanasiou et. al. (2017). Intelligent, model-based control towards the intensification of downstream processes. Computers & Chemical Engineering. Article in Press*
2. *Papathanasiou et. al. (2016). "A centralized/decentralized control approach for periodic systems with application to chromatographic separation processes". 11th IFAC Symposium on Dynamics and Control of Process Systems, including Biosystems; 2016;, IFAC-PapersOnLine 49 Paper 7, pp 159-164*
3. *Papathanasiou et. al. (2016).. "Computational tools for the advanced control of periodic processes - Application to a chromatographic separation", 2016, In Computer Aided Chemical Engineering, Elsevier, Volume 38. pp. 1665-1670.*
4. *Papathanasiou et. al. (2016). "Advanced control strategies for a periodic, two-column chromatographic process". IEEE International Conference on Automation, Quality and Testing, Robotics (AQTR); 2016; pp 387-392.*

5.1 Introduction

In Chapter 4 we investigated the development of advanced control strategies of single-column chromatographic systems with primary goal to design the control schemes in a way that allows continuous process monitoring and stable operation. The case studies presented above can be applied in various examples, where a single column is used or in cases where columns operate in batch mode (e.g. B-phases of the MCSGP process). However, in order to increase the process efficiency, chromatographic processes usually consider multi-column equipment, where the columns interact with each other. Such configurations can be found in SMB or other chromatographic separation processes, where the mixture is transferred from one column to the other. The operation of such systems is considered to be continuous and therefore online measurements become even more challenging to obtain.

In this chapter we focus on the development of advanced control strategies of multi-column systems and in particular a two-column configuration, based on the principles of the MCSGP process (Section 3.3). We follow the PAROC framework and software platform (Pistikopoulos et al., 2015) for the design and testing of the model-based controllers. The main objective of this chapter is the design and testing of novel control strategies for the connected system, handling issues with unavailable measurements when the impure stream is transferred from one column to the other. Section 5.2 describes the twin-column system, as well as the framework followed for the development of the control scheme. The latter is discussed in detail in section 5.3, where we demonstrate how we apply PAROC for the development of two, advanced, single-input multiple-output parametric controllers. Following their design, the controllers are tested in silico, in a 'closed-loop' fashion under two sets of operating flow rates and their performance is assessed. Lastly, in section 5.4 we discuss a novel control concept for the twin-column MCSGP process, where we suggest a centralized/decentralized control approach, monitoring each operating mode independently.

5.2 Two-column System

Based on the principles of the MCSGP process, we consider the system presented in Figure 5.1, comprising two identical chromatographic columns. The thermodynamic and kinetic equations described in Appendix B remain the same for both columns, however the mass balances around them are modified to describe the mixing (Equation 3.2). For simplicity, we will refer to the two columns as: Column 1 (the one eluting the mixture) and Column 2 (the one receiving the recycling stream). For the purposes of this case study, we consider that feed is introduced to Column 1 in a periodic fashion. It should be underlined that this case study aims to design a controller that is able to track the system, capturing its main features such as the periodicity and system non-linearity. Although in chromatographic separation ultimately the process performance in terms of purity and yield needs to be considered, the described controller has a more fundamental purpose and therefore numeric results for these parameters are not further discussed.

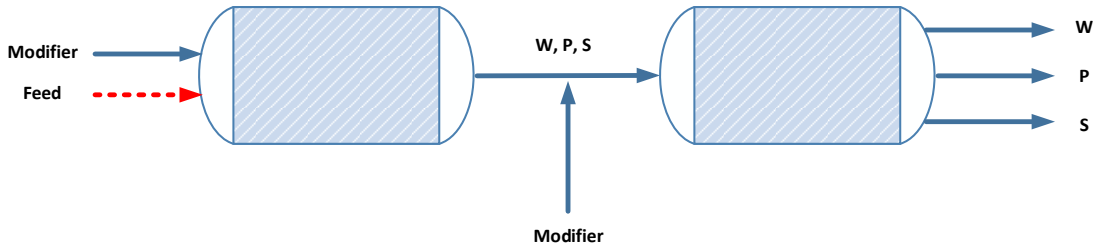

Figure 5.1 Two-column system considering: (1) for Column 1: the modifier concentration as input & the feed composition at the column inlet and the three mixture components at the column outlet and (2) for Column 2: the modifier concentration & the internally recycled components from Column 1 at the column inlet and the three mixture components at the column outlet.

The development of advanced control strategies for such complex systems requires a rigorous procedure that can ensure seamless design and testing of the proposed controllers. Here we follow the PAROC framework and software platform (Pistikopoulos et al., 2015) for the design and in-silico testing of advanced multi-parametric controllers. The framework, as described in Section 0 comprises 4 main steps: (i) model development, (ii) model approximation, (iii) design of the mp-MPC controller and (iv) 'closed-loop' validation. Figure 5.2 illustrates the PAROC framework tailored for the purposes of this work. Section 5.3 describes the step-by-step application of framework for the control of the two-column system.

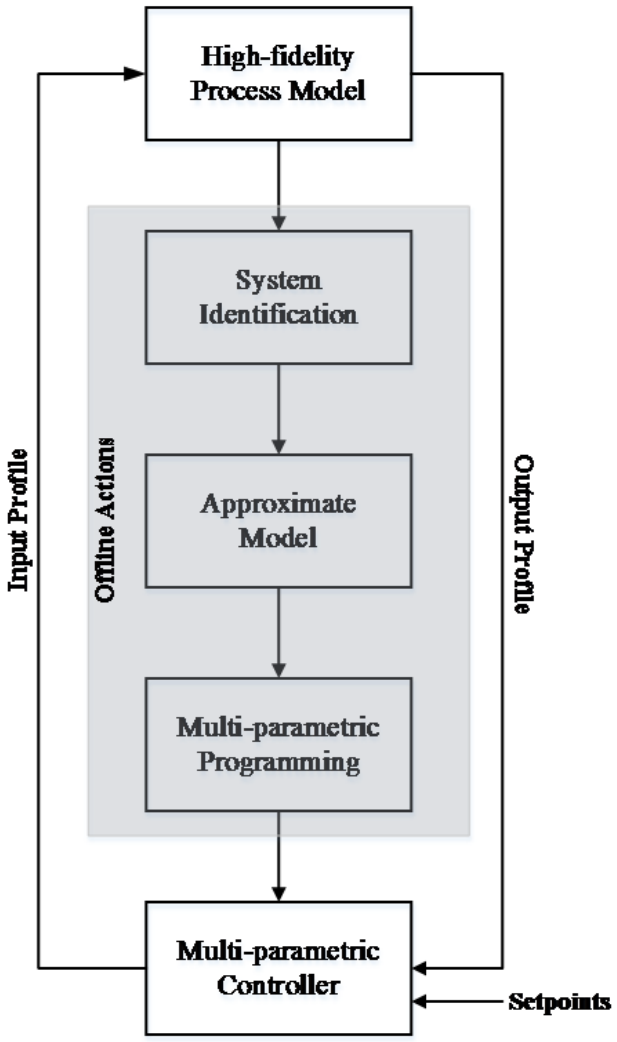

Figure 5.2 PAROC framework as followed for the development of the twin-column control scheme development and testing.

5.3 Control of the Two-column System via PAROC

5.3.1 Model development

The two columns shown in Figure 5.1 operate in series, aiming to increase process efficiency. Based on the operation of the MCSGP process (Section 3.3), during the I-phases, the outlet of Column 1 that elutes the impure fraction becomes the inlet Column 2 that undergoes gradient elution. To achieve separation, the impure fraction is mixed with additional modifier before entering the second column. The columns presented here are the same with the one studied in Chapter 4 and therefore the input/output set selection is based on the results from the sensitivity tests presented earlier (Section 4.2.2).

5.3.1.1 Input & output set selection

(i) Column 1

The operation of Column 1 is not affected by the second column and can be therefore considered similar to the batch operation. Therefore, the controller operating on Column 1 considers the modifier concentration as the sole input, the feed composition as measured disturbances and the integrals of the mixture components at the column outlet as outputs.

(ii) Column 2

As mentioned previously, the two columns are described by the same thermodynamic/kinetic equations, regardless of the system configuration. Consequently, the sensitivity of the inputs as described in Section 4.2.2 applies in this case as well and therefore, the modifier concentration is used as the only input. Similarly to the batch operation, we consider the integral concentrations of the three mixture components at the column exit as tracked outputs. However, in this case Column 2 receives the recycling stream exiting Column 1. Given the continuous nature of the process at this stage, no online measurements are available at the connection point between the two columns. However based on simulation results as well as offline experiments, the range of the mixture composition exiting Column 1 can be pre-defined and can be therefore treated as measured disturbance for the design of Controller 2. It is important to underline that although the output set considers the integrals of the outlet concentrations (mg), the disturbances considered by Controller 2 correspond to the actual concentrations of the mixture components (mg/mL). This is to maintain consistency with the process model that uses the concentration profiles in order to describe the events within the column.

5.3.2 Model approximation

Based on the fact that both the columns and the input/output set remain the same, the approximate model derived in Section 4.4 can be used here as well. In particular, both columns are described by the same model equations. Table 5.1 illustrates the details of the approximate models.

Table 5.1 Input/Output sets and measured disturbances as considered for the two-column system.

	Column 1	**Column 2**
Input	Modifier Concentration	Modifier Concentration
Output	Integrals of the outlet concentrations of W, P, S exiting Column 1	Integrals of the outlet concentrations of W, P, S exiting Column 2
Disturbance	Feed composition	Component concentrations transferred from Column 1
Approximate Model	As presented in Section 4.4.1	

5.3.3 Design of the mp-MPC controllers

Following the PAROC framework, the next step is the formulation and solution of the mp-MPC problem that will lead to the map of optimal control actions. Figure 5.3 demonstrates the control scheme considered for the current configuration, where Controller 1 acts on Column 1, considering: (i) the modifier concentration as input, (ii) the feed as measured disturbances and (iii) the integrals of outlet concentrations of the three mixture components as outputs. Similarly, Controller 2 monitors the activity of Column 2, considering: (i) the modifier concentration as input, (ii) the outlet concentrations of Column 1 as measured disturbances and (iii) the integrals of outlet concentrations of the three mixture components as outputs. It should be underlined that the flow rate has been excluded from the problem formulation and thus is maintained constant for both columns. Given that the two columns are identical, they are described by the same approximate model and the same operational constraints, it suffices to formulate and solve only one mp-P problem. The latter will lead to a map of solutions that can be used for both columns

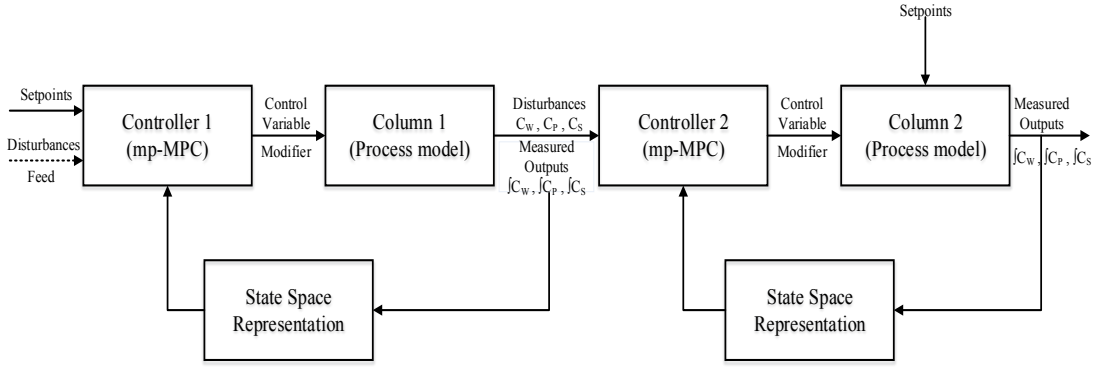

Figure 5.3 mp-MPC control scheme as designed for the two-column system.

Table 5.2 Tuning parameters used for the formulation and solution of the mp-MPC problem.

Tuning Parameter	Explanation	Value	Tuning Parameter	Explanation	Value
OH	Output Horizon	4	**Umin**	Input upper bound	0.2
NC	Control Horizon	2	**Umax**	Input lower bound	12
QR	Weights on the outputs	$[10^2\ 10^4\ 10^2]$	**Dmin**	Disturbance upper bound	[0 0 0]
Q	Weights on the states	$1I$	**Dmax**	Disturbance lower bound	[10 10 10]
R	Weights for the inputs	1	**Total number of critical regions**		9
P	Terminal weight for the states	Riccati equation*			

* The Riccati equation is as follows: $P = A^T PA - (A^T PB)(B^T PB + R)^{-1}(APB) + Q$, where A and B are the matrices of the state space model and P, R, Q the tuning parameters used for the control problem formulation.

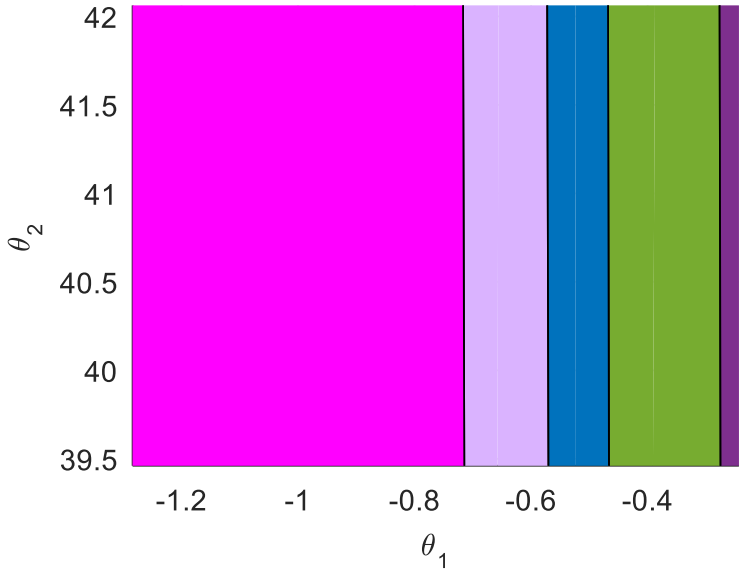

Figure 5.4 Two-dimensional projection of 5 critical regions polyhedral. States: $x_1 = 0.0059$, $x_2 = \theta_2$, $x_3 = 0.1165$, $x_4 = 0.0238$, Disturbances: $C_i^{feed} = [0.01\ 0\ 0.001]$, Outputs: $\int C_i = 1$, Output Setpoints: $\int C_W^{set} = 2$, $\int C_P^{set} = 2$, $\int C_S^{set} = \theta_1$, where $i = W, P, S$.

Table 5.2 illustrates the tuning parameters used for the design of the controller. The multi-parametric programming problem is solved using the POP® toolbox (Oberdieck et al., 2016) for robust/explicit mp-MPC, within PAROC. The map of solutions for this problem comprises 9 critical regions that correspond to the control laws. A higher weight in the objective function is chosen for the targeted product (*QR*) as it is the output of interest. Figure 5.4 illustrates the map of solutions as a function of two of the control problem parameters.

5.3.4 In-silico evaluation of the controller performance

The controllers designed above are tested in-silico against the process model and their performance is assessed. Based on the schematic shown in Figure 5.3, the two columns and therefore the respective controllers are operated in tandem. The two columns start empty, and feed is introduced to Column 1 in a periodic fashion (Figure 5.5) (following the original feeding strategy of the MCSGP process, please refer to Section 3.3). Controller 1 receives feedback from the outlet of Column 1 and returns the respective optimal control action (modifier concentration) to reach the predefined setpoints. Following that, Column 2 receives the fraction exiting Column 1 that is treated as disturbance by Controller 2 (Figure 5.7). The latter, receives feedback from the output

measurement (integrals of the outlet concentrations) and returns the optimal modifier concentration.

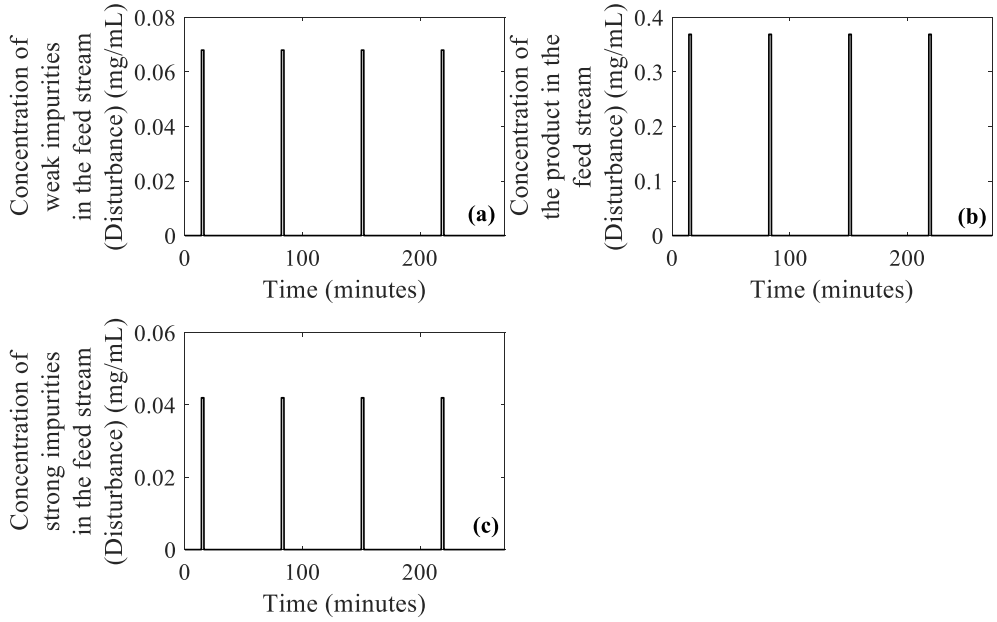

Figure 5.5 Disturbance profile on Column 1 during the 'closed-loop validation' corresponding to the concentrations of: (a) weak impurities, (b) product and (c) strong impurities in the feed stream.

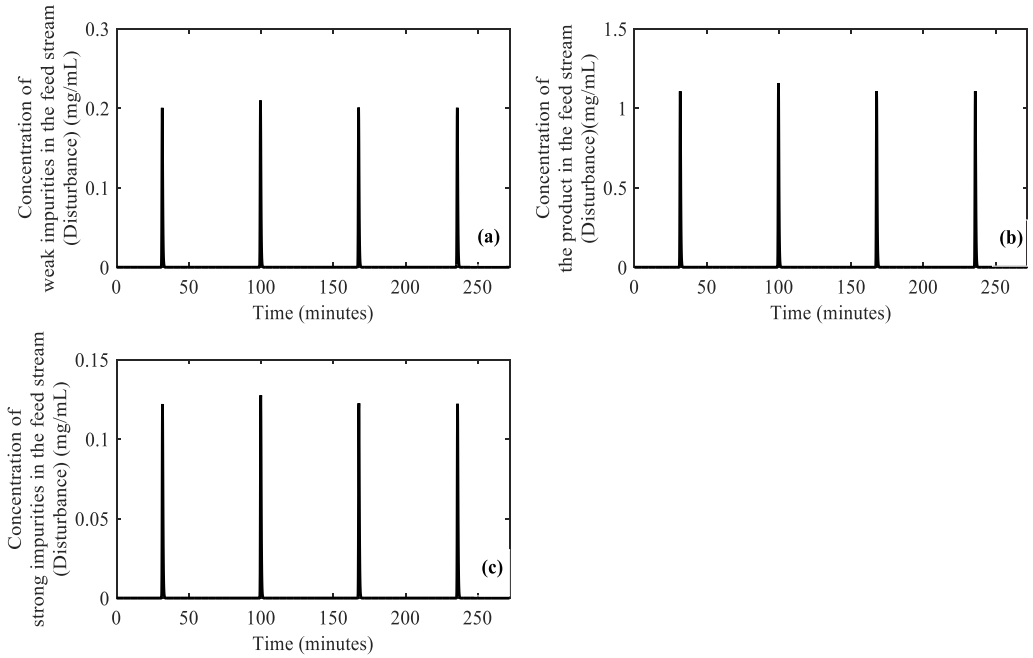

Figure 5.6 Disturbance profile on Column 2 during the 'closed-loop validation' corresponding to the concentrations of: (a) weak impurities, (b) product and (c) strong impurities eluting from Column 1.

For the in-silico validation, we apply both the 'gradient setpoint change' (Section 4.4.4) and the 'setpoint shift' (Section 4.6) strategies. Table 5.3 illustrates the operating conditions used in this example for the calculation of the residence time (time delay). Figure 5.7a and Figure 5.8 illustrate the input profile (modifier concentration) as designed by Controller 1 and the comparison between the predefined setpoints and the outputs, respectively. It is observed that the behavior of Controller 1 is identical to the one of the batch operation (Section 4.5) as the operation of Column 1 and effectively the actions of the controller are not affected by the configuration illustrated in Figure 5.1. Conversely, although Controller 2 shares the same map of solutions with Controller 1, it is characterized by a different behavior during the in-silico validation. In the interconnected mode, Controller 2 is operated under disturbances that occur from the impure fractions transferred from Column 1. The disturbance profile (Figure 5.6) corresponds to the component concentrations at the exit of Column 1 and is a result of the process model simulation under 'closed-loop' in tandem with Controller 1. The disturbance profile can also be post-calculated by the derivation of the outputs of Column 1 (Figure 5.8). The elution peaks are of approximately 1.5 min duration, similarly to the gradient change of the setpoints defined for Controller 1.

Table 5.3 Operating details used during the 'closed-loop', in-silico validation for the two columns. The details are used for the calculation of time delay and therefore the setpoint shift strategy, based on Equation 4.4.*

	Column Volume (mL)	Flow rate (mL/min)	Residence Time (time delay, min)
Column 1	5	0.6	8
Column 2		1	5

In order to track the setpoints (Figure 5.9), Controller 2 is returning the input profile shown in Figure 5.7b. Contrary to the input of Controller 1 (Figure 5.7a), here, the periodic profile is not observed. This can be attributed to the fact that at this stage of the process, Column 2 is continuously receiving the outlet of Column 1. In particular, apart from the impure fractions (disturbances, Figure 5.6), Column 2 is also receiving the amount of the modifier that exits Column 1. This is considered by Controller 2 and therefore feeds only the essential amount of modifier in order to reach the desired setpoints. It is observed (Figure 5.7b) that in all control

* Due to confidentiality agreement with the Morbidelli Group (ETH Zürich) the exact values cannot be disclosed and therefore only estimates are provided.

actions, the controller starts feeding modifier approximately 5 min before the upcoming setpoint change to compensate for the residence time. This is a combined result both from the knowledge transferred from the process model as well as from the "setpoint shift" strategy. Particularly interesting is the second, wide input action, where modifier is fed in the system for approximately 70 min. During this time frame, the controller is aiming to compensate for both the occurring disturbances (Figure 5.6) and the setpoint tracking (Figure 5.9). A satisfactory agreement between the setpoints and the tracked outputs is observed, characterized by less than 2% offset (Figure 5.9). Exceptions to the latter are the first and third setpoints of the strong impurities that demonstrate a significant offset of approximately 10%. This could be attributed to the control tuning parameters and in particular the QR values determining the weight of the three outputs in the objective function of the control problem (please also refer to the studies on the tuning parameters presented in Appendix B). Increasing the weight of the strong impurities could potentially lead to more accurate tracking of the output variable. It should be also underlined that the main objective of the proposed controller is to efficiently track the system, maintaining key features such as the periodicity (Figure 5.7). Therefore, attributes such as purity and/or yield are not assessed here. Nevertheless, since the proposed control strategy can efficiently track the system under various conditions, it can be expected that it will return satisfactory results also in real-time application, where the process is operated under pre-optimized setpoints. Here, however, the setpoints are retrieved from simulations of the validated mathematical model and correspond to a case study designed for this work aiming to test the controller behavior under a variety of conditions. In case the same deviations persist they could be tackled either directly (via the tuning parameters of the control) or indirectly using estimation methods (e.g. integral state or Kalman filter estimation techniques) (Sakizlis et al., 2004b, Voelker et al., 2010).

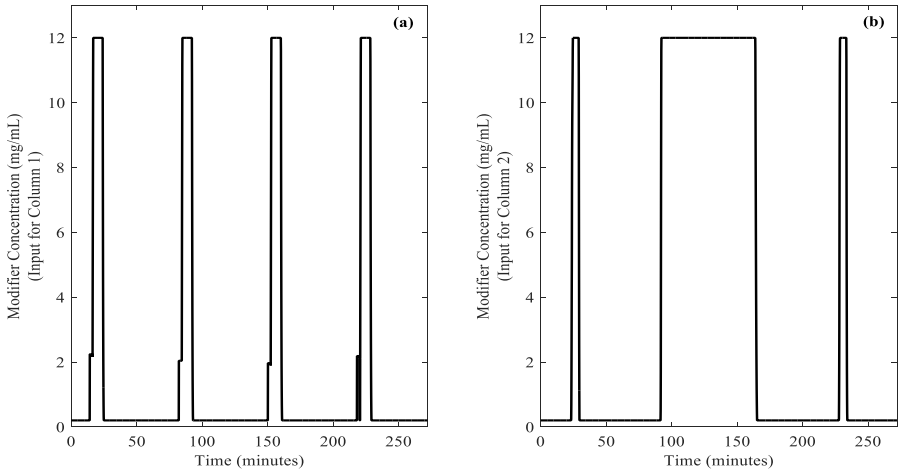

Figure 5.7 Input profiles as generated by: (a) Controller 1 and (b) Controller 2 during the 'closed-loop validation of the interconnected system.

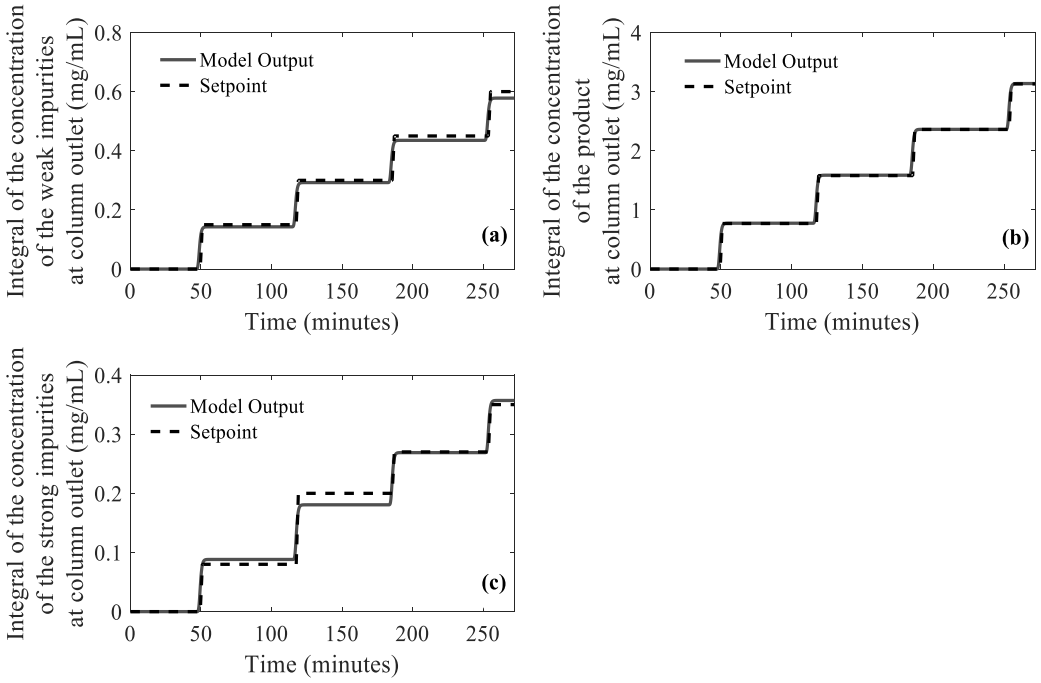

Figure 5.8 Column 1: Comparison of the predefined setpoint (---) [using the setpoint shift strategy] and the output of the process model simulation (—) as resulted from the controller closed-loop validation for (a) weak impurities, (b) product and (c) strong impurities over time [under the disturbance and input profile illustrated in Figure 5.10 and Figure 5.7a respectively].

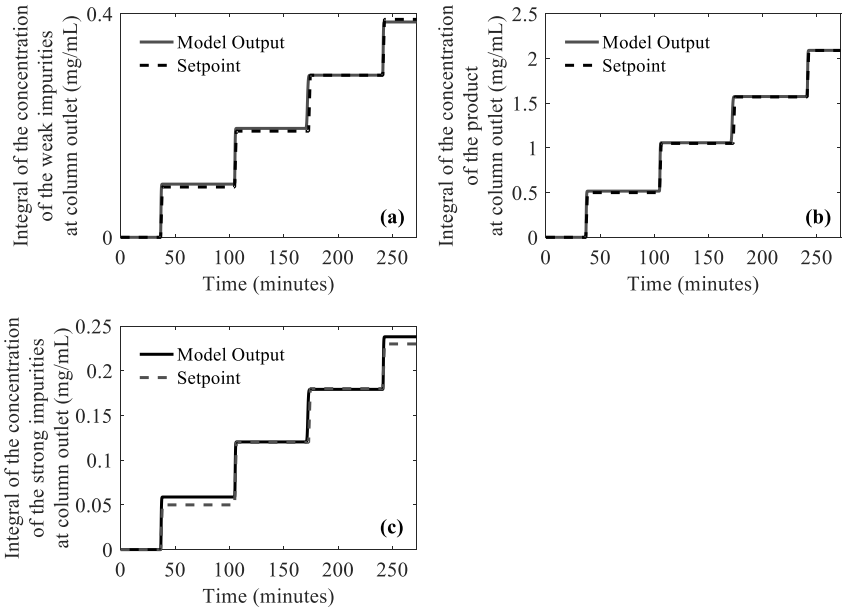

Figure 5.9 Column 2: Comparison of the predefined setpoint (---) [using the setpoint shift strategy] and the output of the process model simulation (—) as resulted from the controller closed-loop validation for (a) weak impurities, (b) product and (c) strong impurities over time [under the disturbance and input profile illustrated in Figure 5.11 and Figure 5.7b respectively].

5.3.5 Testing the controllers under different flow rates

The control scheme presented above is tested here under a different set of flow rates and the controller behavior is assessed. Table 5.4 summarizes the operating flow rate used for the new 'closed-loop' validation for each column. The "setpoint shift" strategy presented in section 4.6 is employed here as well.

Table 5.4 Operating details used during the 'closed-loop', in-silico validation for the two columns. The details are used for the calculation of time delay and therefore the setpoint shift strategy, based on Equation 4.4[*]

	Column Volume (mL)	Flow rate (mL/min)	Residence Time (time delay, min)
Column 1	5	0.2	25
Column 2		1	5

[*] Due to confidentiality agreement with the Morbidelli Group (ETH Zürich) the exact values cannot be disclosed and therefore only estimates are provided.

For the simulation, we consider that periodic feeding of predefined composition (Table 4.4) is introduced to Column 1 (Figure 5.3), while Column 2 received the recycling stream exiting Column 1. The disturbance profiles considered for Column 1 and 2 are illustrated in Figure 5.10 and Figure 5.11 respectively. Figure 5.13 illustrates the comparison between the output and the output setpoints of Controller 1, where a good agreement is observed. The controller manages to track the setpoints without significant offsets, returning a periodic input profile (Figure 5.12a) that is followed by periodicity in the control laws (Figure 5.12b).

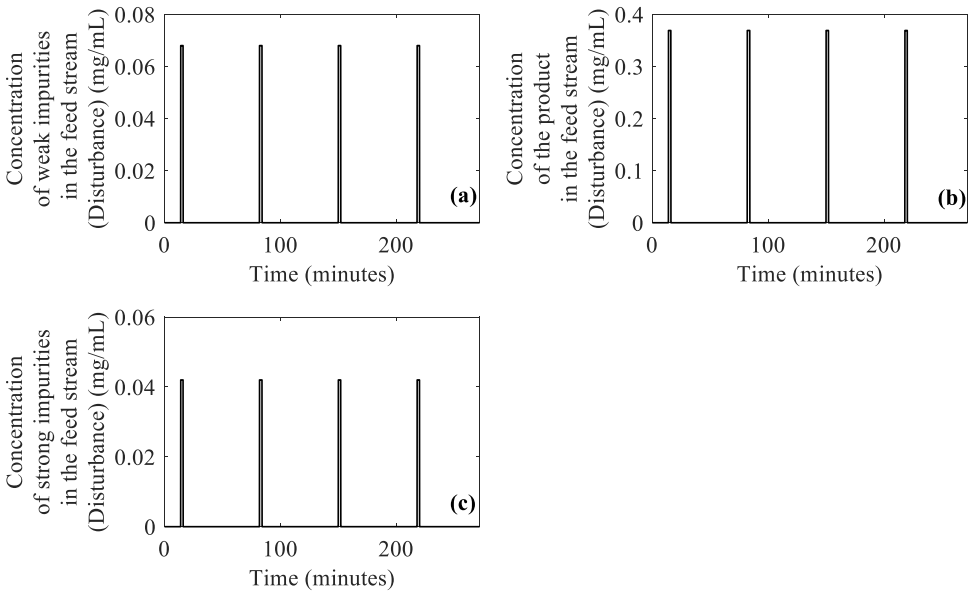

Figure 5.10 Disturbance profile on Column 1 during the 'closed-loop validation' corresponding to the concentrations of: (a) weak impurities, (b) product and (c) strong impurities in the feed stream.

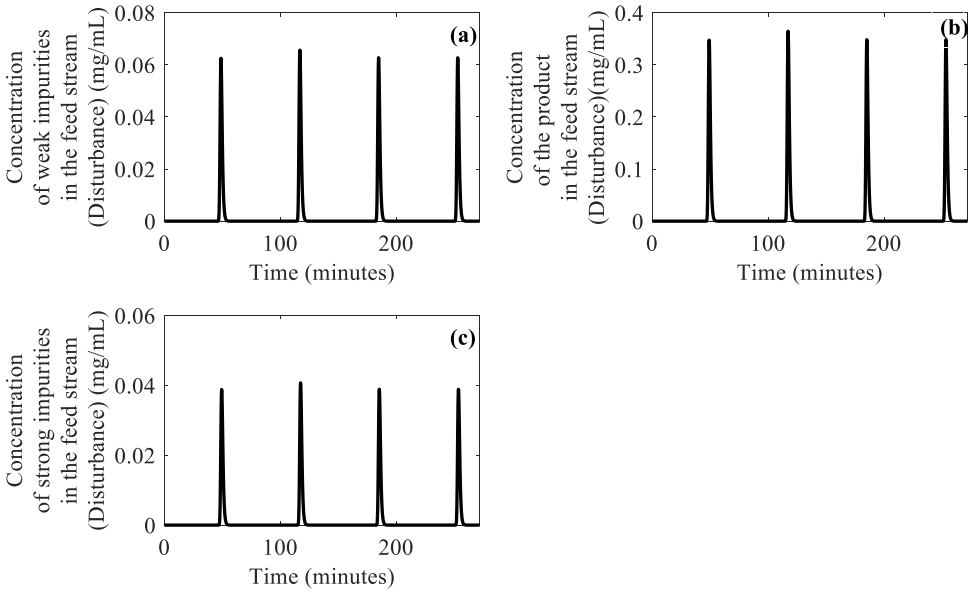

Figure 5.11 Disturbance profile on Column 2 during the 'closed-loop validation' corresponding to the concentrations of: (a) weak impurities, (b) product and (c) strong impurities eluting from Column 1.

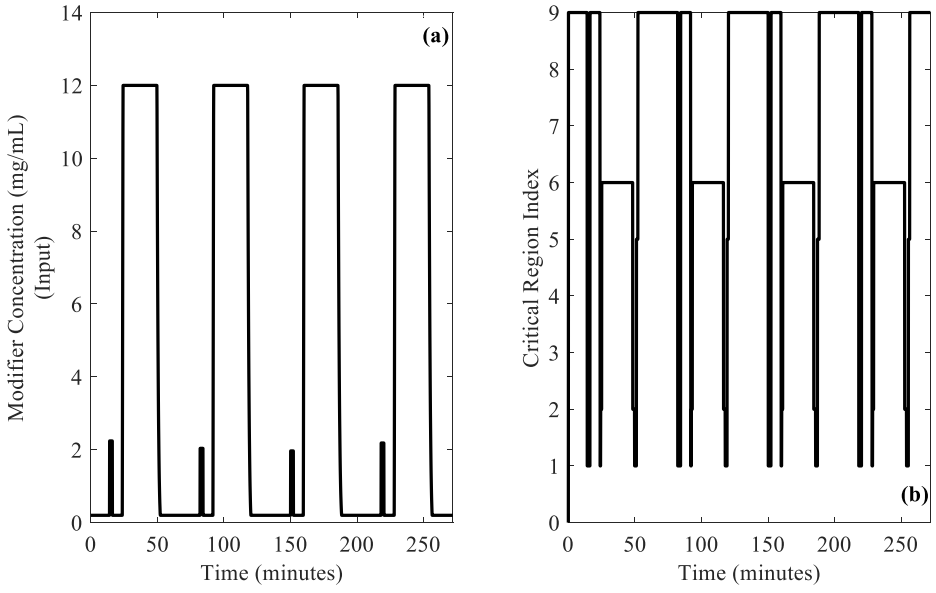

Figure 5.12 Column 1: (a) Input profiles as generated by the controller and (b) Evolution of the critical regions/control laws during the 'closed-loop' controller validation [under constant flow rate (0.2 mL/min), considering the feed composition as measured disturbance].

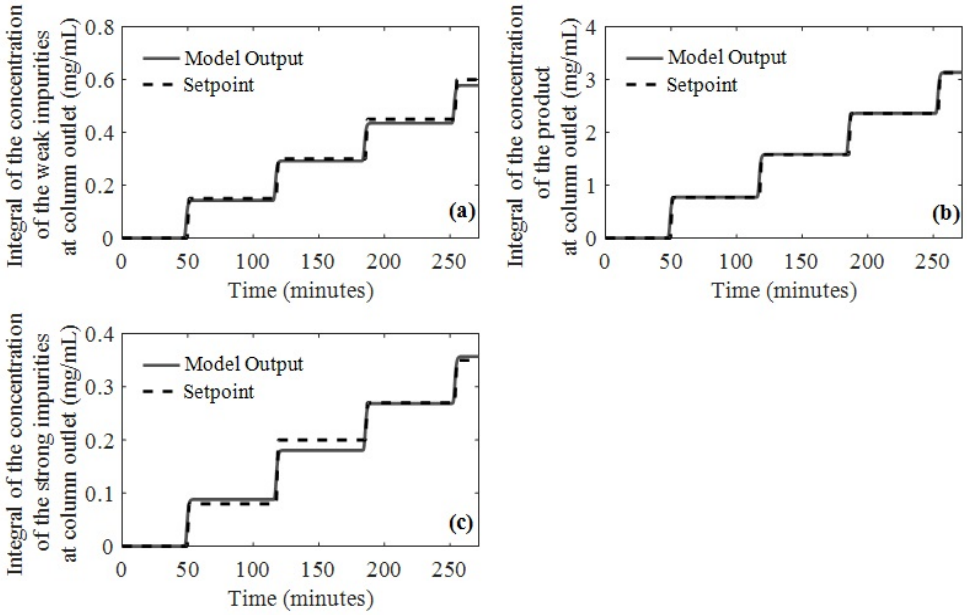

Figure 5.13 Column 1: Comparison of the predefined setpoint (---) and the output of the process model simulation (—) as resulted from the controller closed-loop validation for (a) weak impurities, (b) product and (c) strong impurities over time [under constant flow rate (0.2 mL/min), considering the feed composition as measured disturbance].

Compared to the results demonstrated previously (Figure 5.7a), here we observe broader actions in the input profile. This can be attributed to the fact that in this case Column 1 operates under decreased flow rate that leads to reduced speed within the column. Therefore, the time required for the column to be saturated with modifier is significantly longer, leading to delayed elution. The controller operating on Column 1 recognizes the slower speed of the eluting outputs and therefore suggests that modifier should be introduced to the system for a longer time. Conversely, the second controller operates on Column 2 that runs under maximum flow rate value. Therefore the respective input profile (Figure 5.14) is characterized by narrower peaks. It is observed that Controller 2 introduces decreased amount modifier to the system compared to Controller 1. The latter is a result of the stream transferred from Column 1 to Column 2, where modifier is transferred as well. This behavior indicates that due to their model-based nature, the controllers recognize the system requirements and provide only the necessary amount of raw material, paving the way towards the design of sustainable process of reduced cost. The peaks observed in the input profile, occur at the time points where the setpoints are increased and therefore actions taken by the controller in order to reach the desired setpoints on time. Furthermore, the periodicity characterizing both the input and the selection of optimal control laws, indicate that the cyclic

nature of the system has been inherited by the control scheme that can guarantee stable operation during the online application.

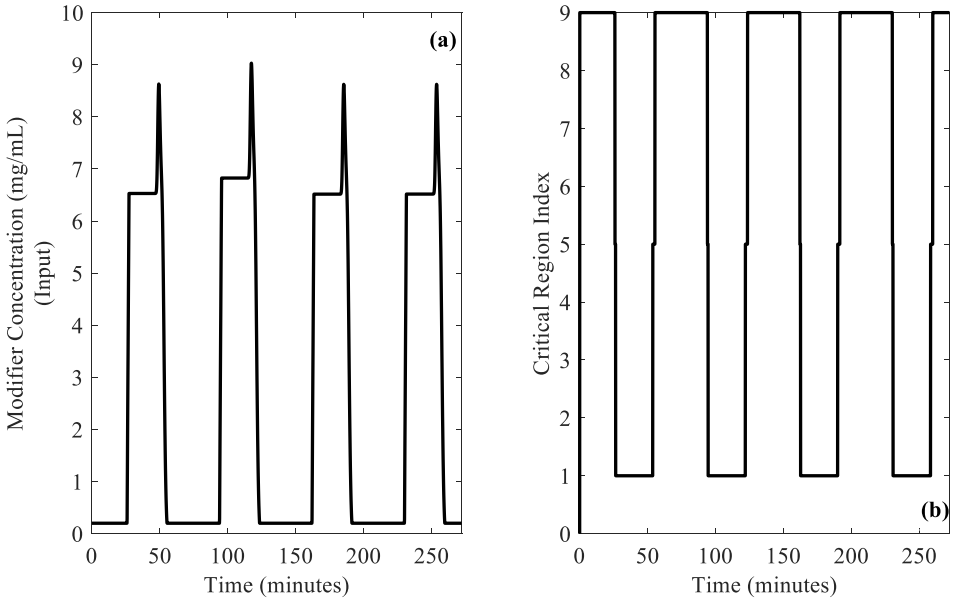

Figure 5.14 Column 2: (a) Input profiles as generated by the controller and (b) Evolution of the critical regions/control laws during the 'closed-loop' controller validation [under constant flow rate (1 mL/min), considering the outlet of Column 1 as measured disturbance].

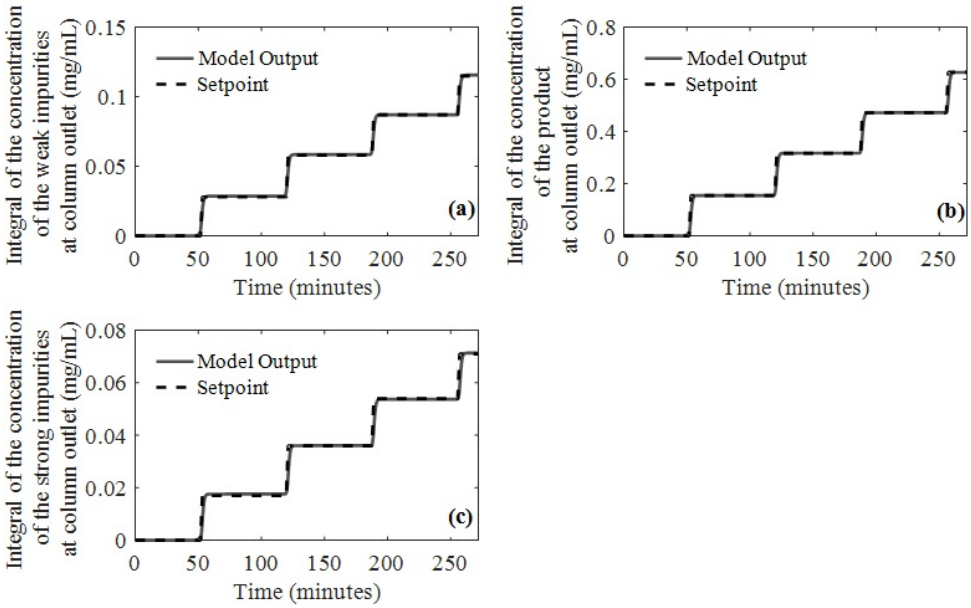

Figure 5.15 Column 2: Comparison of the predefined setpoint (---) and the output of the process model simulation (—) as resulted from the controller closed-loop validation for (a) weak impurities, (b) product and (c) strong impurities over time [under constant flow rate (1 mL/min), considering the feed composition as measured disturbance].

5.4 Control Concept of the Twin-Column MCSGP Process

The twin-column MCSGP process (Section 3.3.1) comprises two, identical chromatographic columns that operate in a semi-continuous fashion. The works that have been presented so far regarding the control of the process suggest 'cycle-to-cycle' approaches, where the setup is treated as a black box and the purity and/or recovery yield are monitored (Grossmann et al., 2010, Krättli et al., 2011, Krättli et al., 2013b). However, the feedback required for such approaches depends on offline measurements that require significant amount of time to be obtained. Additionally, updating the controller once per cycle may entail the risk of unexpected disturbances that will cause the system to deviate from its optimal performance. In addition, at the points where the process operates in a continuous fashion (I-phases) feedback measurements become unavailable and thus the controller cannot receive the required feedback.

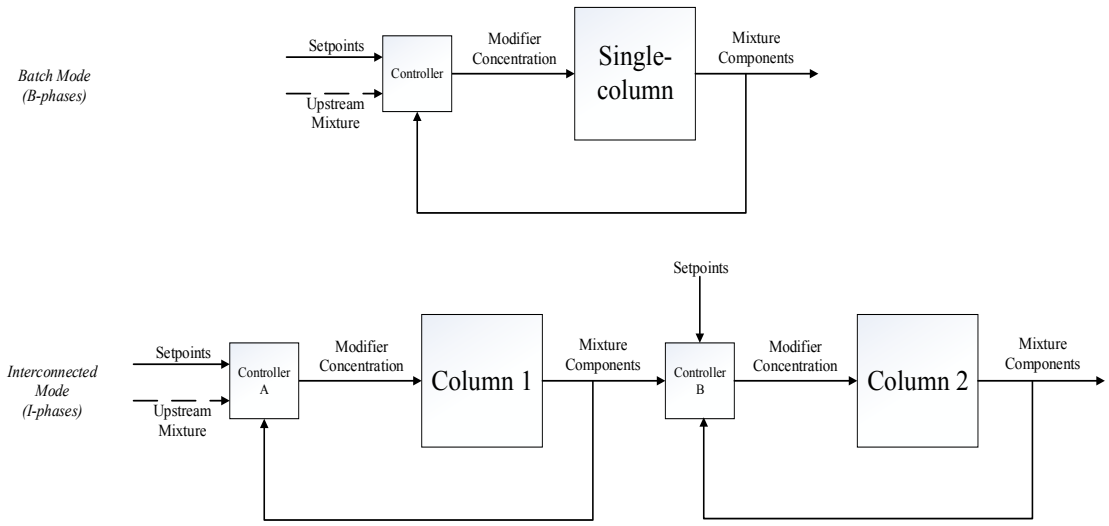

Figure 5.16 Proposed control scheme for the twin-column MCSGP process.

To tackle the above challenges, in this work we distinguish two operating modes of the process: (i) batch (B-phases) and (ii) interconnected (I-phases) mode and we propose a centralized/decentralized control strategy based on the control schemes presented above (Sections 4.5 and 5.3). As illustrated in Figure 5.16, we suggest the design of two independent control schemes, one for each operating mode. The first one accounts for the batch operation (B-phases) and considers that the columns operate independent from one another, while the second scheme is designed for the control of the continuous operation (I-phases) and takes into account the recycling stream from one column to the other. Exploiting the fact that the two columns are identical in terms of technical characteristics and physicochemical

properties, we suggest the formulation of a single control problem that will lead to the design of one parametric controller. The latter can operate on both columns, regardless of their operating mode and/or position in the setup. Following the work presented in the previous sections we suggest the schemes summarized in Table 5.5.

Essentially, the control scheme remains the same throughout the process cycle for both columns, thus reducing the computational work required for the design of the controllers. The key difference between the two operating modes and the column positions is the nature of the disturbances. In particular, during the I-phases the column on the left-hand side of the setup (Figure 5.16) is free of disturbance as no feed is introduced to the system, while the column on the right position receives the recycling stream of the impure fraction that is considered as disturbance by the controller (Section 5.3). Similarly, during batch operation (B-phases) the columns are either free of disturbance or they are receiving the feed that comes from the upstream. In either case, the designed controllers are immunized for a wide range of disturbance values (from 0 to +10% of the predefined experimental value) and thus they can account for any of the aforementioned scenarios.

Another main difference and therefore challenge for the proposed control schemes is the change in the operating flow rate that is adjusted accordingly in every process phase. As mentioned above (Section 4.6), the optimal flow rate values can be defined via dynamic optimization procedures and/or experimental optimization strategies and therefore they are known a priori. Consequently, following the strategy presented in Section 4.6 for the elimination of the time delay, the suggested controllers are able to handle variations in the flow rate simply by shifting the desired setpoints in time.

Table 5.5 Suggested control schemes for the operating modes of the twin-column MCSGP[*] (please refer to Chapter 3, Section 3.3).

Switch	Operating mode	Operating flow rate		Control Scheme	Results
		Column 1	Column 2		
Switch 1	I1	Average (0.4-0.8 mL/min)	Maximum (0.8-1 mL/min)	2 SIMO controllers with disturbance	Chapter 5 (Section 5.3)
	B1	Maximum (0.8-1 mL/min)	Maximum (0.8-1 mL/min)	2 SIMO controllers with disturbance	Chapter 4 (Section 4.5 & 4.6.3)
	I2	Low (0-0.4 mL/min)	Maximum (0.8-1 mL/min)	2 SIMO controllers with disturbance	Chapter 5 (Section 5.4)
	B2	Maximum (0.8-1 mL/min)	Maximum (0.8-1 mL/min)	2 SIMO controllers with disturbance	Chapter 4 (Section 4.5 & 4.6.3)
Switch 2	I1	Maximum (0.8-1 mL/min)	Average (0.4-0.8 mL/min)	2 SIMO controllers with disturbance	Chapter 5 (Section 5.3)
	B1	Maximum (0.8-1 mL/min)	Maximum (0.8-1 mL/min)	2 SIMO controllers with disturbance	Chapter 4 (Section 4.5 & 4.6.3)
	I2	Maximum (0.8-1 mL/min)	Low (0-0.4 mL/min)	2 SIMO controllers with disturbance	Chapter 5 (Section 5.4)
	B2	Maximum (0.8-1 mL/min)	Maximum (0.8-1 mL/min)	2 SIMO controllers with disturbance	Chapter 4 (Section 4.5 & 4.6.3)

[*] Due to confidentiality agreement with the Morbidelli Group, the exact flow rate values cannot be disclosed in this document, therefore their order of magnitude is provided. Flow rate values can vary between 0 mL/min and 1 mL/min.

5.5 Conclusions

This chapter is dedicated to the model-based control of multi-column chromatographic systems. We examine a two-column system based on the principles of the MCSGP process, where the outlet stream of Column 1 is transferred to Column 2 (Figure 5.3). We suggest a control scheme, where we design two, identical multi-parametric controllers, one for each column. The controllers consider the modifier concentration as the sole input and the integrals of the outlet concentrations of the three mixture components as outputs. For this study we consider that feed is introduced to the system in a periodic fashion and is considered as measured disturbance by the controller operating on Column 1. Similarly, the controller operating on Column 2 receives and considers as measured disturbance the concentrations of the mixture components eluting from Column 1. The proposed scheme is tested under two different sets of flow rate values and its performance is assessed.

The key objective of this chapter is the development of a control strategy that is able to handle the stream transferred from one column to the other, where measurements are unavailable, while maintaining the periodicity of the process. Although in chromatographic separation ultimately the process performance in terms of purity and yield needs to be considered, the described controller has a more fundamental purpose and therefore numeric results for these parameters are not further discussed. In real-time application the process is pre-optimized (computationally and/or experimentally) and issues such as optimal feeding strategy, optimal flow rate value and switching times are defined prior to the execution and automation of the process. The optimization policies yield thereafter the optimal setpoints under which the controller should operate. Here, we trust the validated mathematical model in order to specify the setpoints for each presented case study.

The suggested controllers demonstrate a satisfactory behavior, managing to track the predefined setpoints without significant offsets, returning periodic input profiles that are of vital importance for cyclic processes and the achievement of CSS. Additionally, it is observed that due to the internal recycle stream from Column 1 to Column 2, the modifier consumption from the latter is reduced as the controller recognizes that part of the modifier is transferred to the column. The latter indicates that the proposed strategy has the potential to lead to the design of novel process, characterized by reduced costs, as the amount of raw materials used can be significantly reduced. Another distinct advantage of the proposed strategy is that the internal recycle stream is treated as disturbance by the controller and therefore no online measurements are required. Particularly, during continuous operation, online measurements

are often challenging and/or impossible to obtain and can render the application of global control strategies infeasible. Therefore, strategies that could potentially decrease the amount of online measurements required can pave the way towards the intensification of existing processes via continuous operation.

Lastly, this section investigates the development of a control concept for the twin-column MCSGP process, operating in a semi-continuous, periodic fashion. Contrary to previously published works (Grossmann et al., 2010), here we suggest a centralized/decentralized strategy, where the setup is not treated as a 'black box' but every operating mode is controlled independently. We follow the steps presented in previous sections (Chapter 4 and Chapter 5) and we suggest a control scheme for the given setup. Ultimately, a global control strategy on the MCSGP process would look into a combination of the control schemes presented in Chapter 4 (single-column, batch mode) and Chapter 5 (twin-column, interconnected mode). For a fully automated, in-silico demonstration of the proposed scheme, a supervisory controller would be required that will serve as the decision maker for the switching times between the two modes. The latter are usually optimized prior to the controller development, aiming to maximize process productivity under purity constraints.

From a practical standpoint, measurements can be obtained within seconds from the UV/VIS monitors currently used in industry and later on be updated by more accurate measurements resulting from the HPLC that requires longer analysis time. This bi-level feedback offers a two-step verification of the process state and allows the controller to re-estimate a better forward action in case the original feedback received from the UV is not accurate enough. The signal resulting from the on-line and/or at-line equipment provides information on the eluted concentrations of the mixture components that can be translated into integrals using commercially available software packages. Finally, yield and purity can be post-calculated offline based on the average concentrations over a process cycle. Similar to any other online control strategy, it heavily resides on the availability of online (or at-line) measurements and entails risks related to noise and/or unavailable measurements. However, due to the model-based nature of the proposed controllers, the presented approach can benefit from the process model when measurements are unavailable. In the event where the detectors fail to return a feedback measurement, the output from the high-fidelity process model can be used as compensation and be updated by actual experimental values when available. Last but not least, the proposed controllers do not intend to completely eliminate the operator, who can interfere at any point and re-adjust the process parameters as appropriate.

Chapter 6.

Model-based Control of Cell Culture Systems

** The mathematical model used for the design of the optimization and control studies has been developed and validated by Dr. A. Quiroga. The model is also presented in Papathanasiou et. al (2017). "Advanced multi-parametric Model Predictive Control (mp- MPC) strategies towards integrated continuous biomanufacturing". Biotechnology Progress for the Special Issue based on the Berkeley conference on Integrated Continuous Biomanufacturing. Article in Press.*

*** The dynamic optimization studies have been performed in collaboration with Ms M. Elviro (University of Salamanca, Spain). The results are also presented in Papathanasiou et. al (2017). "Advanced multi-parametric Model Predictive Control (mp- MPC) strategies towards integrated continuous biomanufacturing". Biotechnology Progress for the Special Issue based on the Berkeley conference on Integrated Continuous Biomanufacturing. Article in Press*

**** The results presented in this chapter have been included in the following publications:*

1. *Papathanasiou et. al (2017). "Advanced multi-parametric Model Predictive Control (mp-MPC) strategies towards integrated continuous biomanufacturing". Biotechnology Progress for the Special Issue based on the Berkeley conference on Integrated Continuous Biomanufacturing Article in Press.*
2. *Papathanasiou et. al (2016). "Development of advanced computational tools for the intensification of monoclonal antibody production", 2016, In Computer Aided Chemical Engineering, Elsevier, Volume 38; pp. 1581-1586.*

6.1 Introduction

The main interest of this work is the development of advanced computational tools to facilitate the development of an integrated, continuous process for the production of monoclonal antibodies. In the previous two chapters (Chapter 4 and Chapter 5) we demonstrate how the design of advanced control strategies can facilitate the development and monitoring of continuous downstream processes. However, the performance of the downstream separation/purification is tightly linked to the efficiency of its upstream counterpart. In the case of the upstream it is necessary to ensure that the continuous system will be characterized by similar or higher productivity, improved product quality, compared to the batch operation.

Prior to the development of a fully integrated bioprocess, both USP and DSP need to be optimized. Although cell culture systems have been studied for several years, the lack of PAT technologies, limits their capabilities. Currently, cell culture systems are operated to a great extent in fed-batch mode, while their *in situ* monitoring relies on sensors and electrodes measuring basic process parameters (e.g. pH, dissolved oxygen, temperature, airflow, pressure etc.) (Teixeira et al., 2009). Other process parameters, such as cell volume (*offline*), cell concentration and viability (*offline, online or in situ*) and product concentration (*offline or in situ)* can be also measured *(Al-Rubeai, 2015).* However particularly the development of PAT technologies that monitor the aforementioned attributes is still at its early stages, therefore challenging the application of advanced process control tools that can assist process monitoring and improve process performance.

Despite the aforementioned obstacles, significant contributions have been reported in the control of mammalian cell cultures systems (

Table 6.1) that aim to improve process performance and maintain it under optimal operation. Often the optimal feeding profile is computed offline, based on a priori determination of the process parameters (Pörtner et al., 1996) or it is determined through correlation studies, based either on online measurements of the oxygen uptake rate (OUR) (Zhou et al., 1995, Zhou et al., 1997) or offline experiments that monitor the integral of viable cells (deZengotita et al., 2000). Although the presented studies result in improved culture performances, the suggested methodologies are coupled with certain limitations when it comes to their application in large scale. In the case where the course and parameters of the cell culture are determined a priori, the optimal feeding strategy does not encounter for disturbances. Therefore, there is no guarantee that the designed feeding profile will maintain the system under optimal operation

and lead to the desired culture productivity/viability. On the other hand, monitoring OUR, allows the operator to update the information over the culture period and take corrective actions whenever required. However, as reported by Zhou et al. (1997), although OUR is a good indicator of the culture performance, it does not allow the operator to investigate whether changes in the viability are associated to lack of nutrients or variations in other environmental conditions (e.g. osmolality), hindering therefore the design of a tailor-made feeding profile that will satisfy the needs of the cell culture system. Moreover, most of the presented studies employ the optimal feeding profiles through manual administration. However, in continuous manufacturong automated processes are preferred as they allow continuous system monitoring and they minimize variations associated to human error. In that respect, there are works suggesting automated techniques to calculate the optimal feeding profile based on the current culture needs (Ozturk et al., 1997, Frahm et al., 2003, Teixeira et al., 2009). Nevertheless, most of the studies propose re-calculation of the process parameters during online operation and are based on computationally expensive simulations. Therefore, in spite of their experimental success, can become significantly expensive when applied in industrial scale.

Table 6.1 Contributions in the control of mammalian cell culture systems.

Contribution	Reference
Open-loop control for the calculation of optimal feeding strategies using dynamic models.	• Hybridoma cells: Pörtner et al. (1996) • NS0 myeloma cells: deZengotita et al. (2000) & Zhou et al. (1997)
On-line control based on measurements of oxygen uptake rate and estimation of nutrient consumption rate in a hybridoma cell culture system.	Zhou et al. (1995)
On-line control based on feed-forward algorithm for the maintenance of glucose and lactate levels in a hybridoma cell culture system.	Ozturk et al. (1997)
Model-based control based on a hybrid model for the optimization of BHK cell culture systems (integrating metabolic flux analysis & measured data).	Teixeira et al. (2007)
Model-based control for the improvement of culture productivity & cell density in NS0 culture systems.	Frahm et al. (2003)

In continuous operation, additional factors need to be considered in the design of a global control strategy, such as the interaction between the multiple units of the production line (Chatterjee, 2012). In order to overcome regulatory hurdles, the developed schemes need to minimize risk of failure and ensure process robustness prior to their online application. In this fashion, human error needs to be minimized and the suggested optimization and control strategies need to allow the incorporation of disturbances in the mathematical formulation. Model-based optimization and control strategies can prove to be of great assistance when it comes to continuous operation. The model-based nature of such techniques allows the design of control strategies that are trained on the knowledge gained from the process model and therefore the principal interactions of the system at hand. Compared to other classical control methods (e.g. PID control), model-based controllers can be trained against disturbances thus providing an additional level of process robustness against sudden variations during online operation. Moreover, they can be combined with estimation techniques (e.g. Kalman filter) that not only improve the system performance with respect to setpoint-plant mismatch, but they also facilitate state estimation in cases where online measurements are unavailable or influenced by noise. Furthermore, due to their model-based nature, such control systems can be executed in tandem with the process model that can be used to provide the feedback required for the operation of the controller when online measurements are unavailable. The latter can prove to be of vital importance in systems where measurements rely mainly on at line or offline measurements that require longer times in order to be obtained. In this case, the process model can temporarily provide feedback to the controller that will be later on updated by the experimental measurement when it becomes available.

Based on the above, in this chapter we present a model-based control scheme for the performance improvement of a cell culture system used for the production of a monoclonal antibody. The designed controllers are based on the principles of mp-MPC (Appendix A) that combines the features of model-based control techniques with the ability to solve the optimization problem once and offline. The latter allows a priori identification of the optimal regions of operation and simplifies the calculation of the control actions through affine function evaluations (Pistikopoulos, 2009). This can be of great importance at large scale, where the complexity of the process models and the number of parameters become overwhelming thus leading to computationally demanding optimization problems.

In particular, here we investigate the development of advanced computational tools for the intensification of a GS-NS0 cell culture system, used for the production of an IgG4 monoclonal antibody following the systematic PAROC framework/software platform (Pistikopoulos et al., 2015). Section 6.2 explains the main metabolic pathways considered in

this work that are modeled in section 6.3, following first-principles. Section 6.3 demonstrates also dynamic optimization studies executed on the aforementioned system, aiming to explore its capabilities and increase the culture efficiency. Lastly, sections 6.4 and 6.5 are dedicated to the development and testing of 3 control strategies, based on various discretization times (2-hours, 4-hours and 1-minute). The performance of the suggested strategies is assessed and compared to the results of the dynamic optimization. Moreover, the impact of the feedback frequency on the culture performance is also investigated.

6.2 GS-NS0 Cell Culture System

Based on previously presented work (Kiparissides et al., 2015), we investigate a simplified metabolic network (Figure 6.1) that describes the uptake of nutrients used in the examined system. Namely, we consider glucose and four key amino acids: aspartate, arginine, asparagine and glutamate. The nutrients are utilized through different pathways for biosynthesis, energy production and mAb assembling (Figure 6.1). The key importance of the considered nutrients is discussed below. The model development, sensitivity analysis, parameter estimation and experimental validation for the upstream model used in this chapter has been performed by Dr. Ana Quiroga Campano (Imperial College London), while the optimization studies were executed in collaboration with Ms Montaña Elviro Perez (University of Salamanca).

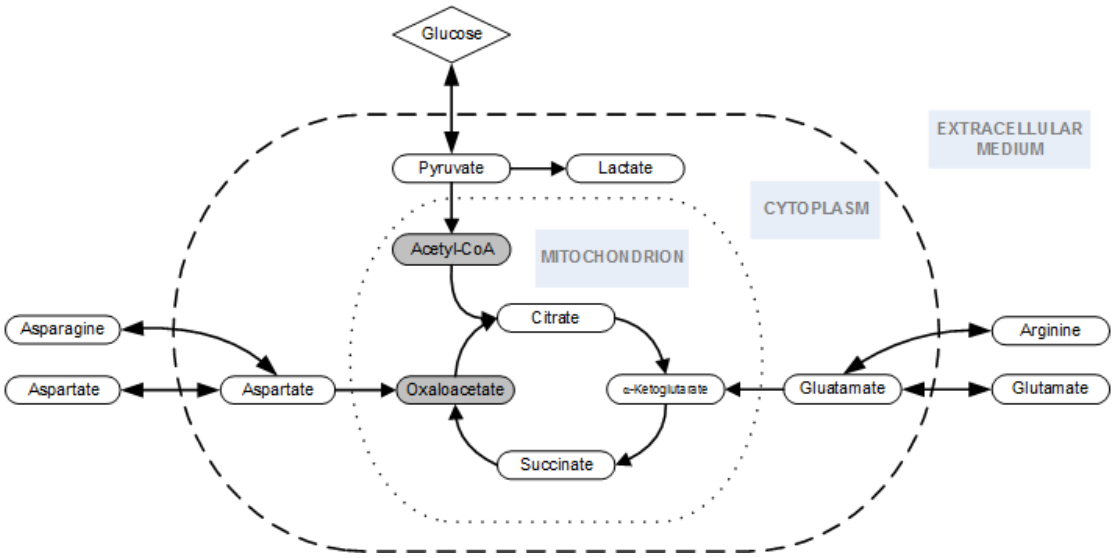

Figure 6.1 Metabolic network considering the basic pathways.

(i) Glucose is the most predominant carbohydrate that participates in various metabolic pathways, such as: (1) the pentose phosphate pathway (PPP) for the production of DNA precursors, (2) the anaerobic pathway or glycolysis for the production of energy

and (3) the aerobic pathway, where it is completely oxidized through the tricarboxylic acid (TCA) cycle.

(ii) Glutamate is a key compound in the cellular metabolism, as it represents the only source of glutamine in the case of GS-NS0 cells (Papathanasiou et al., 2016c, Quiroga et al., 2016). The latter are NS0 cells transfected with plasmids that include the glutamine synthetase gene expression system (GS-system) that allows them to synthesise glutamine from glutamate and ammonium (Barnes et al., 2000). It has been observed that in GS-NS0 cell culture systems its consumption is preferred over glucose and therefore, glutamate depletion leads to a decrease in the growth rate. Nevertheless, the cells can still continue to grow utilizing other amino acids, such as asparagine, whose catabolism leads to glutamate production.

(iii) Aspartate is crucial for energy production (through the TCA cycle). Similarly to the mechanism described above, to compensate for aspartate depletion, the cells can produce the required amino acid amount through asparagine hydrolysis.

For the control studies presented in this section, we consider a cell culture system of the GS-NS0 mammalian cell line, for the production of the chimeric IgG4 antibody, in a 1L flask with 200 mL working volume.

6.3 Model Development & Dynamic Optimization

6.3.1 Model development

For the upstream system we consider a 1L flask with 200 mL working volume, where samples of 1 mL are taken every 6 hours. The system (Figure 6.1) is described by an unstructured, non-segregated, Monod-kinetics model that comprises 22 Differential and Algebraic Equations (DAEs), 24 variables and 27 parameters (Appendix C). Following the framework presented by Kiparissides et al. (2011a) we perform Global Sensitivity Analysis for the identification of the significant model parameters (executed through the gO:MATLAB interface that allows in tandem utilization of gPROMS® ModelBuilder and MATLAB®) that are later estimated using experimental data (gPROMS® ModelBuilder v4.2.0 (P.S.E, 1997-2016)). Moreover, the model is validated against experimental data and its predictive capabilities are assessed using 2 sets of initial conditions (Appendix C). The mathematical model used in this work was previously developed and validated by Dr. A. Quiroga (Quiroga, 2017). For more information on the model development, analysis and validation, the reader is referred to Appendix C.

The presented model describes the batch culture of GS-NS0 cells for the production of an IgG4 antibody. Therefore, the term representing the inlet flow rate (F_{in}) shown in the model equations is set to zero, while the outlet (F_{out}) corresponds to the periodic sampling. However, fed-batch operation is the most common choice when it comes to industrial application of such systems. Therefore, for the optimization and control studies in this work, we consider that feed is introduced to the system in a fed-batch fashion, while part of the culture volume is removed as a result of the sampling.

6.3.2 Model-based dynamic optimization

Dynamic optimization techniques can be used to identify the optimal feeding strategy for the maximization of the efficiency of mammalian cell culture systems based on mathematical models. The two most common indicators that characterize the efficiency of a cell culture system are culture viability and specific productivity (Bibila and Robinson, 1995) and are usually affected by different parameters. Moreover, culture conditions that seem to prolong culture viability may result in reduced productivity and vice versa (Kiparissides et al., 2015). Cell culture optimization can been performed for the design of optimal feeding strategies to increase culture productivity and/or cell viability. There are several works in the open literature addressing the optimization of mammalian cell culture systems employing various methods, such as design of experiments and *in silico* optimization using statistical and/or dynamic tools (Teixeira et al., 2006, Ji, 2012, Koumpouras and Kontoravdi, 2012, Bayrak et al., 2015, Green, 2015, Kiparissides et al., 2015, Bayrak et al., 2016, Chen et al., 2016, Villaverde et al., 2016, Liu and Gunawan, 2017). Particularly dynamic, model-based optimization strategies that employ first-principle models can provide a solid basis for the execution of such studies (Kiparissides et al., 2011b, Koumpouras and Kontoravdi, 2012). Such methods allow the knowledge obtained by the process model to be transferred to the optimization problem formulation, while the latter is applied on a mathematical representation that describes the events of the bioprocess in a dynamic fashion (Farzan et al., 2017). The procedure is usually executed offline, while the results from the dynamic optimization are validated *in vitro,* in lab-scale prior to the application of the feeding strategy on a larger scale. In this fashion, computationally expensive, online optimization procedures can be avoided.

During the formulation of the optimization problem, one can consider various objective functions upon which the mathematical problem will be designed. These could look into the specific antibody production rate, the extracellular antibody concentration, the concentration of viable cells or the integral of viable cells that corresponds to the total number of cells available for antibody production (Koumpouras and Kontoravdi, 2012). In a similar study.

Koumpouras and Kontoravdi (2012), investigated four optimization studies, comparing the four different objective functions and demonstrated that using the antibody concentration as the objective function resulted in increased productivity in terms of extracellular antibody concentration, improved total cell number, while the specific productivity remained the same for all examined cases. Based on the above we aim to explore the system dynamics and in particular to maximize the culture productivity, using the volumetric antibody concentration as the objective function to be maximized. The optimization studies performed in this work aim to provide preliminary information regarding the system behavior under feeding. This information will be used as setpoint for the designed controller. Therefore, the strategy upon which the optimization problem is formulated should be identical to the control problem formulation. Nonetheless, the experimental implementation of the optimization and/or control strategies needs to be considered. Therefore, based on the suggested strategy, the antibody concentration can be measured experimentally using sensors currently available (e.g. Bioprofile® Flex Analyser, Nova Biomedical, Waltham, USA). The latter is of high importance for the control strategy described later on (Section 6.4) as it can provide the measurements required for the controller feedback. Genzyme presented a small-scale example of a fully continuous bioprocess for the production of monoclonal antibodies by a CHO cell culture system (Warikoo et al., 2012). In this study a 12L bioreactor is operated in perfusion mode, utilizing alternating tangential flow (ATF) filtration as the cell retaining procedure. The upstream harvest is pumped into a disposable bag serving as the surge vessel and then loaded to a 4-column Periodic Countercurrent Chromatography (PCC) system for the purification. The volumetric productivity of the culture is measured online using UV detectors at the inlet of the PCC system, while culture viability and mAb Critical Quality Attributes (CQAs) are measured offline. In this application, following the standard procedure of mAb production, cells are removed prior to the collection of the upstream harvest. Therefore, from an experimental standpoint, tracking the volumetric mAb concentration could lead to control schemes that could be applied using existing sensors.

This work is focusing on the design of control strategies that can assist continuous operation and therefore the two control schemes (upstream and downstream) should be designed in a fashion that allows seamless communication amongst them. Using the antibody concentration as the optimization objective and subsequently as the control output will allow seamless communication between the two control schemes. In addition, as demonstrated in Chapter 4, impurities resulting from the cell culture system can be treated as measured disturbances by the downstream controller, eliminating therefore the need for accurate online measurements on their concentration. Furthermore, offline optimization experiments to identify the optimal

culture conditions that will minimize impurity content in the cell culture system can be performed. We use the model developed in the previous section for the design of a dynamic optimization problem. The suggested formulation (Table 6.2) aims to maximize the final volumetric concentration of mAb, administrating GS-Supplement (SAFC Biosciences, Sigma-Aldrich, UK) X40 and 0.4M glucose in fed-batch fashion. This medium is chosen in order to be in line with the procedure presented by Kiparissides et al. (2015) and allow comparison of the generated results. We consider a culture time of 168 hours and we define 76 time intervals, allowing the optimizer to design a feeding strategy that will lead to increased volumetric mAb concentration. Due to the plethora of nutrients available at the beginning of the culture, initially we design a scarcer feeding strategy (6-hour intervals) that we intensify after the 20th hour (2-hour intervals), when nutrient concentrations start to decrease significantly. Aiming to move towards continuous operation, we choose to administrate feeding based 2-hour long pulses, instead of the standard injection-like strategies of 1 min. In order to maintain the culture under optimal conditions, we consider a tight constraint on the total culture volume (± 10% from the base value), as well as on the inlet flow rate of the supplement based on the same criterion. Moreover, we allow 28 mL sampling volume to be removed throughout the culture time. The initial conditions shown in Table 6.2 are based on lab-scale experiments (Appendix C). The optimization studies are executed in gPROMS® ModelBuilder, using g:OPT (P.S.E, 1997-2016).

Table 6.2 Formulation of the dynamic optimization solved for the maximization of the productivity of the GS-NS0 cell culture system.

Objective function	**max** $[\boldsymbol{mAb}]$
subject to	
The process model:	$x_i(t) = f_i\left(X_j(t), u(t), t\right), \quad i,j = 1 \dots 10$
Control variable:	$u(t) = F_{in}(t)$
Inequality constraints:	$0.9{\times}V_0 \leq V \leq 1.1{\times}V_0$
	$F_{LB} \leq F_{in} \leq F_{UB}$
Initial conditions:	
$\boldsymbol{V_0 = 0.2\ L}$	$X_{V,0} = 1.78{\times}10^8$ cells/L
$[\boldsymbol{mAb}]_0 = \boldsymbol{4.06}$ mg/L	$X_{D,0} = 4.4{\times}10^7$ cells/L
$[\boldsymbol{GLC}]_0 = \boldsymbol{19.8}$ mM	$[GLU]_0 = 1.03$ mM
$[\boldsymbol{ASP}]_0 = \boldsymbol{0.45}$ mM	$[ASN]_0 = 1.03$ mM
$[\boldsymbol{ARG}]_0 = \boldsymbol{0.99}$ mM	$[LAC]_0 = 0.73$ mM
Total amount removed from sampling:	$F_{out,tot} = 28$ mL

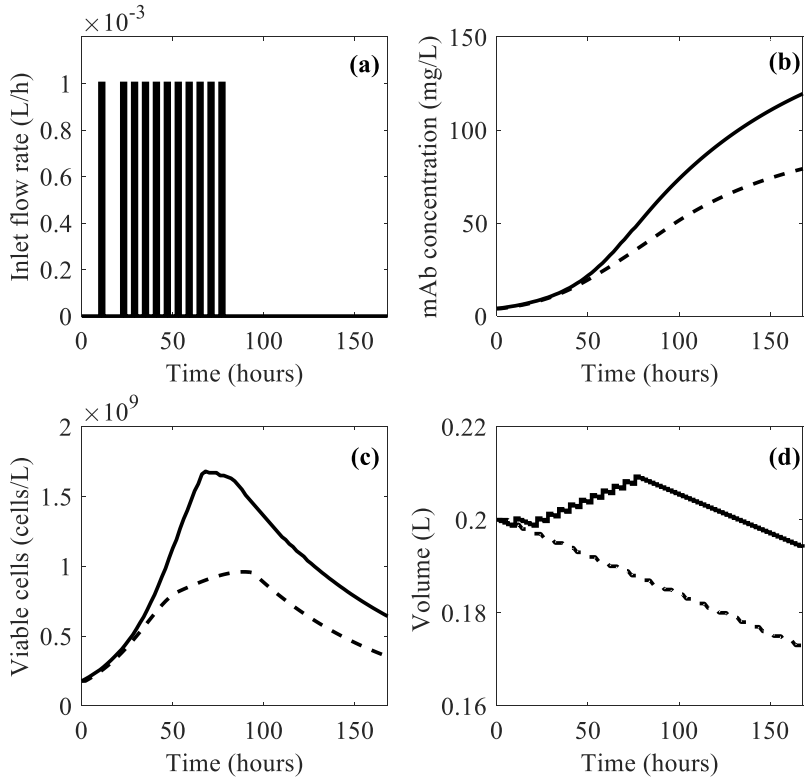

Figure 6.2 Simulation results after the solution of the dynamic optimization problem for 168 hours of culture: (a) optimal feeding strategy, (b) volumetric mAb concentration for batch (- -) and fed-batch (−) system, (c) viable cell population for batch (- -) and fed-batch (−) system and (d) culture volume for batch (- -) and fed-batch (−) system.

Figure 6.2a demonstrates the proposed feeding strategy, where medium is introduced in pulses of 2-hours duration. Based on the applied strategy, the feeding is intensified after the 20th hour, however it is observed that the dynamic optimizer suggests that fresh medium should be administrated only until the 70th hour. This time point corresponds to the end of the growth phase of the culture and the cells start entering the irreversible state of death phase. The profile of the feeding strategy (Figure 6.2a) is similar to the one presented by Kiparissides et al. (2015), where fresh medium introduced during the first hours of the culture and stops approximately after the 75th hour. The schedule proposed here for the feeding results in a higher volumetric mAb concentration by the end of the culture (approximately 1.4 fold higher than the batch system). Moreover, it is demonstrated that the depletion of 3 of the key nutrients (glutamate, aspartate and arginine) (Figure 6.3b, c & e) leads to decreased cell growth and subsequently cell death. The results presented here will serve as setpoints for the design of advanced control strategies of the examined system (Section 6.4).

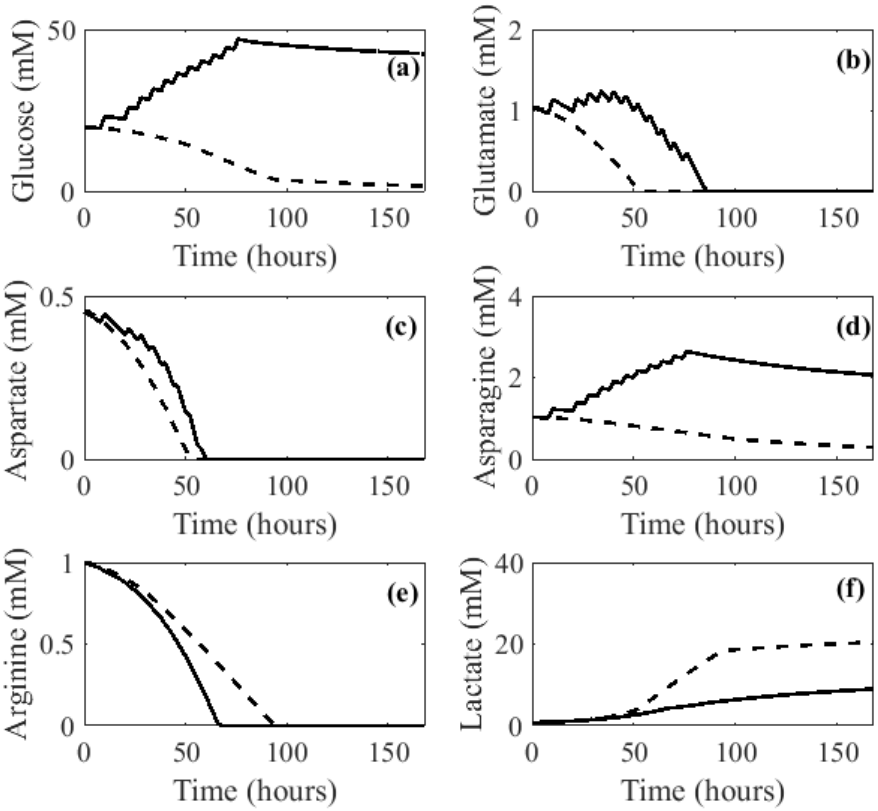

Figure 6.3 Simulation results after the solution of for batch (- -) and fed-batch (−) system: (a) glucose, (b) glutamate, (c) aspartate, (d) asparagine, (e) arginine and (f) lactate over 168 hours of culture.

The computational optimization results presented in this chapter indicate into improved culture productivity and prolonged viability (Figure 6.2 b & c) compared to the batch system. However, comparing the results demonstrated here to the work presented by Kiparissides et al. (2015), it is observed that the suggested feeding strategy (Figure 6.2 a) results into lower final antibody concentration. In particular, here a final concentration of 120 mg/L is achieved, while Kiparissides et al. (2015) reports 175 mg/L. Nevertheless, the feeding strategy illustrated in Figure 6.2a results into an improved profile for the viable cells as on the 168th day the model reports a concentration of $6.42 \cdot 10^8$ cells/L, while in Kiparissides et al. (2015) a concentration of approximately $5.5 \cdot 10^8$ cells/L is achieved. It should be underlined that neither of the optimization approaches considers the viable cells in the objective function. The feeding strategy presented here considers feeding intervals of 2 hours that offer a smoother adaptation of the cells to the new culture conditions, compared to the pulse strategy presented by Kiparissides et al. (2015). The latter could be considered as the reason of the computationally improved cell viability presented here.

6.4 Control of the Cell Culture System via PAROC

The validated process model designed in the previous section (Section 6.3) is used here for the development of an advanced, parametric controller. For the design and testing of the latter we follow the PAROC framework that allows us to seamlessly formulate and solve the mp-programming problem, while it facilitates the in-silico validation of the designed controller. For the latter we exploit the results of the dynamic optimization studies presented above in order to define the setpoints for the proposed control strategy. As discussed in section 6.3, the formulation of the control problem should be in line with the rationale upon which the optimization problem is designed and solved. Therefore, the volumetric antibody concentration is chosen for the design of the control scheme. As discussed earlier (section 6.3) using the antibody concentration as the optimization objective and subsequently as the control output will allow seamless communication between the upstream and downstream control schemes (see also Chapter 4 for a detailed discussion on disturbances considered in the downstream system). In addition, the suggested output can be monitored using sensors available in the market (Warikoo et al., 2012).

6.4.1 Model approximation

The process model (Appendix C) is characterized by nonlinear equations that render the control studies infeasible to perform. Therefore, an intermediate step is required, where the process model is re-formulated to a state space, linear representation. Here this is realized using system identification techniques (*ident* toolbox, MATLAB®). The model input (inlet flow rate of the feeding medium) is adequately excited and the behavior of the tracked output (volumetric mAb concentration) is monitored (Figure 6.4). In addition, here we consider a periodic sampling of 1 mL every 6 hours that is introduced as measured disturbance for the design of the state space model (Figure 6.4c). Moreover, standard practice indicates that the culture volume should not vary more than ± 10% from its starting value. In order to ensure that the volume is maintained within the permitted range, we consider it as an additional system state (4^{th} state) introducing its equation in the state space formulation. Moreover, we introduce the culture volume as an additional output with a predefined setpoint fixed at the original value of 200 mL.

$$\frac{dV}{dt} = F_{IN} - F_{OUT}$$

Equation 6.1 Equation for the calculation of the culture volume.

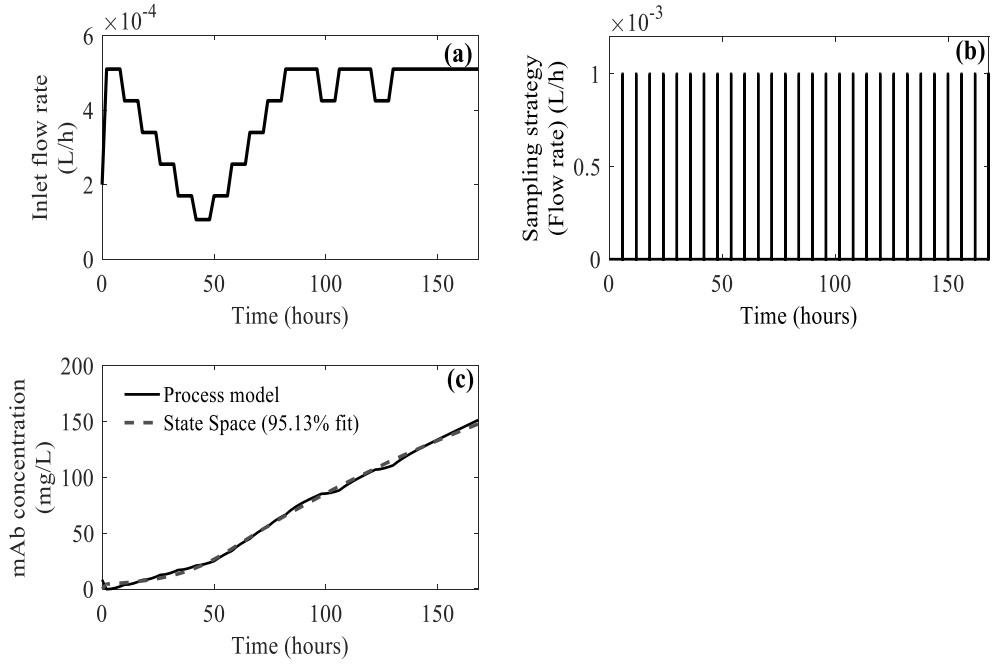

Figure 6.4 Data used for the model approximation of the upstream process model: (a) random pulse input strategy applied on the inlet flow rate (input), (b) periodic sampling strategy applied on the system (1mL/6hours), (c) comparison between the process model (continuous grey line) and the linear state space model (dotted black line).

The resulting linear model is characterized by 95.13% fit to the tracked output and considers 2 hours sampling time (T_s) to be in accordance with the optimization procedure presented above (Section 6.3). The latter is also chosen in order to ensure that the proposed control strategy is capturing the main events taking place in the culture system, such as the metabolic shifts (Quiroga et al., 2016). The model structure is given below (Table 6.3).

Table 6.3 State space model formulation.

$\boldsymbol{x(t+T_s) = Ax(t) + Bu(t) + Dd(t)}$	**Equation 6.2 State space formulation as considered for the upstream system.**
$\boldsymbol{y(t) = Cx(t)}$	

Where *x, u, y* are the states, inputs (inlet flow rate of the feeding medium) and outputs (volumetric mAb concentration) respectively, *t* corresponds to the time, T_s is the sample time and *A, B, C, D* represent the matrices of the state space model.

$$A = \begin{bmatrix} 0.5441 & -0.04234 & 0.04154 & 0 \\ 0.003578 & 0.9867 & 0.001953 & 0 \\ -1.684 & -0.1334 & 1.126 & 0 \\ 0 & 0 & 0 & 1 \end{bmatrix}$$

$$B = \begin{bmatrix} 1.718e+4 \\ -1242 \\ 7.411e+4 \\ 7200 \end{bmatrix}$$

$$C = \begin{bmatrix} 51.69 & -90.72 & -13.25 & 1 \\ 0 & 0 & 0 & 1 \end{bmatrix}$$

$$D = \begin{bmatrix} 0 \\ 0 \\ 0 \\ -120 \end{bmatrix}$$

Equation 6.3 Matrices of the linear state space model of the upstream system with 2 hours sampling time.

As mentioned earlier (Chapter 4) the state space model does not classify as a "result" but rather as an "intermediate compensation" to facilitate the controller design. Subsequently, the state space model designed at this step is considered satisfactory for the design of the controller.

6.4.2 Design of the mp-MPC controller

The state space model designed in the previous step is used here for the development of a parametric controller for the maximization of the culture productivity (mAb volumetric). Figure 6.5 demonstrates the control scheme considered in this work. We investigate the development of advanced control strategies for a bioreactor operating in fed-batch mode and we consider the inlet flow rate of feeding medium as the manipulating variable. Following the optimization strategy presented above (Section 6.3) we consider the feeding of GS-Supplement (SAFC Biosciences, Sigma-Aldrich, UK) X40 and 0.4 M glucose. The proposed

controller is monitoring both the volumetric concentration of the antibody, as well as the levels of the culture volume (allowing variations within ± 10% from the starting value). Moreover, we consider that samples of 1mL are extracted from the bioreactor every 6 hours. This periodic sampling is considered as measured disturbance by the designed controller.

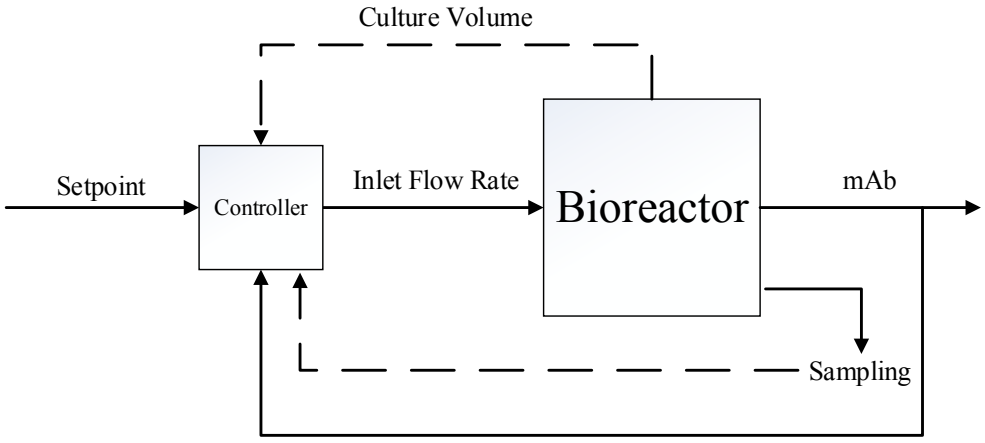

Figure 6.5 Proposed control scheme for the upstream system.

The multi-parametric programming problem is formulated and solved based on the state space model. Table 6.4 summarizes the control parameters chosen for the design of the mp-programming problem. The control problem comprises 8 parameters and is solved using POP (Oberdieck et al., 2016) toolbox in MATLAB®. Figure 6.6 illustrates the map of critical regions that correspond to affine function evaluations of the problem parameters and result into the optimal control actions (Pistikopoulos et al., 2002, Pistikopoulos, 2009).

Table 6.4 Tuning parameters used for the formulation of the mp-MPC problem for the 2 hours, 4 hours and 1 minute discretization.

Tuning Parameter	Explanation	Value	Tuning Parameter	Explanation	Value
OH	Output Horizon	4	**Umin**	Input upper bound	0
NC	Control Horizon	2	**Umax**	Input lower bound	1
QR	Weights on the outputs	$10^3\ I$	**Dmin**	Disturbance upper bound	0
Q	Weights on the states	$1I$	**Dmax**	Disturbance lower bound	0.1
R	Weights for the inputs	0.01	**Total number of critical regions**		64
P	Terminal weight for the states	Riccati equation*			

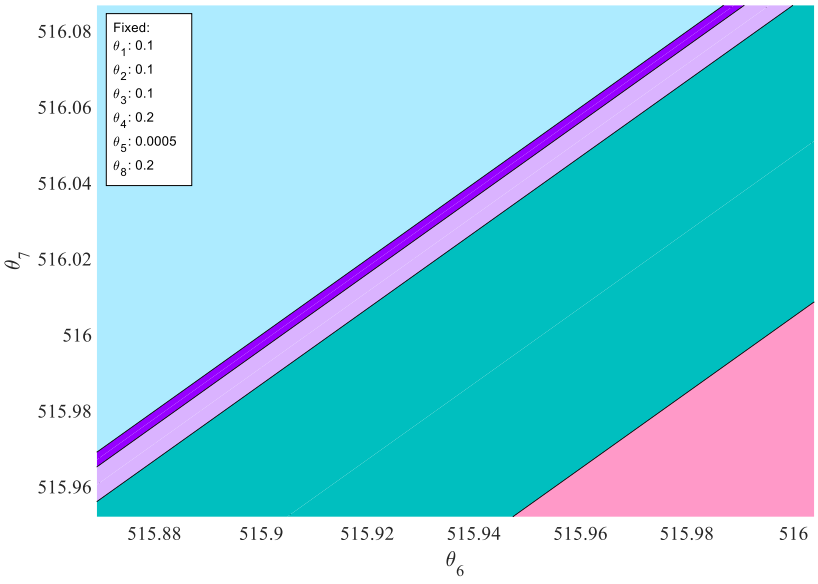

Figure 6.6 Two-dimensional projection of 4 critical regions polyhedral for the 2-hour controller. States: $x_1, \dots, x_4 = \theta_1, \dots \theta_4$, disturbances: θ_5 , volumetric mAb concentration: θ_6 , Output Setpoints: $mAb\ setpoint = \theta_7$, $volume\ setpoint = \theta_8$. The values used for the design of the graph are depicted.

* The Riccati equation is as follows: $P = A^T PA - (A^T PB)(B^T PB + R)^{-1}(APB) + Q$, where A and B are the matrices of the state space model and P, R, Q the tuning parameters used for the control problem formulation.

6.4.3 In silico evaluation of the controller performance

Following its design, the controller is validated in-silico, in 'closed-loop' fashion against the process model. The validation is facilitated using the gO:MATLAB interface that allows seamless data exchange between MATLAB® (control actions) and gPROMS® ModelBuilder (process model). We use the maximum volumetric concentration of antibody as resulted from the optimization studies as the target value (Section 6.3) and we simulate the model for 168 hours (7 days), under periodic sampling (Figure 6.4b). It is observed that the designed controller inherently suggests fed-batch feeding (Figure 6.7a), while the first pulse is introduced 8 hours after the beginning of the culture and the feeding is intensified only after the 20th hour. During the beginning of the culture, the cells are growing slowly (adaptation/lag phase) and therefore the nutrient requirements are lower (Olofsson and Ma, 2011). Consequently, the proposed feeding strategy minimizes the excess of nutrients in the culture and promotes the effective consumption of glucose, reducing the formation of toxic metabolites, such as lactate (Figure 6.9f) (Xie and Wang, 1994, Cruz et al., 2000). In a similar fashion, the controller intensifies the feeding after the 20th hour, when the culture enters the exponential phase and maximum cell growth is achieved. At this stage nutrient uptake increases as well, as nutrients are essential for cell growth.

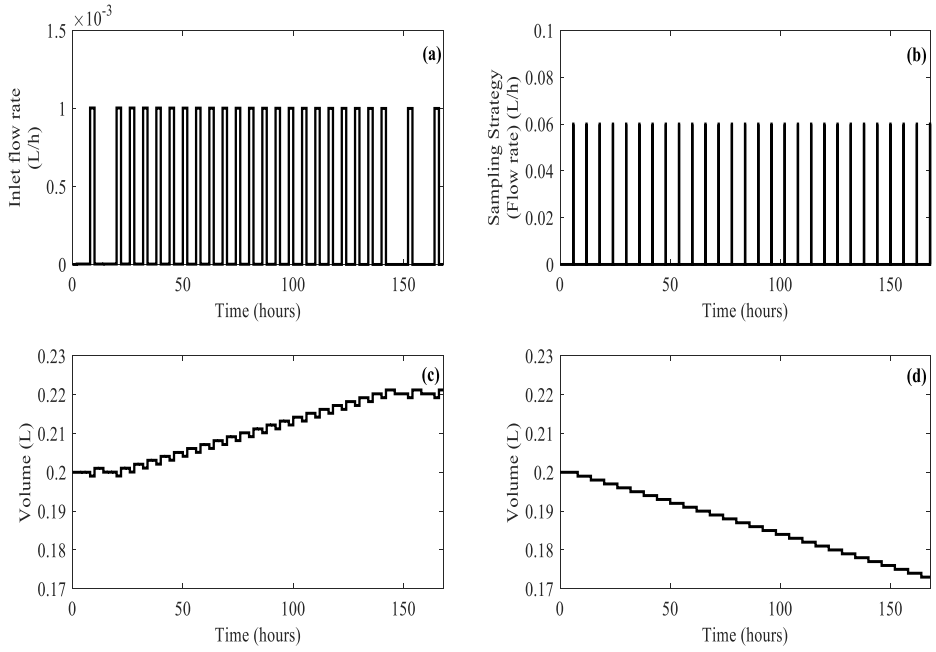

Figure 6.7 (a) Control input (inlet feed flow rate) as designed by the presented controller, (b) sampling strategy applied both to the batch and the fed-batch system, (c) evolution of culture volume for the fed-batch case and (d) evolution of the culture volume for the batch case.

The suggested strategy for nutrient supply (Figure 6.7a) not only increases the number of viable cells, but also prolongs the culture longevity (Figure 6.8b), leading to increased productivity (Figure 6.8a) (Spens and Häggström, 2007). Counter-intuitively, the controller suggests a scarcer feeding towards the end of the culture (beyond the 142nd hour). However, the latter is in agreement with standard experimental/industrial practice, as at this stage the culture starts entering death phase that is an irreversible state. In particular, the exhaustion of arginine (66th hour), followed by the limitation of glutamate (96th hour) decreases the cell growth and activates cell apoptosis via starvation signals (Majors et al., 2007). Therefore, any medium provided beyond this point would increase process waste rather than improve the culture productivity. Furthermore, these results provide a valid indication of the optimal time point that the culture should be terminated in order to minimize product degradation and therefore to improve the performance of the downstream purification. In addition, it is illustrated (Figure 6.7b) that the controller efficiently manages to maintain the working volume within the permitted range (± 10% from the starting value of 0.2 L). The volume of feeding required in order to maintain the system in exponential growth, the accumulation of glucose and asparagine and the limitation of glutamate and arginine reveal the opportunity to use the proposed controller for medium development, in order to simultaneously optimize the feeding composition and feeding profile.

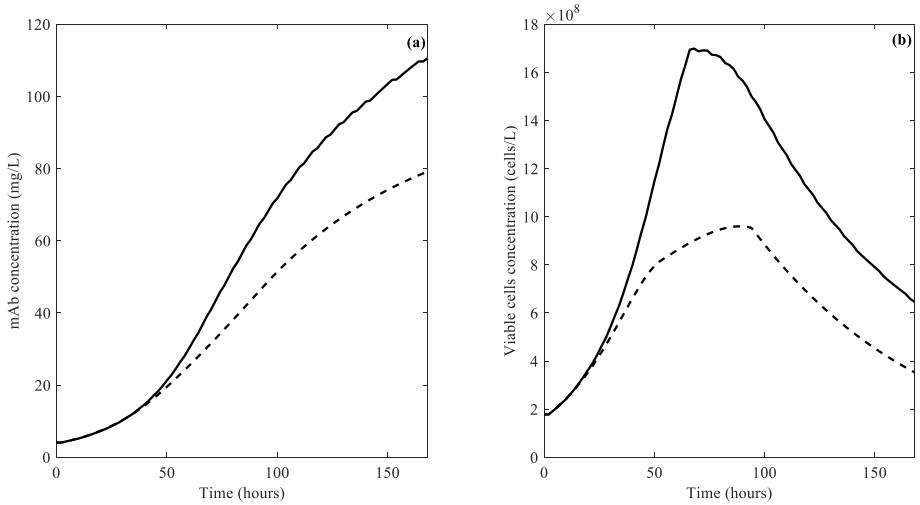

Figure 6.8 Comparison between the fed-batch (continuous black line) and the batch (dotted grey line) system for: (a) the volumetric mAb concentration and (b) the population of viable cells over 168 hours of culture.

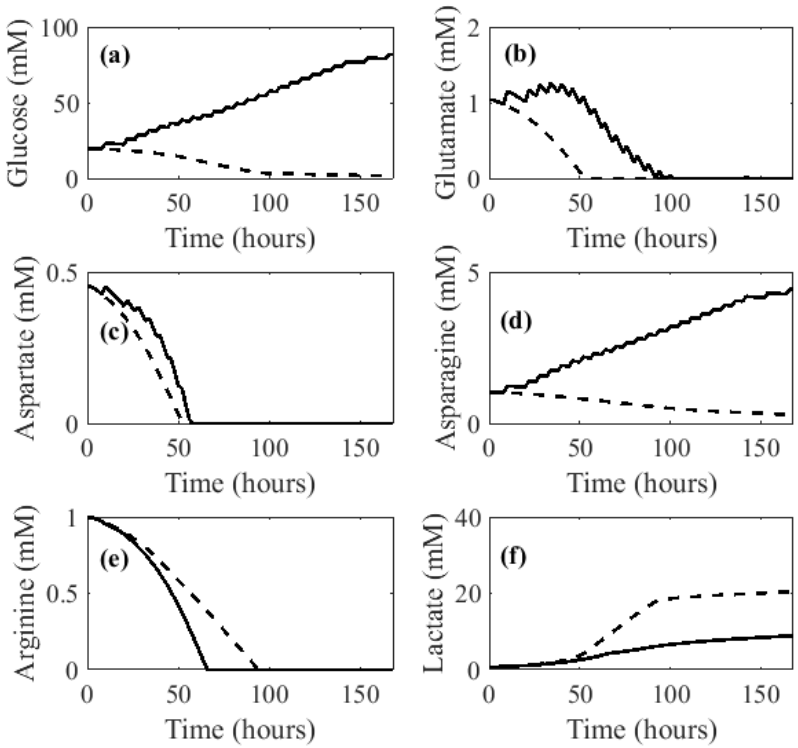

Figure 6.9 Comparison between the fed-batch (continuous black line) and the batch (dotted grey line) system for the concentrations of: (a) glucose, (b) glutamate, (c) aspartate, (d) asparagine, (e) arginine and (f) lactate over 168 hours of culture.

The presented control input (Figure 6.7a) results in increased culture productivity, that is almost 1.4 fold higher compared to the batch system (Figure 6.8), without reaching however the maximum volumetric product concentration acquired in the optimization studies (Section 6.3). Nevertheless, the suggested feeding strategy results in higher cell densities and prolonged culture times. The latter plays a vital role increasing the culture productivity, particularly under continuous operation, where the culture duration should be increased in order to minimize start-up/shut-down costs.

6.5 Comparison of Various Feeding Strategies

Currently, in fed-batch cultures measurements are taken every 24 hours (Kiparissides et al., 2015) and therefore control strategies developed for such systems can only be updated once per day. However, in order to minimize the risk of failure in continuous operation tighter monitoring and control strategies should be investigated. In the previous section (Section 6.3 & 6.4) we examined optimization & control strategies based on a 2-hour interval. Here we examine the impact on the system performance of two new strategies: (a) a 4-hour interval

and (b) a tighter approach of 1-min intervals. The system performance is compared to the one described above (2-hour interval strategy, Section 6.4) as well as to the batch operation.

6.5.1 Model approximation

The linear state space models for the 1-minute and 4-hour cases are derived directly from the linear model designed in the previous section (Section 6.4.1). The system behavior, as well as the interactions between the input (feed flow rate), the disturbance (sampling) and the outputs (culture volume and volumetric mAb concentration) remain the same. The matrices representing the mathematical relationships of the latter are illustrated in the equation sets below (Equation 6.4 and Equation 6.5 respectively) and are constructed based on the respective discretization/sampling times (1 minute & 4 hours respectively). The fitting of the linear representation to the process model remains the same as well.

$$A = \begin{bmatrix} 0.9955 & -0.0004266 & 0.0004173 & 0 \\ 5.614e-05 & 0.9999 & 1.418e-05 & 0 \\ -0.0169 & -0.001404 & 1.001 & 0 \\ 0 & 0 & 0 & 1 \end{bmatrix}$$

$$B = \begin{bmatrix} 167.2 \\ -11.47 \\ 717 \\ 60 \end{bmatrix}$$

$$C = \begin{bmatrix} 51.69 & -90.72 & -13.25 & 1 \\ 0 & 0 & 0 & 1 \end{bmatrix}$$

$$D = \begin{bmatrix} 0 \\ 0 \\ 0 \\ -1 \end{bmatrix}$$

Equation 6.4 Matrices of the linear state space model of the upstream system with 1 minute sampling time.

$$A = \begin{bmatrix} 0.2259 & -0.07035 & 0.06928 & 0 \\ 0.002188 & 0.9732 & 0.004274 & 0 \\ -2.813 & -0.2104 & 1.197 & 0 \\ 0 & 0 & 0 & 1 \end{bmatrix}$$

$$B = \begin{bmatrix} 2.965e+4 \\ -2261 \\ 1.288e+05 \\ 1.44e+04 \end{bmatrix}$$

$$C = \begin{bmatrix} 51.69 & -90.72 & -13.25 & 1 \\ 0 & 0 & 0 & 1 \end{bmatrix}$$

$$D = \begin{bmatrix} 0 \\ 0 \\ 0 \\ -1906 \end{bmatrix}$$

Equation 6.5 Matrices of the linear state space model of the upstream system with 4 hours sampling time.

6.5.2 Design of the mp-MPC controllers

Following the scheme presented in Figure 6.5 and using the state space models with the new discretization times (1 min & 4 hours), we design two new parametric controllers, using the same tuning parameters as for the 2-hour case (Table 6.4). The control problems are solved using POP (Oberdieck et al., 2016) toolbox in MATLAB®. Table 6.5 summarizes the total number of critical regions for each of the three problem solutions.

Table 6.5 Details of the three mp-MPC controllers.

Discretization	Total Number of Critical Regions	Tuning Parameters	Offline Solution Map
2 hours	64	Table 6.4	Figure 6.6
4 hours	65		Figure 6.10
1 min	48		Figure 6.11

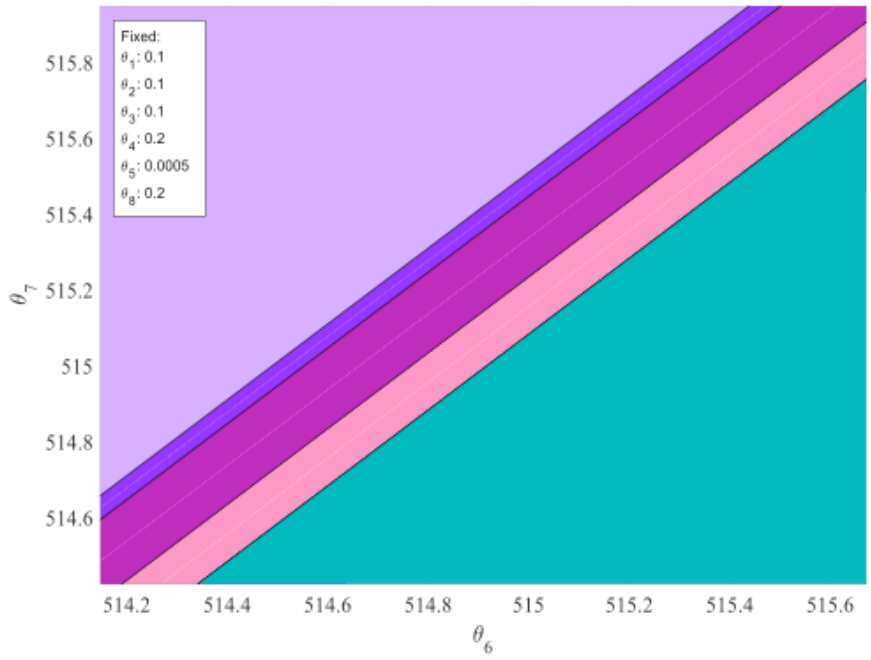

Figure 6.10 Two-dimensional projection of 5 critical regions polyhedral for the 4-hour controller. States: $x_1, \dots, x_4 = \theta_1, \dots \theta_4$, disturbances: θ_5 , volumetric mAb concentration: θ_6 , Output Setpoints: $mAb\ setpoint = \theta_7$, $volume\ setpoint = \theta_8$. The values used for the design of the graph are depicted.

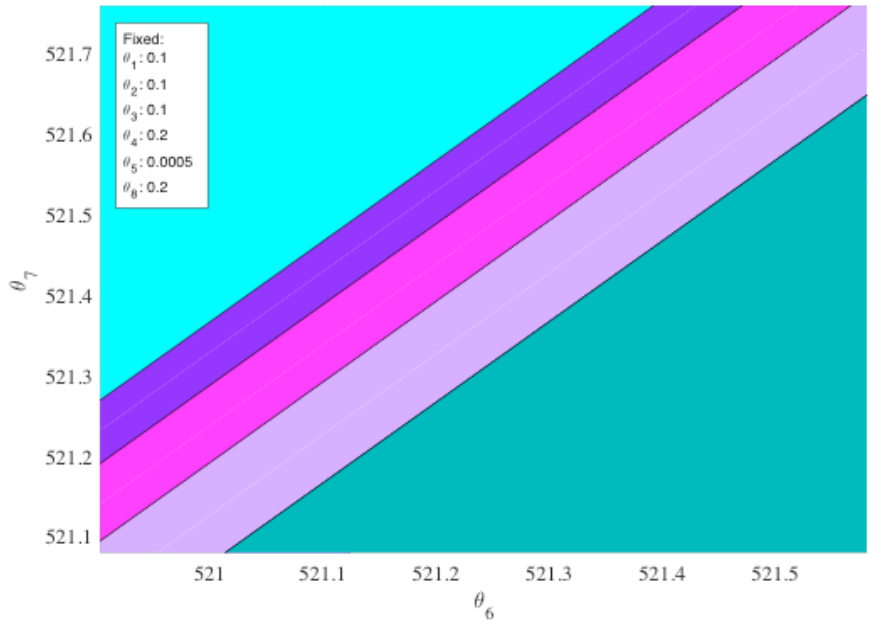

Figure 6.11 Two-dimensional projection of 5 critical regions polyhedral for the 1 minute controller. States: $x_1, \dots, x_4 = \theta_1, \dots \theta_4$, disturbances: θ_5 , volumetric mAb concentration: θ_6 , Output Setpoints: $mAb\ setpoint = \theta_7$, $volume\ setpoint = \theta_8$. The values used for the design of the graph are depicted.

6.5.3 "Closed-loop" validation and comparison of strategies

The performance of the mp-MPC controllers designed in the previous step is assessed here, in silico against the process model. For the "closed-loop" validation we consider periodic sampling of 1mL every 6 hours (disturbance) (Figure 6.7b). Both controllers aim to increase the culture productivity (volumetric mAb concentration) using the setpoint obtained from the dynamic optimization studies (Section 6.3.2) and manipulating the inlet flow rate of the feed. For the latter, we consider feeding of the GS-Supplement (SAFC Biosciences, Sigma-Aldrich, UK) X40 and 0.4 M glucose, as before. The controller is simulated for 168 hours (7 days) of culture and its performance is assessed.

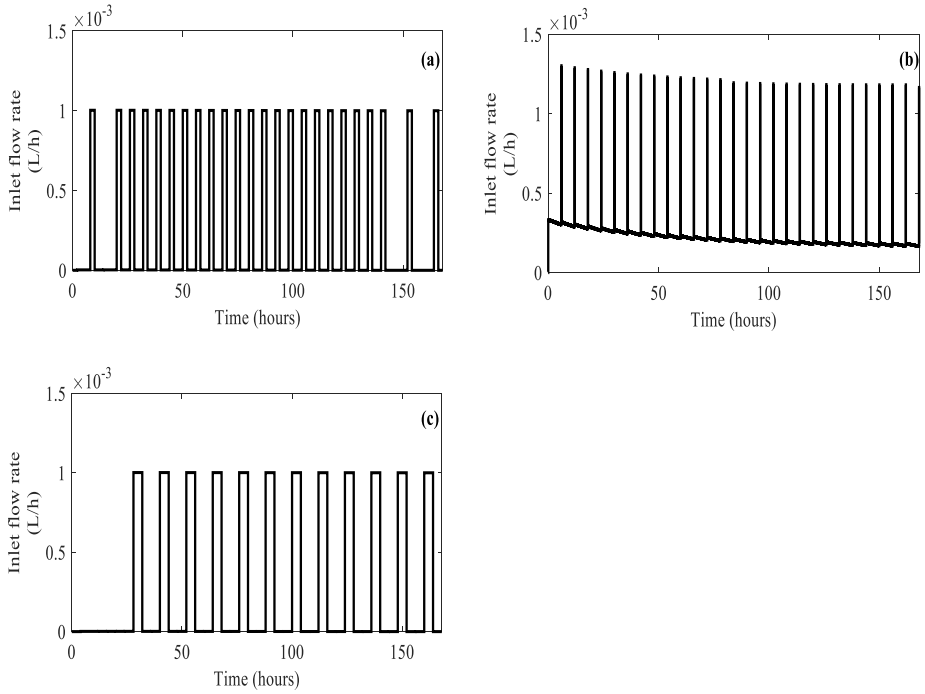

Figure 6.12 Input profile (feeding strategy) for the: a) 2-hour, (b) the 1-minute and (c) 4-hour interval strategy.

Figure 6.12 illustrates the feeding strategies as indicated by the controllers. It is observed that the 2- and 4-hour controller (Figure 6.12a & c) return a pulse feeding strategy that is scarcer in the beginning and is intensified as the culture evolves and enters growth phase. As mentioned previously, the generated profiles are in accordance with the system biologics, as nutrients are mostly required during the exponential phase. In addition, the cell density increases as a function of time (Figure 6.14), leading therefore to increased nutrient demand. A key difference in the two input profiles is that the 2-hour controller decreases the frequency of the feeding towards the last hours of the culture. On the other hand, the 1-minute strategy suggests a different input profile for the feeding that could be characterized semi-continuous.

In particular, the controller (Figure 6.12b) starts introducing 0.3 mL of fresh medium that is gradually decreased throughout the culture time and reaches the value of 0.17 mL on the 168th hour. The continuous profile is interrupted by periodic pulses of approximately 1mL at the points when samples are extracted. The latter are most probably corrective actions taken by the controller as a response to the occurring disturbance (sampling), in order to maintain the culture volume within the permitted window. Although this profile is probably a result of the volume constraint imposed on the control problem formulation, the periodic feeding pulses introduce fresh medium in the cell culture system that affects the cell metabolism and therefore the culture behavior. The model-based nature of the control strategy presented here allows testing of the controller against the process model that describes the main events taking place in the cell culture system. Consequently, any variations in the culture behavior due to the applied feeding strategy are depicted in the closed-loop, in silico simulation results presented in Figures 6.14 and 6.15. Therefore the efficiency of the strategy can be assessed both in process constraints (e.g. culture volume) and culture performance. It should be underlined that all three strategies manage to maintain the culture volume within the predefined ±10% window (Figure 6.13) (<0.5% overshoot for the 2 hour and the 4 hour strategies).

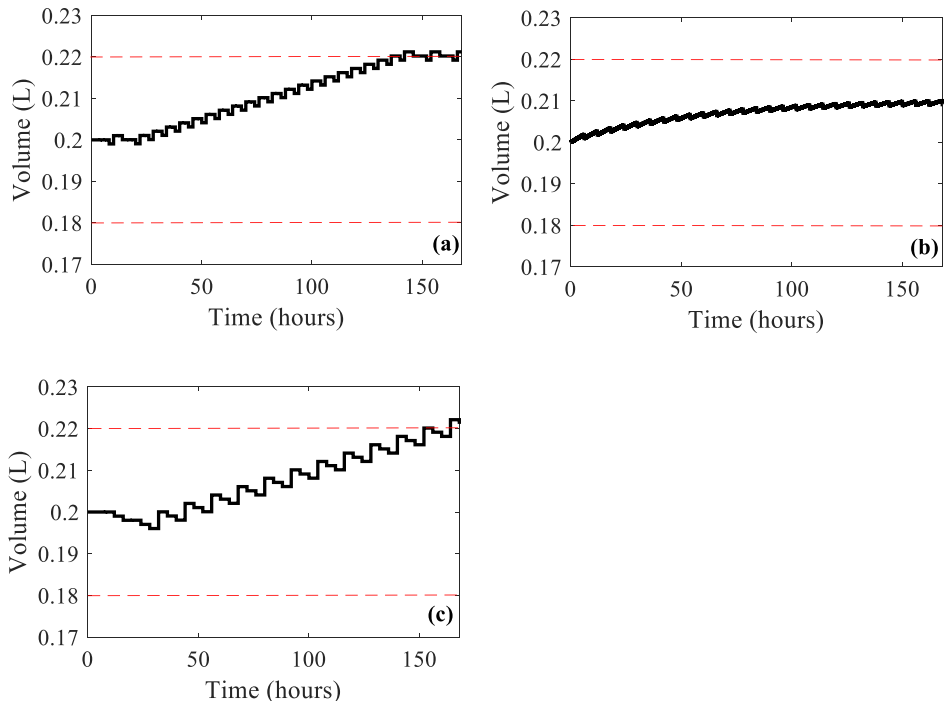

Figure 6.13 Culture volumes during the simulation (black lines) of the: a) 2-hour, (b) 1-minute and (c) 4-hour interval strategy. The red dotted lines correspond to the allowed ±10% threshold for the volume (upper bound: 0.22 L, lower bound: 0.18 L).

Comparing the output profiles (Figure 6.14) we observe that all controllers outperform the batch system, as expected. The 4-hour strategy achieves significantly lower volumetric antibody concentration by the end of the culture, compared to the other two strategies that demonstrate a similar behavior in the output (Figure 6.14a). However, based on the profile of viable cells (Figure 6.14b) it could be concluded that the scarcer the strategy the higher the culture longevity. More specifically, it is observed that although the 4-hour strategy results in lower cell density compared to the other fed-batch systems, it demonstrates a decreased death rate and therefore prolonged culture time.

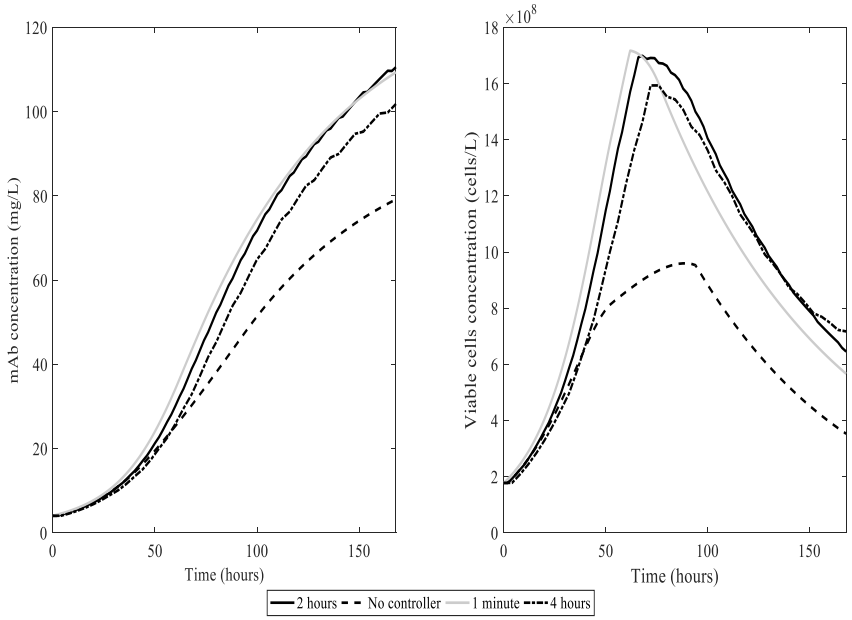

Figure 6.14 Comparison of the 2-hour, 1-minute and 4-hour interval and the batch system for: (a) the mAb concentration and (b) the population of viable cells over 168 hours of culture.

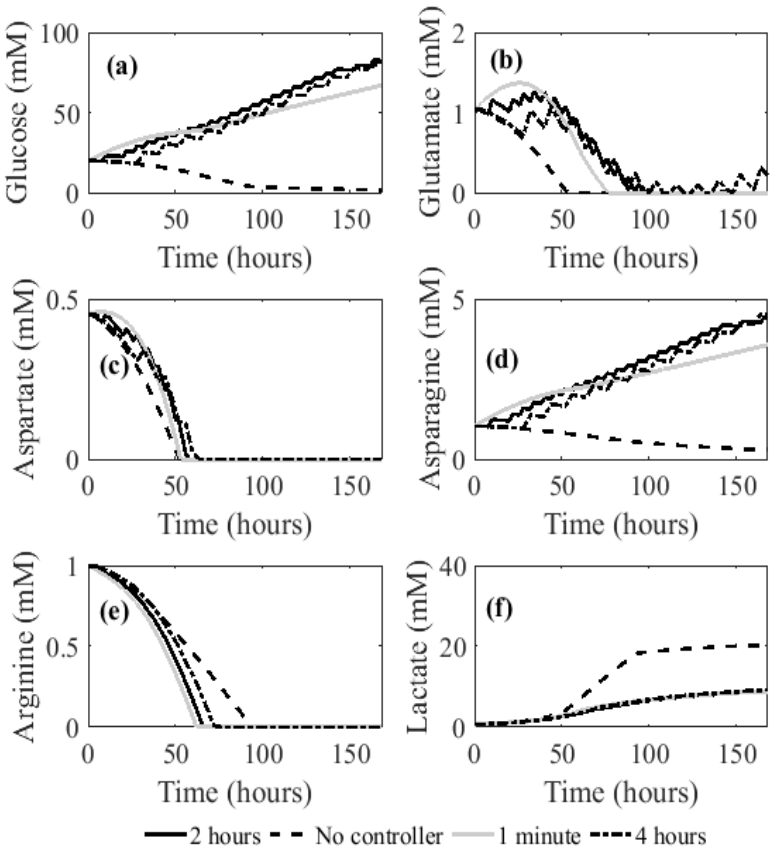

Figure 6.15 Comparison the 2-hour, 1-minute and 4-hour interval and the batch system for the concentrations of: (a) glucose, (b) glutamate, (c) aspartate, (d) asparagine, (e) arginine and (f) lactate over 168 hours of culture.

Figure 6.15 illustrates the profiles of the 5 nutrients considered in this work, where the proposed strategies manage to maintain the levels of most of the amino acids and glucose above zero and therefore guarantee that nutrients are available throughout the culture period. Comparing the amino acid profiles it is evident that the cells utilize them in a preferential manner, rather than all at the same time and rate. According to the metabolic interactions considered here (Figure 6.1), the cell population utilizes different metabolic pathways based on the nutrient availability. Such profiles could therefore lead to the design of combined optimization and/or control strategies where the optimal medium and composition for maximum productivity are defined (Quiroga et al., 2016).

In order to evaluate the overall performance of the examined systems, we compare the total amount of antibody produced within the culture period (Figure 6.16). Therefore we can assess the total amount of product produced, regardless of variations in the culture volume. It can be observed that although the maximum volumetric mAb concentration (mg/L) is reached following the feeding strategy designed by the dynamic optimization (Section 6.3.2), the culture produces higher total amount of product (mg) under the 2-hour and 1-minute strategy.

Interestingly, although the total amount of medium administrated in the 2- and 4-hour strategy is the same and in fact significantly higher (49 mL) than the 1-minute one (37 mL), the latter strategy manages to reach similar amounts of total product to the 2-hour strategy (1965mg). Conversely, the 4-hour strategy can be considered as less efficient (1860 mg). It could be therefore concluded that control strategies with higher feedback frequency and therefore more frequent feeding can lead to more efficient culture operations. That could be attributed to the fact that semi-continuous feeding, such as the 1-minute strategy, introduce the feed in a gradual fashion, allowing the culture to adapt to changes and therefore minimize the risk of cell stress that might jeopardize the cell functions.

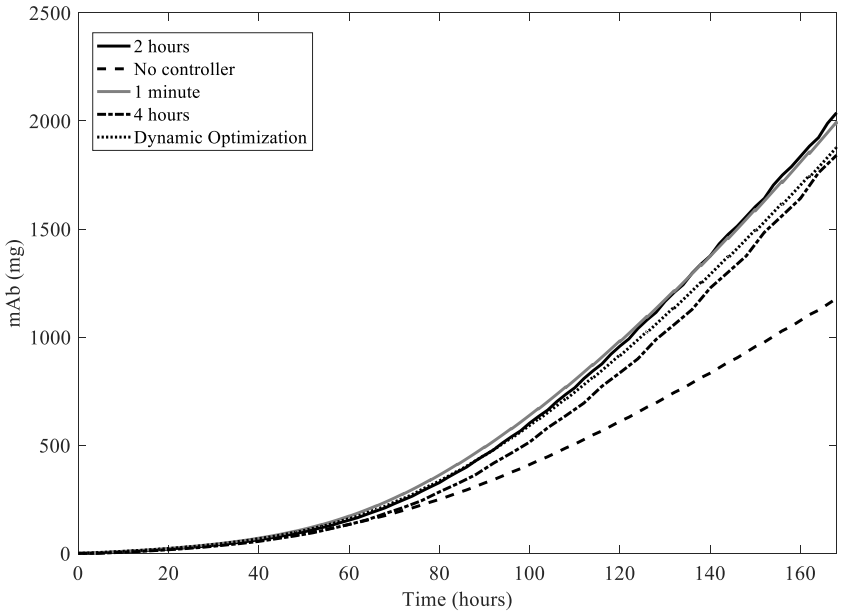

Figure 6.16 Accumulative amount of mAb produced during the culture period for the 2-hour, 1-minute and 4-hour interval and the batch system.

It is acknowledged that the suggested control strategies are associated with certain practical implications when it comes to their implementation and are mostly related to sensor availability. More specifically, currently measurements for mAb concentration are performed at line, thus requiring part of the culture volume to be removed. Therefore, strategies that require frequent sampling (e.g. 1 minute frequency) would compromise almost 1/3 of the culture volume within the timespan of 1 hour. Such strategies would be feasible to implement only in the event where online sensors are available. For this reason, the 2-hour control strategy would result in a more stable system with feasible experimental application. Moreover, the at line measurement for the antibody concentration can be returned to the controller in the order of minutes, thus allowing the controller to re-estimate the system state prior to the next action.

6.6 Conclusions

This chapter presents novel, model-based control strategies where the developed controllers are designed based on a dynamic, process model of a mammalian cell culture system. In particular, we investigate the culturing of GS-NS0 cells in a 1L flask and we design advanced multi-parametric control strategies for the maximization of the culture productivity. Firstly, a dynamic model is developed that considers the main events taking place in the culture. The model is based on a simplified network of the cell metabolism that considers 5 key nutrients: (a) glucose, (b) glutamate, (c) aspartate, (d) asparagine, (e) arginine, and lactate. Those interactions are described through Ordinary Differential and Algebraic Equations (ODAEs) that are assessed also under sensitivity analysis and parameter estimation procedures (Appendix C). The model is experimentally validated and a good agreement between the simulation results and the experimental data is reported. Following the model development, dynamic optimization studies are executed in order to define a feeding strategy that will increase the culture productivity. The optimization problem is formulated using the volumetric antibody concentration as the objective function of interest. Other objective functions reported in the literature are the concentration of viable cells, the integral of viable cells as well as the specific productivity (Schubert et al., 1994, Bibila and Robinson, 1995, Jenzsch et al., 2006, Aehle et al., 2012, Koumpouras and Kontoravdi, 2012, Kiparissides et al., 2015). However, as discussed in section 6.3 the optimization problem forms the basis for the design of the control scheme further on and should therefore follow the same structure. Therefore envisioning to create a computational link between the upstream and the downstream controller, we choose to use the volumetric antibody concentration as the objective function that is the output of interest also in the downstream control schemes presented in this work (Chapter 4 and Chapter 5).

Based on the results obtained from the dynamic optimization three parametric controllers are designed, following the PAROC framework and their performance on the examined system is compared. Based on different discretization profiles we design a: (a) 2-hour, (b) 4-hour and (c) 1-minute control strategy. According to the results from the in-silico validation, all three controllers manage to increase the culture productivity and longevity compared to batch, maintaining the culture volume within the permitted range. Nevertheless, the 2-hour & 1-minute approaches demonstrate significantly improved performances as they achieve higher total amount of product. Comparing the input profiles, all controllers manage to consider the culture requirements and adjust the feeding accordingly, minimizing the excess of nutrients in the flask. From the computational results presented in this section, it could be concluded that

semi-continuous feeding has the potential to lead to more efficient operating profiles, where cell stress due to abrupt change of conditions in the culture can be decreased. Compared to standard practice (

Table 6.1), the control strategies presented here suggest a feeding strategy considering not only the improvement of the system performance, but also a set of operational constraints such as variations in the culture volume. In addition, the use of mp-MPC allows the optimization problem to be solved offline thus reducing the computational demand of the controller during online operation (Pistikopoulos, 2009).

A potential limitation of the proposed control strategies could be associated with feedback measurements, as the latter need to be taken at the same frequency as the discretization step used for the controller design. Therefore, strategies that require frequent sampling (e.g. 1 minute frequency) would compromise a large amount of the culture working volume thus rendering the strategy infeasible in the absence of online sensors. For this reason, control strategies with scarcer discretization step (e.g. 2 hours) would be preferred. Moreover, the at-line measurements available for antibody concentration can be returned to the controller within minutes, thus allowing the controller to re-estimate the system state prior to the next action. The mp-MPC controllers designed here can be modified to account for disturbances that might occur during online operation. These can be a result of the periodic sampling as part of the required monitoring (measured disturbance) or other types of variations in the system that might occur as a result of changes in the culture conditions (e.g. pH, temperature) or noise in the feedback measurements. The latter would be incorporated as unmeasured disturbances in the control problem formulation as they are of unexpected nature and variation and the controller would be robustified against those.

Based on the work presented in this chapter, the proposed control scheme suggests tracking of the volumetric antibody concentration that is also the output of interest in the downstream purification (Chapters 4 &5). Therefore, a computational link between the upstream and the downstream control schemes could be established, using the output of the upstream controller (volumetric antibody concentration) to update the controller operating on the downstream process. In particular, as discussed in Chapter 4 the exact product concentration resulting from the upstream may vary and it is therefore treated as measured disturbance in the downstream control scheme. Another set of crucial variables that need to be considered is the level of impurities that in this work look into fragments and aggregates (weak and strong impurities respectively) that is also treated as measured disturbance, as their concentrations cannot be defined a priori (Chapter 4). In order to realize the in silico integration, their

quantities need to be tracked by the upstream process model. Appendix D demonstrates preliminary, in silico results on the modification of the upstream model to include terms describing the formation of these impurities in the cell culture. At this stage it is not considered necessary to include the impurities in the output set of the upstream controller as their levels can be controlled offline, through experimental and/or computational optimization that will indicate the optimal operating conditions that can lead to improved cell culture performance and reduced impurity levels.

Chapter 7.

Conclusions & Future Directions

7.1 Project Summary

Aiming to design eco-efficient processes of high productivity and operating costs, pharmaceutical industries are embracing the shift from batch to continuous operation (Hillier, 2013). This technological advance could be characterized as "leading-edge" in the field of intensification of chemical engineering processes and beyond. In particular, monoclonal antibody manufacturing can significantly benefit from this paradigm shift, as continuous operation promises higher product titers and reproducible/stable quality. However, for this transition to be realized significant improvements in the current state-of-the-art are required. More specifically, both the process counterparts (upstream & downstream) need to be individually studied, optimized and effectively integrated, considering the entire set of their capabilities/limitations. The main focus of this work is the development of advanced computational tools for the performance improvement of chromatographic separation systems as well as cell culture systems, envisioning their integration under a global control strategy. In this direction:

- Chapters 1, 2 & 3 are dedicated to the investigation and discussion of the current state-of-the-art both in the upstream and the downstream system. The capabilities and limitations of both systems are examined and key contributions in the fields of modeling, control and optimization of such systems are acknowledged.
- Chapters 4 & 5 are focused on the development of advanced, model-based control strategies of chromatographic separation systems. In particular, we present the design & in silico testing of multi-parametric MPC controllers for a single- (Chapter 4) and a twin-column (Chapter 5) system, based on the industrially relevant MCSGP process. The mathematical model used for the control studies has been previously developed and validated by the Morbidelli Group (ETH Zürich). Issues with unavailable measurements, as well as disturbances due to feed variations are discussed. In addition, the inherent time delay due to the residence time is investigated. The controllers are designed and tested within the systematic PAROC framework and software platform for the development of explicit/multi-parametric controllers.
- Chapter 6 presents a model-based control approach for the improvement of the productivity in a GS-NS0 cell culture system. A dynamic model based on the consumption/production of 5 key nutrients and lactate is used for the execution of dynamic optimization experiments for the design of an optimal feeding strategy. The model has been previously developed and validated in collaboration with Dr. Ana Quiroga. Following that, we employ PAROC as the tool for the design and testing of

3 parametric controllers with different feedback requirements (sampling time). The system performance under the proposed strategies is assessed and compared.

7.2 Key Contributions & future steps

The aim of this work was to design advanced control strategies that are able to track the examined systems throughout the process cycle. In the case of the chromatographic separation (Chapter 4 & 5) the main focus was the development of control schemes that can maintain the periodic nature of the studied process, while dealing with variations in the feed stream. Similarly, the main objective for the upstream system (Chapter 6) was the investigation of the effect of feeding frequency on the culture productivity. The contributions of this thesis are discussed below.

7.2.1 Model-based control of chromatographic separation processes

The control scheme presented in this work suggests monitoring every chromatographic column as an independent unit, rather than treating the setup as a "black box", where a general correlation between the input (modifier) and the output (usually product purity and yield (Grossmann et al., 2010)) is utilized. Moreover, as discussed in Chapter 4, the designed controllers are monitoring the integral of the outlet concentrations of the mixture components, allowing for continuous process monitoring, rather than "cycle-to-cycle" control policies. Hence the presented results enable a control of multi-column continuous processes, while dealing with their cyclic and non-linear behavior. The main contributions of the proposed scheme are summarized below:

- Novel multi-parametric control strategies for single- and multi-column chromatographic systems were designed and tested in silico against the process model.
- Integral tracking: Aiming to design advanced control strategies that can facilitate continuous monitoring, we propose tracking of the integrals of the outlet concentrations of the mixture components. The latter can be used for the offline, post-calculation of yield and purity as discussed in Chapter 4.
- Gradient setpoint change: We apply a gradient slope for the change in the predefined setpoints, aiming to follow the profiles encountered in gradient chromatography.
- Setpoint shift strategy: To compensate for the residence time in chromatographic systems, we suggest a novel strategy, where the setpoints are shifted in time, based on the pre-calculated time delay.

- Column integration: We present the column integration, where the recycling streams are treated as disturbance in the control scheme, minimizing the amount of online measurements required.

7.2.2 Model-based control of cell culture systems:

In the context of this work preliminary control studies were also performed on a cell culture system, aiming to investigate the impact of different feeding frequencies on the culture performance. As discussed in Chapter 6 the suggested control schemes manipulated the feed flow rate, tracking the volumetric antibody concentration within the culture. The latter is chosen as the control output amongst other variables (e.g. viable cells, specific productivity) as it provides seamless communication between the upstream and the downstream controller. In addition, in real-life application, as discussed in Chapter 6, feedback measurements can be obtained by sensors already available in the market. Moreover, the proposed controllers are designed taking into consideration constraints associated with changes in the culture volume, minimizing the risk of dilution due to excessive feeding. The main contributions of the proposed scheme are summarized below:

- Novel, model-based control strategies for GS-NS0 cell culture system are designed and tested in silico, based on a dynamic, process model.
- Dynamic optimization policies are designed for the maximization of the culture productivity under fed-batch feeding of 5 key nutrients and lactate.
- Different sampling strategies are tested for the improvement of the performance of the cell culture system. The designed controllers are trained against disturbances that can occur from noise in the measurements and/or periodic sampling (or outlet flow in the case of continuous operation).

7.3 Discussion

This work presents the development of advanced controllers, based on multi-parametric techniques for: (i) a chromatographic separation process and (ii) a cell culture system. Compared to previously presented works on such systems, the control schemes suggested here benefit from the advantages of multi-parametric MPC that allows the solution of the optimization problem offline thus enabling faster control actions (Pistikopoulos, 2009). Moreover, "online via offline" optimization allows the solution of more complex problems, as the computational burden is transferred offline without having the timing restrictions existing during the online operation. The contributions from this work along with their applicability and potential limitations are discussed below.

7.3.1 Chromatographic separation systems

The strategies developed for the MCSGP system have demonstrated their capabilities with respect to setpoint tracking. Moreover, as demonstrated in Chapter 4 and 5, the controllers manage to return cyclic input profiles, thus revealing the potential of the suggested techniques to maintain the process periodicity and ensure cyclic steady state. As discussed earlier (Chapter 4) the control schemes designed in this work consider variations in the feed stream as measured disturbances, aiming to prevent deviations due to process variability to affect the process performance. The latter can prove to be of great significance as it has been reported that changes in the feed composition affect the robustness of the separation (Mazzotti et al., 1997). It has to be underlined that the case studies upon which the controllers were tested (Chapter 5) focus on their performance under different operating conditions (e.g. periodic feeding, various flow rates). The latter was successfully assessed with respect to system tracking rather than final product purity and recovery yield. For completeness, the next step should look into a unified simulation of the whole MCSGP process course, where purity and yield can be assessed.

Feedback measurements are often a challenge for most control schemes in downstream processing. Also, in this case, the presented controllers will require a series of online measurements when applied on the setup. These can result from equipment that is already established on such units, such as UV/VIS. The latter can provide measurements within few seconds on the eluted concentrations that can later be updated by more accurate measurements resulting from the HPLC that requires longer analysis time. Software packages such as MATLAB® or similar can be used in tandem in order to calculate the value of the integral concentration, while yield and purity can be post-calculated offline as per current standard practice. The model-based nature of the proposed controllers minimizes the risk of failure in case measurements are unavailable, as the process model can be used to temporarily obtain the required feedback. In addition, the suggested approach takes into consideration the lack of measurements during continuous mode, treating the internal recycle stream as disturbance.

7.3.2 Cell culture system

Compared to previously developed control schemes (please refer to Chapter 6 for a detailed discussion) the one presented in this work benefits both from the model-based nature of the controller, as well as the ability offered by multi-parametric control, to solve the optimization problem offline. The first element, not only allows the controller to be trained on the

knowledge gained from the process model, but offers also the advantage of using the validated process model to obtain feedback for the controller during online operation in case of unexpected events and/or noisy measurements. To add to that, mp-MPC suggests the solution of the optimization problem offline (Pistikopoulos, 2009), thus minimizing the computational demand and time required for the calculation of the optimal action during the online operation. Similar to all control strategies, also the one presented in this work, relies on the availability of online measurements. Using the volumetric antibody concentration as the tracked output, the controller feedback can be obtained via sensors available in the market (e.g. Bioprofile® Flex Analyser, Nova Biomedical, Waltham, USA).

Currently, the input profile suggested by the presented control strategies is characterized by relatively low flow rate values that are close to the operating lower bound of current commercial pumps, thus posing a challenge in their experimental application. The latter could be potentially tackled through the use of micro-pumps. The study presented here, focuses on the examination of the effect of different feeding frequencies on the volumetric antibody concentration, based on a simplified mathematical model. Current and future research is looking into the development of similar control strategies using a more sophisticated mathematical model that incorporates elements such as metabolic shifts and energy metabolism (Quiroga, 2017). Moreover, replacing the feeding medium used here with a medium of optimized composition would lead to the development of tailor-made, automated feeding strategies that satisfy the culture needs while using the optimal amount of nutrients required.

7.4 Future Research Directions

The main vision of this work is the advancement of computational tools used in the biomanufacturing of monoclonal antibodies for the. In this framework, current and future developments are looking into further optimization and development of: (a) upstream processes, (b) chromatographic separation processes and (c) the integrated bioprocess.

7.4.1 Upstream processes

In Chapter 6, we demonstrate the development of dynamic optimization and model-based control strategies based on a simplified network that considers 5 key nutrients as the principal components of the cell metabolic functions. This work is currently being expanded and applied to an energy-based model, monitoring ATP and the full set of amino-acids (Quiroga, 2017). Moreover, the use of model-based media as the input for the control problem formulation can also be considered. Aiming to shift towards continuous processing, the model

parameters could be re-estimated to serve cases where there is continuous outlet flow. The latter will not affect the control methodology presented in this work, as the outlet flow rate is already considered as disturbance by the problem formulation. A change in the outlet profile, however, may result into changes in the input profile that is expected to present a more continuous behavior. In addition, alternative control schemes where the concentrations of the key amino-acids are monitored independently could also be investigated. In addition, in order to determine the effect of the human error, an automated feeding strategy as designed and provided by the controllers can be compared to a human-operated feeding.

7.4.2 Chromatographic separation processes

The work presented in Chapters 4 & 5 can be employed for the control of multi-column chromatographic separation processes, such as the MCSGP process. In collaboration with the Morbidelli Group (ETH Zürich) we are investigating the experimental application of the proposed control schemes. From a computational standpoint, dynamic optimization policies of the MCSGP process can be investigated, aiming to improve the experimentally optimized input profiles and setpoints. The online application of the proposed methodology could be facilitated by the design of a supervisory controller that will determine the optimal duration of each phase (batch or continuous, please refer to Chapter 3, Section 3.3) and consequently the switch between the two proposed control schemes (batch (Chapter 4) and interconnected (Chapter 5) respectively). For completeness, it would be also interesting to investigate the development of robust control schemes that will account for unexpected disturbances during the online operation. In order to immunize the controller against a greater variety of feed compositions, the latter could also be predicted using a systematic approach as presented by Chan et al. (2008a) that could be used afterwards as disturbance bounds for the controller development.

7.4.3 Integrated biomanufacturing system

As mentioned earlier, the vision of this work is the intensification of the production of monoclonal antibodies via continuous operation. On that end, work is being carried out towards the integration of all the units utilized in the bioprocess. Figure 7.1 demonstrates the concept based on which a global control policy will be designed.

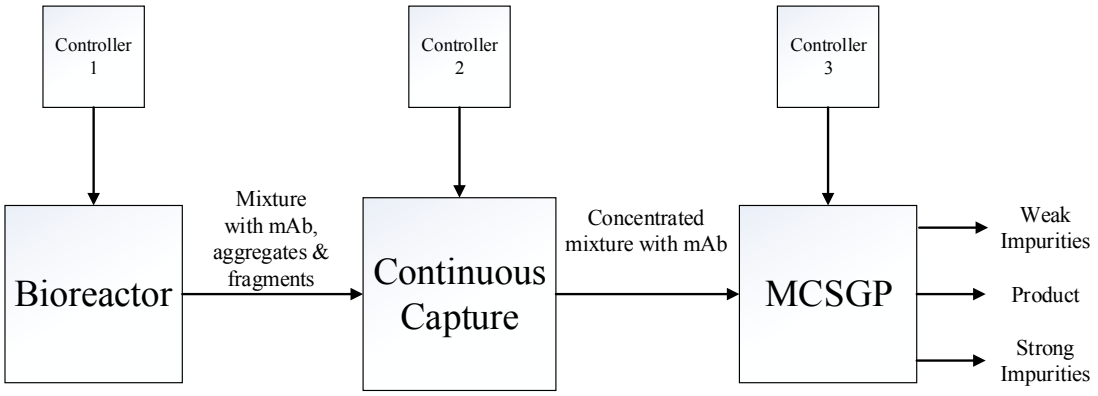

Figure 7.1 Integrated bioprocess under a global control scheme.

In collaboration with the Morbidelli Group (ETH Zürich), we are studying the integration of:

- A continuous upstream system,
- a continuous capture system based on Protein A chromatography (Steinebach et al., 2016a) and
- the MCSGP process.

Current research is focusing on the improvement and unification of the aforementioned systems under an interoperable software platform, employing the PAROC framework and software platform (Pistikopoulos et al., 2015). For the model integration to be achieved, the outputs of the three process models (cell culture, capture and MCSGP) need to be unified, in order to monitor: impurities (weak & strong) as well as the targeted product (mAb). In particular, with respect to the upstream system; the incorporation of terms describing the formation of aggregates and fragments needs to be investigated. Preliminary results on the modification of the upstream process model are presented in Appendix C, however, due to the fact that aggregation kinetics and fragmentation are complex effects that are associated with the culture conditions, the selected cell line as well as the type of antibody produced, a thorough investigation is needed, coupled with the required experimentation. Therefore, the results demonstrated in Appendix D serve as a proof of concept that identifies the computational requirements for the unification of the three process models. In order to smoothen the integration of the process models at hand the simulation of the capture model in gPROMS® Modelbuilder (P.S.E, 1997-2016) is being realized. Appendix D discusses preliminary results on the model integration under an interoperable software environment.

7.4.4 Other applications

The presented control strategies can be further expanded to other types of industries, where continuous processing and/or monitoring can improve the process efficiency. For example,

chromatography is extensively used in food industries for the clarification of various mixtures (Bubnik et al., 2004, Ni et al., 2016). Intensifying their operation via advanced computational tools could lead to increased productivity and significantly improve product quality, as holdup steps will be minimized. Other areas of application of the suggested strategies could be fermentation systems as well as periodic separation processes such as pressure swing adsorption systems (Jiang et al., 2003, Kawajiri and Biegler, 2006b, Khajuria and Pistikopoulos, 2011a, Khajuria and Pistikopoulos, 2011b, Khajuria and Pistikopoulos, 2013).

Contributions from this work

A. Journal Publications

1. **Papathanasiou M.M**., Mantalaris A., Pistikopoulos E.N. 2017. "Intelligent, model-based control towards the intensification of downstream processes". *Submitted to Computers and Chemical Engineering for the Special Issue on Process Intensification. Aritcle in Press*

2. **Papathanasiou M. M.**, Quiroga-Campano A, Elviro Perez M., Mantalaris A., Pistikopoulos E. N. "Advanced multi-parametric Model Predictive Control (mp-MPC) strategies towards integrated continuous biomanufacturing". 2017. *Biotechnology Progress for the Special Issue based on the Berkeley conference on Integrated Continuous Biomanufacturing. Article in Press*

3. **Papathanasiou, M. M.**, Avraamidou, S., Oberdieck, R., Mantalaris, A., Steinebach, F., Morbidelli, M., Mueller-Spaeth, T. and Pistikopoulos, E. N., **2016**. "Advanced control strategies for the multicolumn countercurrent solvent gradient purification process." *AIChE Journal*, 62: 2341–2357.

4. Pistikopoulos, E.N., Diangelakis N.A., Oberdieck R., **Papathanasiou M.M**., Nascu I. and Sun M., **2015**. PAROC—An integrated framework and software platform for the optimisation and advanced model-based control of process systems. *Chemical Engineering Science*, *136*, pp.115-138.

5. Oberdieck, R., Diangelakis, N. A., **Papathanasiou, M. M**., Nascu, I. & Pistikopoulos, E. N. 2016. POP – Parametric Optimization Toolbox. *Industrial & Engineering Chemistry Research,* 55**,** 8979-8991

B. Conference Publications

1. **Papathanasiou M.M.,** Oberdieck R., Avraamidou S., Nascu I., Mantalaris A., Pistikopoulos E.N: "Development of advanced control strategies for periodic systems: An application to chromatographic separation processes", **2016**, *In American Control Conference (ACC)*. IEEE. *pp. 4175-4180.*

2. Nascu I., Diangelakis N. A., Oberdieck R. **Papathanasiou M.M.,** Pistikopoulos E. N., "Explicit MPC in real-world applications: the PAROC framework", **2016**, *In American Control Conference (ACC)*. IEEE. *pp. 913-918.*

3. **Papathanasiou, M. M.**; Sun, M.; Oberdieck, R.; Mantalaris, A.; Pistikopoulos, E. N. "A centralized/decentralized control approach for periodic systems with application to chromatographic separation processes". *11th IFAC Symposium on Dynamics and Control of Process Systems, including Biosystems; 2016;, IFAC-PapersOnLine* 49 Paper 7, pp 159-164.

4. **Papathanasiou M.M.,** Oberdieck R., Mantalaris A., Pistikopoulos E.N. "Computational tools for the advanced control of periodic processes - Application to a chromatographic separation", **2016** , *In Computer Aided Chemical Engineering, Elsevier, Volume 38. pp. 1665-1670.*

5. **Papathanasiou M.M.,** Quiroga-Campano A., Oberdieck R., Mantalaris A., Pistikopoulos E.N., "Development of advanced computational tools for the intensification of monoclonal antibody production", **2016**, *In Computer Aided Chemical Engineering, Elsevier, Volume 38; pp. 1581-1586.*

6. Quiroga-Campano A., **Papathanasiou M.M.,** Mantalaris A., Pistikopoulos E.N., "A Predictive Model for Energy Metabolism and ATP Balance in Mammalian Cells: Towards the Energy-Based Optimization of mAb Production", **2016**, *In Computer Aided Chemical Engineering, Elsevier, Volume 38; pp 1659-1664.*

7. **Papathanasiou, M. M.**; Mantalaris, A.; Pistikopoulos, E. N. "Advanced control strategies for a periodic, two-column chromatographic process". *IEEE International Conference on Automation, Quality and Testing, Robotics (AQTR)*; **2016**; pp 1-6**.**

8. **Papathanasiou M.M**, Steinebach F., Stroehlein G., Müller-Späth T., Nascu I., Oberdieck R., Morbidelli M., Mantalaris A., Pistikopoulos E.N., "A control strategy for periodic systems – application to the twin-column MCSGP", **2015**, *In Computer Aided Chemical Engineering, Elsevier, Volume 37,* pp. 1505-1510.

C. Oral & Poster Presentations

1. **13 – 18 Nov '16: AIChE Annual Meeting 2016 (San Francisco, CA, USA)**

- **Papathanasiou M.M.,** Mantalaris A., Pistikopoulos E.N., "Towards Optimal and Sustainable Operation of Separation Processes: The Computational Approach" (Oral Presentation)
- **Papathanasiou M.M.**, Mantalaris A., Pistikopoulos E.N., "Intelligent Control Strategies Towards the Intensification of Monoclonal Antibody Production Via Continuous Operation" (Oral Presentation)
- Quiroga-Campano A., **Papathanasiou M.M.,** Mantalaris A., Pistikopoulos E.N., "Energy-Based Medium Design for Mammalian Cell Fed-Batch Cultures" (Oral Presentation)

2. **5 – 7 July '16 : American Control Conference (ACC) 2016 (Boston, MA, USA)**

- **Papathanasiou M.M.,** Oberdieck R., Avraamidou S., Nascu I., Mantalaris A., Pistikopoulos E.N: "Development of advanced control strategies for periodic systems: An application to chromatographic separation processes" (Oral Presentation)
- Nascu I., Diangelakis N. A., Oberdieck R. **Papathanasiou M.M.,** Pistikopoulos E. N., "Explicit MPC in real-world applications: the PAROC framework" (Oral Presentation)

3. **12 – 15 June ’16: European Symposium on Computer Aided Process Engineering (ESCAPE) 26 (Portoroz, Slovenia)**

- **Papathanasiou M.M.,** Oberdieck R., Mantalaris A., Pistikopoulos E.N: “Computational tools for the advanced control of periodic processes - Application to a chromatographic separation” (Oral Presentation)
- **Papathanasiou M.M.,** Quiroga-Campano A., Oberdieck R., Mantalaris A., Pistikopoulos E.N., “Development of advanced computational tools for the intensification of monoclonal antibody production” (Oral Presentation)
- Quiroga-Campano A., **Papathanasiou M.M.,** Mantalaris A., Pistikopoulos E.N., “A Predictive Model for Energy Metabolism and ATP Balance in Mammalian Cells: Towards the Energy-Based Optimization of mAb Production” (Oral Presentation)

4. **6 – 8 June ’16: 11th IFAC Symposium on Dynamics and Control of Process Systems, including Biosystems (DYCOPS-CAB) 2016 (Trondheim, Norway)**

- **Papathanasiou M.M.,**Sun M., Oberdieck R., Mantalaris A., Pistikopoulos E.N: “A Centralized/Centralized Control Approach for Periodic Systems with Application to Chromatographic Separation Processes” (Oral Presentation)

5. **19 – 21 May ’16: International Conference on Automation, Quality and Testing, Robotics (AQTR) 2016 (Cluj-Napoca, Romania)**

- **Papathanasiou M.M.,** Mantalaris A., Pistikopoulos E.N., “Advanced control strategies for a periodic, two-column chromatographic process” (Oral Presentation)

6. **27 – 29 April’16: 10th European PhD Workshop on Food Engineering and Technology (Buhler Group, Uzwil, Switzerland)**

- **Papathanasiou M.M.,** Mantalaris A., Pistikopoulos E.N., “ From Batch to Continuous Operation: Through the Prism of Computational Tools” (Oral Presentation)

7. **2 – 4 Feb ’16: Cell Culture Conference (Euroscicon) (London, UK)**

- **Papathanasiou M.M.,** Quiroga-Campano A., Oberdieck R. Mantalaris A., Pistikopoulos E.N., “ Towards the Intensification of Mammalian Cell Culture Systems” (Oral Presentation)

8. **8 – 13 Nov ’15: AIChE Annual Meeting (Salt Lake City, UT, USA)**

- **Papathanasiou M.M**., Sun M., Steinebach F., Mueller-Spaeth T., Morbidelli M., Mantalaris A., Pistikopoulos E.N., “ A Centralized/Decentralized Control Approach for the Multicolumn Countercurrent Solvent Gradient Purification (MCSGP) Process” (Oral Presentation)

- **Papathanasiou M.M.,** Quiroga-Campano A Steinebach F., Mueller-Spaeth T., Morbidelli M., Mantalaris A., Pistikopoulos E.N., “ Advanced Control Strategies Towards the Intensification of Monoclonal Antibody Production” (Oral Presentation)

- Oberdieck R., Diangelakis N.A., **Papathanasiou M. M.,** Nascu I., Sun M., Avraamidou S., Pistikopoulos E.N., “ Pop – the Parametric Optimization Toolbox” (Oral Presentation)

- Pistikopoulos E.N., Oberdieck R., Diangelakis N.A., **Papathanasiou M. M.,** Nascu I., “ PAROC - a Unified Framework Towards the Optimal Design, Operational Operation and Model-Based Control of Process Systems” (Oral Presentation)

9. **1 – 5 Nov ’15: Integrated Continuous Biomanufacturing (San Fransisco, CA, USA)**

- **Papathanasiou M.M.,** Quiroga-Campano A., Oberdieck R., Mantalaris A. Pistikopoulos E.N., “Advanced Computational tools to enhance continuous monoclonal antibody production” (Poster & Snapshot presentation)
-

10. **31 May – 4 June ’15: Process Systems Engineering 2015/ European Symposium on Computer Aided Process Engineering 25 (PSE 2015/ESCAPE 25) (Copenhagen, Denmark)**

- **Papathanasiou M.M.,** Steinebach F., Stroehlein G., Mueller-Spaeth T., Nascu I., Oberdieck R., Morbidelli M., Mantalaris A. Pistikopoulos E.N., “A control strategy for periodic systems: Application to a chromatographic separation process” (Oral Presentation)

11. **4 – 5 Dec ’14: CPSE Autumn Industrial Consortium Meeting (London, UK)**

- **Papathanasiou M.M**., Manthanwar A., Nascu I., Diangelakis N.A., Oberdieck R., Sun M., Avraamidou S., Mantalaris A., Pistikopoulos E.N., “PAROC An Integrated Framework & Software Platform for Multi-parametric Programming & Control” (Oral & Poster Presentation)

12. **16 – 21 Nov ’14 : AIChE Annual Meeting (Atlanta, GA, USA)**

- **Papathanasiou M.M**., Steinebach F., Stroehlein G., Diangelakis N.A. M., Mantalaris A. Pistikopoulos E.N., “On the development of multi-parametric controllers for the twin-column MCSGP” (Oral Presentation)

13. **2 – 3 April ’14: Advanced Process Modelling (APM) Forum 2014 (London, UK)**

- **Papathanasiou M.M**., Nascu I., Diangelakis N.A., Oberdieck R., Mantalaris A., Pistikopoulos E.N., “An integrated software platform for the development and testing of multi-parametric controllers” (Poster presentation)

References

Absoluteantibody. 2017. Antibody Fragments. 2017. Available: http://absoluteantibody.com/antibody-resources/antibody-engineering/antibody-fragments/.

Aehle, M., Bork K., Schaepe S., Kuprijanov A., Horstkorte R., Simutis R. & Lübbert A. 2012. Increasing batch-to-batch reproducibility of CHO-cell cultures using a model predictive control approach. *Cytotechnology,* 64**,** 623-634.

Al-Rubeai, M. 2015. Animal Cell Culture. Springer.

Al-Rubeai, M. & Emery A. N. 1990. Mechanisms and kinetics of monoclonal antibody synthesis and secretion in synchronous and asynchronous hybridoma cell cultures. *Journal of Biotechnology,* 16**,** 67-85.

Altamirano, C., Illanes A., Casablancas A., Gámez X., Cairó J. J. & Gòdia C. 2001. Analysis of CHO Cells Metabolic Redistribution in a Glutamate-Based Defined Medium in Continuous Culture. *Biotechnology Progress,* 17**,** 1032-1041.

Anderson, N. G. 2001. Practical Use of Continuous Processing in Developing and Scaling Up Laboratory Processes. *Organic Process Research & Development,* 5**,** 613-621.

Angarita, M. B. D. B. M., Stroehlein R. L. G. L. G. & Massimo P. T. M.-S. P. 2013. Increasing Capacity Utilization in Protein A Chromatography. *BioPharm International,* 26.

Arathoon, W. R. & Birch 1986. Large-scale cell culture in biotechnology. *Science,* 232**,** 1390-1395.

Arosio, P., Rima S., Lattuada M. & Morbidelli M. 2012. Population Balance Modeling of Antibodies Aggregation Kinetics. *The Journal of Physical Chemistry B,* 116**,** 7066-7075.

Aumann, L. & Morbidelli M. 2005. *European Patent*. EP 05405327.7, EP 05405421.8.

Aumann, L. & Morbidelli M. 2007. A continuous multicolumn countercurrent solvent gradient purification (MCSGP) process. *Biotechnology and Bioengineering,* 98**,** 1043-1055.

Aumann, L. & Morbidelli M. 2008. A semicontinuous 3-column countercurrent solvent gradient purification (MCSGP) process. *Biotechnology and Bioengineering,* 99**,** 728-733.

Aumann, L., Stroehlein G. & Morbidelli M. 2007. Parametric study of a 6-column countercurrent solvent gradient purification (MCSGP) unit. *Biotechnology and Bioengineering,* 98**,** 1029-1042.

Aumann, L., Stroehlein G., Schenkel B. & Morbidelli M. 2009. Protein Peptide Purification using the Multicolumn Countercurrent Solvent Gradient Purification (MCSGP) Process. *Biopharm International* 22(1).

Aumann, L., Strohlein G., Muller-Spath T., Hansen T. B., Frederiksen S. S., Hansen E., Staby A. & Morbidelli M. 2011. Preparative insulin purification by continuous countercurrent chromatography (MCSGP). *Abstracts of Papers of the American Chemical Society,* 241.

Báez, J., Olsen D. & Polarek J. W. 2005. Recombinant microbial systems for the production of human collagen and gelatin. *Applied Microbiology and Biotechnology,* 69**,** 245-252.

Bai, J. P. 2011. Monoclonal antibodies: from benchtop to bedside. *Therapeutic delivery,* 2**,** 329-331.

Bailey, L. A., Hatton D., Field R. & Dickson A. J. 2012. Determination of Chinese hamster ovary cell line stability and recombinant antibody expression during long-term culture. *Biotechnology and Bioengineering,* 109**,** 2093-2103.

Barnes, L., Bentley C. & Dickson A. 2000. Advances in animal cell recombinant protein production: GS-NS0 expression system. *Cytotechnology,* 32**,** 109-123.

Barnes, L. M., Bentley C. M. & Dickson A. J. 2004. Molecular definition of predictive indicators of stable protein expression in recombinant NS0 myeloma cells. *Biotechnology and Bioengineering,* 85**,** 115-121.

Barton, P. I. & Lee C. K. 2002. Modeling, Simulation, Sensitivity Analysis, and Optimization of Hybrid Systems. *ACM Trans. Model. Comput. Simul.,* 12**,** 256.

Bayrak, E. S., Wang T., Cinar A. & Undey C. 2015. Computational Modeling of Fed-Batch Cell Culture Bioreactor: Hybrid Agent-Based Approach. *IFAC-PapersOnLine,* 48**,** 1252-1257.

Bayrak, E. S., Wang T., Jerums M., Coufal M., Goudar C., Cinar A. & Undey C. 2016. In Silico Cell Cycle Predictor for Mammalian Cell Culture Bioreactor Using Agent-Based Modeling Approach. *IFAC-PapersOnLine,* 49**,** 200-205.

Behrens, M., Khobkhun P., Potschka A. & Engell S. Optimizing set point control of the MCSGP process. Control Conference (ECC), 2014 European, 24-27 June 2014 2014. 1139-1144.

Bemporad, A., Morari M., Dua V. & Pistikopoulos E. N. Explicit solution of model predictive control via multiparametric quadratic programming. 2000. 872-876.

Bemporad, A., Morari M., Dua V. & Pistikopoulos E. N. 2002. The explicit linear quadratic regulator for constrained systems. *Automatica,* 38**,** 3-20.

Bentley, J. & Kawajiri Y. 2013. Prediction-correction method for optimization of simulated moving bed chromatography. *AIChE Journal,* 59**,** 736-746.

Bentley, J., Sloan C. & Kawajiri Y. 2013. Simultaneous modeling and optimization of nonlinear simulated moving bed chromatography by the prediction–correction method. *Journal of Chromatography A,* 1280**,** 51-63.

Berlec, A. & Strukelj B. 2013. Current state and recent advances in biopharmaceutical production in Escherichia coli, yeasts and mammalian cells. *Journal of Industrial Microbiology & Biotechnology,* 40**,** 257-274.

Bibila, T. A. & Robinson D. K. 1995. In Pursuit of the Optimal Fed-Batch Process for Monoclonal Antibody Production. *Biotechnology Progress,* 11**,** 1-13.

Birch, J. R., Mainwaring D. O. & Racher A. J. 2008. Use of the Glutamine Synthetase (GS) Expression System for the Rapid Development of Highly Productive Mammalian Cell Processes. *Modern Biopharmaceuticals*. Wiley-VCH Verlag GmbH.

Blackstone, E. A. & Fuhr J. P. 2012. Innovation and Competition: Will Biosimilars Succeed?: The creation of an FDA approval pathway for biosimilars is complex and fraught with hazard. Yes, innovation and market competition are at stake. But so are efficacy and patient safety. *Biotechnology healthcare,* 9**,** 24-27.

Boukouvala, F., Niotis V., Ramachandran R., Muzzio F. J. & Ierapetritou M. G. 2012. An integrated approach for dynamic flowsheet modeling and sensitivity analysis of a continuous tablet manufacturing process. *Computers & Chemical Engineering,* 42**,** 30-47.

Brooks, C. A. & Cramer S. M. 1992. Steric mass‐action ion exchange: displacement profiles and induced salt gradients. *AIChE Journal,* 38**,** 1969-1978.

Bubnik, Z., Pour V., Gruberova A., Starhova H., Hinkova A. & Kadlec P. 2004. Application of continuous chromatographic separation in sugar processing. *Journal of Food Engineering,* 61**,** 509-513.

Butler, M. 2005. Animal cell cultures: recent achievements and perspectives in the production of biopharmaceuticals. *Applied Microbiology and Biotechnology,* 68**,** 283-291.

Carta, G. & Jungbauer A. 2010. Protein Chromatography: Process Development and Scale-Up. Wiley-VCH Verlag GmbH & Co. KGaA.

Chan, S., Titchener-Hooker N., Bracewell D. G. & Sørensen E. 2008a. A systematic approach for modeling chromatographic processes—Application to protein purification. *AIChE Journal,* 54**,** 965-977.

Chan, S., Titchener-Hooker N. & Sørensen E. 2008b. Optimal Economic Design and Operation of Single- and Multi-column Chromatographic Processes. *Biotechnology Progress,* 24**,** 389-401.

Chatterjee, S. 2012. FDA Perspective on Continuous Manufacturing.

Chen, C., Le H. & Goudar C. T. 2016. Integration of systems biology in cell line and process development for biopharmaceutical manufacturing. *Biochemical Engineering Journal,* 107**,** 11-17.

Chon, J. H. & Zarbis-Papastoitsis G. 2011. Advances in the production and downstream processing of antibodies. *New Biotechnology,* 28**,** 458-463.

Chromacon. 2017. *ChromaCon AG* [Online]. Available: http://www.chromacon.ch/en/ [Accessed 14.03 2017].

Close, E., Bracewell D. G. & Sorensen E. 2013. A model based approach to an adaptive design space in chromatography. *In:* Andrzej, K. & Ilkka, T. (eds.) *Computer Aided Chemical Engineering.* Elsevier.

Close, E. J., Salm J. R., Bracewell D. G. & Sorensen E. 2014a. A model based approach for identifying robust operating conditions for industrial chromatography with process variability. *Chemical Engineering Science,* 116**,** 284-295.

Close, E. J., Salm J. R., Bracewell D. G. & Sorensen E. 2014b. Modelling of industrial biopharmaceutical multicomponent chromatography. *Chemical Engineering Research and Design,* 92**,** 1304-1314.

Cordoba-Rodriguez, R. V. 2008. Aggregates in MAbs and recombinant therapeutic proteins: a regulatory perspective. *BioPharm International,* 21.

Cramer, S. M. & Holstein M. A. 2011. Downstream bioprocessing: recent advances and future promise. *Current Opinion in Chemical Engineering,* 1**,** 27-37.

Cruz, H. J., Freitas C. M., Alves P. M., Moreira J. L. & Carrondo M. J. T. 2000. Effects of ammonia and lactate on growth, metabolism, and productivity of BHK cells. *Enzyme and Microbial Technology,* 27**,** 43-52.

Curling, J. M. 1980. *Methods of Plasma Protein Fractionation,* London, Academic Press.

Darby, M. L. & Nikolaou M. 2007. A parametric programming approach to moving-horizon state estimation. *Automatica,* 43**,** 885-891.

De Neuville, B. C., Tarafder A. & Morbidelli M. 2013. Distributed pore model for bio-molecule chromatography. *Journal of Chromatography A,* 1298**,** 26-34.

De Palma, A. 2016. Special Report on Continuous Bioprocessing: Upstream, Downstream, Ready for Prime Time? *In:* International, B. (ed.).

Degerman, M., Jakobsson N. & Nilsson B. 2006. Constrained optimization of a preparative ion-exchange step for antibody purification. *Journal of Chromatography A,* 1113**,** 92-100.

Degerman, M., Jakobsson N. & Nilsson B. 2007. Modeling and optimization of preparative reversed-phase liquid chromatography for insulin purification. *Journal of Chromatography A,* 1162**,** 41-49.

Degerman, M., Westerberg K. & Nilsson B. 2009. A Model‐Based Approach to Determine the Design Space of Preparative Chromatography. *Chemical engineering & technology,* 32**,** 1195-1202.

Del Val, I. J., Kontoravdi C. & Nagy J. M. 2010. Towards the implementation of quality by design to the production of therapeutic monoclonal antibodies with desired glycosylation patterns. *Biotechnology Progress,* 26**,** 1505-1527.

Dezengotita, V. M., Miller W. M., Aunins J. G. & Zhou W. 2000. Phosphate feeding improves high-cell-concentration NS0 myeloma culture performance for monoclonal antibody production. *Biotechnology and Bioengineering,* 69**,** 566-576.

Diangelakis, N. A., Manthanwar A. M. & Pistikopoulos E. N. 2014. A Framework for Design and Control Optimisation: Application on a CHP System. *In:* Mario R. Eden, J. D. S. & Gavin, P. T. (eds.) *Computer Aided Chemical Engineering.* Elsevier.

Doneanu, C. E., Xenopoulos A., Fadgen K., Murphy J., Skilton S. J., Prentice H., Stapels M. & Chen W. 2012. Analysis of host-cell proteins in biotherapeutic proteins by

comprehensive online two-dimensional liquid chromatography/mass spectrometry. *mAbs,* 4**,** 24-44.

Drgan, V., Novič M. & Novič M. 2009. Computational method for modeling of gradient separation in ion-exchange chromatography. *Journal of Chromatography A,* 1216**,** 6502-6510.

Dua, P., Doyle F. J. & Pistikopoulos E. N. 2006. Model-based blood glucose control for type 1 diabetes via parametric programming. *Biomedical Engineering, IEEE Transactions on,* 53**,** 1478-1491.

Dua, P., Doyle Iii F. J. & Pistikopoulos E. N. 2009. Multi-objective blood glucose control for type 1 diabetes. *Medical & biological engineering & computing,* 47**,** 343-352.

Dua, P., Kouramas K., Dua V. & Pistikopoulos E. N. 2008. MPC on a chip-Recent advances on the application of multi-parametric model-based control. *Computers and Chemical Engineering,* 32**,** 754-765.

Dünnebier, G., Engell S., Epping A., Hanisch F., Jupke A., Klatt K. U. & Schmidt‐Traub H. 2001. Model‐based control of batch chromatography. *AIChE journal,* 47**,** 2493-2502.

Dünnebier, G., Fricke J. & Klatt K.-U. 2000. Optimal design and operation of simulated moving bed chromatographic reactors. *Industrial & Engineering Chemistry Research,* 39**,** 2290-2304.

Dünnebier, G. & Klatt K. U. 2000. Modelling and simulation of nonlinear chromatographic separation processes: a comparison of different modelling approaches. *Chemical Engineering Science,* 55**,** 373-380.

Dünnebier, G., Weirich I. & Klatt K.-U. 1998. Computationally efficient dynamic modelling and simulation of simulated moving bed chromatographic processes with linear isotherms. *Chemical engineering science,* 53**,** 2537-2546.

Dutta, A. K., Tran T., Napadensky B., Teella A., Brookhart G., Ropp P. A., Zhang A. W., Tustian A. D., Zydney A. L. & Shinkazh O. 2015. Purification of monoclonal antibodies from clarified cell culture fluid using Protein A capture continuous countercurrent tangential chromatography. *Journal of Biotechnology,* 213**,** 54-64.

E.M.A 2016a. European Medicines Agency. Committee for medicinal products for human use (CHMP). Guideline: Development, production, characterisation and specifications for monoclonal antibodies and related products. 7 Westferry Circus, Canary Wharf, London, E14 4HB, UK.

E.M.A. 2016b. *European public assessment reports* [Online]. European Medicines Agency. Available: http://www.ema.europa.eu/ema/index.jsp?curl=pages%2Fmedicines%2Flanding%2Fepar_search.jsp&mid=WC0b01ac058001d124&searchTab=searchByAuthType&alreadyLoaded=true&isNewQuery=true&status=Authorised&keyword=Enter+keywords&searchType=name&taxonomyPath=&treeNumber=&searchGenericType=biosimilars&genericsKeywordSearch=Submit.

Engell, S. & Toumi A. 2005. Optimisation and control of chromatography. *Computers & Chemical Engineering,* 29**,** 1243-1252.

Eon-Duval, A., Broly H. & Gleixner R. 2012. Quality attributes of recombinant therapeutic proteins: An assessment of impact on safety and efficacy as part of a quality by design development approach. *Biotechnology Progress,* 28**,** 608-622.

F.D.A 2004. Guidance for Industry, PAT — A Framework for Innovative Pharmaceutical Development, Manufacturing, and Quality Assurance. FDA, (U.S. Department of Health and Human Services Food and Drug Administration), CDER, (Center for Drug Evaluation and Research),, CVM, (Center for Veterinary Medicine), ORA, (Office of Regulatory Affairs.

F.D.A. 2015a. U.S. Department of Health and Human Services Food and Drug Administration. Available: http://www.fda.gov/newsevents/newsroom/pressannouncements/ucm436648.htm [Accessed 28.09.2016.

F.D.A 2015b. U.S. Department of Health and Human Services Food and Drug Administration

Center for Drug Evaluation and Research (CDER). FDA Guidance: Advancement of Emerging Technology Applications to Modernize the Pharmaceutical Manufacturing Base Guidance for Industry. . *Pharmaceutical Quality/CMC.*

F.D.A, C.D.E.R, C.V.M & O.R.A 2004. Guidance for Industry, PAT — A Framework for Innovative Pharmaceutical Development, Manufacturing, and Quality Assurance. U.S. Department of Health and Human Services Food and Drug Administration, Center for Drug Evaluation and Research, Center for Veterinary Medicine, Office of Regulatory Affairs.

Farid, S. S. 2007. Process economics of industrial monoclonal antibody manufacture. *Journal of Chromatography B,* 848**,** 8-18.

Farid, S. S., Novais J. L., Karri S., Washbrook J. & Titchener-Hooker N. J. 2000. A Tool for Modeling Strategic Decisions in Cell Culture Manufacturing. *Biotechnology Progress,* 16**,** 829-836.

Farzan, P., Mistry B. & Ierapetritou M. G. 2017. Review of the important challenges and opportunities related to modeling of mammalian cell bioreactors. *AIChE Journal,* 63**,** 398-408.

Felinger, A. & Guiochon G. 1992. Optimization of the experimental conditions and the column design parameters in displacement chromatography. *Journal of Chromatography A,* 609**,** 35-47.

Felinger, A. & Guiochon G. 1993. Comparison of maximum production rates and optimum operating/design parameters in overloaded elution and displacement chromatography. *Biotechnology and Bioengineering,* 41**,** 134-147.

Felinger, A. & Guiochon G. 1996. Optimizing Experimental Conditions in Overloaded Gradient Elution Chromatography. *Biotechnology Progress,* 12**,** 638-644.

Fitzpatrick, L., Jenkins H. A. & Butler M. 1993. Glucose and glutamine metabolism of a murine B-lymphocyte hybridoma grown in batch culture. *Applied Biochemistry and Biotechnology,* 43**,** 93-116.

Forrer, N., Butte A. & Morbidelli M. 2008. Chromatographic behavior of a polyclonal antibody mixture on a strong cation exchanger column. Part I: Adsorption characterization. *Journal of Chromatography A,* 1214**,** 59-70.

Frahm, B., Lane P., Märkl H. & Pörtner R. 2003. Improvement of a mammalian cell culture process by adaptive, model-based dialysis fed-batch cultivation and suppression of apoptosis. *Bioprocess and Biosystems Engineering,* 26**,** 1-10.

Gallant, S. R. 1996. Optimization of Preparative Ion‐Exchange Chromatography of Proteins: Linear Gradient Separations. *Journal of Chromatography A,* 725**,** 295.

Gallant, S. R., Vunnum S. & Cramer S. M. 1996. Optimization of preparative ion-exchange chromatography of proteins: linear gradient separations. *Journal of Chromatography A,* 725**,** 295-314.

Garcia, C. E., Prett D. M. & Morari M. 1989. Model predictive control: theory and practice—a survey. *Automatica,* 25**,** 335-348.

Georgiadis, M. C., Kikkinides E. S., Makridis S. S., Kouramas K. & Pistikopoulos E. N. 2009. Design and optimization of advanced materials and processes for efficient hydrogen storage. *Computers & Chemical Engineering,* 33**,** 1077-1090.

Gernaey, K. V., Cervera-Padrell A. E. & Woodley J. M. 2012. A perspective on PSE in pharmaceutical process development and innovation. *Computers & Chemical Engineering,* 42**,** 15-29.

Gernaey, K. V. & Gani R. 2010. A model-based systems approach to pharmaceutical product-process design and analysis. *Chemical Engineering Science,* 65**,** 5757-5769.

Gerontas, S., Shapiro M. S. & Bracewell D. G. 2013. Chromatography modelling to describe protein adsorption at bead level. *Journal of Chromatography A,* 1284**,** 44-52.

Getaz, D., Hariharan S. B., Butte A. & Morbidelli M. 2012. Modeling of ion-pairing effect in peptide reversed-phase chromatography. *Journal of Chromatography A,* 1249**,** 92-102.

Gillespie, R., Nguyen T., Macneil S., Jones L., Crampton S. & Vunnum S. 2012. Cation exchange surface-mediated denaturation of an aglycosylated immunoglobulin (IgG1). *Journal of Chromatography A,* 1251**,** 101-110.

Girard, V., Hilbold N.-J., Ng C. K. S., Pegon L., Chahim W., Rousset F. & Monchois V. 2015. Large-scale monoclonal antibody purification by continuous chromatography, from process design to scale-up. *Journal of Biotechnology,* 213**,** 65-73.

Gnoth, S., Jenzsch M., Simutis R. & Lübbert A. 2008. Control of cultivation processes for recombinant protein production: a review. *Bioprocess and Biosystems Engineering,* 31**,** 21-39.

Godawat, R., Brower K., Jain S., Konstantinov K., Riske F. & Warikoo V. 2012. Periodic counter-current chromatography – design and operational considerations for integrated and continuous purification of proteins. *Biotechnology Journal,* 7**,** 1496-1508.

Godawat, R., Konstantinov K., Rohani M. & Warikoo V. 2015. End-to-end integrated fully continuous production of recombinant monoclonal antibodies. *Journal of Biotechnology,* 213**,** 13-19.

Golshan, S. & Guiochon G. 1990. Optimization of the experimental conditions in preparative liquid chromatography with touching bands. *Journal of Chromatography A,* 517**,** 229-256.

Golshan-Shirazi, S. & Guiochon G. 1991. Combined effects of finite axial dispersion and slow adsorption desorption kinetics on band profiles in nonlinear chromatography. *The Journal of Physical Chemistry,* 95**,** 6390-6395.

Gospodarek, A. M., Hiser D. E., O'connell J. P. & Fernandez E. J. 2014. Unfolding of a model protein on ion exchange and mixed mode chromatography surfaces. *Journal of Chromatography A,* 1355**,** 238-252.

Gottschalk, U. 2005. Downstream processing of monoclonal antibodies: From high dilution to high purity. *Biopharm International,* 18**,** 42-+.

Grancharova, A., Johansen T. A. & Kocijan J. 2004. Explicit model predictive control of gas–liquid separation plant via orthogonal search tree partitioning. *Computers & Chemical Engineering,* 28**,** 2481-2491.

Green, A. J. 2015. *Model based process design for a monoclonal antibody-producing cell line: optimisation using hybrid modelling and an agent based system*. PhD, Newcastle University.

Gritti, F. & Guiochon G. 2012a. Mass transfer kinetics, band broadening and column efficiency. *Journal of Chromatography A,* 1221**,** 2-40.

Gritti, F. & Guiochon G. 2012b. A revisit of the concept of external film mass transfer resistance in the packed beds used in high-performance liquid chromatography. *Chemical engineering science,* 72**,** 108-114.

Gronemeyer, P., Ditz R. & Strube J. 2014. Trends in Upstream and Downstream Process Development for Antibody Manufacturing. *Bioengineering,* 1**,** 188-212.

Grossmann, C. 2009. *Optimizing model predictive control of multi-column chromatographic processes*. PhD, ETH Zurich.

Grossmann, C., Amanullah M., Erdem G., Mazzotti M., Morbidelli M. & Morari M. 2008. 'Cycle to cycle' optimizing control of simulated moving beds. *AIChE Journal,* 54**,** 194-208.

Grossmann, C., Ströhlein G., Morari M. & Morbidelli M. 2010. Optimizing model predictive control of the chromatographic multi-column solvent gradient purification (MCSGP) process. *Journal of Process Control,* 20**,** 618-629.

Guélat, B., Delegrange L., Valax P. & Morbidelli M. 2013. Model-based prediction of monoclonal antibody retention in ion-exchange chromatography. *Journal of Chromatography A,* 1298**,** 17-25.

Guiochon, G. 2002. Preparative liquid chromatography. *Journal of Chromatography A,* 965**,** 129-161.

Guiochon, G. 2012. Basic principles of chromatography. *Ullmann's Encyclopedia of Industrial Chemistry*.

Guiochon, G., Golshan-Shirazi S. & Katti A. 1994. Fundamentals of nonlinear and preparative chromatography. Academic Press, Boston.

Guzlek, H., Baptista I. I., Wood P. L. & Livingston A. 2010. A novel approach to modelling counter-current chromatography. *Journal of Chromatography A,* 1217**,** 6230-6240.

Haas, N. T., Ierapetritou M. & Singh R. 2017. Advanced Model Predictive Feedforward/Feedback Control of a Tablet Press. *Journal of Pharmaceutical Innovation***,** 1-14.

Healthcare, G. 2015. Continuous Chromatography in Downstream Processing of a Monoclonal Antibody. Björkgatan 30, 75184 Uppsala, Sweden: GE Healthcare Bio-Sciences AB.

Hegrenæs, Ø., Gravdahl J. T. & Tøndel P. 2005. Spacecraft attitude control using explicit model predictive control. *Automatica,* 41**,** 2107-2114.

Hernandez, R. 2015. Continuous manufacturing: a changing processing paradigm. *BioPharm International,* 28.

Hillier, S. 2013. Making the chemical industries more sustainable. *The Chemical Engineer*.

Holmqvist, A. & Magnusson F. 2016. Open-loop optimal control of batch chromatographic separation processes using direct collocation. *Journal of Process Control,* 46**,** 55-74.

Hunt, B., Goddard C., Middelberg A. P. J. & O'neill B. K. 2001. Economic analysis of immunoadsorption systems. *Biochemical Engineering Journal,* 9**,** 135-145.

Ierapetritou, M., Muzzio F. & Reklaitis G. 2016. Perspectives on the continuous manufacturing of powder-based pharmaceutical processes. *AIChE Journal,* 62**,** 1846-1862.

Jagschies, G. 2000. Process-Scale Chromatography. *Ullmann's Encyclopedia of Industrial Chemistry.* Wiley-VCH Verlag GmbH & Co. KGaA.

Jandera, P., Komers D. & Guiochon G. 1998. Optimization of the recovery yield and of the production rate in overloaded gradient-elution reversed-phase chromatography. *Journal of Chromatography A,* 796**,** 115-127.

Jandera, P. & Lembke P. 2000. Liquid Chromatography, 2. Methods, Programmed and Coupling Techniques. *Ullmann's Encyclopedia of Industrial Chemistry.* Wiley-VCH Verlag GmbH & Co. KGaA.

Jedrzejewski, P., Del Val I., Constantinou A., Dell A., Haslam S., Polizzi K. & Kontoravdi C. 2014. Towards Controlling the Glycoform: A Model Framework Linking Extracellular Metabolites to Antibody Glycosylation. *International Journal of Molecular Sciences,* 15**,** 4492.

Jenzsch, M., Gnoth S., Beck M., Kleinschmidt M., Simutis R. & Lübbert A. 2006. Open-loop control of the biomass concentration within the growth phase of recombinant protein production processes. *Journal of Biotechnology,* 127**,** 84-94.

Ji, Y. 2012. *Model based process design for bioprocess optimisation: case studies on precipitation with its applications in antibody purification.* University College London.

Jiang, L., Biegler L. T. & Fox V. G. 2003. Simulation and optimization of pressure‐swing adsorption systems for air separation. *AIChE Journal,* 49**,** 1140-1157.

Johnson, S. A., Brown M. R., Lute S. C. & Brorson K. A. 2017. Adapting viral safety assurance strategies to continuous processing of biological products. *Biotechnology and Bioengineering,* 114**,** 21-32.

Jungbauer, A. 1993. Preparative chromatography of biomolecules. *Journal of Chromatography A,* 639**,** 3-16.

Karra, S., Sager B. & Karim M. N. 2010. Multi-Scale Modeling of Heterogeneities in Mammalian Cell Culture Processes. *Industrial & Engineering Chemistry Research,* 49**,** 7990-8006.

Kawajiri, Y. & Biegler L. T. 2006a. Large scale nonlinear optimization for asymmetric operation and design of Simulated Moving Beds. *Journal of Chromatography A,* 1133**,** 226-240.

Kawajiri, Y. & Biegler L. T. 2006b. Optimization strategies for simulated moving bed and PowerFeed processes. *AIChE Journal,* 52**,** 1343-1350.

Kawajiri, Y. & Biegler L. T. 2008. Comparison of configurations of a four-column simulated moving bed process by multi-objective optimization. *Adsorption,* 14**,** 433-442.

Kelley, B. 2009a. Industrialization of mAb production technology: The bioprocessing industry at a crossroads. *mAbs,* 1**,** 440-449.

Kelley, B. Industrialization of mAb production technology: the bioprocessing industry at a crossroads. MAbs, 2009b. Taylor & Francis, 443-452.

Kelley, B., Blank G. & Lee A. 2009. Downstream processing of monoclonal antibodies: current practices and future opportunities. *Process Scale Purification of Antibodies, Hoboken, NJ: J Wiley & Sons***,** 1-23.

Khajuria, H. & Pistikopoulos E. N. 2011a. Dynamic modeling and explicit/multi-parametric MPC control of pressure swing adsorption systems. *Journal of Process Control,* 21**,** 151-163.

Khajuria, H. & Pistikopoulos E. N. 2011b. Integrated Design and Control of Pressure Swing Adsorption Systems. *In:* E.N. Pistikopoulos, M. C. G. & Kokossis, A. C. (eds.) *Computer Aided Chemical Engineering.* Elsevier.

Khajuria, H. & Pistikopoulos E. N. 2013. Optimization and control of pressure swing adsorption processes under uncertainty. *AIChE Journal,* 59**,** 120-131.

Khalaf, R., Heymann J., Lesaout X., Monard F., Costioli M. & Morbidelli M. 2016. Model-based high-throughput design of ion exchange protein chromatography. *Journal of Chromatography A,* 1459**,** 67-77.

Kiparissides, A., Koutinas M., Kontoravdi C., Mantalaris A. & Pistikopoulos E. N. 2011a. 'Closing the loop' in biological systems modeling — From the in silico to the in vitro. *Automatica,* 47**,** 1147-1155.

Kiparissides, A., Koutinas M., Pistikopoulos E. N. & Mantalaris A. 2011b. Model Development and Analysis of Mammalian Cell Culture Systems. *Process Systems Engineering.* Wiley-VCH.

Kiparissides, A., Kucherenko S. S., Mantalaris A. & Pistikopoulos E. N. 2009. Global Sensitivity Analysis Challenges in Biological Systems Modeling. *Industrial & Engineering Chemistry Research,* 48**,** 7168-7180.

Kiparissides, A., Pistikopoulos E. N. & Mantalaris A. 2011c. On the model based optimization of secreting mammalian cell cultures via minimal glucose provision. *In:*

E.N. Pistikopoulos, M. C. G. & Kokossis, A. C. (eds.) *Computer Aided Chemical Engineering*. Elsevier.

Kiparissides, A., Pistikopoulos E. N. & Mantalaris A. 2015. On the model-based optimization of secreting mammalian cell (GS-NS0) cultures. *Biotechnology and Bioengineering,* 112**,** 536-548.

Klatt, K.-U., Hanisch F., Dünnebier G. & Engell S. 2000. Model-based optimization and control of chromatographic processes. *Computers & Chemical Engineering,* 24**,** 1119-1126.

Klatt, K.-U. & Marquardt W. 2009. Perspectives for process systems engineering—Personal views from academia and industry. *Computers & Chemical Engineering,* 33**,** 536-550.

Klutz, S., Holtmann L., Lobedann M. & Schembecker G. 2016. Cost evaluation of antibody production processes in different operation modes. *Chemical Engineering Science,* 141**,** 63-74.

Konstantinov, K. B. & Cooney C. L. 2015. White Paper on Continuous Bioprocessing May 20-21, 2014 Continuous Manufacturing Symposium. *Journal of Pharmaceutical Sciences,* 104**,** 813-820.

Kontoravdi, C., Asprey S. P., Pistikopoulos E. N. & Mantalaris A. 2005a. Application of Global Sensitivity Analysis to Determine Goals for Design of Experiments: An Example Study on Antibody-Producing Cell Cultures. *Biotechnology Progress,* 21**,** 1128-1135.

Kontoravdi, C., Asprey S. P., Pistikopoulos S. & Mantalaris A. 2005b. Dynamic model of MAb production and glycosylation for the purpose of product quality control. *In:* Puigjaner, L. E. A. (ed.) *European Symposium on Computer-Aided Process Engineering-15, 20A and 20B*.

Kontoravdi, C., Pistikopoulos E. N. & Mantalaris A. 2010. Systematic development of predictive mathematical models for animal cell cultures. *Computers & Chemical Engineering,* 34**,** 1192-1198.

Kontoravdi, C., Wong D., Lam C., Lee Y. Y., Yap M. G. S., Pistikopoulos E. N. & Mantalaris A. 2007. Modeling amino acid metabolism in mammalian cells-toward the development of a model library. *Biotechnology Progress,* 23**,** 1261-1269.

Kopaciewicz, W., Rounds M., Fausnaugh J. & Regnier F. 1983. Retention model for high-performance ion-exchange chromatography. *Journal of Chromatography A,* 266**,** 3-21.

Koumpouras, G. & Kontoravdi C. 2012. Dynamic Optimization of Bioprocesses.

Kováts, E. S. 1985. Retention in liquid/solid chromatography. *Journal of Chromatography Library,* 32**,** 205-217.

Kraettli, M. 2012. *Online Control Development and Process Intensification in Continuous Chromatography (MCSGP).* PhD, ETH Zurich

Krättli, M., Müller-Späth T. & Morbidelli M. 2013a. Multifraction separation in countercurrent chromatography (MCSGP). *Biotechnology and Bioengineering,* 110**,** 2436-2444.

Krättli, M., Steinebach F. & Morbidelli M. 2013b. Online control of the twin-column countercurrent solvent gradient process for biochromatography. *Journal of Chromatography A,* 1293**,** 51-59.

Krattli, M., Strohlein G., Aumann L., Muller-Spath T. & Morbidelli M. 2011. Closed loop control of the multi-column solvent gradient purification process. *Journal of Chromatography A,* 1218**,** 9028-9036.

Krättli, M., Ströhlein G., Aumann L., Müller-Späth T. & Morbidelli M. 2011. Closed loop control of the multi-column solvent gradient purification process. *Journal of Chromatography A,* 1218**,** 9028-9036.

Kumar, V., Leweke S., Von Lieres E. & Rathore A. S. 2015. Mechanistic modeling of ion-exchange process chromatography of charge variants of monoclonal antibody products. *Journal of Chromatography A,* 1426**,** 140-153.

Küpper, A., Diehl M., Schlöder J. P., Bock H. G. & Engell S. 2009. Efficient moving horizon state and parameter estimation for SMB processes. *Journal of Process Control,* 19**,** 785-802.

Kurz, M. 2007. Upstream Processing: Regulatory Considerations Regarding Quality Aspects of Monoclonal Antibodies. *BioPharm International.*

Kvasnica, M., Grieder P., Baotić M. & Morari M. Multi-parametric toolbox (MPT). International Workshop on Hybrid Systems: Computation and Control, 2004. Springer, 448-462.

Laird, T. 2007. Continuous processes in small-scale manufacture. *Organic Process Research & Development,* 11**,** 927-927.

Lakerveld, R., Benyahia B., Braatz R. D. & Barton P. I. 2013. Model-based design of a plant-wide control strategy for a continuous pharmaceutical plant. *AIChE Journal,* 59**,** 3671-3685.

Lakerveld, R., Benyahia B., Heider P. L., Zhang H., Wolfe A., Testa C. J., Ogden S., Hersey D. R., Mascia S., Evans J. M. B., Braatz R. D. & Barton P. I. 2015. The Application of an Automated Control Strategy for an Integrated Continuous Pharmaceutical Pilot Plant. *Org. Process Res. Dev.,* 19**,** 1088.

Lam, C. M., Sriyudthsak K., Kontoravdi C., Kothari K., Park H. H., Pistikopoulos E. N. & Mantalaris A. 2008. Cell Cycle Modelling for Off-line Dynamic Optimisation of Mammalian Cultures. *In:* Braunschweig, B. & Joulia, X. (eds.) *18th European Symposium on Computer Aided Process Engineering.* Amsterdam: Elsevier Science Bv.

Lambert, R. S. C., Rivotti P. & Pistikopoulos E. N. 2013. A Monte-Carlo based model approximation technique for linear model predictive control of nonlinear systems. *Computers & Chemical Engineering,* 54**,** 60-67.

Langer, E. S. 2011. Trends in Perfusion Bioreactors: The next Revolution in Bioprocessing? *BioProcess International***,** 18-22.

Langer, E. S. & Rader R. A. 2014. Introduction to Continuous Manufacturing: Technology Landscape and Trends. Available: http://www.biopharma.com/continuous.pdf.

Li, G. Y., Wang S. W. & Rabitz H. 2002. Practical approaches to construct RS-HDMR component functions. *The journal of physical chemistry. A,* 106**,** 8721-8733.

Li, S., Feng L., Benner P. & Seidel-Morgenstern A. 2014. Using surrogate models for efficient optimization of simulated moving bed chromatography. *Computers & Chemical Engineering,* 67**,** 121-132.

Lim, J. a. C., Sinclair A., Kim D. S. & Gottschalk U. 2007. Economic benefits of single-use membrane chromatography in polishing. *BioProcess Int. Feb*.

Liu, S., Simaria A. S., Farid S. S. & Papageorgiou L. G. 2014a. An Optimisation-based Approach for Biopharmaceutical Manufacturing. *In:* Jiří Jaromír Klemeš, P. S. V. & Peng Yen, L. (eds.) *Computer Aided Chemical Engineering.* Elsevier.

Liu, S. S., Simaria A. S., Farid S. S. & Papageorgiou L. G. 2014b. Optimising chromatography strategies of antibody purification processes by mixed integer fractional programming techniques. *Computers & Chemical Engineering,* 68**,** 151-164.

Liu, Y. & Gunawan R. 2017. Bioprocess optimization under uncertainty using ensemble modeling. *Journal of Biotechnology,* 244**,** 34-44.

Love, J. C., Love K. R. & Barone P. W. 2013. Enabling global access to high-quality biopharmaceuticals. *Current Opinion in Chemical Engineering,* 2**,** 383-390.

Low, D., O'leary R. & Pujar N. S. 2007. Future of antibody purification. *Journal of Chromatography B,* 848**,** 48-63.

Luo, J., Vijayasankaran N., Autsen J., Santuray R., Hudson T., Amanullah A. & Li F. 2012. Comparative metabolite analysis to understand lactate metabolism shift in Chinese hamster ovary cell culture process. *Biotechnology and Bioengineering,* 109**,** 146-156.

Ma, N., Ellet J., Okediadi C., Hermes P., Mccormick E. & Casnocha S. 2009. A single nutrient feed supports both chemically defined NS0 and CHO fed-batch processes: Improved productivity and lactate metabolism. *Biotechnology Progress,* 25**,** 1353-1363.

Mabion. 2013. *Mabion* [Online]. Available: http://www.mabion.eu/en/Product-market/ [Accessed 03/07 2013].

Majors, B. S., Betenbaugh M. J. & Chiang G. G. 2007. Links between metabolism and apoptosis in mammalian cells: Applications for anti-apoptosis engineering. *Metabolic Engineering,* 9**,** 317-326.

Martin, M., Blu G. & Guiochon G. 1973. The Effect of Pressure on the Retention Time and the Retention Volume of an Inert Compound In Liquid Chromatography. *Journal of Chromatographic Science,* 11**,** 641-654.

Mazzotti, M., Storti G. & Morbidelli M. 1997. Optimal operation of simulated moving bed units for nonlinear chromatographic separations. *Journal of Chromatography A,* 769**,** 3-24.

Mellstedt, H., Niederwieser D. & Ludwig H. 2008. The challenge of biosimilars. *Annals of Oncology,* 19**,** 411-419.

Melter, L., Butte A. & Morbidelli M. 2008. Preparative weak cation-exchange chromatography of monoclonal antibody variants: I. Single-component adsorption. *Journal of Chromatography A,* 1200**,** 156-165.

Melter, L., Ströhlein G., Butté A. & Morbidelli M. 2007. Adsorption of monoclonal antibody variants on analytical cation-exchange resin. *Journal of Chromatography A,* 1154**,** 121-131.

Miesegaes, G., Lute S., Strauss D., Read E., Venkiteshwaran A., Kreuzman A., Shah R., Shamlou P., Chen D. & Brorson K. 2012. Monoclonal antibody capture and viral clearance by cation exchange chromatography. *Biotechnology and bioengineering,* 109**,** 2048-2058.

Miyabe, K. & Guiochon G. 1999. Influence of column radial heterogeneity on peak fronting in linear chromatography. *Journal of Chromatography A,* 857**,** 69-87.

Moorhouse, K. G., Nashabeh W., Deveney J., Bjork N. S., Mulkerrin M. G. & Ryskamp T. 1997. Validation of an HPLC method for the analysis of the charge heterogeneity of the recombinant monoclonal antibody IDEC-C2B8 after papain digestion1. *Journal of Pharmaceutical and Biomedical Analysis,* 16**,** 593-603.

Mukherjee, S., Chiu R., Leung S.-M. & Shields D. 2007. Fragmentation of the Golgi Apparatus: An Early Apoptotic Event Independent of the Cytoskeleton. *Traffic,* 8**,** 369-378.

Müller-Späth, T., Aumann L., Melter L., Ströhlein G. & Morbidelli M. 2008. Chromatographic separation of three monoclonal antibody variants using multicolumn countercurrent solvent gradient purification (MCSGP). *Biotechnology and Bioengineering,* 100**,** 1166-1177.

Müller-Späth, T., Aumann L. & Morbidelli M. 2009. Role of Cleaning-in-Place in the Purification of mAb Supernatants Using Continuous Cation Exchange Chromatography. *Separation Science and Technology,* 44**,** 1-26.

Müller-Späth, T., Aumann L., Ströhlein G., Kornmann H., Valax P., Delegrange L., Charbaut E., Baer G., Lamproye A., Jöhnck M., Schulte M. & Morbidelli M. 2010a. Two step capture and purification of IgG2 using multicolumn countercurrent solvent gradient purification (MCSGP). *Biotechnology and Bioengineering,* 107**,** 974-984.

Muller-Spath, T., Krattli M., Aumann L., Strohlein G. & Morbidelli M. 2011. Extended MCSGP process for continuous four-fraction separation: Case study of monoclonal antibody variants. *Abstracts of Papers of the American Chemical Society,* 241.

Müller-Späth, T., Krättli M., Aumann L., Ströhlein G. & Morbidelli M. 2010b. Increasing the activity of monoclonal antibody therapeutics by continuous chromatography (MCSGP). *Biotechnology and Bioengineering,* 107**,** 652-662.

Müller-Späth, T., Ströhlein G., Aumann L., Kornmann H., Valax P., Delegrange L., Charbaut E., Baer G., Lamproye A., Jöhnck M., Schulte M. & Morbidelli M. 2011. Model simulation and experimental verification of a cation-exchange IgG capture step in batch and continuous chromatography. *Journal of Chromatography A,* 1218**,** 5195-5204.

Müller-Späth, T., Ulmer N., Aumann L., Ströhlein G., Bavand M., Hendriks L. J., De Kruif J., Throsby M. & Bakker A. B. 2013. Purifying Common Light-Chain Bispecific Antibodies. *BioProcess International,* 11**,** 36-45.

Mulukutla, B. C., Gramer M. & Hu W.-S. 2012. On metabolic shift to lactate consumption in fed-batch culture of mammalian cells. *Metabolic Engineering,* 14**,** 138-149.

Nagrath, D., Bequette B. W., Cramer S. M. & Messac A. 2005. Multiobjective optimization strategies for linear gradient chromatography. *AIChE Journal,* 51**,** 511-525.

Nascu, I., Lambert R. S. C., Krieger A. & Pistikopoulos E. N. 2014. Simultaneous Multi-Parametric Model Predictive Control and State Estimation with Application to Distillation Column and Intravenous Anaesthesia. *In:* Jiří Jaromír Klemeš, P. S. V. & Peng Yen, L. (eds.) *Computer Aided Chemical Engineering.* Elsevier.

Natarajan, V., Wayne Bequette B. & Cramer S. M. 2000. Optimization of ion-exchange displacement separations: I. Validation of an iterative scheme and its use as a methods development tool. *Journal of Chromatography A,* 876**,** 51-62.

Ng, C. K., Osuna-Sanchez H., Valéry E., Sørensen E. & Bracewell D. G. 2012. Design of high productivity antibody capture by protein A chromatography using an integrated experimental and modeling approach. *Journal of Chromatography B,* 899**,** 116-126.

Ng, C. K. S., Rousset F., Valery E., Bracewell D. G. & Sorensen E. 2014. Design of high productivity sequential multi-column chromatography for antibody capture. *Food and Bioproducts Processing,* 92**,** 233-241.

Ni, C., Zhu B., Wang N., Wang M., Chen S., Zhang J. & Zhu Y. 2016. Simple column-switching ion chromatography method for determining eight monosaccharides and oligosaccharides in honeydew and nectar. *Food Chemistry,* 194**,** 555-560.

Nichols, J. 2008. Reducing the Cost of Manufacturing through Targeted Processes, Process Intensification, and Lean/Continuous Manufacturing. International Society for Pharmaceutical Engineering.

Nicoud, R.-M. 2014. The Amazing Ability of Continuous Chromatography To Adapt to a Moving Environment. *Industrial & Engineering Chemistry Research,* 53**,** 3755-3765.

Nicoud, R.-M. 2015. *Chromatographic Processes Modeling, Simulation and Design,* Cambridge, Cambridge University Press.

Nilchan, S. & Pantelides C. C. 1998. On the optimisation of periodic adsorption processes. *Adsorption-Journal of the International Adsorption Society,* 4**,** 113-147.

Oberdieck, R., Diangelakis N. A., Papathanasiou M. M., Nascu I. & Pistikopoulos E. N. 2016. POP – Parametric Optimization Toolbox. *Industrial & Engineering Chemistry Research,* 55**,** 8979-8991.

Olofsson, P. & Ma X. 2011. Modeling and estimating bacterial lag phase. *Mathematical Biosciences,* 234**,** 127-131.

Ozturk, S. S., Thrift J. C., Blackie J. D. & Naveh D. 1997. Real-time monitoring and control of glucose and lactate concentrations in a mammalian cell perfusion reactor. *Biotechnology and Bioengineering,* 53**,** 372-378.

P.S.E 1997-2016. gPROMS ModelBuilder (R). Process Systems Enterpise.

Panos, C., Kouramas K. I., Georgiadis M. C. & Pistikopoulos E. N. 2010. Dynamic optimization and robust explicit model predictive control of hydrogen storage tank. *Computers & Chemical Engineering,* 34**,** 1341-1347.

Papathanasiou, M. M., Avraamidou S., Oberdieck R., Mantalaris A., Steinebach F., Morbidelli M., Mueller-Spaeth T. & Pistikopoulos E. N. 2016a. Advanced control strategies for the multicolumn countercurrent solvent gradient purification process. *AIChE Journal***,** n/a-n/a.

Papathanasiou, M. M., Avraamidou S., Oberdieck R., Mantalaris A., Steinebach F., Morbidelli M., Mueller-Spaeth T. & Pistikopoulos E. N. 2016b. Advanced control strategies for the multicolumn countercurrent solvent gradient purification process. *AIChE Journal,* 62**,** 2341-2357.

Papathanasiou, M. M., Quiroga-Campano A. L., Oberdieck R., Mantalaris A. & Pistikopoulos E. N. 2016c. Development of advanced computational tools for the intensification of monoclonal antibody production. *In:* Zdravko, K. & Miloš, B. (eds.) *Computer Aided Chemical Engineering.* Elsevier.

Papathanasiou, M. M., Steinebach F., Morbidelli M., Mantalaris A. & Pistikopoulos E. N. 2017. Intelligent, model-based control towards the intensification of downstream processes. *Computers & Chemical Engineering*.

Paul, A. & Hesse F. 2013. Characterization of mAb aggregates in a mammalian cell culture production process. *BMC Proceedings,* 7**,** P80-P80.

Perez-Almodovar, E. X. & Carta G. 2009. IgG adsorption on a new protein A adsorbent based on macroporous hydrophilic polymers: II. Pressure–flow curves and optimization for capture. *Journal of Chromatography A,* 1216**,** 8348-8354.

Pfister, D., Morbidelli M. & Nicoud R.-M. 2016. A continuum theory for multicomponent chromatography modeling. *Journal of Chromatography A,* 1446**,** 50-58.

Pistikopoulos, E. 1997. Parametric and Stochastic Programming Algorithm for Process Optimization under Uuncertainty. *AspenWorld 1997 proceedings*.

Pistikopoulos, E. 2000. On-line optimization via off-line optimization!-A guided tour to parametric programming. *AspenWorld 2000*.

Pistikopoulos, E. N. 2009. Perspectives in multiparametric programming and explicit model predictive control. *AIChE Journal,* 55**,** 1918-1925.

Pistikopoulos, E. N. 2012. From multi-parametric programming theory to MPC-on-a-chip multi-scale systems applications. *Computers and Chemical Engineering,* 47**,** 57-66.

Pistikopoulos, E. N., Bozinis, N. A., Dua, V., Perking, J. D. & Sakizlis, V. 2004. *Improved Process Control*. European Patent EP1399784.

Pistikopoulos, E. N., Bozinis, N. A., Dua, V., Perking, J. D. & Sakizlis, V. 2008. *Process Control Using Co-ordinate Space*.

Pistikopoulos, E. N., Diangelakis N. A., Oberdieck R., Papathanasiou M. M., Nascu I. & Sun M. 2015. PAROC—An integrated framework and software platform for the optimisation and advanced model-based control of process systems. *Chemical Engineering Science,* 136**,** 115-138.

Pistikopoulos, E. N., Dua V., Bozinis N. A., Bemporad A. & Morari M. 2002. On-line optimization via off-line parametric optimization tools. *Computers & Chemical Engineering,* 26**,** 175-185.

Plumb, K. 2005. Continuous Processing in the Pharmaceutical Industry: Changing the Mind Set. *Chemical Engineering Research and Design,* 83**,** 730-738.

Pollock, J., Ho S. & Farid S. 2012. Computer-Aided Design and Evaluation of Batch and Continuous Multi-Mode Biopharmaceutical Manufacturing Processes.

Pörtner, R., Schilling A., Lüdemann I. & Märkl H. 1996. High density fed-batch cultures for hybridoma cells performed with the aid of a kinetic model. *Bioprocess Engineering,* 15**,** 117-124.

Q5a 1998. FDA Q5A Guidance Document: Viral Safety Evaluation of Biotech- nology Products Derived from Cell Lines of Human or Animal Origin. *Federal Register.*

Q6b 1999. International Conference on Harmonisation of Technical Requirements for Registration of Pharmaceuticals for Human Use (ICH). Guidance for Industry Q6B Specifications: Test procedures and acceptance criteria for biotechnological/biological products.

Quiroga, A. L. 2017. *Mathematical modelling and experimental validation for optimisation and control of mammalian cell culture systems.* PhD, Imperial College London.

Quiroga, A. L., Papathanasiou M. M., Pistikopoulos E. N. & Mantalaris A. 2016. A Predictive Model for Energy Metabolism and ATP Balance in Mammalian Cells: Towards the Energy-Based Optimization of mAb Production. *In:* Zdravko, K. & Miloš, B. (eds.) *Computer Aided Chemical Engineering.* Elsevier.

Quon, J. L., Zhang H., Alvarez A., Evans J., Myerson A. S. & Trout B. L. 2012. Continuous Crystallization of Aliskiren Hemifumarate. *Crystal Growth & Design,* 12**,** 3036-3044.

Rao, C. V. 2000. *Moving Horizon Strategies for the Constrained Monitoring and Control of Nonlinear Discrete-time Systems.* Ph.D. Ph.D. Thesis, University of Wisconsin-Madison.

Rawlings, J. B. & Mayne D. Q. 2009. *Model Predictive Control: Theory and Design*, Nob Hill Publishing.

Reitzer, L. J., Wice B. M. & Kennell D. 1979. Evidence that glutamine, not sugar, is the major energy source for cultured HeLa cells. *Journal of Biological Chemistry,* 254**,** 2669-2676.

Reklaitis, G. V., Khinast J. & Muzzio F. 2010. Pharmaceutical engineering science—New approaches to pharmaceutical development and manufacturing. *Chemical Engineering Science,* 65**,** iv-vii.

Riedo, F. 1982. Adsorption from liquid mixtures and liquid chromatography. *Journal of Chromatography A,* 239**,** 1-28.

Rivotti, P., Lambert R. S. C. & Pistikopoulos E. N. 2012. Combined model approximation techniques and multiparametric programming for explicit nonlinear model predictive control. *Computers & Chemical Engineering,* 42**,** 277-287.

Rogers, A. & Ierapetritou M. 2015. Challenges and opportunities in modeling pharmaceutical manufacturing processes. *Computers & Chemical Engineering,* 81**,** 32-39.

Royle, K. E., Jimenez Del Val I. & Kontoravdi C. 2013. Integration of models and experimentation to optimise the production of potential biotherapeutics. *Drug Discovery Today,* 18**,** 1250-1255.

Sahlodin, A. M. & Barton P. I. 2015. Optimal Campaign Continuous Manufacturing. *Industrial & Engineering Chemistry Research,* 54**,** 11344-11359.

Sakizlis, V., Dua V., Perkins J. D. & Pistikopoulos E. N. 2004a. Robust model-based tracking control using parametric programming. *Computers & Chemical Engineering,* 28**,** 195-207.

Sakizlis, V., M.P. Kakalis N., Dua V., D. Perkins J. & Pistikopoulos E. N. 2004b. Design of robust model-based controllers via parametric programming. *Automatica,* 40**,** 189-201.

Schaber, S. D., Gerogiorgis D. I., Ramachandran R., Evans J. M. B., Barton P. I. & Trout B. L. 2011. Economic Analysis of Integrated Continuous and Batch Pharmaceutical Manufacturing. *Ind. Eng. Chem. Res.,* 50**,** 10083.

Schubert, J., Simutis R., Dors M., Havlik I. & Lübbert A. 1994. Bioprocess optimization and control: Application of hybrid modelling. *Journal of Biotechnology,* 35**,** 51-68.

Sebastian Escotet-Espinoza, M., Rogers A. & Ierapetritou M. G. 2016. Optimization methodologies for the production of pharmaceutical products. *Methods in Pharmacology and Toxicology.*

Sercinoglu, O., Platas Barradas O., Sandig V., Zeng A.-P. & Pörtner R. 2011. DoE of fed-batch processes – model-based design and experimental evaluation. *BMC Proceedings,* 5**,** P46-P46.

Sharfstein, S. T. 2008. Advances in Cell Culture Process Development: Tools and Techniques for Improving Cell Line Development and Process Optimization. *Biotechnology Progress,* 24**,** 727-734.

Shpritzer, R., Vicik S., Orlando S., Acharya H. & Coffman J. L. Calcium phosphate flocculation of antibody-producing mammalian cells at pilot scale. 232nd ACS Meeting, 2006 San Francisco, CA

Shukla, A. A. & Gottschalk U. 2013. Single-use disposable technologies for biopharmaceutical manufacturing. *Trends in Biotechnology,* 31**,** 147-154.

Shukla, A. A., Hubbard B., Tressel T., Guhan S. & Low D. 2007. Downstream processing of monoclonal antibodies—Application of platform approaches. *Journal of Chromatography B,* 848**,** 28-39.

Shukla, A. A. & Thömmes J. 2010. Recent advances in large-scale production of monoclonal antibodies and related proteins. *Trends in Biotechnology,* 28**,** 253-261.

Sidoli, F. R., Mantalaris A. & Asprey S. P. 2004. Modelling of mammalian cells and cell culture processes. *Cytotechnology,* 44**,** 27-46.

Singh, R., Muzzio F. J., Ierapetritou M. & Ramachnadran R. 2016a. A Systematic Framework for the Design and Implementation of Sensing and Control Architecture for a Continuous Pharmaceutical Manufacturing Plant. *Computer Aided Chemical Engineering.*

Singh, R., Velazquez C., Sahay A., Karry K. M., Muzzio F. J., Ierapetritou M. G. & Ramachandran R. 2016b. Advanced control of continuous pharmaceutical tablet manufacturing processes. *Methods in Pharmacology and Toxicology.*

Sommerfeld, S. & Strube J. 2005. Challenges in biotechnology production—generic processes and process optimization for monoclonal antibodies. *Chemical Engineering and Processing: Process Intensification,* 44**,** 1123-1137.

Spens, E. & Häggström L. 2007. Defined protein and animal component-free NS0 fed-batch culture. *Biotechnology and Bioengineering,* 98**,** 1183-1194.

Steinebach, F., Angarita M., Karst D. J., Müller-Späth T. & Morbidelli M. 2016a. Model based adaptive control of a continuous capture process for monoclonal antibodies production. *Journal of Chromatography A,* 1444**,** 50-56.

Steinebach, F., Müller‐Späth T. & Morbidelli M. 2016b. Continuous counter‐current chromatography for capture and polishing steps in biopharmaceutical production. *Biotechnology Journal,* 11**,** 1126-1141.

Stroehlein, G., Aumann L., Mueller-Spaeth T., Tarafder A. & Morbidelli M. 2007. The multicolumn countercurrent solvent gradient purification process: A continuous chromatographic process for monoclonal antibodies without using protein A. *Biopharm international***,** 42-48.

Ströhlein, G., Aumann L., Mazzotti M. & Morbidelli M. 2006a. A continuous, counter-current multi-column chromatographic process incorporating modifier gradients for ternary separations. *J Chromatogr A,* 1126**,** 338-46.

Ströhlein, G., Aumann L., Melter L., Büscher K., Schenkel B., Mazzotti M. & Morbidelli M. 2006b. Experimental verification of sample-solvent induced modifier–solute peak interactions in biochromatography. *Journal of Chromatography A,* 1117**,** 146-153.

Ströhlein, G., Müller-Späth T., Lyngberg O. & Maclean D. Purification of a synthetic peptide using multi-column chromatography (Contichrom® & MCSGP). 25th International Symposium on Preparative and Process Chromatography (PREP), 2012.

Strube, J., Grote F. & Ditz R. 2012. Bioprocess Design and Production Technology for the Future. *Biopharmaceutical Production Technology.* Wiley-VCH Verlag GmbH & Co. KGaA.

Sung, S. W., Lee J. & Lee I.-B. 2009. *Process identification and PID control*, John Wiley & Sons.

Suvarov, P., Kienle A., Nobre C., De Weireld G. & Vande Wouwer A. 2014. Cycle to cycle adaptive control of simulated moving bed chromatographic separation processes. *Journal of Process Control,* 24**,** 357-367.

Taylor, P. 2015. GSK and Pfizer team up on continuous manufacturing project. Available: http://www.in-pharmatechnologist.com/Processing/GSK-and-Pfizer-team-up-on-continuous-manufacturing-project.

Teixeira, A., Cunha A. E., Clemente J. J., Moreira J. L., Cruz H. J., Alves P. M., Carrondo M. J. & Oliveira R. 2005. Modelling and optimization of a recombinant BHK-21 cultivation process using hybrid grey-box systems. *J Biotechnol,* 118.

Teixeira, A. P., Alves C., Alves P. M., Carrondo M. J. & Oliveira R. 2007. Hybrid elementary flux analysis/nonparametric modeling: application for bioprocess control. *BMC Bioinformatics,* 8**,** 1-15.

Teixeira, A. P., Clemente J. J., Cunha A. E., Carrondo M. J. & Oliveira R. 2006. Bioprocess iterative batch-to-batch optimization based on hybrid parametric/nonparametric models. *Biotechnol Prog,* 22.

Teixeira, A. P., Oliveira R., Alves P. M. & Carrondo M. J. T. 2009. Advances in on-line monitoring and control of mammalian cell cultures: Supporting the PAT initiative. *Biotechnology Advances,* 27**,** 726-732.

Teoh, H. K., Sørensen E., Turner M. & Titchener-Hooker N. 2001a. Dynamic modelling of chromatographic processes: A systematic procedure for isotherms determination. *In:* Rafiqul, G. & Sten Bay, J. (eds.) *Computer Aided Chemical Engineering.* Elsevier.

Teoh, H. K., Turner M., Titchener-Hooker N. & Sorensen E. 2001b. Experimental verification and optimisation of a detailed dynamic high performance liquid chromatography column model. *Computers & Chemical Engineering,* 25**,** 893-903.

Torphy, T. J. 2002. Monoclonal antibodies: Boundless potential, daunting challenges. *Current Opinion in Biotechnology,* 13**,** 589-591.

Toumi, A. & Engell S. 2004. Optimization-based control of a reactive simulated moving bed process for glucose isomerization. *Chemical Engineering Science,* 59**,** 3777-3792.

Toussaint, C., Henry O. & Durocher Y. 2016. Metabolic engineering of CHO cells to alter lactate metabolism during fed-batch cultures. *Journal of Biotechnology,* 217**,** 122-131.

Unger, J., Kolios G. & Eigenberger G. 1997. On the efficient simulation and analysis of regenerative processes in cyclic operation. *Computers & Chemical Engineering,* 21**,** S167-S172.

Varma, A. & Morbidelli M. 1997. *Mathematical methods in chemical engineering,* New York, Oxford University Press.

Vázquez-Rey, M. & Lang D. A. 2011. Aggregates in monoclonal antibody manufacturing processes. *Biotechnology and Bioengineering,* 108**,** 1494-1508.

Villaverde, A. F., Bongard S., Mauch K., Balsa-Canto E. & Banga J. R. 2016. Metabolic engineering with multi-objective optimization of kinetic models. *Journal of Biotechnology,* 222**,** 1-8.

Vlasak, J. & Ionescu R. 2011. Fragmentation of monoclonal antibodies. *mAbs,* 3**,** 253-263.

Voelker, A., Kouramas K. & Pistikopoulos E. N. 2010. Simultaneous State Estimation and Model Predictive Control by Multi-Parametric Programming. ELSEVIER SCIENCE BV.

Voitl, A., Müller-Späth T. & Morbidelli M. 2010. Application of mixed mode resins for the purification of antibodies. *Journal of Chromatography A,* 1217**,** 5753-5760.

Wakankar, A., Chen Y., Gokarn Y. & Jacobson F. S. 2011. Analytical methods for physicochemical characterization of antibody drug conjugates. *mAbs,* 3**,** 161-172.

Walther, J., Godawat R., Hwang C., Abe Y., Sinclair A. & Konstantinov K. 2015. The business impact of an integrated continuous biomanufacturing platform for recombinant protein production. *Journal of Biotechnology,* 213**,** 3-12.

Wang, C., Engell S. & Hanisch F. 2002. Neural network-based identification and MPC control of SMB chromatography. *IFAC Proceedings Volumes,* 35**,** 31-36.

Wang, Z., Escotet-Espinoza M. S. & Ierapetritou M. 2017. Process analysis and optimization of continuous pharmaceutical manufacturing using flowsheet models. *Computers & Chemical Engineering*.

Wang, Z. & Georgakis C. 2017. An in silico evaluation of data-driven optimization of biopharmaceutical processes. *AIChE Journal*.

Warikoo, V., Godawat R., Brower K., Jain S., Cummings D., Simons E., Johnson T., Walther J., Yu M., Wright B., Mclarty J., Karey K. P., Hwang C., Zhou W., Riske F. & Konstantinov K. 2012. Integrated continuous production of recombinant therapeutic proteins. *Biotechnology and Bioengineering,* 109**,** 3018-3029.

Welch, G. & Bishop G. 2001. *An introduction to the Kalman filter,* http://www.cs.unc.edu/tracker/media/pdf/SIGGRAPH2001_CoursePack_08.pdf.

Westerberg, K., Broberg Hansen E., Degerman M., Budde Hansen T. & Nilsson B. 2012. Model-based process challenge of an industrial ion-exchange chromatography step. *Chemical Engineering and Technology,* 35**,** 183-190.

Wurm, F. M. 2004. Production of recombinant protein therapeutics in cultivated mammalian cells. *Nature biotechnology,* 22**,** 1393-1398.

Xenopoulos, A. 2015. A new, integrated, continuous purification process template for monoclonal antibodies: Process modeling and cost of goods studies. *J Biotechnol,* 213**,** 42-53.

Xie, L. & Wang D. I. C. 1994. Applications of improved stoichiometric model in medium design and fed-batch cultivation of animal cells in bioreactor. *Cytotechnology,* 15**,** 17-29.

Zavitsanou, S., Mantalaris A., Georgiadis M. C. & Pistikopoulos E. N. 2014. Optimization of Insulin Dosing in Patients with Type 1 Diabetes Mellitus. *In:* Jiří Jaromír Klemeš, P. S. V. & Peng Yen, L. (eds.) *Computer Aided Chemical Engineering.* Elsevier.

Zhang, H., Lakerveld R., Heider P. L., Tao M., Su M., Testa C. J., D'antonio A. N., Barton P. I., Braatz R. D., Trout B. L., Myerson A. S., Jensen K. F. & Evans J. M. B. 2014a. Application of Continuous Crystallization in an Integrated Continuous Pharmaceutical Pilot Plant. *Crystal Growth & Design,* 14**,** 2148-2157.

Zhang, J. 2010. Mammalian Cell Culture for Biopharmaceutical Production. *In:* H, B. R. (ed.) *Manual of Industrial Microbiology and Biotechnology.* 3rd ed.: ASM Press, Washington, DC.

Zhang, Q., Goetze A. M., Cui H., Wylie J., Trimble S., Hewig A. & Flynn G. C. 2014b. Comprehensive tracking of host cell proteins during monoclonal antibody purifications using mass spectrometry. *mAbs,* 6**,** 659-670.

Zhou, J. X. & Tressel T. 2006. Basic Concepts in Q Membrane Chromatography for Large-Scale Antibody Production. *Biotechnology Progress,* 22**,** 341-349.

Zhou, W., Chen C.-C., Buckland B. & Aunins J. 1997. Fed-batch culture of recombinant NS0 myeloma cells with high monoclonal antibody production. *Biotechnology and Bioengineering,* 55**,** 783-792.

Zhou, W., Rehm J. & Hu W.-S. 1995. High viable cell concentration fed-batch cultures of hybridoma cells through on-line nutrient feeding. *Biotechnology and Bioengineering,* 46**,** 579-587.

Zhu, J. 2012. Mammalian cell protein expression for biopharmaceutical production. *Biotechnology advances,* 30**,** 1158-1170.

Zydney, A. L. 2016. Continuous downstream processing for high value biological products: A Review. *Biotechnology and Bioengineering,* 113**,** 465-475.

Appendix A

Computational Tools

A.1 Global Sensitivity Analysis (GSA)

GSA is the mathematical procedure according to which the model parameters are simultaneously excited, within the range of interest, and their effect on the model outputs is monitored. Such procedures enable the examination of the global parameter space, cope well with non-linearities, providing a complete set of results that demonstrates both the sensitivity of the model to the uncertainty of the parameter values, as well as the effect of one model parameter to the other (Li et al., 2002, Kiparissides et al., 2011a).

In this work, the sensitivity of the model to the parameter values is assessed using High Dimensional Model Representation (HDMR) method. HDMR is a global method that examines the entire parameter space and is based on the ANOVA decomposition method. More specifically, for the purposes of this work Random Sampling HDMR (RS-HDMR) is used. RS-HDMR is a technique that was introduced to generate the ANOVA decomposition (Equation A.1) of a model function with random input (Li et al., 2002).

$$f(x) = f_0 + \sum_{s=1}^{n} \sum_{i_1<\cdots<i_s}^{n} f_{i_1 \ldots i_s}(x_{i_1}, \ldots, x_{i_s})$$

Equation A.1 ANOVA decomposition.

HDMR aims to efficiently build the map of the input-output behaviour of a model function involving high dimensional inputs ($n \sim 10^2 - 10^3$). Li *et al.* (2002) postulated that in most engineering problems the expansion of functions can be truncated to the second order component function (Equation A.2).

$$f(x) \approx h(x) = f_0 + \sum_{i=1}^{n} f_i(x_i) + \sum_{1 \le i < j \le n} f_{ij}(x_i, x_j)$$

Equation A.2 Second order component function.

A.2 Multi-parametric Model Predictive Control (mp-MPC)

A.2.1 Fundamentals of MPC

Model predictive control (MPC) is an advanced control methodology that is used to predict the future state of the system and take the appropriate control actions to ensure that optimal operation is always maintained. The aim of MPC is to provide a sequence of control actions over a future horizon that will optimize the controller performance based on predictions of the system states (Pistikopoulos, 2009). This is realized by solving online the optimization problem that describes the system behavior.

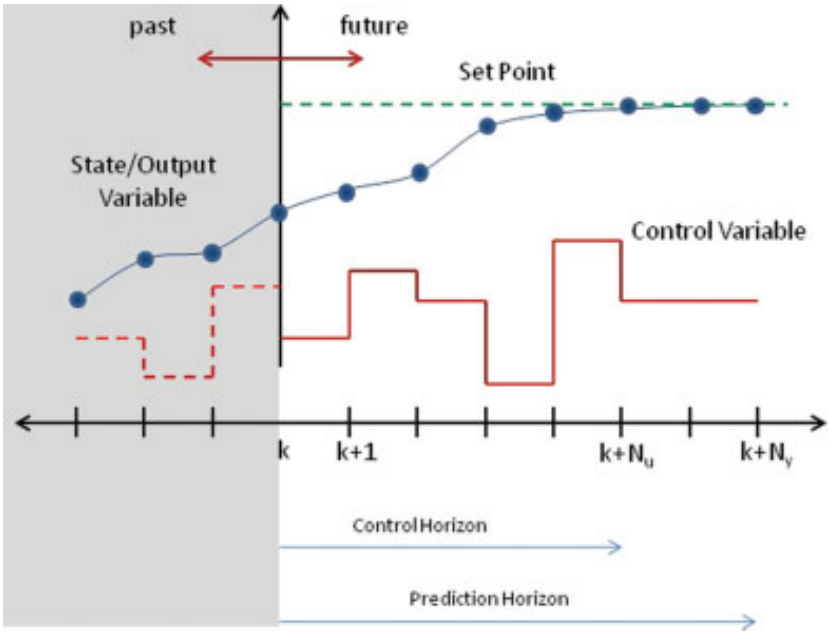

Figure A.1 Moving horizon policy used in the MPC implementation (Pistikopoulos, 2009).

As illustrated in Figure A.1 the method is based on a moving horizon policy, according to which the optimal control problem is solved at each time step (Bemporad et al., 2002). Starting at the current time interval (k), the optimization problem is solved, aiming to minimize the state and control deviations from the setpoint (Pistikopoulos, 2009). Then, the computation is repeated for the next time step ($k+1$) starting from the new state and the horizon is shifted by one time interval (Garcia et al., 1989, Bemporad et al., 2002, Pistikopoulos, 2009). The sequence is repeated until the values of the setpoint are obtained. The key advantage of MPC is that it is designed to handle multivariable applications and take into consideration the constraints on the state and control variables (Garcia et al., 1989, Pistikopoulos, 2009). However, MPC's implicit nature requires the optimization problem to be solved online for every time interval, demanding large computational effort.

Equation A.3 illustrates the standard equation used as objective function in the formulation of the MPC problem.

$$\min_{x,y,u} J = x'_N P x_N + \sum_{k=1}^{N-1} x_k Q_k x_k + \sum_{k=1}^{N-1} (y_k - y_k^R)' Q R_k (y_k - y_k^R) + \sum_{k=0}^{M-1} (u_k - u^R)' R_k (u_k - u^R) + \sum_{k=0}^{M-1} \Delta u_k R1_k \Delta u_k$$

$$\boldsymbol{s.t.\ x_{t+1} = A\, x_t + B\, u_t + D\, d}$$

$$y_t = C x_t$$

$$\boldsymbol{x_{min} \le x_t \le x_{max}}$$

$$\boldsymbol{u_{min} \le u_t \le u_{max}}$$

$$\boldsymbol{y_{min} \le y_t \le y_{max}}$$

$$\boldsymbol{\Delta u_{min} \le \Delta u_t \le \Delta u_{max}}$$

$$d_{min} \le d_t \le d_{max}$$

Equation A.3 General form of the the MPC problem formulation.

Table A.1 Explanation of the various entities and tuning parameters used in the MPC formulation.

Entity	Description	Entity	Description
M	Control Horizon (NC)	Δu	Changes in the control actions
N	Output/Prediction Horizon (OH)	d	Disturbances
k	Time intervals	P	Terminal weight matrix for states (t=N)
$\boldsymbol{x}$	States	Q	Objective coefficient for states (x)
$\boldsymbol{y}$	Outputs	QR	Quadratic matrix for tracked outputs (y)
$\boldsymbol{y^R}$	Output setpoints	R	Quadratic matrix for manipulated variables (u)
$\boldsymbol{u}$	Control actions	R1	Weight matrix for output moves (Δu)

A.2.2 Explicit/multi-parametric MPC

Aiming to simplify the online implementation of MPC, Bemporad et al. (2000) first suggested a methodology that has the ability to obtain the MPC control law offline. This is realized by reformulating the initial MPC problem into a multi-parametric optimization problem and obtaining the complete map of the optimal solution as a function of the problem parameters (Pistikopoulos, 2000). The nature of the mathematical model that describes the dynamic system indicates the type of functions that formulate the optimization problem (e.g. linear, nonlinear, quadratic, convex, differentiable and non-differentiable). Another aspect that is of key importance for the choice of the solution procedure is the type of decision variables and parameters (e.g. continuous, binary, time-varying or not) (Pistikopoulos, 2009, Pistikopoulos et al., 2015). The combination of various types of objective functions and variables gives rise to mp-MPC problems of different structure, such as:

(i) Multi-parametric linear programming (mp-LP)
(ii) Multi-parametric quadratic programming (mp-QP)
(iii) Multi-parametric mixed-integer programming (mp-MILP)
(iv) Multi-parametric mixed-integer quadratic programming (mp-MIQP)

One of the key advantages of multi-parametric MPC (mp-MPC) is that it reduces the online optimization problem to a sequence of function evaluations. The parametric control profiles that are obtained by the offline solution can be stored in a computational hardware (e.g. microchip) (Pistikopoulos, 2009). "Online optimization via offline optimization" (Pistikopoulos, 1997, Pistikopoulos, 2000), enables the mapping of the optimal multi-parametric solution without the need of an online optimization software. "MPC-on-a-chip" technology allows the storage of the parametric profiles on a simple hardware and enables thus the incorporation of advanced model-based controllers in portable and/or embedded devices (Pistikopoulos, 2004, Pistikopoulos, 2008). Explicit/mp-MPC has been successfully applied to a number of case studies. Some of them are illustrated in Table A.2.

Table A.2 Applications of the multi-parametric model predictive control (mp-MPC).

Applicaiton	Reference
Control of a two-input two-output gas-liquid separation plant.	Grancharova et al. (2004)
Controller development for the attitude of a satellite.	Hegrenæs et al. (2005)
Control of insulin delivery in patients with Type I diabetes.	Dua et al. (2006)
Optimal design and optimization of a metal-hydride based hydrogen storage tank.	Georgiadis et al. (2009)
Automatic control of blood glucose to avoid hypoglycemia.	Dua et al. (2009)
Robust explicit MPC of hydrogen storage tank.	Panos et al. (2010)
Control of PSA systems.	Khajuria and Pistikopoulos (2011a), Khajuria and Pistikopoulos (2013)
Optimization of insulin dosing to patients with Type I diabetes.	Zavitsanou et al. (2014)

Appendix B

Downstream Process

**The mathematical model of the MCSGP process presented in this chapter has been developed and validated by the Morbidelli Group (ETH Zürich). The model is also presented in Appendix A of Papathanasiou et al. (2016). Advanced control strategies for the multicolumn countercurrent solvent gradient purification process. AIChE J., 62: 2341–2357. doi:10.1002/aic.15203s*

***The work on the development of the PID controllers for the single-column system presented here have been performed in collaboration with Ms Styliana Avraamidou and are presented in: Papathanasiou et al. (2016). Advanced control strategies for the multicolumn countercurrent solvent gradient purification process. AIChE J., 62: 2341–2357. doi:10.1002/aic.15203*

B.1 The Mathematical Model of the MCSGP Process

B.1.3 Model development

The mathematical model describing the MCSGP process has been developed by ETH Zürich and has been tested for various case studies (see Section 3.3). The model comprises Partial Differential and Algebraic Equations (PDAEs) and describes the main events taking place in in the chromatographic column.

(i) Liquid Phase Concentration

Equation B.1 corresponds to the mass balance equation of chromatography that assumes the column is radially homogenous and all column properties are constant in a given cross section. The differential equation is derived by material balances, lumping all non-convective transport phenomena in a dispersion term (Guiochon et al., 1994).

$$\frac{\partial c(z,t)_{i,h}}{\partial t} = D_{ax}\frac{\partial^2 c(z,t)_{i,h}}{\partial z^2} - \frac{Q_h}{A_{col}\,\varepsilon_i}\frac{\partial c(z,t)_{i,h}}{\partial z} - \frac{(1-\varepsilon_i)}{\varepsilon_i}\frac{\partial q(z,t)_{i,h}}{\partial t}$$

Equation B.1 Liquid phase concentration

The system considers two independent domains: (i) time (*t*) and (ii) space (*z*) with limits from 0 to column length, as well as the concentration of the liquid phase concentration of species *i* at column *h* $c(z,t)_{i,h}$ *(mg/mL)* and the solid phase concentration of species *i* at column *h*, $q(z,t)_{i,h}$ *(mg/mL).* The indices *i* and *h* correspond to the number of species in the column (here: modifier, weak impurities, product and strong impurities) and the number of columns used in the setup, respectively. The term on the right hand-side of the equation, describes the evolution of the liquid phase concentration over time (accumulation in the mobile phase). On the left hand-side, starting from left to right: (i) $D_{ax}\frac{\partial^2 c(z,t)_{i,h}}{\partial z^2}$ corresponds to the dispersion term, where D_{ax} is the axial dispersion coefficient *(cm²/min)*, (ii) $\frac{Q_h}{A_{col}\,\varepsilon_i}\frac{\partial c(z,t)_{i,h}}{\partial z}$ describes the convective transport, where Q_h is the operating flow rate *(mL/min)* of column *h*, A_{col} *(cm²)* is the column cross-section and ε_i corresponds to the column porosity for component *i (dimensionless),* the ratio

$\frac{Q_h}{A_{col}\,\varepsilon_i}$ describes the local average mobile velocity, and (iii) $\frac{(1-\varepsilon_i)}{\varepsilon_i}\frac{\partial q(z,t)_{i,h}}{\partial t}$ is the term describing the adsorptive interaction (accumulation in the stationary phase) for species *i* at column *h* .

(ii) Solid Phase Concentration

The mass balance (Equation B.2) is combined with a kinetic equation based on the linear driving force model, following lumped kinetics (Guiochon et al., 1994).

$$\frac{\partial q(z,t)_{i,h}}{\partial t} = k_i\left(q^*\left(c(z,t)_{i,h}\right) - q(z,t)_{i,h}\right)$$

Equation B.2 Solid phase concentration

The term on the left hand side describes the evolution of the liquid phase concentration over time (accumulation in the mobile phase), while on the right hand side: k_i corresponds to the lumped mass transfer coefficient of species *i (min^{-1})*, $q^*\left(c(z,t)_{i,h}\right)$is the equilibrium solid phase concentration as a function of the mobile phase concentration *(mg/mL)* for species *i* at column *h* and $q(z,t)_{i,h}$ is the solid phase concentration of species *i* at column *h (mg/mL)*.

(iii) Initial Conditions

At the start of the operation (*t=0*) columns are considered empty and equilibrated:

$$c(z,t=0)_{i,h} = 0$$

Equation B.3 Initial conditions

(iv) Boundary Conditions

At the column inlet (*z=0*) the concentration of species *i* is assumed to be equal to its concentration in the feed $c_{i,h}^{in}$ *(mg/mL)*.

$$c(z=0,t)_{i,h} = c_{i,h}^{in}$$

Equation B.4 Boundary conditions at the column inlet

At the column outlet, Danckwerts boundary condition is applied (Guiochon et al., 1994), where no axial change in the concentration is assumed.

$$\frac{\partial c(z = L_{col}, t)_{i,h}}{\partial z} = 0$$

Equation B.5 Boundary conditions at the column outlet

where *t* represents the time, *z* the column length, *i* the component and *h* the column index:

$$t \in [0, t_{end}] \ , \qquad z \in [0, L_{col}] \ , \qquad i = 1, \dots, n_{comp} \ , \qquad h = 1, .., n_{col}$$

(v) Isotherms: The Competitive Bi-Langmuir Isotherm

The model uses the competitive bi-Langmuir isotherm to describe the competition between the species during adsorption. The solid phase equilibrium concentration $q^*\left(c(z,t)_{i,h}\right)$ *(mg/mL)* is calculated by the following equation:

$$q^*\left(c(z,t)_{i,h}\right) = \frac{c_{i,h} \cdot H_{i,h}^{I}}{1 + \sum_{i=2}^{n_{comp}} \frac{c_{i,h} \cdot H_{i,h}^{I}}{q_{i,h}^{I}}} + \frac{c_{i,h} \cdot H_{i,h}^{II}}{1 + \sum_{i=2}^{n_{comp}} \frac{c_{i,h} \cdot H_{i,h}^{II}}{q_{i,h}^{II}}}$$

Equation B.6 Solid phase concentration at equilibrium

As discussed in Chapter 3, one can consider other types of isotherms, however the bi-Langmuir isotherm used here is commonly applied in protein systems (Kraettli, 2012). Equation B.6 is valid under the assumption of ideal behavior of the mobile phase and the adsorbed layer and equal column saturation capacities of both types of sites for the two components. $H_{i,h}^{I}$ and $H_{i,h}^{II}$ correspond to the Henry constants for the adsorption sites 1 and 2 of species *i* in column *h* respectively, while $q_{i,h}^{I}$ and $q_{i,h}^{II}$ are the saturation capacities for the adsorption sites 1 and 2 *(mg/mL)*.

The Henry constants and saturation capacities for the mixture components are shown below:

$$H_{i,h} = \alpha_{i,1} \cdot \left(c(z,t)_{1,h}\right)^{\alpha_{i,2}}$$

$$H_{i,h}^{II} = \alpha_{i,3} \cdot \left(H_{i,h}\right)^{\alpha_{i,4}}$$

$$H_{i,h}^{I} = H_{i,h} - H_{i,h}^{II}$$

Equation B.7 Henry constants

$$q_{i,h}^{I} = \alpha_{i,5} \cdot \left(H_{i,h}^{I}\right)^{\alpha_{i,6}}$$

Equation B.8 Saturation capacities for the two

$$q_{i,h}^{II} = \alpha_{i,7} \cdot (H_{i,h}^{II})^{\alpha_{i,8}}$$

adsorption sites

where i here is the number of the components and h represents the column index. $H_{i,h}$ corresponds to the Henry constant of species *i* in column *h, while* α_i are dimensionless, species dependents constants.

For the modifier, the equilibrium solid phase concentration is solely a function of its liquid phase concentration:

$$q^*(c(z,t)_{1,h}) = H_{mod} \cdot c(z,t)_h$$

Equation B.9 Solid equilibrium phase concentration for the modifier

In addition to the equations shown above, the model includes a set of equations describing the mass balance around each column (Chapter 3). Those equations depend on the configuration of the setup at any given time point. The efficiency of the separation process can be evaluated using two main criteria. The first and most important constraint to be fulfilled is purity. That is what defines whether the product is suitable to be used as end-product or needs to be further processed. Secondly, the process needs to reach high levels of recovery yield, so as to minimize product loss. To calculate purity and yield we use the equations presented by Grossmann et al. (2010).

$$Pur_{av_j} = \frac{c_{av_{P,s,j}}}{c_{av_{W,s,j}} + c_{av_{P,s,j}} + c_{av_{S,s,j}}}$$

Equation B.10 Product purity as a function of the component concentration in the product outlet stream

$$Y_j = \frac{c_{av_{P,s,j}}}{c_p^{feed}}$$

$$j = 1, \dots, n_{cycle}, s = 1, \dots, n_{outlet}$$

Equation B.11 Recovery yield

Where, Pur_{av_j} and Y_j correspond to the average purity and recovery yield over a process cycle, $c_{av,s,j}$ *(mg/mL)*. is the average concentration of the mixture components at the end of each cycle,

c_p^{feed} *(mg/mL)*. indicates the feed concentration of the targeted product, *j* indicates the cycle index and s the outlet stream.

Table B.1 illustrates the model parameters used for the simulation of the above presented process model. Due to confidentiality agreement, the exact parameter values cannot be disclosed in this document, therefore their order of magnitude is provided.

Table B.1 Model parameters and the respective order of magnitude (data obtained by ETHZ, group of Prof. Morbidelli)

Parameter	Significance	Value (range)	Units
$\mathbf{A_{col}}$	Column cross-section	0.2-0.5	cm^2
$\mathbf{L_{col}}$	Column length	10-16	cm
$\mathbf{k_i}$	Lumped mass transfer coefficient of species *i*	20-100 [Species dependent]	min^{-1}
$\mathbf{D_{ax}}$	Effective axial dispersion coefficient	0-0.001	cm^2/min
$\boldsymbol{\varepsilon}$	Column porosity for component *i*	0.5-0.8 [Species dependent]	Dimensionless
$\mathbf{H_{mod}}$	Henry constant for the modifier	0.2	Dimensionless
$\boldsymbol{\alpha_i}$	Species dependent constants	Species dependent	Dimensionless

B.1.4 Model simulation

The MCSGP process model is simulated in gPROMS® ModelBuilder v4.2.0 (P.S.E, 1997-2016) (using a first order backward finite discretization method with 50 collocation points) and the results are represented below *(It should be underlined that for confidentiality agreement signed with the Morbidelli Group (ETH Zürich) tables and figures illustrate qualitative information, rather than quantitative)*. The separation process depends highly on the modifier concentration, since the latter is responsible for detaching the impurities and/or product from the resins and facilitating the elution. Figure B.1 illustrates the dynamics of the modifier

concentration over one cycle during CSS. It can be observed that the applied input strategy imposes the modifier to move from low to high concentration profiles, aiming to achieve gradient elution. Furthermore, the two columns are characterized by identical profiles for both the inputs and the outputs, shifted by a phase difference of half a cycle. During *Switch 1,* column 1 starts from a moderate modifier concentration for the elution of the overlapping fraction of W and P. Gradually, the modifier concentration increases following a linear change, until the maximum concentration is reached and the strong impurities are eluted. Figure B.2 illustrates the concentration of W, P and S during at the column inlet. It can be observed that during the I1 phase, the overlapping fractions of W and P enter the column in order to be further separated. Following that, B1 is the phase that the feed is introduced into the system. The feed stream contains W, P ,S and the modifier and is introduced once per cycle in each column. B1 phase is followed by I2 phase, where the overlapping fractions of P and S exit the column placed on the right position and enter the column on the left. After the completion of one switch (half a cycle) the columns swap places and the input strategy is repeated.

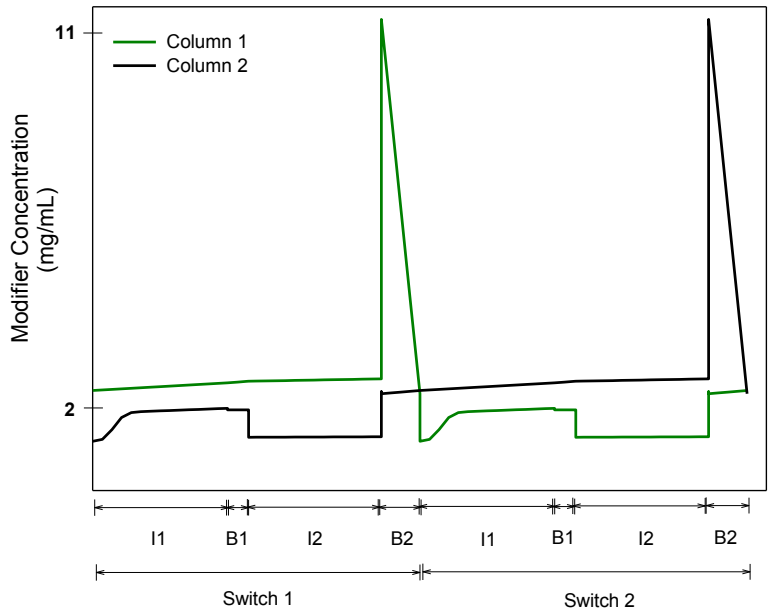

Figure B.1 Modifier concentration over one cycle under CSS for column 1 and column 2.

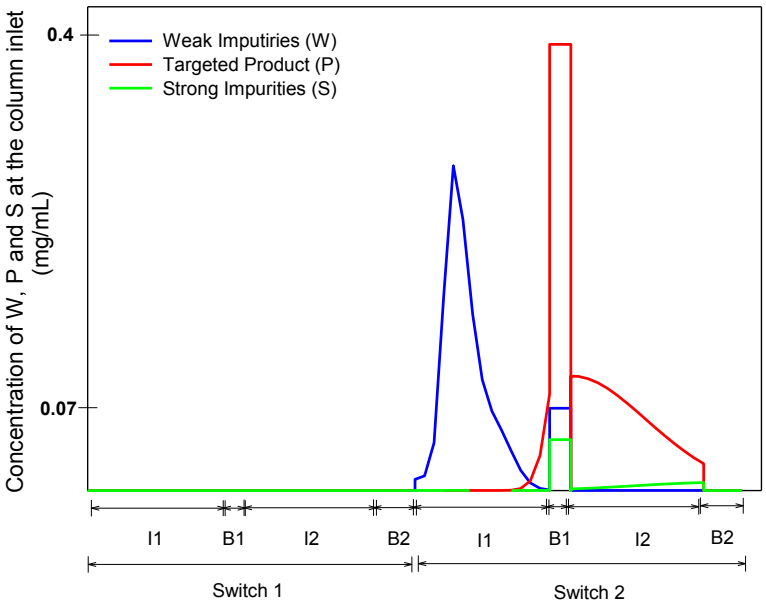

Figure B.2 Inlet concentrations and feeding strategy for one column over a cycle under CSS for weak impurities, targeted product and strong impurities.

The elution profiles of the three components for one column over one cycle are depicted in Figure B.3 It can be observed that the three components (W, P, S) are eluted gradually in three distinct fractions. However, there are overlapping regions between W & P and P & S that according to the process are recycled in order to be separated further. The results illustrated in Figure B.3 have been favorably compared to the results generated by ETHZ in FORTRAN programming language that have been experimentally validated.

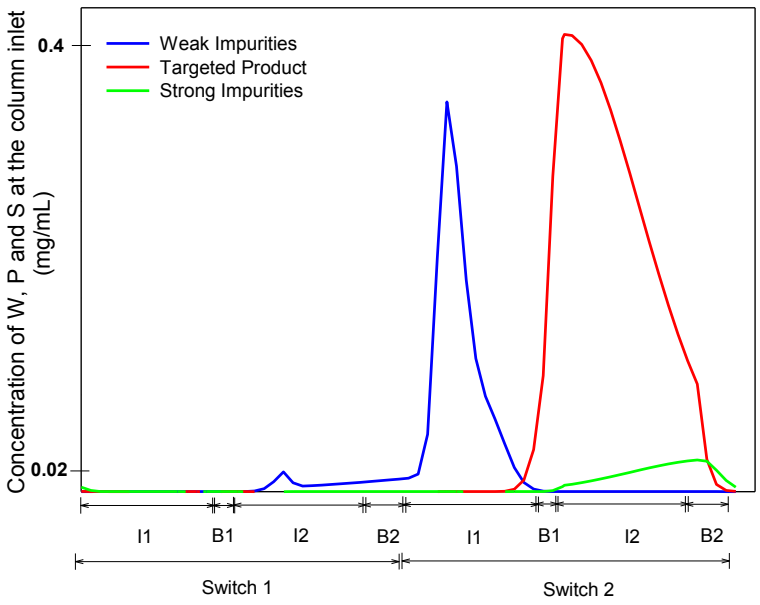

Figure B.3 Elution profiles of weak impurities, targeted product and strong impurities for one column over a cycle under CSS.

B.1.5 Cyclic Steady State

The first thing to be investigated was the time point at which the CSS is attained. The steady state is defined as the point at which the difference between the initial and the final state of the system is less or equal to a number very close to zero:

$$\left\| x(t_{cycletime})_k - x(t_0)_k \right\| \leq ess_k$$

Here, k is the iteration counter, $x(t_0)_k$ represents the initial state of the system, $x(t_{cycletime})_k$ is the state of the system after a cycle and ess_k shows the development of $\left\| x(t_{cycletime})_k - x(t_0)_k \right\|$ of cycles computed.

Table B.2 summarizes the time-points that CSS is attained for different values of ess_k. It can be observed that the time point at which the CSS is attained depends highly on the choice of ess_k. More specifically, for very low values of ess_k, a large number of cycles needs to be computed for CSS to be attained. Additionally, it should be noted that CSS is not attained for all the variables simultaneously. As shown in Table B.2, for a tolerance of ***1e-4,*** the concentration of

the weakly adsorbed impurities reached the steady state significantly slower compared to the rest of the variables. This has also a physical meaning, since the weak impurities are highly affected by small changes in the modifier concentration, whereas the desired product and the strong impurities are more resistant. The rest of the variables (not shown here) follow the behavior of the concentration of the respective species.

Table B.2 Monitoring the CSS under different tolerance (ess_k).

Variable	**Number of Cycle where CSS is achieved**				
ess_k Value	**10^{-1}**	**10^{-2}**	**10^{-3}**	**10^{-4}**	**10^{-5}**
C_{mod}	2nd	2nd	2nd	3rd	15th
C_{weak}	2nd	8th	12th	17th	17th
$C_{product}$	2nd	3rd	5th	6th	10th
C_{strong}	2nd	2nd	2nd	4th	5th

B.1.6 System Efficiency

As it has been previously discussed, there are two main criteria that indicate the efficiency of a separation process. The first and most important criterion is the *purity* of the desired product, as it indicates whether the latter qualifies for an end- product. For the calculation of purity function the approach suggested by Grossmann et al. (2010) was followed and is presented below. As it is illustrated in Figure B.3, the elution of the product takes place during the B1 phases and the product is extracted only from the column placed on the right position. Consequently, product elution is realized twice per cycle and therefore the average concentration needs to be computed (Equation 4.5).

$$c_{av_{i,s}} = \frac{\int_{\tau} c_{i,s}^{out} \cdot Q_s dt}{\int_{\tau} Q_s dt}$$

Equation B.12 Average concentration of the mixture components over one process cycle.

$$i = 2, \dots, n_{comp}, s = 1, \dots, n_{outlet}$$

Here s is the outlet stream, $c_{i,s}^{out}$ *(mg/mL)*. is the outlet concentration, Q_s represents the flow rate *(mL/min)* of the respective stream and τ the time *(min)*. for which the elution is realized.

The average purity is given by the following equation, where j indicates the cycle index and s the outlet stream.

$$Pur_{av\,j} = \frac{c_{avP,s,j}}{c_{avW,s,j}+c_{avP,s,j}+c_{avS,s,j}}$$

Equation B.13 Average product purity over one process cycle.

$$i = 2, \dots, n_{comp}, s = 1, \dots, n_{outlet}$$

The second criterion for the evaluation of the purification process is the *yield* that refers to the amount of the product recovered during the separation process, with c_p^{feed} *(mg/mL)* to indicate the feed concentration of the targeted product.

$$Y_j = \frac{c_{avP,s,j}}{c_p^{feed}}$$

Equation B.14 Average process yield over one process cycle.

$$i = 2, \dots, n_{comp}, s = 1, \dots, n_{outlet}$$

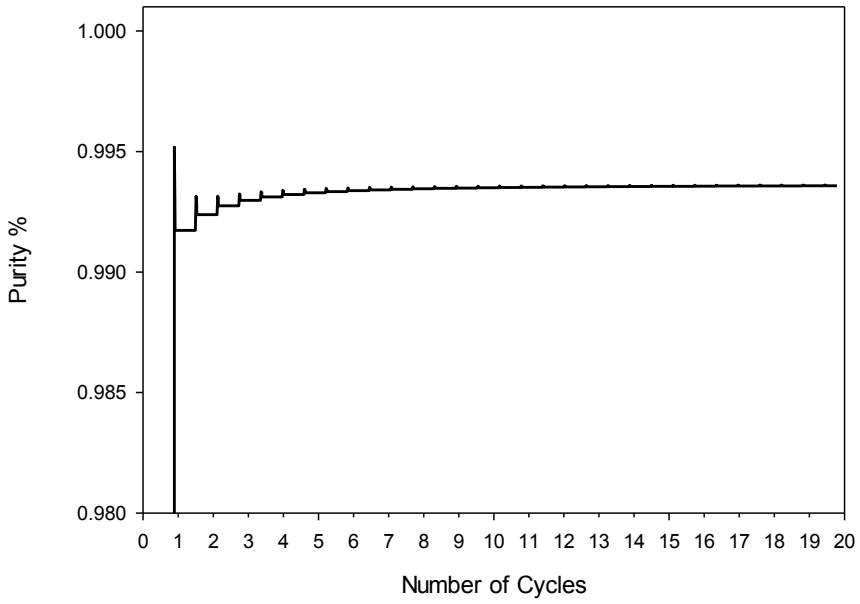

Figure B.4 The evolution of the % purity over 19 simulation cycles.

Figure B.4 illustrates the dynamics of purity for a time span of 18 cycles (cycles 0 to 19). For the sake of clarity, cycle 0 is not included in the graph. It can be observed, that at the end of the first cycle (cycle 0) the extracted product is ≅ 99% pure. For the first 3 cycles, the value of the function shows a relative variation that is in the order of magnitude of $1e^{-3,}$ while the value is stabilized at 0.993 at the end of the 4th cycle. On the contrary, yield (Figure B.5) starts from relatively low levels (2%) and rises gradually.

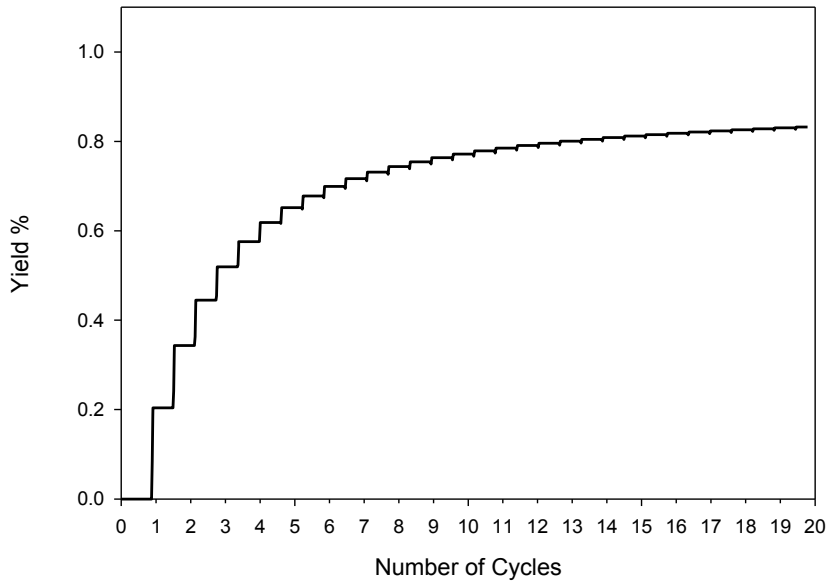

Figure B.5 The evolution of the % yield over 19 simulation cycles.

Judging by the results discussed above, the need for optimization is evident. Although purity, almost instantly reaches the desired levels, yield starts from lower levels. The latter means that under the current operational conditions, the system has a product loss of almost 13% for the first 9 cycles. Therefore the optimal operation point needs to be found, for the minimization of product losses and maintenance of product purity.

B.2 Sensitivity Analysis of the Control Tuning Parameters

The study presented in tis section is complementary to the work demonstrated in Chapter 4. Here, we examine the sensitivity of the mp-MPC tuning parameters and their effect on the controller behavior. We consider a single-column, chromatographic system (Figure B.6) based on the principles of MCSGP.

Figure B.6 Single-column Single Input-Multiple Output system under measured disturbances.

For the formulation and solution of the mp-MPC problem we use the linear state space model presented in section 4.5, where we consider: one input (modifier concentration), 3 outputs ($\int C_W$, $\int C_P$, $\int C_S$) and measured disturbances (feed composition).

B.2.1 Base case controller

Firstly, we formulate and test the following base case mp-MPC problem (MPC1). The controller is tested in-silico against the high-fidelity process model under the disturbance profile (feeding) illustrated in Figure B.7.

Table B.3 Tuning parameters used for the development of the base case controller.

Tuning Parameter	Explanation	Value
OH	Output horizon	2
NC	Control horizon	2
QR	Weights on the outputs	[100 10000 100]
Q	Weights on the states	1*I*
R	Weights for the inputs	1
P	Terminal weight for the states	Riccati equation
Umax	Input upper bound	12
Umin	Input lower bound	0.2
Ymax	Output upper bound	100
Ymin	Output lower bound	0
Dmax	Disturbance upper bound	[0 0 0]
Dmin	Disturbance lower bound	[0.0748 0.4059 0.0462]
Xmax	States upper bound	[-10000 -10000 -10000]
Xmin	States lower bound	[10000 10000 10000]

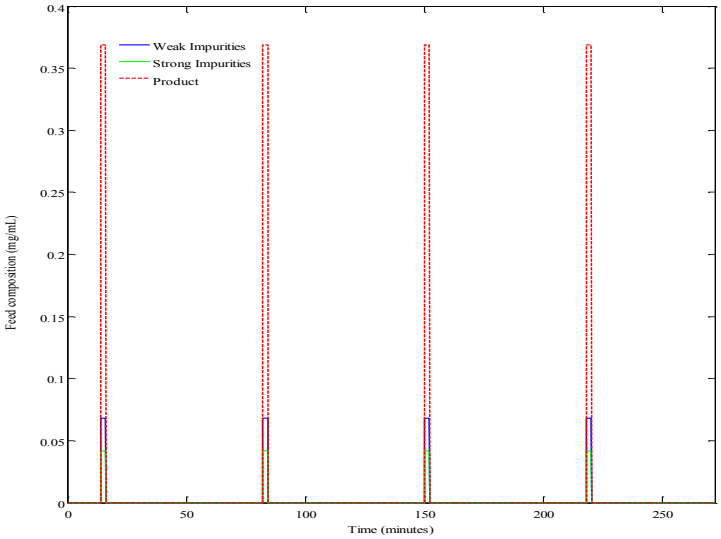

Figure B.7 Disturbance profile corresponding to the feed composition applied to the system during the closed-loop, in-silico validation.

Figure B.8 shows the input profile as indicated by the controller, while the output behavior with respect to the setpoints is shown in Figure B.9.

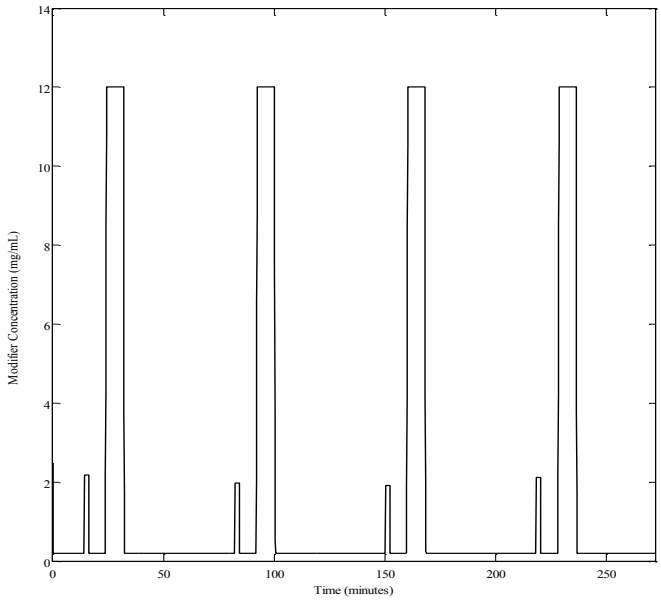

Figure B.8 Input profile indicated by the controller during the closed-loop validation.

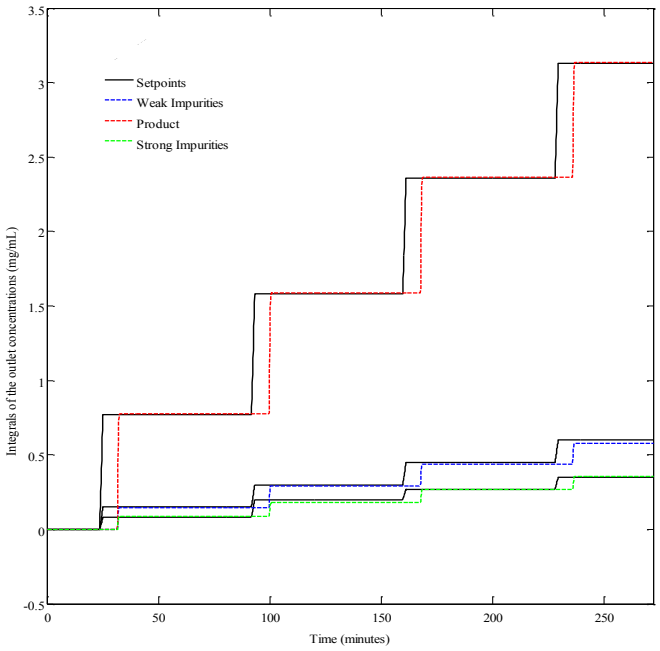

Figure B.9 Output behaviour under closed-loop validation.

It can be observed that the controller manages to reach and maintain the desired setpoitnts, however, with a significant, repetitive time delay. The latter can be attributed to the physicochemical properties of the system and in particular to the operational flow rate.

$$t_{delay} = \frac{V_{column}}{Q}$$

Equation B.15 Time delay as a function of the column volume and the operating flow rate.

Where, t_{delay} is the time delay in minutes, V_{column} the volume of the chromatographic column and Q corresponds to the flow rate.

We have previously demonstrated that pre-calculating and adjusting the setpoints based on the flow rate can lead to elimination of the delay. However, here, we are interested in exploring the effect of the controller tuning parameters on the system behavior. Aiming to explore the possibilities of eliminating the time delay in a generic way, we formulate and assess the behavior of 7 different mp-controllers (Table B.5). In particular, the problems are solved for a wide range of output and control horizons and their performance is assessed. In addition to varying horizons, here, we examine the effect of other parameters (such as the weight on output,

states and the bounds posed on the input) on the controller behavior. The controllers are tested in closed-loop against the high-fidelity process model and their behavior is discussed below

B.2.2 The effect of the output horizon

In this section we examine the effect of the output horizon solely. It should be noted that out of the 7 mp-MPC designed controllers, mp-MPC5 and mp-MPC7 did not manage to capture the setpoints and are therefore excluded from any further analysis, while mp-MPC4 and mp-MPC6 resulted in identical profiles for all the tested horizons. Moreover, the 2x2 combination (output x control horizon) was unsuccessful for all presented cases. For simplicity, in all the graphs below we focus on the behavior of 1 output (the product).

- mp-MPC 1

Figure B.10 illustrates the results from the closed loop validation for mp-MPC1 for a set of 4 different output horizons. In this case, no significant difference in the output behavior is observed (Figure B.10a, c). The gradient increase occurs of the output for all controllers simultaneously, while the differences in the absolute value are not considered significant. Interestingly, however, it is observed that changes in the output horizon affect also the input profile. In particular, the control actions for the period 14.2 min – 16.2 min (when the disturbance occurs) are different for every controller.

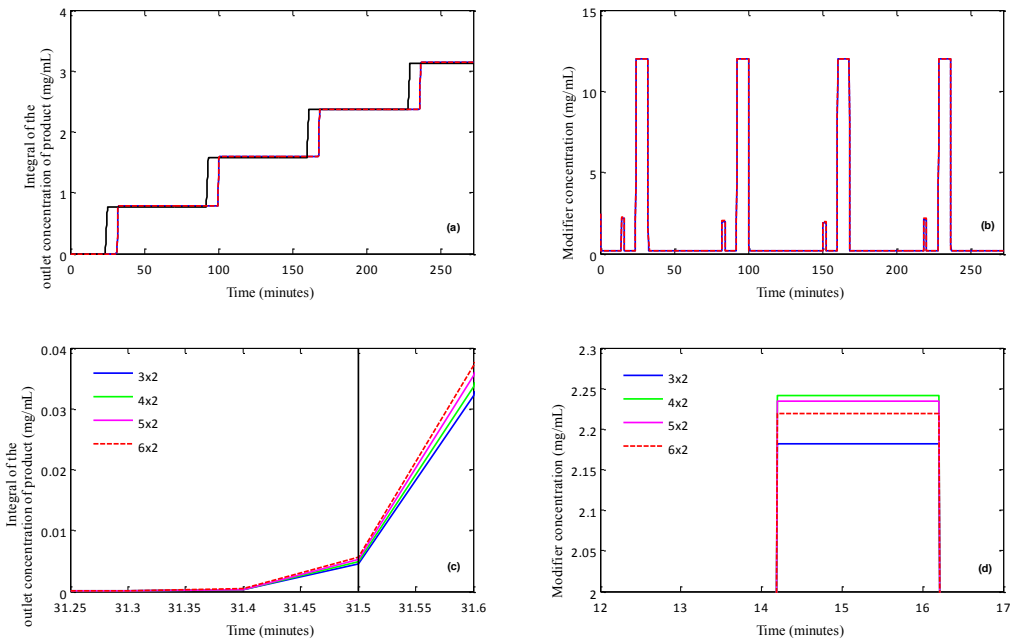

Figure B.10 Closed-loop validation results for mp-MPC1 using control horizon 2 and output horizons: 3, 4, 5, 6. (a) Comparison of the setpoint (solid black line) to the controllers output, (b) Input sets as indicated by the controllers under closed-cloop validation, (c) Close-up image on the output behaviour of graph 5a, (d) Close-up on the input profile of graph 5b.

Similarly, Figure B.11 demonstrates the results for mp-MPC2. In this case, we observe that there is a consistent increase in the slope of the output and is directly correlated to the increase of the output horizon (Figure B.11c). Particularly, the output of the 3x2 controller increases with significantly lower speed that could lead to increased dead time. As expected, the input profiles of the assessed controllers (Figure B.11d) differ both in absolute value, as well as steepness of the slope. More specifically, the steeper the increase in the input, the faster the elution of the output. The latter is in agreement with the physicochemical properties of the system, as the higher the modifier concentration (or the steeper the gradient) is, the higher the amount of the eluting components. In addition to that, the observed input/output interplay is a result of the QR/R ratio of the control problem.

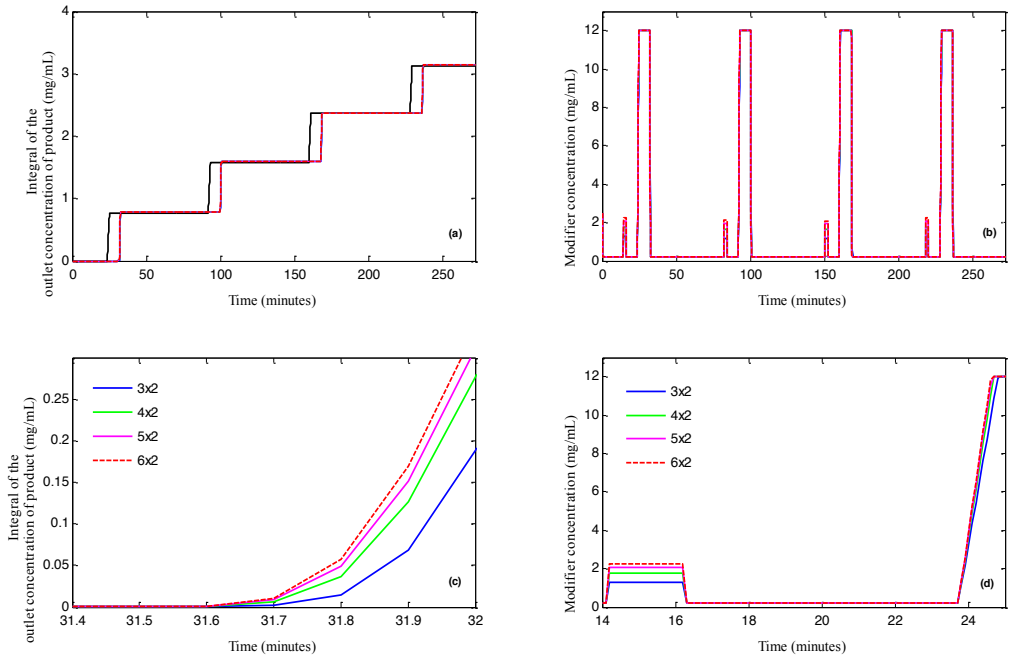

Figure B.11 Closed-loop validation results for mp-MPC2 using control horizon 2 and output horizons: 3, 4, 5, 6. (a) Comparison of the setpoint (solid black line) to the controllers output, (b) Input sets as indicated by the controllers under closed-cloop validation, (c) Close-up image on the output behaviour of graph B11.a, (d) Close-up on the input profile of graph B.11b.

- mp-MPC3

Figure B.12 illustrates the results from the closed loop validation of MPC3.

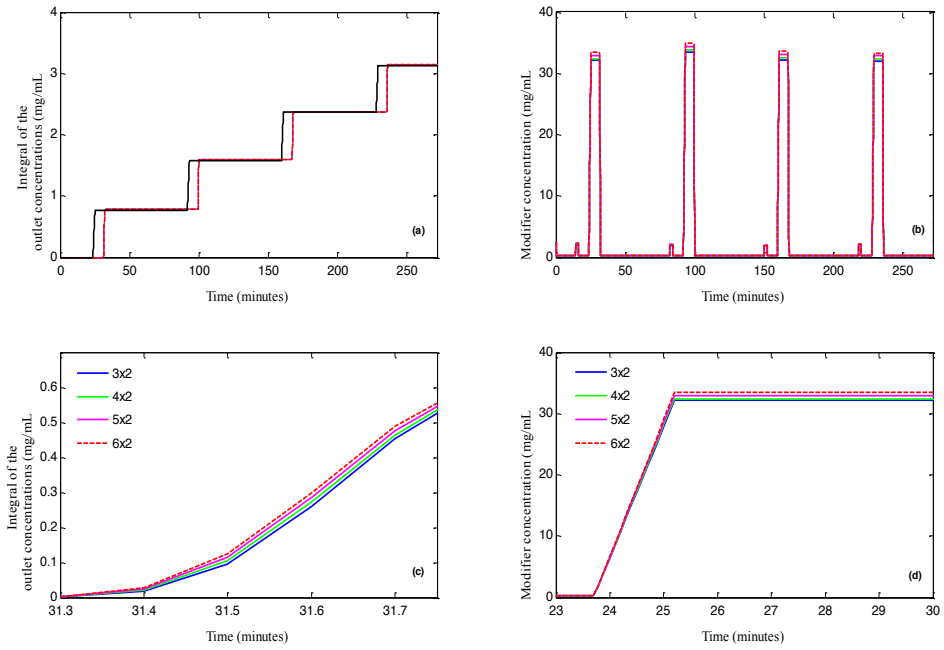

Figure B.12 Closed-loop validation results for mp-MPC3 using control horizon 2 and output horizons: 3, 4, 5, 6. (a) Comparison of the setpoint (solid black line) to the controllers output, (b) Input sets as indicated by the controllers under closed-cloop validation, (c) Close-up image on the output behaviour of graph B.12a, (d) Close-up on the input profile of graph B.12b.

It can be observed that with the increase in the output horizon there is a consistent increase and therefore improvement in the output (Figure B.12c). Additionally, the input profile (Figure B.12b) differs with respect to the maximum value reached that could possibly result in the different profiles we observe in the output. Similarly to mp-MPC2, the most significant changes are observed in the steepness of the output curve.

Judging from the closed loop simulation results it could be concluded that the choice of the output horizon has a more significant impact on the steepness of the output curve rather than the elution times, as one would expect. In particular, a consistent improvement in the output profile with the increase of the output horizon is observed. Counter intuitively, the output horizon does not seem to affect the controller responses with respect to time. Additionally, it can be concluded that the input maximum bound does not play a significant role, as all the controllers manage to reach the setpoint value equally efficiently. Therefore, from a process perspective it

might be better to operate under a tight control strategy (e.g. MPC1) that could potentially lead to decreased modifier use and therefore minimize production costs.

B.2.3 The effect of the tuning parameters

Following the investigation of the effect of the output horizon, the next step is to explore the impact of other tuning parameters in the problem formulation. Here, we compare 5 out of the 7 control schemes (excluding the unsuccessful mp-MPC5 and mp-MPC7), using the 3x2 (output x control horizon) results. It can be observed that mp-MPC3 & mp-MPC6 result in the best output profile, followed by mp-MPC1 & mp-MPC4 and, the input profiles generated by the controllers. In particular, the output of schemes 3 & 6 is characterized by the highest steepness and reaches the setpoint approximately 0.2 min faster, compared to mp-MPC1 and mp-MPC4. In addition, each pair is characterized by the same input actions (Figure B.13b&d). Interestingly, all 4 schemes are characterized by the same corrective action when disturbances occur (Figure B.13d, 14.2-16.2 min), while mp-MPC2 operates at a lower value. Moreover, mp-MPC2 follows a smoother, less steep increase in the input profile compared to the rest of the schemes. Aiming to relate the resulting profiles to the control parameters, it is observed that all four schemes are using the same QR matrix, whereas mp-MPC2 is tuned using weight of an order of magnitude less for output 2 (product). It could be concluded therefore that the QR/R ratio is the most significant parameter that determines the input profile, both in absolute values and steepness. It would be advisable to test control schemes of intermediate upper bounds in order to examine whether the actions of mp-MPC1 & mp-MPC4 are saturated. Furthermore, comparing mp-MPC3 & mp-MPC6 to mp-MPC1 & mp-MPC4 we observe that the upper bound of the input is significantly affecting the steepness of the output slope (i.e. the elution profile). That is also in accordance to the physicochemical properties as the modifier concentration is the sole factor responsible for the elution. However, the controller performance has to be further assessed and the trade-off between modifier use and product elution had to be determined in order to be able to avoid unnecessary costs.

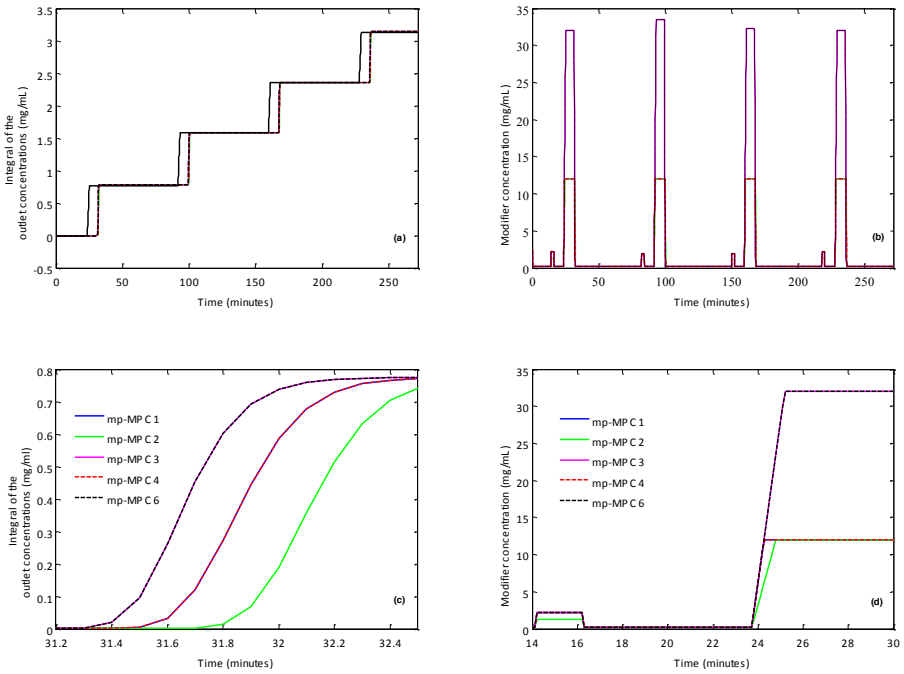

Figure B.13 Closed-loop validation results for mp-MPC1, 2, 3, 4 & 6 using control horizon 2 and output horizon 3. (a) Comparison of the setpoint (solid black line) to the controllers output, (b) Input sets as indicated by the controllers under closed-cloop validation, (c) Close-up image on the output behaviour of graph B.13a, (d) Close-up on the input profile of graph B.13b.

Comparing now mp-MPC3 to mp-MPC6 it can be concluded that the weight for the states (Q) has no significant effect on the controller behavior and can be therefore eliminated from the formulation. Similarly, as expected, the bounds of the disturbances do not affect the performance, as mp-MPC1 and mp-MPC4 operate under different disturbance bounds and result in the same profiles.

B.2.4 The effect of the control horizon

In this section we investigate the effect of the control horizon on the response of the controller. In particular we examine mp-MPC2, mp-MPC3, mp-MPC4 and mp-MPC6 for an output horizon of 6 and control horizon 2 to 6. Mp-MPC1 is eliminated from the comparison as it is characterized by tighter disturbance bounds and it cannot be applied on the twin-column system. Table B.4 summarizes the performance of the examined controllers. The sets for which the controllers failed to reach the setpoints are not included in the comparative figures.

Table B.4 Summary of the performance of the 4 mp-MPC schemes assessed in closed loop validation, using output horizon 6 and control horizons 2 to 6. The performance assessment is based on the efficiency of the controller to reach the predefined setpoints.

Control Scheme	Control Horizon	Performance
mp-MPC2	2	Good
	3	Good
	4	Good
	5	*Failed*
	6	Good
mp-MPC3	2	Good
	3	Good
	4	*Failed*
	5	Good
	6	Good
mp-MPC4	2	Good
	3	Good
	4	*Failed*
	5	Good
	6	Good
mp-MPC6	2	*Failed*
	3	Good
	4	*Failed*
	5	Good
	6	Good

- mp-MPC2

Figure B.14 illustrates the results from the closed loop validation of mp-MPC2 using an output horizon of 6 and 4 different control horizons. It can be observed that the change in the control horizon has a significant effect on the controller performance. In particular, the results indicate that the control horizon affects the controller behavior much more than the output horizon (Figure B.11). Counter intuitively, Figure B.14c demonstrates that the best performance is given by the 6x2 controller, as its output elutes significantly earlier, decreasing the system delay by approximately 1.2 min (compared to the 6x4 controller). A closer observation in the input behavior (Figure B.14d) indicates that the choice of the control horizon affects both the steepness of the slope and the absolute maximum value of the input. In addition to that, it can be observed that the output behavior does not depend solely on the amount of modifier (input) injected in the system, but also on the speed that the input enters the system (steepness of the slope). It could be assumed that, in fact, the output behavior depends in a higher extent to the speed rather than the actual concentration. A characteristic example that supports this assumption is the behavior of the 6x2 controller. Although, it is characterized by the smallest control horizon, its input is following the steepest increase compare to the other 3 cases. However, its maximum input value is lower than the respective one of the 6x6 controller. Moreover, it is observed that the fastest the increase in the modifier concentration is, the fastest is the elution. The latter is also in agreement with the system physicochemical properties, as the gradient of the modifier (i.e. the steepness of the slope) is one of the most significant parameters that determine separation.

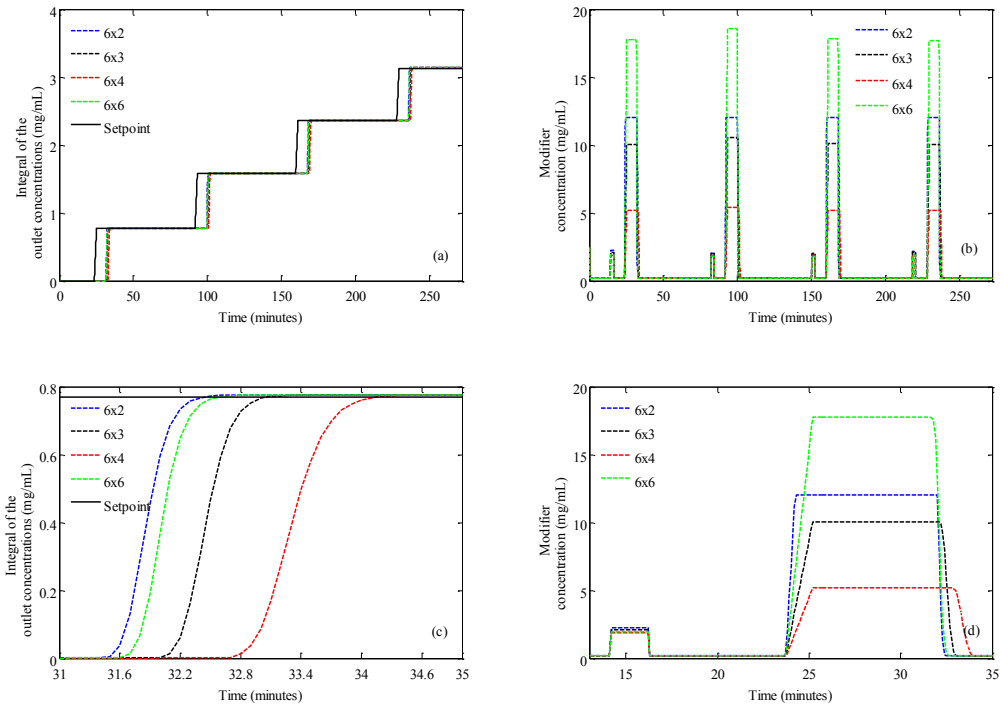

Figure B.14 Closed-loop validation results for mp-MPC2 output control horizon 6 and control horizons: 2, 3 , 4, 6. (a) Comparison of the setpoint (solid black line) to the controllers output, (b) Input sets as indicated by the controllers under closed-cloop validation, (c) Close-up image on the output behaviour of graph B.14a, (d) Close-up on the input profile of graph B.14b.

In addition to the above, the control horizon affects also the control action against the disturbance (Figure B.14 d, 14-16.2 min). In particular, it is observed that for each control horizon, the controller chooses a different absolute maximum value. Consequently, this is reflected to the output profile. More specifically, the 6x2 controller reached the highest concentration amongst the 4 examined controllers for this time period. Therefore, in this case, the column is filled faster with modifier and results to earlier elution.

- mp-MPC3

Similarly, to mp-MPC2, here we observe that the steepest the change in the input (Figure B.15d) the faster the elution (Figure B.15c). In addition, it is clear that the elution profile depends almost solely on the gradient of the input rather than the absolute values, as the 6x2 and 6x6 controllers are characterized by the exact same gradient but different final value in the input. If we compare now in pairs the controllers that are characterized by the same gradient in the input, it can be observed that the control horizon does impact the output behavior. However,

it is indicated by the results that the higher the control horizon, the slower the elution (i.e. the output responds slower to the control actions).

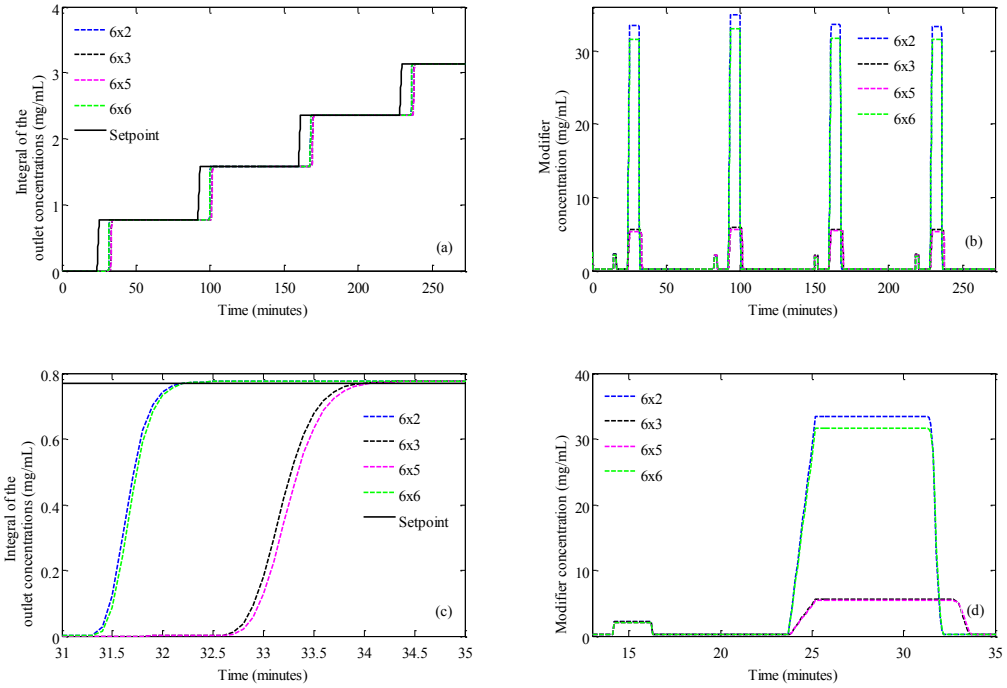

Figure B.15 Closed-loop validation results for mp-MPC3 output control horizon 6 and control horizons: 2, 3 , 4, 6. (a) Comparison of the setpoint (solid black line) to the controllers output, (b) Input sets as indicated by the controllers under closed-cloop validation, (c) Close-up image on the output behaviour of graph B.15a, (d) Close-up on the input profile of graph B.15b.

- mp-MPC4 & mp-MPC6

Mp-MPC4 (Figure B.16) and mp-MPC6 (Figure B.17) behave similarly to the above-described controllers. Also, in these two cases it is consistently observed that the gradient of the input has the most significant effect on the output behavior. That cannot be linked however to the choice of control horizon as there is no repetitive pattern.

However, in cases where two controllers share the same gradient input profile (Figure B.16d: 6x2 and 6x6, Figure B.17: 6x3 and 6x5) then the higher the control horizon, the later the output elution.

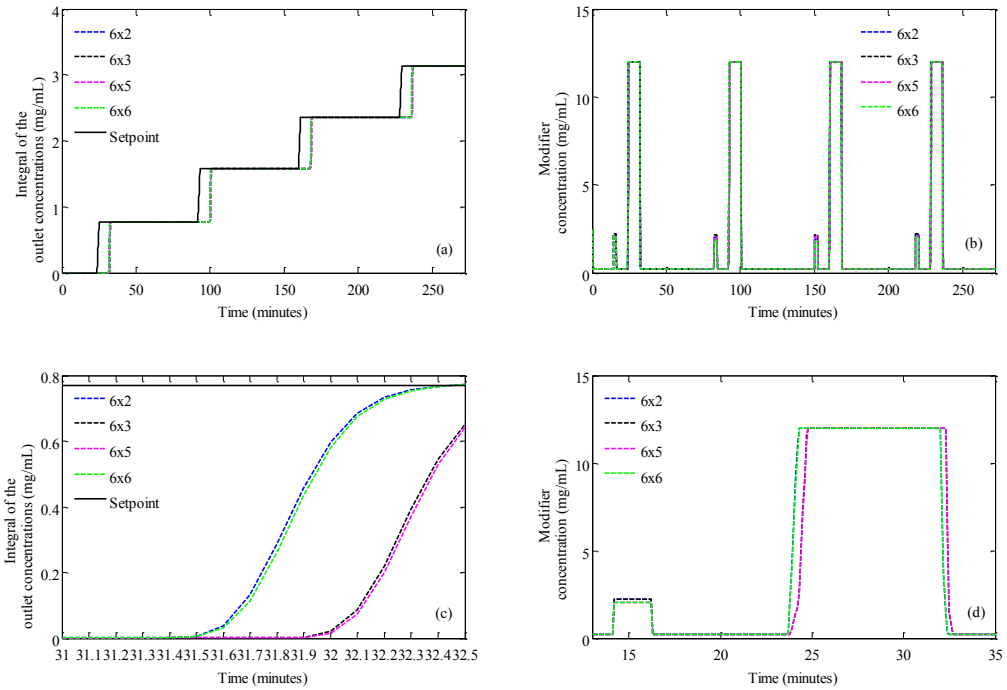

Figure B.16 Closed-loop validation results for mp-MPC4 output control horizon 6 and control horizons: 2, 3 , 4, 6. (a) Comparison of the setpoint (solid black line) to the controllers output, (b) Input sets as indicated by the controllers under closed-cloop validation, (c) Close-up image on the output behaviour of graph B.16a, (d) Close-up on the input profile of graph B.16b.

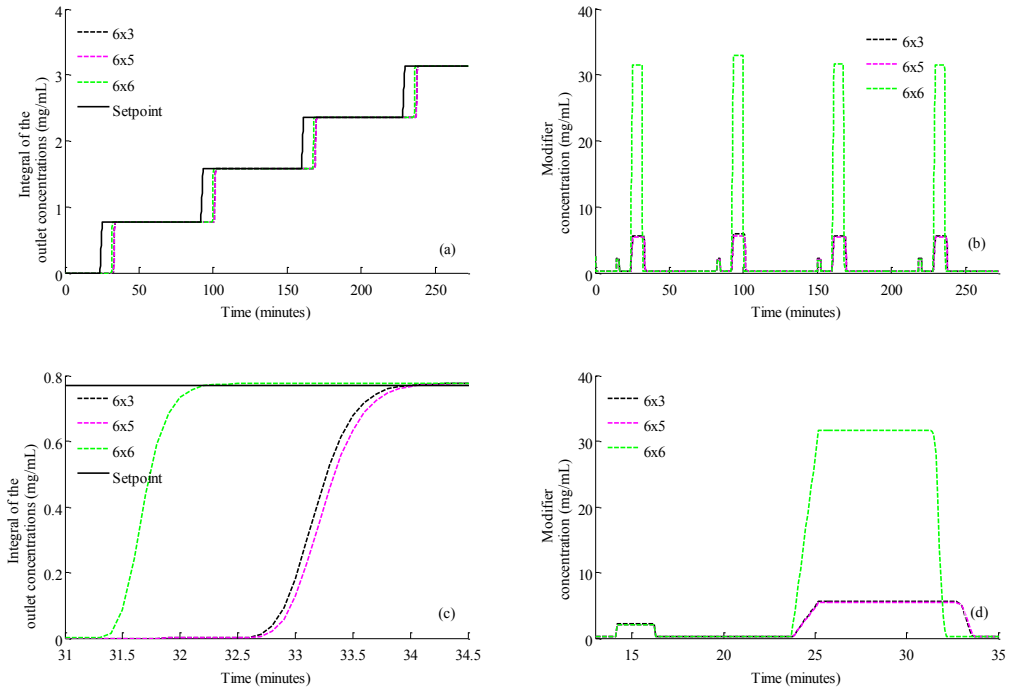

Figure B.17 Closed-loop validation results for mp-MPC6 output control horizon 6 and control horizons: 2, 3 , 4, 6. (a) Comparison of the setpoint (solid black line) to the controllers output, (b) Input sets as indicated by the controllers under closed-cloop validation, (c) Close-up image on the output behaviour of graph B.17a, (d) Close-up on the input profile of graph B.17b.

Table B.5 Tuning parameters for all mp-MPC problems tested

Tuning Parameter	**Values**						
	mp-MPC1	**mp-MPC2**	**mp-MPC3**	**mp-MPC4**	**mp-MPC5**	**mp-MPC6**	**mp-MPC7**
QR	[100 10000 100]	[100 1000 100]	[100 10000 100]	[100 10000 100]	[100 1000 100]	[100 10000 100]	[100 1000 100]
Q	1*I*	1*I*	1*I*	1*I*	-	-	-
R	1						
P	Riccati equation	Riccati equation	Riccati equation	Riccati equation	-	-	-
Umax	12[1]	50[1]	50	12	50	50	12
Umin	0.2[1]						
Ymax	100						
Ymin	0						
Dmax	[0 0 0]						
Dmin	[0.0748 0.4059 0.0462][2]	[10 10 10][3]	[10 10 10][3]	[10 10 10][3]	[10 10 10][3]	[10 10 10][3]	[10 10 10][3]
Xmax	[-10000 -10000 -10000]						
Xmin	[10000 10000 10000]						

[1] The modifier concentration can actually vary between 0 mg/mL and 50 mg/mL. The maximum value of 12 mg/mL is chosen as upper bound for some of the cases as it approximately matches the maximum value used in the real process (11.69 mg/mL). The minimum of 0.2 mg/mL is chosen as in reality the modifier concentration never drops to 0 mg/mL. [2] The bounds of the disturbances correspond to a ±10% experimentally defined variation range. [3] The maximum bound is increased to meet the specifications of the connected system later on.

B.3 Comparison of mp-MPC Performance to PID Control

PID is one of the most common control algorithms used in industry primarily due to its simplicity, good control performance and robustness to uncertainties in a wide range of operating conditions (Sung et al., 2009). PID control is based on the calculation of an error value as the difference between a measured process variable and a desired setpoint. The controller computes the desired actuator output by calculating proportional, integral, and derivative responses to minimise the original error (Equation B.16**).**

$$u(t) = K_p e(t) + K_i \int_{t_0}^{t} e(\tau)\,\mathrm{d}\tau + \mathrm{K}_d \frac{\mathrm{d}e(t)}{\mathrm{d}t}$$

Equation B.16 Output of the PID controller.

where $u(t)$ is the output of the controller, therefore the control action at time t, $e(t)$ is the error between the measured data and the set value ($e = y_{sp} - y$), K_p is the proportional gain, K_i is the integral gain, and K_d is the derivative gain. Furthermore, t is the instantaneous time (the present), and τ is variable of integration and takes on values from time 0 to the present t. The values of K_p, K_i and K_d correspond to the weights and determine the performance of the controller.

Here we develop a P-only controller for the SIMO system presented above (Section 4.4), with three different gains for each control variable. Tracking the integral of the outlet concentrations ensures that no oscillation will be observed in the control variables, therefore there is no need for the integral (I) and derivative (D) parts of the PID controller. The performance of a PI controller for this case has exactly the same performance as the P-only controller, and no reduction of the offset is observed. This is because the integral of the outlet concentrations is tracked. Once the proportional part (faster) of the controller takes action, the output would either reach the set point or overpass it with an offset. This offset cannot be decreased by the integral part of the controller due to the integral nature of the controlled variables. The developed controller has a control output composed of a linear combination of the three different proportional parts, one for every control variable (Equation B.17). Table B.6 illustrates the tuning parameters used for the development of the P-controller.

$$u(t) = K_p^w e_w(t) + K_p^S e_w(t) + K_p^w e_w(t)$$

Equation B.17 Control output composed of a linear combination of the three different proportional parts

Table B.6 Design parameters of the P-controller.

Design Parameter (Gain)	Value
$\boldsymbol{K_W}$ (weak impurities)	503.80
$\boldsymbol{K_P}$ (product)	727.56
$\boldsymbol{K_S}$ (strong impurities)	707.62

The controller is tested in 'closed-loop' using the process model described above and its performance is evaluated. The choice of setpoints is made in the same fashion as described for the mp-MPC controller. It is observed that the response of the system operating under the P-controller is characterized by a significant delay especially when the system operates close to the allowed limits. This kind of dead time cannot be decreased by a dead time compensator (e.g. Smith predictor). The P-controller cannot project the setpoint change and therefore cannot take proactive actions.

The P-controller is further tested against different flow rate values (Figure B.18). It is observed that the setpoint shift leads to the elimination of the delay for all flow rate cases except for the 0.2mL/min (Figure B.18c.2). On the contrary, in the case of mp-MPC no delay is observed (Section 4.4). That could be due to the fact that in the 0.2 mL/min case the delay is significantly higher and affects not only the output elution, but also the speed of the input and the disturbances within the column. Therefore, due to the fact that the P-only controller does not compensate for disturbances (feed composition) its performance is limited when the process operates close to the bounds. Moreover, for the P-only controller an offset is observed for most of the setpoints, whereas the mp-MPC controller is able to reach the setpoints with no offset due to its predictive nature, as well as the disturbance compensation. Similarly to the mp-MPC, the P-controller indicates a cyclic profile for the input for all presented cases (Figure B.18).

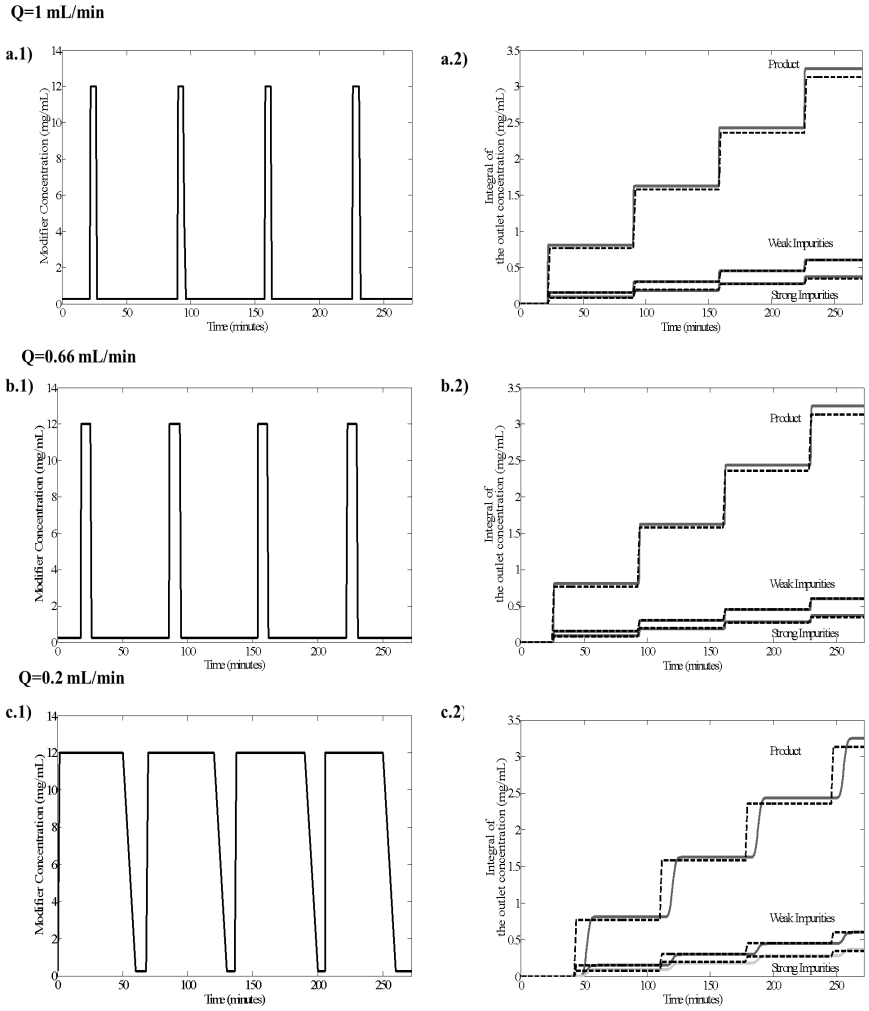

Figure B.18 Results of P-only controller for three flow rate values (Q= 1, 0.66 and 0.2 mL/min).. The column on the left represents the input profile (modifier concentration) indicated by the control that leads to the output profile (integrals of the components concentrations, right column) [using the setpoint shift strategy].

B.4 Investigating the Periodicity in the Control Laws for the Single-Column Case

To elucidate the periodicity in the selection of critical regions, Table B.7 and Table B.8 illustrate the input expressions for the first group of control actions as functions of the problem parameters. Once the cycle has finished, the controller returns to first action and repeats the sequence. The tables include the expressions of the critical regions used by the designed controller. However, it can be observed that the controller does not operate within regions 3, 7 and 8 (omitted from Table B.7 & Table B.8) and that is probably due to the particular conditions chosen in the 'closed-loop' simulation. The general mathematical expression for the input action in this case is given by the following equation:

$$u(\theta) = c_1 \cdot x_1 + c_2 \cdot x_2 + c_3 \cdot x_3 + c_4 \cdot x_4 + c_5 \cdot {C_W^{feed}}_{(t+0)} + c_6 \cdot {C_P^{feed}}_{(t+0)} + c_7 \cdot {C_S^{feed}}_{(t+0)} + c_8 \cdot {C_W^{feed}}_{(t+1)} + c_9 \cdot {C_P^{feed}}_{(t+1)} + c_{10} \cdot {C_S^{feed}}_{(t+1)} + c_{11} \cdot {C_W^{feed}}_{(t+1)} + c_{12} \cdot {C_P^{feed}}_{(t+2)} + c_{13} \cdot {C_S^{feed}}_{(t+2)} + c_{14} \cdot {C_W^{feed}}_{(t+3)} + c_{15} \cdot {C_P^{feed}}_{(t+3)} + c_{16} \cdot {C_S^{feed}}_{(t+3)} + c_{17} \cdot \int {C_W}^{real} + c_{18} \cdot \int {C_P}^{real} + c_{19} \cdot \int {C_S}^{real} + c_{20} \cdot \int {C_W}^{SP} + c_{21} \cdot \int {C_P}^{SP} + c_{22} \cdot \int {C_S}^{SP} + c_{23}$$

Equation B.18 General mathematical expression of the control laws for the single-column case.

where $x_1,\ x_2,\ x_3,\ x_4$ correspond to the states of the state space representation, ${C_W^{feed}}_{(t+i)}$, ${C_P^{feed}}_{(t+i)}$, ${C_S^{feed}}_{(t+i)}$ represent the disturbances over output horizon *i*, $\int {C_W}^{real}$, $\int {C_P}^{real}$, $\int {C_S}^{real}$ are the outputs and their respective setpoints: $\int {C_W}^{SP}$, $\int {C_P}^{SP}$, $\int {C_S}^{SP}$ and $c_{1,\dots}$, c_{23} are the corresponding coefficients as resulted from the solution of the multi-parametric programming problem.

The actions demonstrated here are the same for all flow rate values. The sole difference is that the profile is shifted in time depending on how aggressive the control response should be.

Table B.7 Coefficients c1, …, c11 for the problem parameters in Equation B.18.

Critical Region	c_1	c_2	c_3	c_4	c_5	c_6	c_7	c_8	c_9	c_{10}	c_{11}
9	8.88E-16	4.26E-14	2.84E-14	1.42E-14	-1.11E-16	0	0	3.33E-16	1.78E-15	0	1.11E-16
1	3.210249	47.72769	42.01113	51.42858	0.844549	4.582932	0.521634	0.253192	1.373942	0.156383	-0.0284
5	5.535566	81.65332	71.76297	87.91981	0.913323	4.956133	0.564112	0.609107	3.305311	0.376214	0.304667
9	8.88E-16	4.26E-14	2.84E-14	1.42E-14	-1.11E-16	0	0	3.33E-16	1.78E-15	0	1.11E-16
5	5.535566	81.65332	71.76297	87.91981	0.913323	4.956133	0.564112	0.609107	3.305311	0.376214	0.304667
1	3.210249	47.72769	42.01113	51.42858	0.844549	4.582932	0.521634	0.253192	1.373942	0.156383	-0.0284
2	4.44E-16	7.11E-15	7.11E-15	7.11E-15	0	8.88E-16	0	5.55E-17	0	0	-3.47E-18
4	4.44E-16	7.11E-15	7.11E-15	7.11E-15	0	8.88E-16	0	5.55E-17	0	0	-3.47E-18
6	8.88E-16	4.26E-14	2.84E-14	1.42E-14	-1.11E-16	0	0	3.33E-16	1.78E-15	0	1.11E-16
2	4.44E-16	7.11E-15	7.11E-15	7.11E-15	0	8.88E-16	0	5.55E-17	0	0	-3.47E-18
1	3.210249	47.72769	42.01113	51.42858	0.844549	4.582932	0.521634	0.253192	1.373942	0.156383	-0.0284
9	8.88E-16	4.26E-14	2.84E-14	1.42E-14	-1.11E-16	0	0	3.33E-16	1.78E-15	0	1.11E-16

Table B.8 Coefficients c12, …, c23 for the problem parameters in Equation B.18.

Critical Region	c_{12}	c_{13}	c_{14}	c_{15}	c_{16}	c_{17}	c_{18}	c_{19}	c_{20}	c_{21}	c_{22}	c_{23}
9	4.44E-16	5.55E-17	5.29E-23	4.24E-22	7.94E-23	0	0	1.39E-17	0	0	-1.39E-17	0.2
1	-0.15412	-0.01754	-1.15E-07	-6.26E-07	-7.13E-08	-0.0421	-42.1067	-0.06076	0.042099	42.10666	0.060761	0
5	1.653269	0.188177	1.03E-07	5.60E-07	6.38E-08	-0.04556	-45.6548	-0.06589	0.045565	45.65484	0.065888	-0.18497
9	4.44E-16	5.55E-17	5.29E-23	4.24E-22	7.94E-23	0	0	1.39E-17	0	0	-1.39E-17	0.2
5	1.653269	0.188177	1.03E-07	5.60E-07	6.38E-08	-0.04556	-45.6548	-0.06589	0.045565	45.65484	0.065888	-0.18497
1	-0.15412	-0.01754	-1.15E-07	-6.26E-07	-7.13E-08	-0.0421	-42.1067	-0.06076	0.042099	42.10666	0.060761	0
2	-2.78E-17	0	-2.65E-23	-1.06E-22	-1.32E-23	-6.94E-18	-7.11E-15	0	6.94E-18	7.11E-15	0	12
4	-2.78E-17	0	-2.65E-23	-1.06E-22	-1.32E-23	-6.94E-18	-7.11E-15	0	6.94E-18	7.11E-15	0	0.2
6	4.44E-16	5.55E-17	5.29E-23	4.24E-22	7.94E-23	0	0	1.39E-17	0	0	-1.39E-17	12
2	-2.78E-17	0	-2.65E-23	-1.06E-22	-1.32E-23	-6.94E-18	-7.11E-15	0	6.94E-18	7.11E-15	0	12
1	-0.15412	-0.01754	-1.15E-07	-6.26E-07	-7.13E-08	-0.0421	-42.1067	-0.06076	0.042099	42.10666	0.060761	0
9	4.44E-16	5.55E-17	5.29E-23	4.24E-22	7.94E-23	0	0	1.39E-17	0	0	-1.39E-17	0.2

Appendix C

Upstream Process

** The mathematical model presented in this chapter has been developed and validated by Dr. A. Quiroga (A. Quiroga 2017. "Mathematical modelling and experimental validation for optimisation and control of mammalian cell culture systems", Imperial College London). The model is also presented in the Appendix of Papathanasiou et. al (2017). "Advanced multi-parametric Model Predictive Control (mp- MPC) strategies towards integrated continuous biomanufacturing". Submitted (in Review) to Biotechnology Progress for the Special Issue based on the Berkeley conference on Integrated Continuous Biomanufacturing*

C.1 Model Development & Experimental Validation for the GS-NS0 Cell Culture System

The system presented in Section 4.1.1, is described by an Ordinary and Differential Equation (ODE) model that features the main metabolic interactions and pathways. Following the framework presented by Kiparissides et al. (2011a) the first step is the construction of the equation set, followed by Global Sensitivity Analysis (GSA), Parameter Estimation (PE) and experimental validation. Here we present how these steps are applied for the development of a dynamic model, describing a GS-NS0 cell culture system. The modeling and experimental results presented in this section have been performed by Dr. Ana Quiroga Campano (Imperial College London).

C.1.1 Materials & Methods

The model is validated against a series of experimental data, the methodology for which is described below.

(i) Cell line and culture conditions: GS-NS0 mouse myeloma cells were cultured in triplicate 1L Erlenmeyer flasks (Corning) with 200mL working volume, agitated at 130rpm, incubated at 37^{o}C and 5% CO_2. The media contained Advanced-DMEM X1 (Invitrogen Ltd.), MEM Non-essential amino acids (Sigma–Aldrich) X2, MEM-Essential amino acids (Sigma –Aldrich) X2, GS-Supplement (Sigma-Aldrich) X1, MEM-Vitamins (Gibco) X1, Penicillin/Streptomycin (Gibco) X1, 5 mg/L MSX (Sigma-Aldrich) and 10% Dialyzed Fetal bovine serum (Gibco). The monoclonal antibody produced by the cell is a chimeric IgG4 antibody, cB72.3, which recognizes the Tag-72 tumor marker in colorectal cancer.

(ii) Feeding medium composition: A concentrated medium comprising GS-Supplement (SAFC Biosciences, Sigma-Aldrich, UK) X40 and 0.4M glucose was considered as fed-batch concentrated medium for the development of the optimization and control strategies.

(iii) Detection of viable and dead cells: The number of cells in different states was determined by flow cytometry using Guava ViaCount® assay (Merck Millipore). Every 24 hours 50μL of the culture were extracted and subsequently incubated with 450μL of ViaCount®, for 5 min at room temperature. The data was acquired using a bench top flow cytometer, Guava EasyCyte™ (Merck Millipore) and processed using GuavaSoft software (V 2.6).

(iv) Glucose and toxic metabolites analysis: Extracellular glucose and lactate concentrations were measured using Nova BioProfile 400 Analyser. 700µL samples were collected from each flask on 24h intervals and centrifuged at 800rpm for 5 minutes to remove cells and analyze the supernatant.

(v) Amino Acids Analysis: High-pressure liquid chromatography (HPLC) assay was used to determine the concentration of amino acids in samples collected every 24 hours. The samples were centrifuged for 5 minutes at 800 rpm; the supernatant was filtrated through a 10kDa cut-off ultrafiltration membrane at 22,000 rpm, 4^{o}C for 1 hour and stored at -20^{o}C prior to analysis. Amino acid analysis was performed with Agilent 1260 Infinity Quaternary LC, equipped with RRLC in-line filter, 4.6mm, 0.2um; and ZORBAX Eclipse Plus C18 LC, 4.6 mm, 100 mm, 1.8 µm column (Agilent Technologies).

(vi) Monoclonal antibody production: The product was measured using HPLC techniques. The samples were centrifuged for 5 minutes at 800rpm, the supernatants were filtrated through 0.2µm filter and stored at -20^{o}C prior to analysis. The mAb assay was performed with Agilent 1260 Infinity Quaternary LC, equipped with RRLC in-line filter, 4.6mm, 0.2um; and Bio-Monolith Protein A, 4.95 mm x 5.2 mm column (Agilent Technologies Ltd).

C.1.2 Model Development and Validation

The proposed model describes a simplified metabolic network of GS-NS0 cells, based on four key nutrients and glucose. The model equations as well as the interactions considered in this work are described below.

Cell growth depends on the availability of a wide variety of nutrients, in particular carbohydrates and amino acids. Glucose is the most predominant carbohydrate consumed by mammalian cells and it follows different metabolic pathways: (1) the pentose phosphate pathway (PPP) to produce DNA precursors, (2) the anaerobic pathway or glycolysis to produce energy and (3) the aerobic pathway where glucose is completely oxidized through the tricarboxylic acid (TCA) cycle that also incorporates amino acids to produce energy. Amino acids are considered as the building blocks for the production monoclonal antibodies and proteins that correspond to 70% of the cell composition. In the case of GS-NS0 cells, glutamate is considered as the main source of glutamine used for biosynthesis of cellular structures and product. However, it has been reported that glutamate is not only used as a biosynthesis precursor but also as one of the main energy sources in mammalian cells, contributing more than 50% of the produced ATP (Reitzer et al., 1979, Fitzpatrick et al.,

1993, Altamirano et al., 2001). Cells require glutamate also for glutamine production, proliferation, mAb assembly and energy production. The depletion of glutamate and aspartate are followed by decreased growth rate and two metabolic shifts where arginine and asparagine uptakes are increased. Metabolic shifts have been extensively reported in NS0 and CHO cultures but their mechanism still remains an open challenge (Ma et al., 2009, Luo et al., 2012, Mulukutla et al., 2012, Toussaint et al., 2016).

Table C.1 Model equations for the GS-NS0 cell culture system.

$\frac{dV}{dt} = F_{IN} - F_{OUT}$	(E.1)	$\frac{d(V[GLU])}{dt} = VX_v(Q_{glu,arg} - Q_{x,glu} - Q_{tca,glu}) + F_{IN}[GLU]_{IN} - F_{OUT}[GLU]$	(E.12)
$\frac{dVX_v}{dt} = VX_v(\mu - \mu_d) - F_{OUT}X_V$	(E.2)	$Q_{glu,arg} = C_{arg}Q_{tca,glu}$	(E.13)
$\frac{dVX_d}{dt} = VX_v\mu_d - F_{OUT}X_d$	(E.3)	$Q_{x,glu} = \frac{\mu}{Y_{x,glu}}$	(E.14)
$\mu = \mu_{max}\left(\frac{[GLC]}{K_{glc}+[GLC]}\right)\left(\frac{[GLU]}{K_{glu}+[GLU]} + \frac{[ARG]}{K_{arg}+[ARG]}\right)\left(\frac{[ASP]}{K_{asp}+[ASP]} + \frac{[ASN]}{K_{asn}+[ASN]}\right)$	(E.4)	$Q_{tca,glu} = \frac{\mu}{Y_{tca,glu}} + m_{tca,glu}$	(E.15)
$\mu_d = \mu_{d,max}\left(\frac{K_{glc,lim}}{K_{glc,lim}+[GLC]} + \frac{K_{glu,lim}}{K_{glu,lim}+[GLU]} + \frac{K_{asp,lim}}{K_{asp,lim}+[ASP]} + \frac{K_{arg,lim}}{K_{arg,lim}+[ARG]} + \frac{K_{asn,lim}}{K_{asn,lim}+[ASN]}\right)$	(E.5)	$\frac{d(V[ARG])}{dt} = -VX_v(Q_{glu,arg} + Q_{x,arg}) + F_{IN}[ARG]_{IN} - F_{OUT}[ARG]$	(E.16)
$\frac{d(V[GLC])}{dt} = -VX_v(Q_{x,glc} + Q_{glyc,glc} + Q_{tca,glc}) + F_{IN}[GLC]_{IN} - F_{OUT}[GLC]$	(E.6)	$\frac{d(V[ASP])}{dt} = VX_v(Q_{asp,asn} - Q_{x,asp} + Q_{tca,asp}) + F_{IN}[ASP]_{IN} - F_{OUT}[ASP]$	(E.17)
$Q_{x,glc} = \frac{\mu}{Y_{x,glc}}$	(E.7)	$Q_{asp,asn} = C_{asn}Q_{tca,glu}$	(E.18)
$Q_{glyc,glc} = (1 - Q_{MET})\left(\frac{\mu}{Y_{glyc,glc}} + m_{glyc,glc}\right)$	(E.8)	$Q_{x,asp} = \frac{\mu}{Y_{x,asp}}$	(E.19)
$Q_{MET} = \frac{K_{MET}}{K_{MET}+[GLU]}$	(E.9)	$Q_{tca,asp} = C_{asp}Q_{tca,glu}$	(E.20)
$Q_{tca,glc} = \frac{\mu}{Y_{tca,glc}} + m_{tca,glc}$	(E.10)	$\frac{d(V[ASN])}{dt} = -VX_v(Q_{asp,asn} + Q_{x,asn}) + F_{IN}[ASN]_{IN} - F_{OUT}[ASN]$	(E.21)
$\frac{d(V[LAC])}{dt} = VX_v 2 * Q_{gly,glc} - F_{OUT}[LAC]$	(E.11)	$\frac{d(V[mAb])}{dt} = VX_v m_{mAb,x}$	(E.22)

The suggested model assumes that arginine and asparagine are used to supply glutamate and aspartate, respectively, as well as for cell proliferation and survival. Cell growth rate depends on the availability of nutrients in the culture. Namely, the depletion of glutamate and/or aspartate leads to decrease in the growth rate, while cell growth is diminished with the exhaustion of either glutamate/arginine or aspartate/asparagine (Table C.1, E14 & E19). In addition, cell starvation (exhaustion of nutrients) produces cellular stress and activates apoptosis pathways and subsequently cell death. The independent effect of each nutrient has been depicted as an additive effect (Table C.1).

The specific glucose consumption for biomass production ($Q_{x,glc}$) is described by biomass yield from glucose ($Y_{x,glc}$), that is modeled as a function of the growth rate (μ) and considers the consumption of glucose for biosynthesis of multiple structural components of the cell, including non-essential amino acids, lipids, nucleotides and DNA. Furthermore, $Q_{glyc,glc}$ corresponds to the specific consumption of glucose per cell for the production of energy through glycolysis, while Q_{MET} depicts the effect of glutamate concentration in glucose uptake for the production of energy trough glycolysis (Kiparissides et al., 2015). The specific consumption of glucose per cell to produce energy through the TCA cycle is described by $Q_{tca,glc.}$ Moreover the specific consumption of amino acids is linked to both biomass ($Q_{x,glu}$) and energy ($Q_{tca,glu}$) production. The balance for the mAb is described by a non-growth associated/maintenance term that ($m_{mAb,xv}$) that describes the constant production of mAb by viable cells.

The model consists of 22 differential and algebraic equations, 24 variables and 27 parameters. The model is simulated in gPROMS ModelBuilder ® v.4.2.0. Following the framework presented by Kiparissides et al. (2011a), the model is subjected to sensitivity analysis for the identification of the significant parameter set.

C.1.3 Global Sensitivity Analysis (GSA)

Following the formulation of the mathematical equations presented above, the model is subjected to Global Sensitivity Analysis (GSA). GSA (Appendix A) is the mathematical procedure according to which the model parameters are simultaneously excited, within the range of interest, and their effect on the model outputs is monitored. The procedure allows the identification of the factors that contribute most to output variability (Kontoravdi et al., 2005a, Kiparissides et al., 2009, Kiparissides et al., 2011a). Such procedures enable the examination of the global parameter space, cope well with non-linearities, providing a complete set of results that demonstrates both the sensitivity of the model to the uncertainty

of the parameter values, as well as the effect of one model parameter to the other (Li et al., 2002, Kiparissides et al., 2011a).

Here we apply RS-HDMR for the analysis of 27 parameters. The parameters are allowed to vary ± 50% from their base case value and data is collected every 24 hours (i.e. at 24, 48, 72, 96, 120 and 144 h). This strategy is decided in order to be in line with the collection of experimental data and covers all three phases of the cell culture (lag, growth/exponential and death phase) (Kiparissides et al., 2015). In particular, the chosen intervals correspond to the early exponential growth phase (up to the 24^{th} hour) the exponential growth (48^{th} hour), aspartate and glutamate exhaustion (approximately at the 72^{nd} hour) and the beginning of the stationary phase, the end of the stationary phase (96^{th} hour) and the death phase (120^{th} – 140^{th} hour). The sampling intervals are chosen based on the process dynamics as well as the mathematical complexity of the studied model. Here intervals of 1-hour frequency are chosen, allowing the solver to converge in a smoother manner. The data used for the sensitivity assessment, however, is collected at the time points mentioned above (every 24 hours), in order to be in accordance with the experimental sampling.

The 27 parameters (Table C.2) are studied all together and assessed choosing a 10% significance threshold for the sensitivity index for viable cells and volumetric mAb concentration. The latter are chosen as two of the most representative indicators of culture efficiency (Bibila and Robinson, 1995). Indices higher than 10% indicate that the respective parameters can be considered as “significant”, while any index <10% renders the parameter “non-significant”. The 10% threshold corresponds to the minimum experimental error (Kontoravdi et al., 2005a, Kiparissides et al., 2009, Kiparissides et al., 2011b). The GSA results indicate 6 significant parameters related either to viable cells and/or monoclonal antibody concentration (Figure C.1).

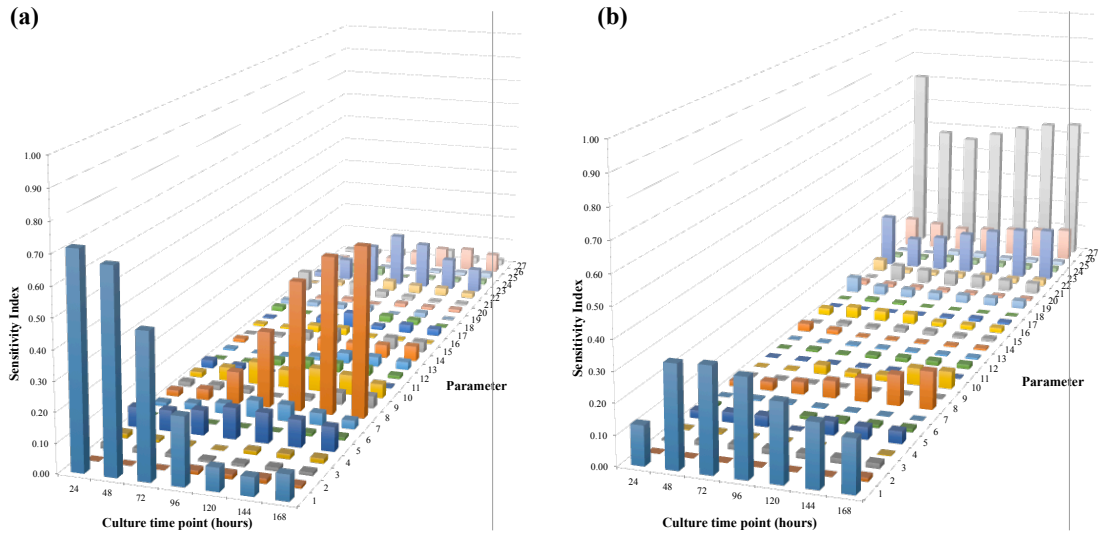

Figure C.1 Sensitivity indices for all 27 parameters at all simulation times for: (a) viable cells and (b) mAb concentration. The parameter indices (1-27) correspond to the numbering used in Table C.2.

Figures C.2 & C.3 illustrate the individual sensitivity indices for all 27 parameters for the two examined differential variables. In particular, it is observed (Figures C.2a & C.3a) that at the early culture stages (24 h – 72 h) and until the culture enters death phase (approximately after the 96th hour) the maximum theoretical growth rate (μ_{max}) is the most significant parameter for both monitored variables (Figure C.1). This is in accordance with the underlying biology as especially during the exponential phase, the cells experience maximum growth. Conversely, after the 96th hour and until the end of the culture, the maximum theoretical death rate ($\mu_{d,max}$) becomes significant (Figures C.2c & C.3b). Interestingly, the significance of these two parameters increases in an inverse fashion. More specifically, as the significance of μ_{max} decreases over time, $\mu_{d,max}$ becomes more significant. This finding agrees with the principles of such culture systems, where the cells experience growth until approximately the 90th hour of the culture, while cell viability declines past this time point (Kontoravdi et al., 2005a, Kiparissides et al., 2009).

Another parameter significant for both examined entities is the requirement of glutamate for the production of energy for maintenance purposes ($m_{tca,glu}$) (Figure C.2d & C.3c) that is participating in Eq. 15 (Table C.1) for the calculation of the specific consumption of glutamate. More specifically, in the case of viable cells (Figure C.2d), the parameter starts becoming significant at the 72nd hour that corresponds to the beginning of the stationary phase and the exhaustion of glutamate, while the index reaches its highest value (20%) at the end of the stationary phase (96 h). For the case of the volumetric monoclonal antibody concentration

(Figure C.3), the significance of $m_{tca,glu}$ varies from 10% - 20% throughout the culture period. The latter is expected, as glutamate is one of the key amino acids considered in this model (Table C.1) and is essential for basic cell functions, involving the maintenance of the homeostasis in the cell and mAb assembling, and consequently mAb production.

The saturation Monod constant for growth on aspartate (K_{asp}) (Figure C.2b) is the fourth and last significant parameter in the case of viable cell concentration (Eq. 4, Table C.1). In particular, the parameter becomes significant on the 96th and 120th hour of culture that corresponds to the beginning of death stage of the culture and aspartate depletion. Although, aspartate is a non-essential amino acid, and can be derived from asparagine, it affects the cell metabolism and its depletion reduces the growth rate.

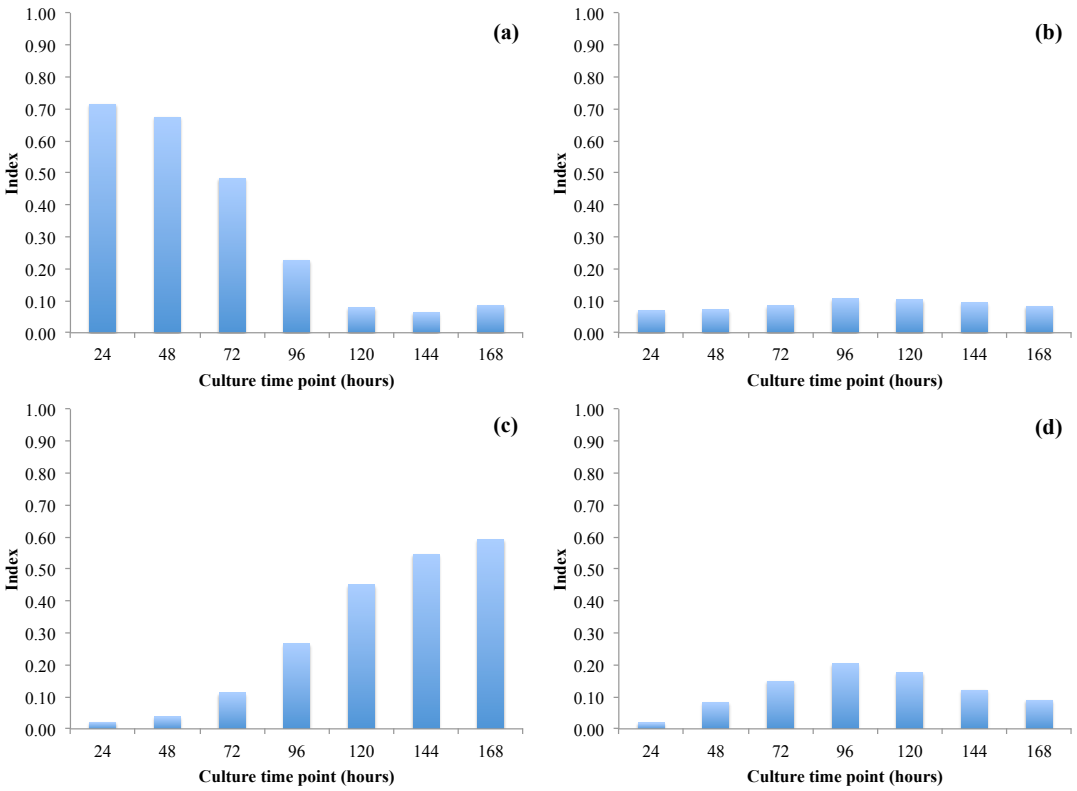

Figure C.2 Results of sensitivity analysis for viable cells for: (a) μ_{max} , (b) K_{asp} , (c) $\mu_{d,max}$ and (d) $M_{tac,glu}$.

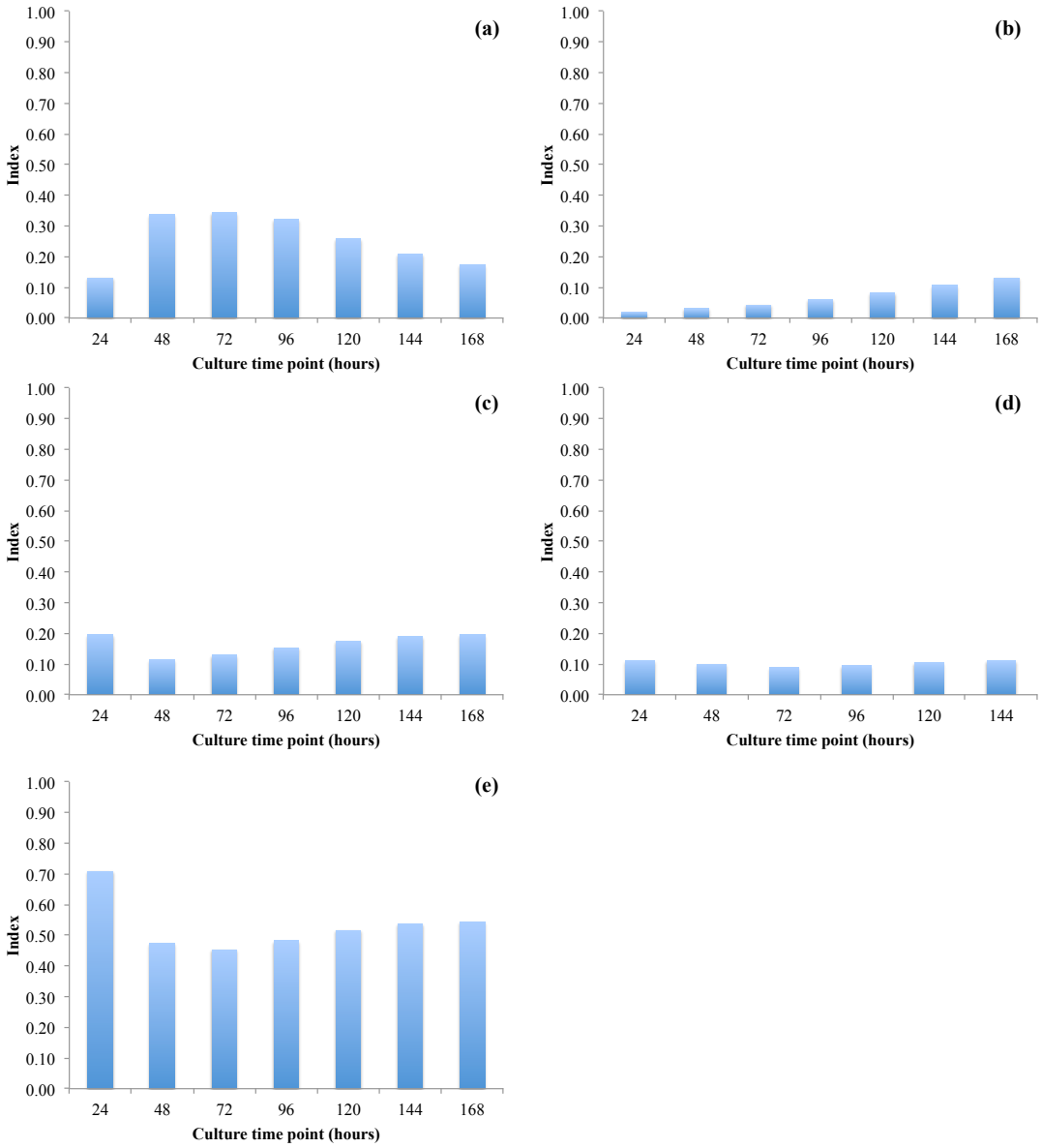

Figure C.3 Results of sensitivity analysis for mAb concentration for: (a) μ_{max} , (b) $\mu_{d,max}$, (c) $M_{tac,glu}$, (d) C_{arg} and (e) $m_{mab,x}$

For the case of the volumetric monoclonal antibody concentration the sensitivity analysis resulted into two more significant parameters, namely C_{arg} and $m_{mab,x}$ (Figure C.3d & e). The former participates in Eq.13 (Table C.1) and corresponds to the consumption of arginine to produce energy. The parameter becomes significant towards the end of the culture period (120 h – 144 h) (Figure C.3d) that translates into the culture death stage, where almost all amino acids are depleted. At this point, glutamate has been depleted (72 h) and the cells use arginine as the source to produce glutamate, essential for mAb assembly. Consequently, the depletion of arginine as well (120 h) renders parameters related to its consumption significant at this time point. Lastly, the production of mAb per viable cells per hour ($m_{mab,x}$) is

significant throughout the culture period (Figure C.3e) as cells produce the antibody as part of their normal metabolic functions throughout the culture time.

C.1.4 Parameter Estimation (PE)

The 6 significant parameters discussed in section C.1.3 are estimated using the Minimum Likelihood Estimation method available in gPROMS ModelBuilder® v.4.2.0, considering a constant relative variance of 25% that captures the variation amongst for 4 independent experimental replicates. Table C.2 illustrates the initial and final values of the six significant parameters, as well as the 95% confidence intervals. For most of the parameters the t-values showed 95% accuracy apart from K_{asp} and μ_{max} that presented t-values (0.17 and 1.2 respectively) lower than the reference (1.69), indicating that more experimental data is required for their estimation. However, the Lack of Fit test showed that the weighted residual (40.5191) is smaller than the Chi-squared value (48.6024) indicating that the model can adequately represent the physical system.

Table C.2 Initial and final values of re-estimated parameters.

Parameter	Initial Guess	Final Value	95% Confidence Interval	Units
$\boldsymbol{\mu_{max}}$	0.021	0.0229552	1.201	h^{-1}
$\boldsymbol{K_{asp}}$	0.5	0.465278	0.1764	mM
$\boldsymbol{\mu_{d,max}}$	0.0033	0.0033736	3.694	h^{-1}
$\boldsymbol{M_{tca,glu}}$	2.8E-11	2.54E-11	2.386	mmol/Cell/h
$\boldsymbol{C_{arg}}$	0.4	0.33818	3.156	-
$\boldsymbol{m_{mab,x}}$	7.05E-10	6.59E-10	3.295	mg/Cell/g

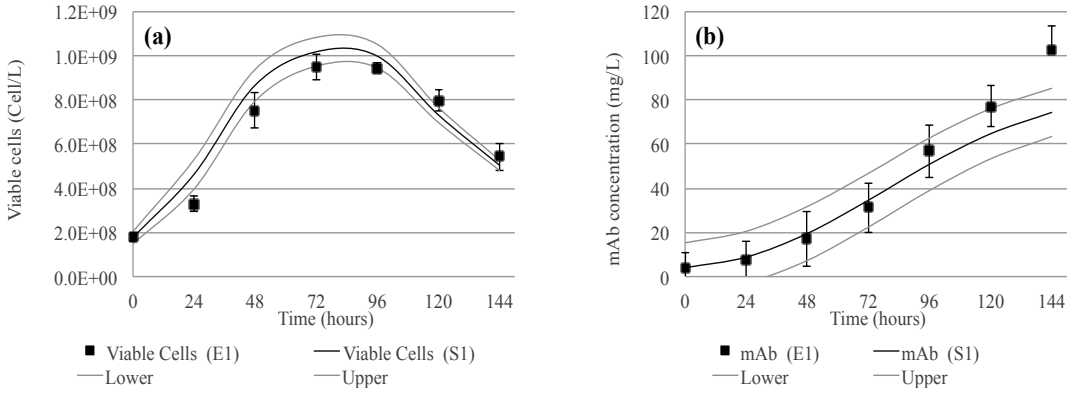

Figure C.4 Parameter estimation results for: (a) viable cells and (b) mAb concentration. The graphs demonstrate the model simulation output (continuous black line), the average experimental value of the variable with the respective standard deviation (square points) and the 95% confidence interval (lower and upper with grey lines).

Figure C.4 & C.5 correspond to the experimental data (square points) used for the parameter estimation in comparison to the process model simulation results (continuous black line) using the same initial conditions, after parameter estimation. The grey lines shown on the graphs depict the 95% confidence intervals for: viable cells (Figure C.4a), monoclonal antibody concentration (Figure C.4b), the 5 nutrients (Figure C.5a-e) considered here and lactate (Figure C.5f). For most of the monitored variables, the experimental data points with the corresponding standard deviation and/or the model simulation lie within the 95% confidence interval, indicating that the designed model can be considered reliable. An exception to this is the profile of glucose (Figure C.5a), where the model fails to capture the trend indicated by the experimental data. In this case, it would be advised to consider glucose in the sensitivity analysis and re-perform the estimation of the parameters. However, the focus of this work is the development of a control scheme to maximize the monoclonal antibody concentration. Therefore, the analysis is focused on the output variable of interest, while it is demonstrated that the model is able to adequately capture the main events taking place in the cell culture system. Of course one could design a more detailed model and/or re-perform the analysis to conclude to more accurate simulation results for all presented variables, however there is also a trade-off between model rigor and computational demand that needs to be considered. Consequently, having successfully assessed the model also using the Lack of Fit test, it is concluded that the presented model can be used to efficiently describe the effect of the manipulated inputs (feed composition) on the output variable of interest (volumetric monoclonal antibody concentration) and therefore it can be used for control studies. As discussed in Chapter 6, current and future work look into the development of a similar control concept based on a more sophisticated process model based on energy metabolism (Quiroga, 2017).

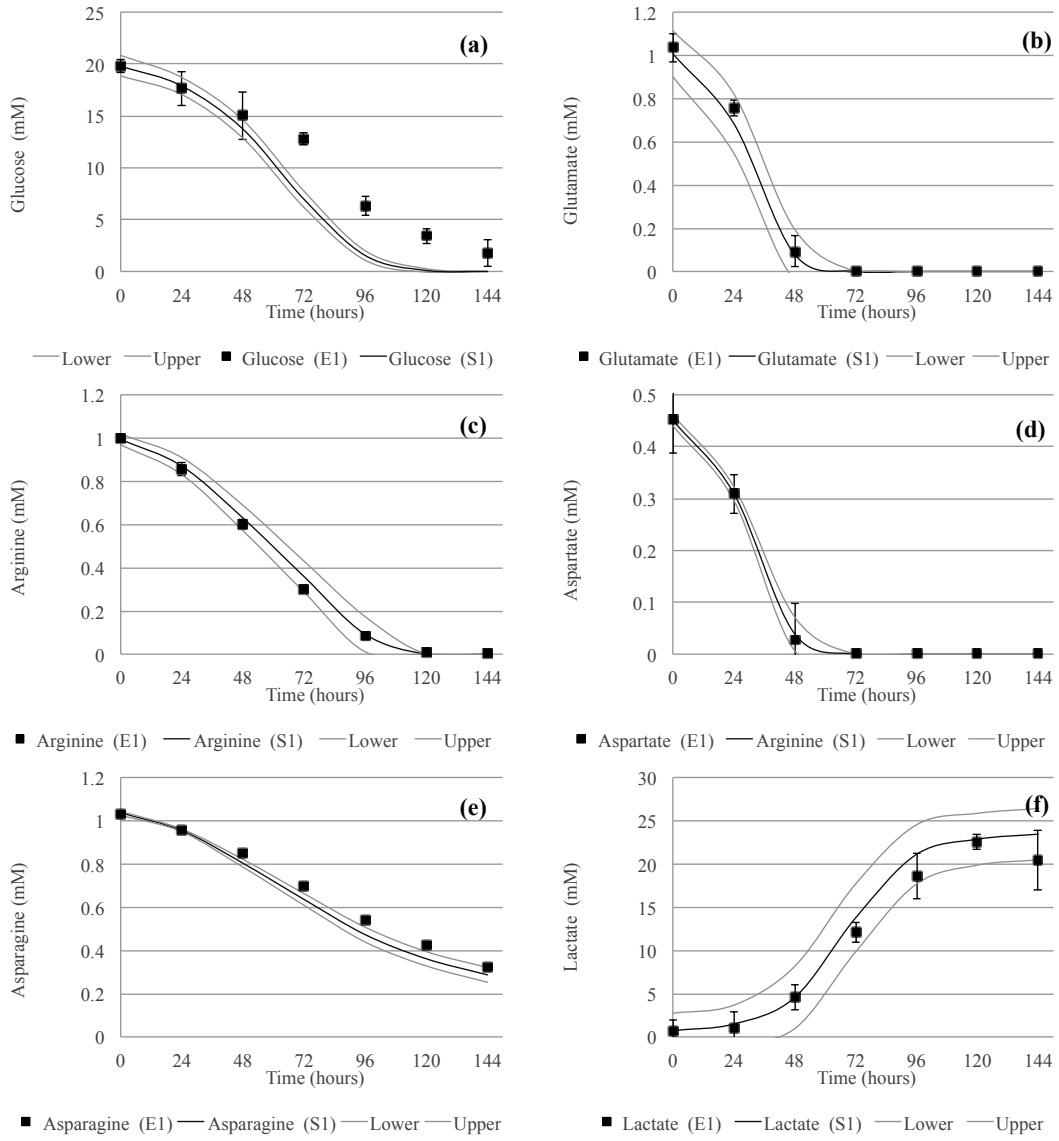

Figure C.5 Parameter estimation results for: (a) glucose and (b) glutamate, (c) arginine, (d) aspartate, (e) asparagine and (d) lactate. The graphs demonstrate the model simulation output (continuous black line), the average experimental value (square points) of the variable with the respective standard deviation and the 95% confidence interval (lower and upper with grey lines).

Table C.3 Results of the GSA procedure and the final parameter values. (*) corresponds to the significant parameters that are re-estimated using experimental data

Order number	Parameter	Value	Units	Order number	Parameter	Value	Units
1	μ^*_{max}	0.0229552	h^{-1}	15	$Y_{glyc,glc}$	9.00E+07	Cell/mmol
2	K_{met}	0.09	mM	16	$M_{glyc,glc}$	2.00E-11	mmol/Cell/h
3	K_{glc}	3.5	mM	*17*	$Y_{tca,glc}$	3.00E+08	Cell/mmol
4	K_{glu}	0.5	mM	18	$M_{tca,glc}$	2.00E-11	mmol/Cell/h
5	K^*_{asp}	0.465278	mM	19	$Y_{tca,lac}$	2.00E+07	Cell/mmol
6	K_{arg}	0.001	mM	20	$M_{tca,lac}$	2.00E-11	mmol/Cell/h
7	K_{asn}	0.001	mM	21	$Y_{x,glu}$	9.25E+09	Cell/mmol
8	$\mu^*_{d,max}$	0.0033736	h^{-1}	22	$Y_{tca,glu}$	4.00E+09	Cell/mmol
9	$K_{lim,glc}$	3.5	mM	23	$M^*_{tca,glu}$	2.54E-11	mmol/Cell/h
10	$K_{lim,glu}$	0.5	mM	24	C_{asp}	0.6	-
11	$K_{lim,asp}$	0.5	mM	25	C_{asn}	0.2	-
12	$K_{lim,arg}$	0.5	mM	26	C^*_{arg}	0.33818	-
13	$K_{lim,asn}$	0.5	mM	27	$m^*_{mab,x}$	6.59E-10	mg/Cell h
14	$Y_{x,glc}$	1.00E+09	Cell/mmol				

C.1.5 Model validation

The model validation is performed comparing the model simulation results to the experimental data obtained from 3 experiments with 3 independent replicates each, using 3 different initial cell densities. Table C.4 illustrates the initial conditions used for the experiment and/or simulation results.

Table C.4 Experimental conditions and initial conditions used for the simulation of the 3 scenarios.

Variable	Scenario1	Scenario2	Scenario3	Units
Viable Cells (E2)	2,76E+08	3,49E+08	4,43E+08	Cells/L
Dead Cells (E2)	8,12E+07	6,72E+07	1,76E+08	Cells/L
Total Cells (E2)	3,57E+08	4,17E+08	6,19E+08	Cells/L
Glucose (E2)	19,20	19,13	21,33	mM
Lactate (E2)	0,00	0,00	0,00	mM
Glutamate (E2)	1,04	1,03	1,04	mM
Arginine (E2)	1,02	1,02	1,03	mM
Aspartate (E2)	0,45	0,45	0,45	mM
Asparagine (E2)	1,03	1,03	1,04	mM
mAb (E2)	0,00	0,00	0,00	mg/L

Viable & dead cell concentration

It is observed (Figure C.6a) that the suggested model efficiently captures the culture entry to exponential phase (post 24th hour) after a short lag period. In addition, the peak in the viable cell concentration is also predicted as the results from the model simulation fall within the range of the reported experimental error. The population of dead cells is also accurately described by the process model.

Monoclonal antibody concentration

In the case of the mAb concentration, a quite good agreement between the model simulation and the experimental data is observed (Figure C.6d). However, a significant discrepancy is observed from 120 to 144 hours, where the model under predicts antibody concentration and the predicted value does not lie within the experimental error. At the end of the culture, when the growth is inhibited and the death process is more prominent, the unspecific release of

product increases, and this phenomenon is not described in the model equations. It has been documented that apoptosis triggers the Golgi apparatus fragmentation (Mukherjee et al., 2007) and there is a passive release of the product in the culture medium (Al-Rubeai and Emery, 1990), to capture this phenomenon, a term should be included a term that accounts for mAb release during dead phase.

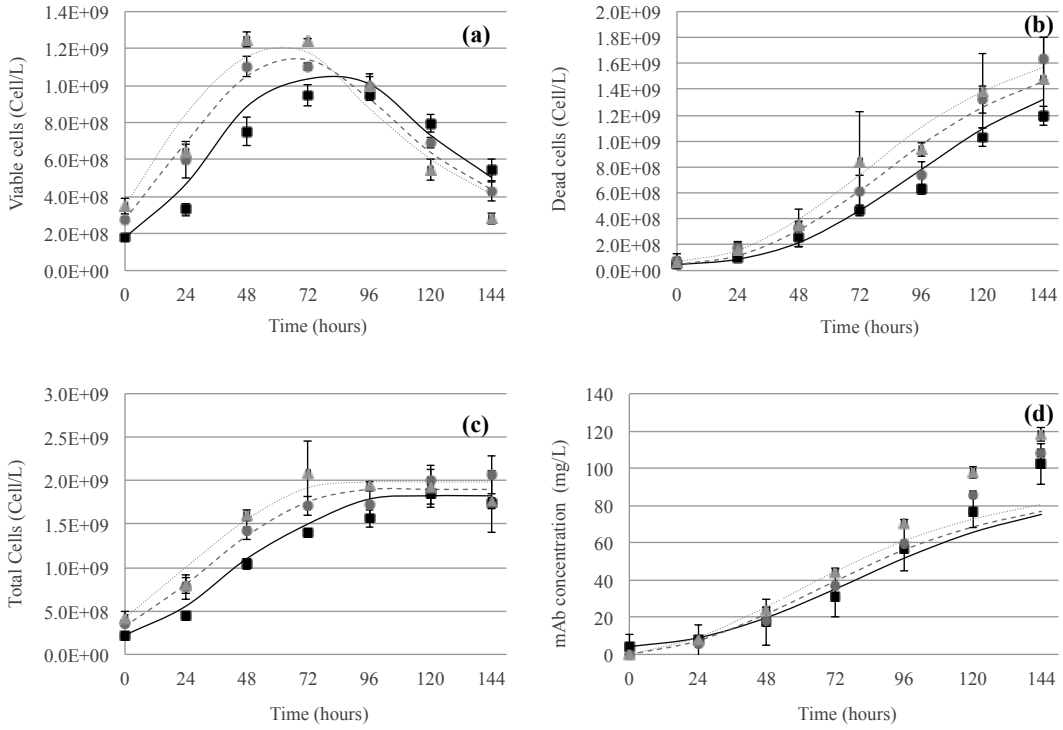

Figure C.6 Model validation: comparison of 3 different simulation results (grey, black and grey dotted lines) against 3 different experimental data sets (points) for: populations of (a) viable, (b) dead and (c) total cells and (d) the concentrations of mAb.

Glucose uptake and lactate production

Although the initial decrease in the glucose concentration (Figure C.7a) is efficiently captured, the model does not manage to describe the experimentally defined plateau reached after the 96th hour. Nevertheless, as mentioned earlier, for the purposes of this work, this model is designed as the basis for development of a control concept for the maximization of the volumetric antibody concentration. Therefore, the description of the effect of the model inputs to the outputs is of outmost importance. Consequently, this discrepancy in the glucose profile can be accepted, as long as the behavior of the output variable of interest is efficiently described. On the other hand, lactate production is adequately described (Figure C.7f).

Glutamate, arginine, asparagine and aspartate uptake

The model captures efficiently the depletion of both glutamate and aspartate at the 48th hour of the culture (Figure C.7b & d). Similarly, the profiles of asparagine and arginine (Figure C.7c & e) are also characterized by good agreement between the simulation results and the experimental data. It should be underlined that amino acids are the building blocks for the production of mAb (output variable). Consequently, accurate monitoring of those components is of high importance, particularly in cases where they are exhausted (e.g. batch cultures).

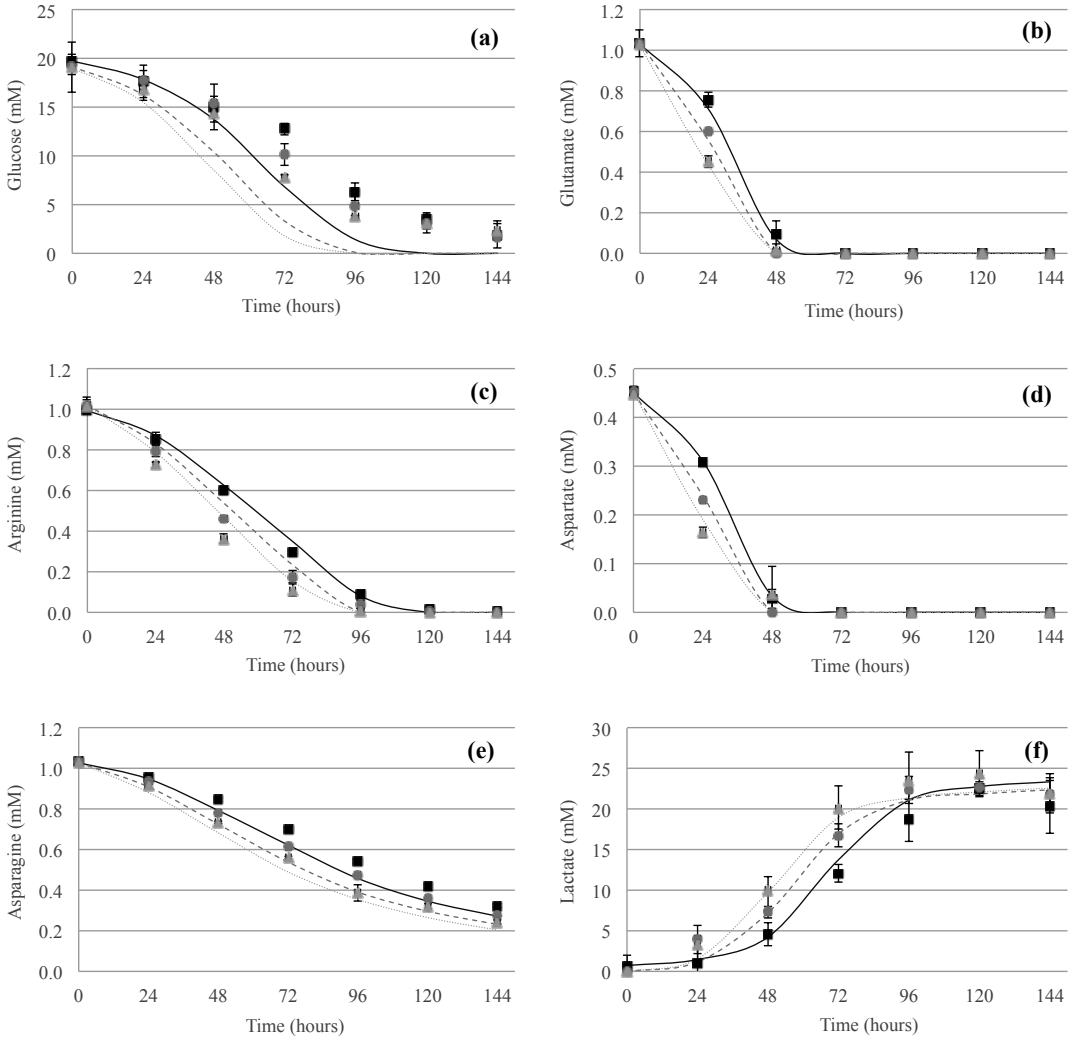

Figure C.7 Model validation: comparison of 3 different simulation results (grey, black and grey dotted lines) against 3 different experimental data sets (points) for: (a) glucose, (b) glutamate, (c) arginine, (d) aspartate, (e) asparagine and (f) lactate.

C.2 Testing the Controller under Disturbance (*no sampling*)

The 2-hour interval controller designed in section 6.4 is validated in-silico, in 'closed-loop' fashion against the process model, considering a periodic disturbance, where a total of 0.5 mL of the culture volume is removed (Figure C.9) in pulses of 1 min. For this case study no sampling is considered. The validation is facilitated using the gO:MATLAB interface that allows seamless data exchange between MATLAB® (control actions) and gPROMS® ModelBuilder (process model). We use the concentration of antibody as resulted from the optimization studies (Section 6.3) as setpoint and we simulate model for 168 hours (7 days). The behaviour of the controller is compared to the profiles of the batch system, where the same disturbance profile is applied.

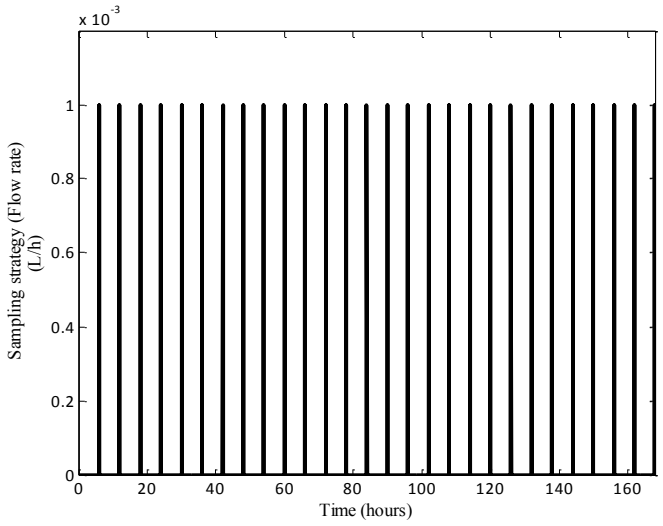

Figure C.8 Sampling considered as disturbance for the controller validation.

It is observed that the designed controller inherently suggests fed-batch feeding (Figure C.9a), while the first pulse is introduced 8 hours after the beginning of the culture and the feeding is intensified only after the 20th hour. Similarly to the results presented earlier, the controller intensifies the feeding after the 20th hour of culture and terminates it on the 76th hour, contrary to the results presented in Chapter 6 where the controller continued the feeding until the 168th hour. This difference observed in the controller behaviour could be attributed to the sampling that significantly reduces the culture volume in the case presented above (Section 6.4). Moreover, also in this case the suggested input is introduced based on the culture needs. More specifically, in the beginning of the culture, where nutrient concentrations are high, the pulses are scarcer and they are intensified later on, when nutrients start to be depleted (Figure C.11). Despite the disturbance introduced to the system and the absence of sampling that would compensate for the increase in the culture volume, the controller manages to maintain the

latter within the permitted range (± 10% from the starting value) (Figure C.9b). Furthermore, the feeding strategy suggested by the controller (Figure C.9a) in this case results in improved culture productivity and higher cell population (Figure C.10) compared to the batch system.

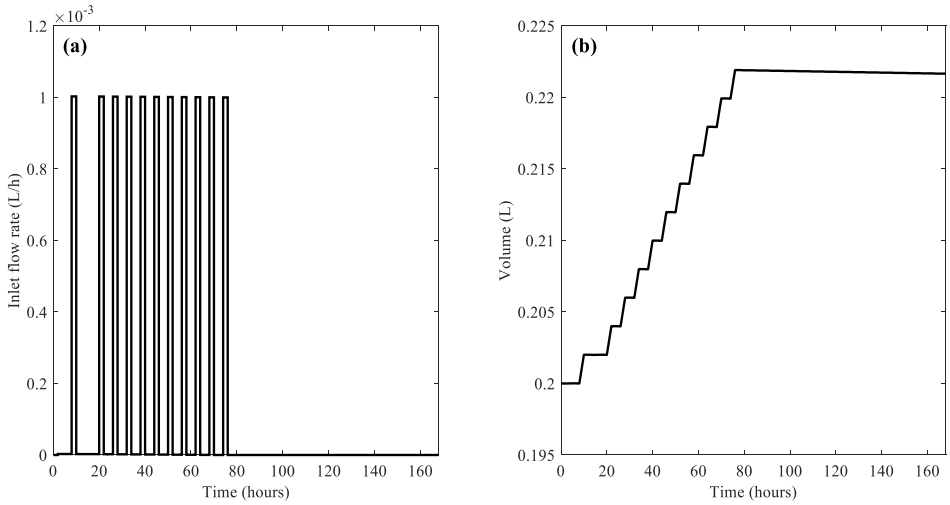

Figure C.9 (a) Control input (inlet feed flow rate) as designed by the presented controller, (b) Evolution of culture volume under the suggested feeding strategy.

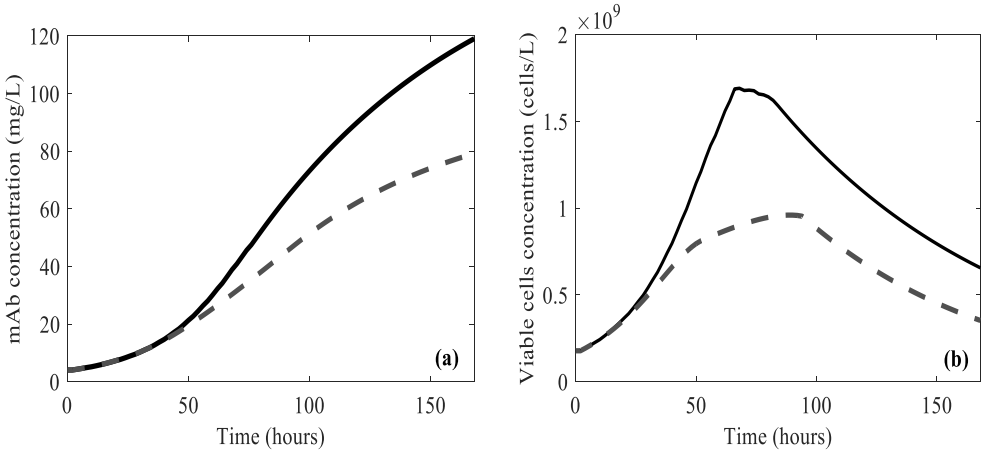

Figure C.10 Comparison between the fed-batch (continuous black line) and the batch (dotted grey line) system for: (a) the mAb concentration and (b) the population of viable cells over 168 hours of culture.

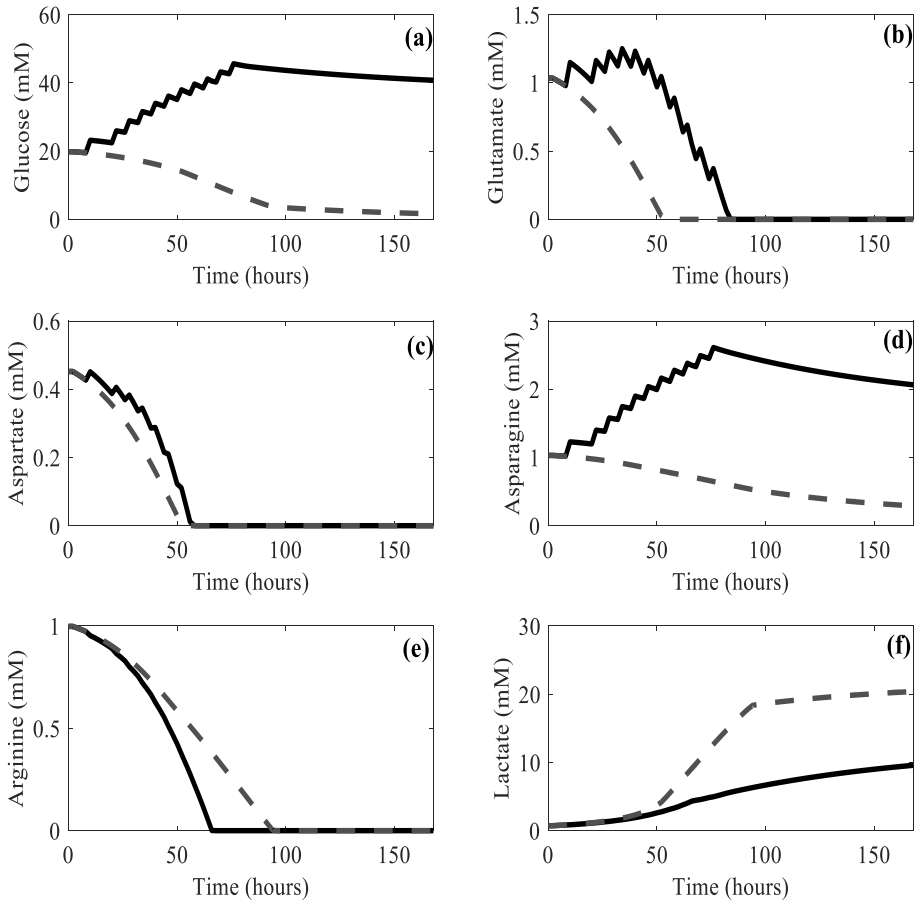

Figure C.11 Comparison between the fed-batch (continuous black line) and the batch (dotted grey line) system for the concentrations of: (a) glucose, (b) glutamate, (c) aspartate, (d) asparagine, (e) arginine and (f) lactate over 168 hours of culture.

Appendix D

Towards an Integrated Biomanufacturing Process

D.1 Model Integration

As mentioned in Chapter 7, the vision of this work is the development of a computational platform that will allow the investigation, as well as the optimization of the integrated, continuous bioprocess (Figure D.1). However, for this to be realized, all process parts need to be modeled under the same platform. The latter will allow seamless communication of the process models and therefore facilitate not only their integration, but also further optimization and control studies. On-going and future work is focusing on the in silico integration of the 3 main process units: (i) the bioreactor system as presented in Chapter 6, (ii) a capture step and (iii) the twin-column MCSGP process as discussed in Appendix B. The project on process integration and control is being performed in collaboration with the Morbidelli Group (ETH Zürich), Dr. Ana Quiroga Campano (Imperial College London) and Ms Montaña Elviro Perez (University of Salamanca). Here we demonstrate preliminary results on:

(i) The upstream system, where terms for the formation of aggregates and fragments are included in the process model and

(ii) The capture step, where we model the process described by Steinebach et al. (2016a) in gPROMS® ModelBuilder v.4.2.0.

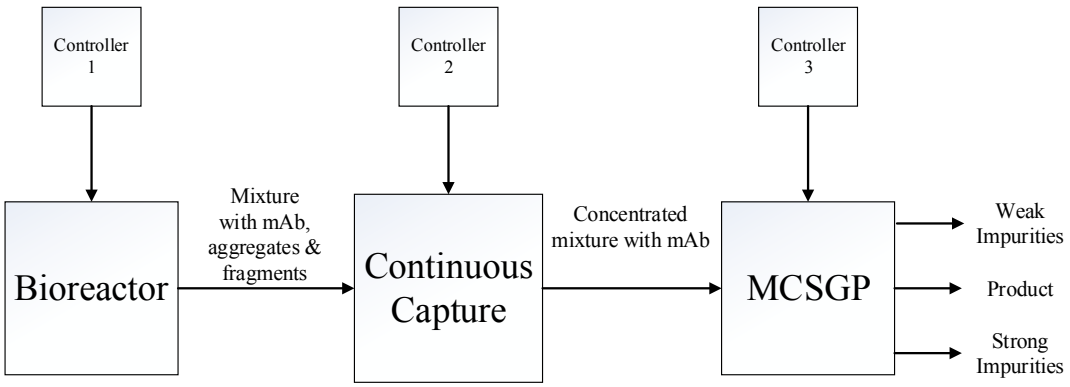

Figure D.1 Conceptual design of the integrated bioprocess.

D.1.6 Upstream Model: Modeling the formation of aggregates and fragments

The model described in Appendix C does not consider the formation of aggregates and fragments during the culture. However, the latter are essential for the in silico integration of the bioprocess as they represent the impurities present in the mixture that is fed in the downstream purification processes. Here we assume that the formation of aggregates and fragments is taking place following second and first order kinetics respectively (Equation D.1 and Equation D.2) (Vázquez-Rey and Lang, 2011, Vlasak and Ionescu, 2011, Arosio et al., 2012). Therefore, the equation set presented in Appendix C is modified to include the following two equations:

$$\frac{d[V[Agg]]}{dt} = k_{agg} V [mAb]^2$$

Equation D.1 Aggregates formation following second order kinetics.

$$\frac{d[V[Frg]]}{dt} = k_{frg} V [mAb]$$

Equation D.2 Fragments formation following first order kinetics.

As a result, the equation describing the antibody is modified accordingly to account for the formation of the impurities (Equation D.3).

$$\frac{d[V[mAb]]}{dt} = V X_v m_{mAb,X} - k_{agg} V [mAb]^2 - k_{frg} V [mAb]$$

Equation D.3 Monoclonal antibody concentration.

For the preliminary simulations, the values of the kinetic constants for the formation of aggregates and fragments are extrapolated based on the results presented by Müller-Späth et al. (2010a) (Table D.1). The model is simulated in open loop using the initial conditions and parameter values as presented in Appendix C and the results for the three examined entities are presented in Figure D.2. For the simulation we assume that no aggregates and/or fragments are present in the culture at time zero.

Table D.1 Initial parameter values used for the kinetic constants of aggregates and fragments based on the results presented by

Parameter	Value	Units
k_{agg}	$1.339 \cdot 10^{-7}$	$Lmg^{-1}h^{-1}$
k_{frg}	$1.029 \cdot 10^{-3}$	h^{-1}

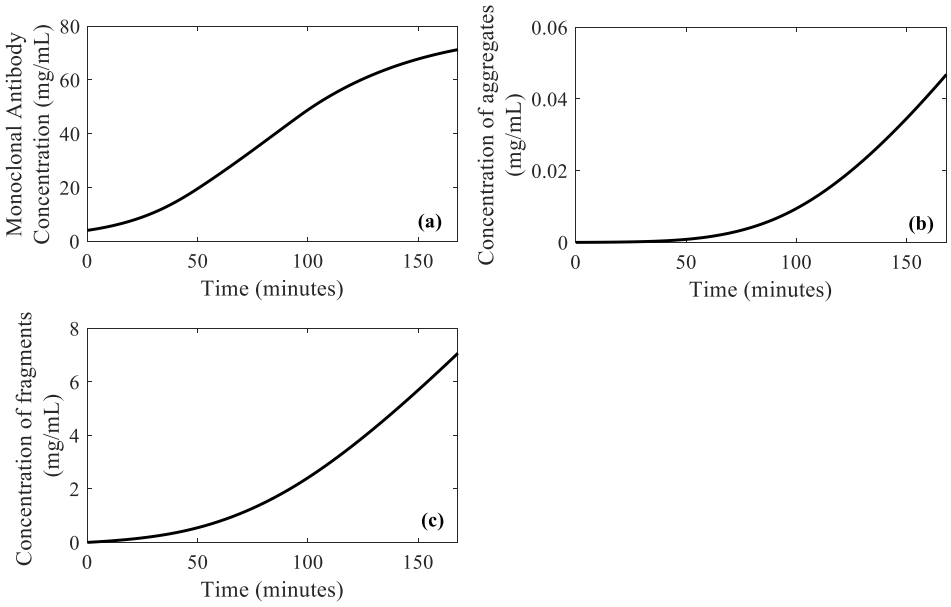

Figure D.2 Profiles of the: (a) monoclonal antibody concentration, (b) aggregates and (c) fragments under open loop model simulation.

It can be observed that the dynamics of the newly introduced model entities are in line with data presented in the open literature However, for completion, following the framework presented by (Kiparissides et al., 2011a) the next step is the execution of tailor-made experiments for the exact determination of the aforementioned kinetic parameters and the validation of the new model.

D.1.7 Capture step: simulation of the process model

For the capture step we use the model described by Steinebach et al. (2016a). The setup considers the continuous operation of two chromatographic columns based on Protein A chromatography. Figure D.3 illustrates the steps followed during the operation of the capture process presented by Steinebach et al. (2016a). In particular, the two columns start interconnected and feed is introduced to the column in the left position aiming to exceed its dynamic binding capacity. This is followed by a second interconnected step, where the column on the left is washed and any unbound protein is transferred to the column on the right position, mixed with additional feed (cell culture harvest). During the last step, the column in the left position is regenerated, while the second one is loaded in batch mode.

The process model describing the above process is based on a lumped mass-transfer model coupled with a heterogeneous binding model. It considers PDAEs and is simulated in gPROMS® ModelBuilder v.4.2.0, using a first order backward finite discretization method with 50 collocation points. The results have been favorably compared to experimental results

provided by Steinebach et al. (2016a) and the Morbidelli Group (ETH Zürich). Figure D.4 illustrates a set of indicative results from the open loop simulation of the process model for one process cycle. The results demonstrate the profiles for the inlet product concentration, the operating flow rate and the product concentration at the pore phase for both columns (Figure D.3). It can be observed that the column profiles are identical with half a cycle difference.

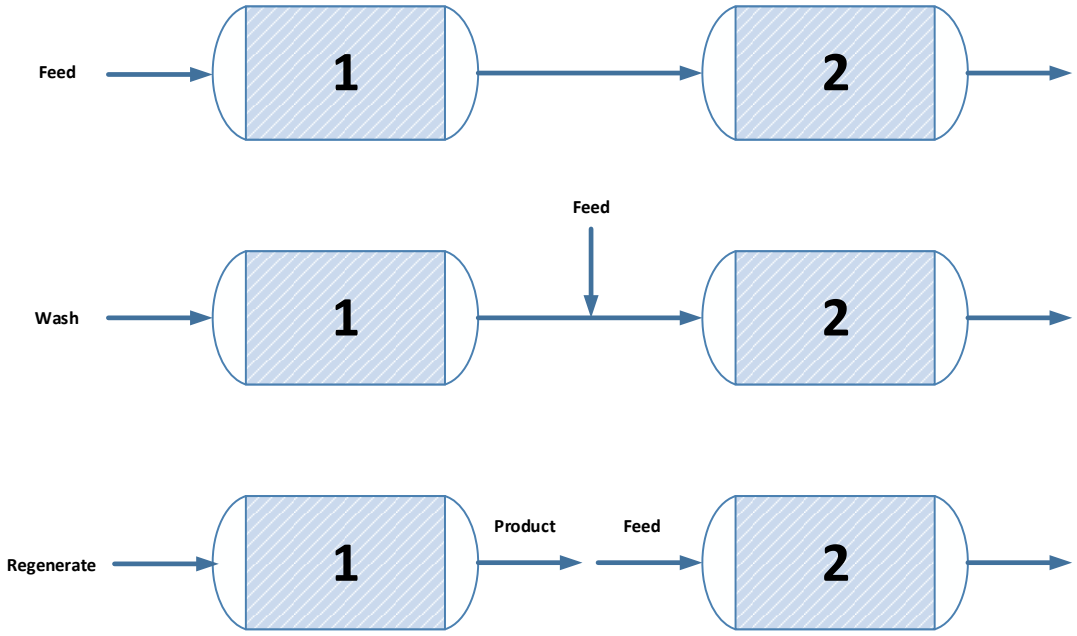

Figure D.3 Step sequence of the continuous capture step presented by Steinebach et al. (2016a).

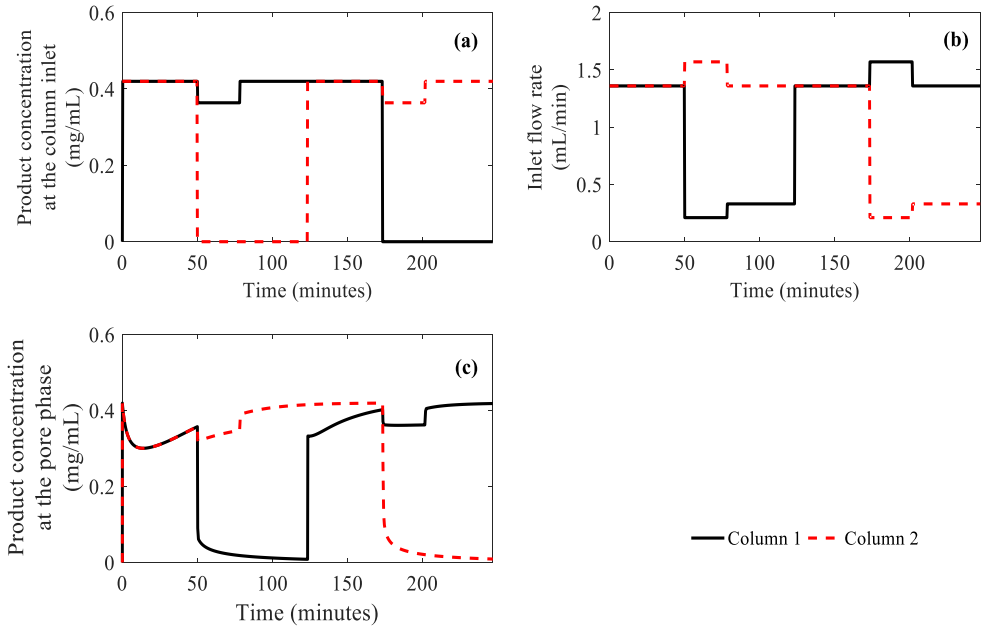

Figure D.4 Results from the open loop simulation of the capture model (Steinebach et al., 2016a) (gPROMS® ModelBuilder v.4.2.0) for one process cycle for: (a) the product concentration at the column inlet, (b) the operating flow rate and (c) the concentration of the pore phase, at the column inlet.

D.2 Conclusions

In this section we focused on the modeling work required for the seamless integration of the bioprocess (Figure D.1). In particular, the mathematical model describing the upstream system (cell culture) is updated to account for the formation of aggregate and fragments during the culturing of the cells. For the initial guesses of the kinetic parameters, experimental data from similar works in the open literature are employed (Müller-Späth et al., 2010a). As illustrated by the open loop simulation results, the model can successfully capture the dynamics of the proposed kinetics and therefore the current model structure can be used for further studies. In addition, aiming to design a interoperable environment for in silico experimentation of the continuous bioprocess, the capture step as suggested by Steinebach et al. (2016) is modeled in gPROMS® ModelBuilder. The presented model has been previously validated using experimental data (Steinebach et al., 2016a).

The results presented here provide the missing link for the integration of the three process models considered in the bioprocess. Currently, all the models are simulated under the same unit system and software platform, facilitating therefore further tests and analysis of the bioprocess performance. The connection of the three models can be easily realized using: (i) the upstream model output (antibody concentration) as feed for the capture model and (ii) the concentration of aggregates & fragments resulting from the upstream as well as the concentrated mAb from the capture step as input for the MCSGP process model.

On-going and future research is looking into the optimization of the bioprocess as well as investigation of the economic impact of the upstream performance on the downstream. Moreover, as shown in Figure D.1 the development of a global control strategy is investigated. The latter can be seamlessly facilitated as the controllers for the upstream system and the purification process have been previously developed (Chapter 6 & 5 respectively), while the design of a control strategy for the capture step will follow the procedure of the model-based control of single-/multi-column systems as presented in Chapter 4 & 5.